Universidad Autónoma de Madrid

Programa de Doctorado en Biociencias Moleculares

Novel vaccines based on poxvirus vector MVA against human viral diseases HIV/AIDS and Zika

Patricia Pérez Ramírez

MADRID, 2019

Departamento de Biología Molecular

Facultad de Ciencias

Universidad Autónoma de Madrid

Novel vaccines based on poxvirus vector MVA against human viral diseases HIV/AIDS and Zika

Memoria de Tesis Doctoral presentada por **Patricia Pérez Ramírez,** licenciada en Farmacia por la Universidad Complutense de Madrid, para optar al título de Doctora en Biología Molecular por la Universidad Autónoma de Madrid.

Directores de Tesis:

Mariano Esteban Rodríguez

Juan Francisco García Arriaza

Centro Nacional de Biotecnología (CNB-CSIC)

Madrid, 2019

Oblivisci tempta quod didicisti

(Epica – Consign to Oblivion)

Si quieres triunfar en la vida, haz de la perseverancia tu amigo del alma, de la experiencia tu sabio consejero, de la advertencia tu hermano mayor y de la esperanza tu genio guardián

(Joseph Addison)

El continuo esfuerzo, no la fortaleza o inteligencia, es la clave para desbloquear nuestro potencial

(Winston S. Churchill)

Tras escalar una gran colina, uno solo encuentra que hay muchas más colinas que escalar

(Nelson Mandela)

We are one

We are a universe

Aeons pass

Writing the tale of us all

A day-to-day new opening

For the greatest show on Earth

-We were Here-

AGRADECIMIENTOS

Después de cinco años y de un gran esfuerzo llega uno de los momentos más importantes de mi vida. Llega con mucha ilusión, pero también con mucha tristeza. Ilusión porque he alcanzado una gran meta, que en ocasiones se me ha tornado imposible. Y tristeza porque dejo atrás una de las etapas más exigentes, pero más reconfortantes y más bonitas de mi vida. Al llegar este momento lo primero que tengo es que dar mil gracias….

Gracias Mariano, por darme la oportunidad de emprender este camino de la ciencia. Por hacerme un hueco en tu laboratorio y enseñarme que con esfuerzo y perseverancia todo se puede alcanzar. Y también gracias al MINECO por la beca predoctoral FPI asignada al proyecto SAF2013-45232-R concedido a M. Esteban que me ha permitido realizar esta Tesis.

Gracias Juan por tus incansables ganas de hacer ciencia, por tus ganas de enseñar todo lo que sabes y por tu infinita paciencia. En todos estos años nunca han flaqueado tus ganas de enseñarnos, y también de aprender cosas nuevas con nosotros. Tus esfuerzos por hacer de nosotros un equipo sólido han sido constantes y creo que han tenido sus frutos ya que has conseguido que montemos nuestra pequeña familia JGA que tantos buenos momentos, profesionales y también personales, nos ha dado. Muchas gracias.

Gracias María. Mil gracias. La mitad de esta Tesis es tuya, lo sabes. Eres mucho más que una compañera o una amiga, eres una hermana. No me imagino que hubiese sido el doctorado sin ti. Hemos compartido momentos fantásticos, de viaje, de congreso, de fiesta, pero también confesiones en momentos muy duros y, sobre todo en esos momentos es donde una persona se hace un hueco en tu corazón; y en el mío hay una parcelita con tu nombre.

Gracias Adri. Desde que llegaste has sido como mi hermano pequeño en el laboratorio. Contigo no sólo he aprendido a enseñar. También hemos compartido muchas conversaciones sobre música, cine y series. También alguna receta y, sobre todo, muy buenos momentos.

Gracias a todos los miembros del laboratorio. Gracias Cris, por estar siempre dispuesta a ayudar en todo lo que estaba en tu mano. A Carmen y Bea, por compartir vuestro conocimiento conmigo siempre que me he acercado a vuestras mesas con una y mil preguntas. A Suresh, por ayudarme siempre con todo lo que te he pedido y siempre con una sonrisa y palabras amables, eres un cielo de persona; no cambies nunca. A Chogüi, por su inestimable ayuda en la preparación de cultivos celulares y crecimiento y purificación de virus. A los antiguos miembros del laboratorio: Ernesto, Lucas y Mauro, por todos los consejos y todo lo que me habéis aportado. A todo el departamento de Biología Molecular y Celular del CNB, a Carlos Óscar Sánchez Sorzano, , Iván Jareño, Luis Almonacid, Sylvia Gutiérrez, Ana Oña, Cristina Patiño y toda la gente del CNB que me ha ayudado con los experimentos. También gracias a nuestros colaboradores Miguel Ángel Martín-Acebes y Juan Carlos Saiz.

Gracias Dani, mi otro hermano pequeño, por todas las risas en los viajes, tu hiperactividad y por los momentos tan divertidos bien en el teatro, en la montaña o en una cueva. Gracias Nokaut (Carmen, Marcos, Lore, Esther, Lucía, Manu, Edu, Miguel,

Javi, Carlos, Isa, a todos) por hacer que ir al CNB fuese mucho más que ir a trabajar o a hacer experimentos, fuese ir a pasar buenos ratos, risas, conocer gente increíble y sobre todo llevarme unos recuerdos preciosos e inolvidables.

Gracias a todos mis amig@s por todo el apoyo estos años en todo lo relacionado con la Tesis (y en lo que no), por ser mis amigos, por escuchar mis problemas y ofrecerme apoyo y soluciones, por los momentos divertidos y los momentos duros.

Gracias a mis amig@s de Farmacia: María, Neibla, Cris, Mery, Ana, Michu y también a Patri, Kilian, Richi, Javi y Pableras. A mis amig@s de Moratalaz: Carlitos, Edu, Cude, Myri, Rake, Bruno, Pablo, Noe, Juanpa y, sobre todo, gracias a mis chicas *Peligrosas*: Nuri, Sara, Ampy e Isa, mis grandes descubrimientos, mis mejores y más leales amigas, por estar siempre a mi lado. Os quiero.

Gracias a mis hermanas de otra madre, Ana y Ampy. Os quiero, igual que quiero a mis niñas Lucía y Alicia y a mis padres postizos Julián y Amparo. Sois mi segunda familia, la que yo he elegido y elegiría una y mil veces. Ampy, esta Tesis también es en parte tuya, tú has estado conmigo en cada paso de este camino, me conoces mejor que yo misma y eres mi consuelo cuando todo parece ir mal y mi compañera de viajes, de fiesta y de vida. Pase lo que pase… y a pesar de…

Gracias a mi nene, Rafa. El que me dio el empujón para ese primer e-mail (tú ya sabes a cuál me refiero). Por ser mi compañero de vida y mi apoyo durante estos años. Por escucharme tanto cuando los experimentos iban mal y llegaba a casa abatida, como cuando llegaba entusiasmada porque un resultado había salido genial. Por compartir mis éxitos, mis desilusiones y mi vida. Te quiero.

Gracias a mis padres. Por todo el esfuerzo en darnos una educación, empezando por casa. Soy lo que soy gracias a vosotros, me habéis ensenado el valor del esfuerzo y la perseverancia, me habéis enseñado a ser buena persona y sobre todo me habéis inculcado el apoyo incondicional de la familia. Os quiero mucho.

Y, por último, pero no menos importante, gracias a mi familia. A mi hermano, Kike; a mis yayos Pepe, Pepa, Victoria y Kubala (aunque ya no estés entre nosotros); a mis queridos tíos y tías Fran, Charo, Ana, Rosi (mi Tachi), Esther, María y Antonio; y también Pamela, Pedro, Alberto y David. A mis niñas Lorena y Sandra. A mis chicos Sergio, Raúl y David. Y también a mis pequeños Carlota, Miri (mi brujita), José y Alex. Gracias familia por el apoyo, por ser una piña y por haberme dado una infancia y una vida rodeada de amor.

¡¡Gracias, a todos una y mil gracias!!

RESUMEN

El virus vaccinia modificado de Ankara (MVA) es una cepa altamente atenuada del virus vaccinia (VACV) y uno de los vectores más prometedores utilizados para generar vacunas recombinantes frente a varias enfermedades infecciosas. Sin embargo, se necesitan vacunas basadas en MVA novedosas, más eficientes y optimizadas, capaces de inducir mejores respuestas inmunitarias celulares y humorales específicas del antígeno. Por lo tanto, el objetivo principal de esta Tesis es mejorar la inmunogenicidad del vector MVA mediante diferentes enfoques: i) fortalecer el promotor del VACV que dirige la expresión del antígeno heterólogo, ii) delecionar un gen del MVA con un supuesto papel inmunosupresor, y iii) diseño racional del antígeno heterólogo para optimizar su expresión y presentación. Estas modificaciones se han aplicado en primer lugar a vectores MVA que expresan antígenos del VIH-1 para demostrar si se observa un aumento en la inmunogenicidad específica frente al VIH-1 en ratones inmunizados; y, en segundo lugar, para generar una nueva vacuna basada en MVA frente al patógeno emergente virus Zika (ZIKV), para tratar directamente de correlacionar un beneficio en la mejora de las respuestas inmunitarias específicas frente al ZIKV con protección frente a un desafío con ZIKV en un modelo de ratón.

Como primera modificación para mejorar la inmunogenicidad frente a antígenos del VIH-1, un nuevo promotor sintético del VACV, denominado LEO160, diseñado y optimizado para potenciar la expresión de genes heterólogos a tiempos tempranos, se insertó en un vector MVA que expresa el antígeno gp120 del VIH-1. Los resultados mostraron un aumento en la expresión y liberación celular de la proteína gp120 del VIH-1 *in vitro*, y un incremento de las respuestas inmunitarias celulares y humorales específicas frente a gp120 en ratones inmunizados, en comparación con el candidato vacunal MVA-B que expresa la proteína gp120 del VIH-1 bajo el control del promotor sintético temprano/tardío usado convencionalmente.

La segunda modificación consistió en la deleción del gen *A40R* del MVA, que codifica una proteína con una supuesta función inmunosupresora. Por lo tanto, la deleción y posterior reinserción del gen *A40R* del MVA en el candidato vacunal MVA-B, que expresa varios antígenos del VIH-1, demostró su papel inmunosupresor tanto *in vitro* como *in vivo*. En ratones inmunizados, el candidato vacunal MVA-B que carece del gen *A40R* incrementó las respuestas inmunitarias celulares y humorales específicas frente al VIH-1, en comparación con el virus parental MVA-B.

Finalmente, ambas estrategias (el fortalecimiento del promotor del VACV y la deleción de genes inmunosupresores del VACV) se combinaron junto con un diseño racional para optimizar la expresión y presentación de los antígenos estructurales del

ZIKV para generar un nuevo candidato vacunal basado en MVA frente al ZIKV, MVA-ZIKV. MVA-ZIKV expresó altos niveles de partículas similares al virus e indujo robustas respuestas inmunitarias celular y humoral específicas frente al ZIKV en ratones inmunizados, que correlacionaron con la capacidad de controlar la replicación del ZIKV después de un desafío con ZIKV en un modelo de ratón susceptible.

Estos hallazgos demuestran la importancia de desarrollar nuevas vacunas basadas en MVA más optimizadas, capaces de mejorar las respuestas inmunitarias celular y humoral específicas del antígeno, y de aumentar su eficacia.

SUMMARY

Modified vaccinia virus Ankara (MVA) is a highly attenuated vaccinia virus (VACV) strain, and one of the most promising vectors used to generate recombinant vaccines against several infectious diseases. However, novel, more efficient and optimized MVA-based vaccines able to induce better antigen-specific cellular and humoral immune responses are needed. Thus, the main aim of this Thesis is to enhance the immunogenicity of the MVA vector by using different approaches: i) strengthening the VACV promoter that drives the expression of the heterologous antigen, ii) deleting an MVA gene with a supposed immunosuppressive role, and iii) rational designing of the heterologous antigen for optimizing its expression and presentation. These modifications have been applied first, to MVA vectors expressing HIV-1 antigens to demonstrate whether an enhancement in the HIV-1-specific immunogenicity is observed in immunized mice; and second, to generate a novel MVA-based vaccine against the emerging pathogen Zika virus (ZIKV), to directly try to correlate a benefit in the improved ZIKV-specific immune responses with protection against ZIKV challenge in a mouse model.

As the first modification to improve the immunogenicity against HIV-1 antigens, a novel VACV synthetic promoter, termed LEO160, designed and optimized to enhance the expression of heterologous genes at early times, was inserted in an MVA vector expressing the HIV-1 gp120 antigen. The results showed an increase in the expression and cell release of HIV-1 gp120 protein *in vitro* and an enhancement in the Env-specific cellular and humoral immune responses in immunized mice, compared to the MVA-B vaccine candidate expressing the HIV-1 gp120 protein under the control of the widely used synthetic early/late (sE/L) promoter.

The second modification consisted in the deletion of the MVA *A40R* gene, encoding a protein with a presumed immunosuppressive function. Thus, deletion and subsequent reinsertion of the MVA *A40R* gene in the MVA-B vaccine candidate, expressing several HIV-1 antigens, demonstrated its immunosuppressive role both *in vitro* and *in vivo.* In immunized mice, the MVA-B vaccine candidate lacking the *A40R* gene enhanced the HIV-1-specific cellular and humoral immune responses.

Finally, both strategies (increasing VACV promoter strength and deleting immunosuppressive VACV genes) were combined together with a rational design for optimize expression and presentation of ZIKV structural antigens to generate a novel MVA-based vaccine candidate against ZIKV, MVA-ZIKV. MVA-ZIKV expressed high levels of virus-like particles and induced robust ZIKV-specific cellular and humoral immune responses in immunized mice that linked with the ability to control ZIKV replication after a ZIKV challenge in a susceptible mouse model.

These findings prove the importance of develop novel MVA-based vaccines more optimized, able to enhance the antigen-specific cellular and humoral immune responses and to increase its efficacy.

INDEX

ABBREVIATIONS

A

Ab	Antibody
Ad	Adenovirus
ADCC	Antibody-dependent cell-mediated cytotoxicity
Ag	Antigen
ANOVA	Analysis of variance
AP-1	Activator protein-1
APC	Allophycocyanin
ART	Antiretroviral therapy
A.U.	Arbitrary units

B

BFA	Brefeldin A
bNAb	Broadly neutralizing antibody
bp	base pairs

C

CA	Capsid
CCL3	Chemokine C-motif ligand-3
CCL5	Chemokine C-motif ligand-5
CD	Cluster of differentiation
CDR	Complementarity determining region
CEF	Chick embryo fibroblasts
CEV	Cell-associated enveloped virions
CNB	Centro Nacional de Biotecnología
CMV	Cytomegalovirus
COP	Copenhagen vaccinia virus strain
CVA	Chorioallontoic vaccinia virus Ankara
CXCR5	C-X-C chemokine receptor type 5
Cy	Cyanine

D

DAB	Diaminobenzidine tetrahydrochloride
DAPI	4′,6′-diamidino-2-phenylindole
DDX58	DEAD box helicase-58
DMEM	Dulbecco´s modified Eagle´s medium
dNTP	Deoxyribose nucleoside triphosphate
dsRed2	Red fluorescent protein from *Discosoma sp*.

E

E	Envelope protein (ZIKV)
EBOV	Ebola virus
E.coli	*Escherichia coli*
EMEM	Eagle's minimal essential medium
Env	Envelope (HIV)
ER	Endoplasmic reticulum
EV	Enveloped virion

F

FBS	Fetal bovine serum
FCS	Fetal calf serum
Fig.	Figure

G

Gag	Group-specific antigen (HIV)
GAPDH	Glyceraldehyde-3-phosphate dehydrogenase gene
GBS	Guillain-Barré syndrome
GM-CSF	Granulocyte-macrophage colony-stimulating factor
GPN	Gag-Pol-Nef (HIV)

H

HA	Hemagglutinin
HCV	Hepatitis C virus
HPRT	Hypoxanthine phosphoribosyl transferase
HRP	Horseradish peroxidase
h.p.i.	Hours post-infection

I

ICS	Intracellular cytokine staining

IEV	Intracellular enveloped virion
IFIH1	Interferon induced with helicase C domain-1
IFIT1	Interferon induced protein with tetratricopeptide repeats-1
IFIT2	Interferon induced protein with tetratricopeptide repeats-2
FITC	Fluorescein isothiocyanate
IFN	Interferon
IFNAR	Interferon-α/β receptor
IFN-R	Interferon receptor
IFNβ	Interferon beta
IL	Interleukin
IN	Integrase
ITR	Inverted terminal repeat
IRF	Interferon-regulatory factor
ISG	Interferon-stimulated gene
ISRE	Interferon-stimulated response element
i.d	Intradermal
i.m	Intramuscular
i.p	Intraperitoneal

J

JAK	Janus kinase
JEV	Japanese encephalitis virus

L

LB	Luria-Bertani
LF	Left flank
LPS	Lipopolysaccharide

M

MA	Matrix
mAb	Monoclonal antibody
MCS	Multiple cloning site
MDA-5	Melanoma differentiation antigen-5
MHC	Major histocompatibility complex
MIP-1α	Macrophage inflammatory protein-1 alpha
MOI	Multiplicity of infection
MT	Microtubules
MV	Mature virion
MVA	Modified vaccinia virus Ankara

N

NC	Nucleocapsid
NCS	Newborn calf serum
NF	Nuclear factor
NK	Natural Killer
NYVAC	New York vaccinia virus

O

OAS	2’-5’-oligoadenylate synthase
OD	Optical density
OPV	Orthopoxvirus
ORF	Open reading frame

P

PAMP	Pathogen-associated molecular pattern
PD-1	Programmed cell death protein 1
PE	Phycoerythrin
PerCP	Peridinin-Chlorophyll-protein
PFU	Plaque-forming unit
PKR	Protein kinase R
PMA	Phorbol 12-myristate 13-acetate
Pol	Polymerase
PPR	Pattern recognition receptor
PR	Protease
prM	Premembrane protein (ZIKV)
PRNT	Plaque reduction neutralization
p.i	Post-infection

R

RANTES	Regulated upon Activation Normal T cell Expressed and Secreted gene
RF	Right flank
RIG-I	Retinoic acid inducible gene I
RLR	Retinoic acid inducible gene I-like receptor

RPMI	Roswell Park Memorial Institute medium
RT	Reverse transcriptase
RT	Room temperature

S

SDS-PAGE	Sodium dodecyl sulfate-polyacrylamide gel electrophoresis
sE/L	Synthetic early/late
ssRNA	Single-stranded ribonucleic acid
STAT	Signal Transducer and Activator of Transcription

T

TF	Transcription factor
TGN	Trans-Golgi network
TK	Thymidine kinase
TLR	Toll-like receptor
TMB	3,3',5,5' Tetramethyl benzidine
TNFα	Tumor necrosis factor-α

V

VACV	Vaccinia virus
VARV	Variola virus
VLP	Virus-like particles
VSV	Vesicular stomatitis virus

W

WHO	World Health Organization
WR	Western Reserve

Y

YFV	Yellow fever virus

Z

ZIKV	Zika virus
β-glus	β-glucuronidase

INTRODUCTION

1. INTRODUCTION

1.1. Vaccinia virus

Vaccinia virus (VACV) is the prototype species of the *Orthopoxvirus* (OPV) genus, among whose members is included *Variola virus* (VARV), the causative agent of smallpox. OPV genus belongs to the *Poxviridae* family, which comprises complex enveloped viruses with double-stranded DNA genome that replicate entirely in the cytoplasm of infected cells [1].

VACV was the agent most commonly used as a vaccine against smallpox by the World Health Organization (WHO) eradication program. Smallpox is the only human disease that has been eradicated worldwide through human intervention, starting at the end of the XVIII century when Edward Jenner in the United Kingdom proved that the inoculation with cowpox (another OPV), called variolation, in a healthy individual prevented the subsequent infection with VARV and the development of smallpox. The expansion of the variolation process all over the world during the following 200 years culminated when the WHO declared the eradication of the smallpox in 1980. Near four decades since the eradication of smallpox, VACV continues to be a focus of intensive research because its many interactions with the host cell and the immune system have provided tremendous insights into virology, cell biology and immunology. More importantly, in 1982 VACV was developed as an expression vector [2,3] and, from then, it has become a recombinant expression vector widely used for the development of vaccines [4–8]. Nowadays, attenuated VACV strains such as modified vaccinia virus Ankara (MVA), one of the most promising poxvirus vectors, are widely used as improved vaccine candidates against several prevalent and emerging infectious diseases, probing to be extremely safe, and highly immunogenic and protective against several pathogens.

1.1.1. Genomic structure

VACV has a linear AT-rich (67%) double-stranded DNA of about 190 kbp, which has relatively low inter-gene spacing and noncoding regions [9]. The two DNA strands are covalently linked at the termini by incompletely base-impaired loops into one continuous molecule [9]. At either end of the genome there are inverted terminal repeat (ITR) regions that consist of identical but oppositely orientated sequences which play a key role during DNA replication (Fig. 1) [10,11]. VACV genetic nomenclature was adopted from the Copenhagen (COP) strain in which the open reading frames (ORFs), about 200, were named according to their relative position (left or right) in the 16 fragments (A to P) produced upon digestion with *Hind*III restriction endonuclease [12]. The central conserved region of the genome contains the genes responsible for essential functions

such as replication and assembly, while the left and right variable terminal regions contain non-essential genes, such as those related to host-virus interactions and immune evasion (Fig. 1).

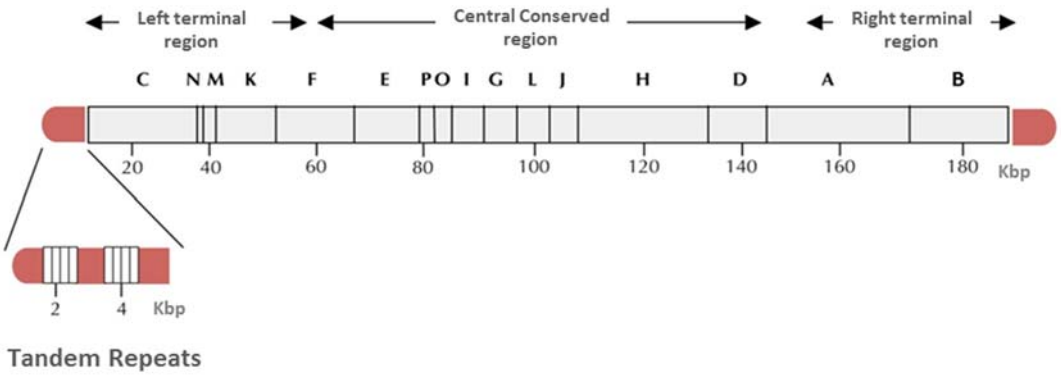

Figure 1. Genomic organization of the VACV genome. The DNA genome is divided into a central conserved region and two variable terminal regions (left and right) and consists in 16 regions named from A to P, containing about 200 ORFs. Two sets of 70 bp tandemly repeated sequences are located 2 and 4 kbp from the 5´and 3´ends and are covalently linked to form a hairpin. Adapted from [12].

1.1.2. Virion structure

VACV particles are large (360 x 270 x 250 nm), brick-shaped virus particles with lack of symmetry (Fig. 2). Infective VACV produces two forms of virions, the mature virion (MV) and the enveloped virion (EV), that have different structures, locations, abundance and roles in the virus life-cycle [13,14]. The MVs are enveloped by an outer layer and an inner lipid membrane, while the EVs have an additional outer plasma-membrane-derived envelope containing viral and cellular proteins (absent in the MV) [1,14]. Inside the virions, the genomic DNA, structural proteins and transcriptional enzymes are located, covered by a core wall [15] (Fig. 2).

During the replication cycle, two more intracellular forms are produced: i) the intracellular enveloped virion (IEV) that is formed through the wrapping of an assembled MV by a Golgi-derived lipid membrane, and ii) the cell-associated enveloped virion (CEV) that is formed when the IEV fuses to the cell membrane prior to release.

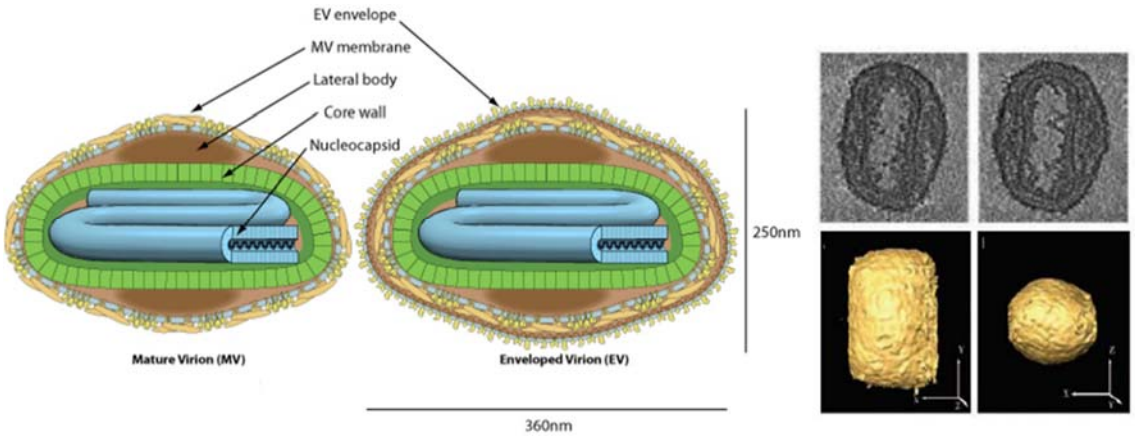

Figure 2. Structure of the infective VACV particles. Left panel: Mature virion (MV) and enveloped virion (EV). Adapted from "© ViralZone 2016, Swiss Institute of Bioinformatics (https://viralzone.expasy.org/174). Right panel: Cryo-electron microscopy sections (top) and volumetric representation (bottom) of an MV using tomographic reconstruction. Adapted from [15].

1.1.3. Life cycle

VACV infects a wide variety of cells and its replication cycle takes place entirely in the cytoplasm of the infected cell. As illustrated in Fig. 3, the viral infection cycle takes place in four steps: i) entry, ii) uncoating, iii) gene expression and DNA replication, and iv) virion assembly and release. i) Virion entry differs between the different virion forms and could be by direct fusion to the plasma membrane, assisted by a complex of several viral proteins; or through macropinocytosis into acidified endosomes. In the case of EVs, the additional membrane is disrupted before entry using a non-fusogenic mechanism that is dependent on cellular and viral surface proteins [16]. ii) Following entry, the virions are transported through microtubules to be uncoated in the viral factories, where they loss viral lipids and viral genome is exposed to the DNA exonucleases [17,18]. iii) Viral factories are the hotspots of viral DNA replication within the cytoplasm and are established early during the infection [9,19]. About 50% of the replicated DNA is packaged into new virions [20]. During gene expression viral genome transcription is highly regulated and takes place in three stages: early, intermediate and late [12,21–23]. Within 20 minutes after entry, viral proteins are produced [21], and the enzymes and transcription factors packaged into the core of the virions come together to carry out early transcription of about half of the viral genome. The mRNAs thus produced encode proteins that are involved in host antiviral response modulation, DNA replication and intermediate gene transcription [1]. Intermediate transcription occurs simultaneously with DNA replication and encodes factors necessary for late transcription [24]. Finally, late transcription of genes encoding structural proteins, virulence factors and other enzymes is carried out. iv) Newly formed virions undergo various changes until they reach the final

EV or MV forms. Spherical immature virions (IVs) are first formed in the viral factories where they mature into MVs after the proteolytic processing of some of the viral proteins and core condensation [25]. Most MVs stay in the cytoplasm until they are released following cell lysis, while a small fraction is transported through the Golgi, where they acquire a second membrane to form the IEVs. The IEVs are transported again by microtubules to the plasma membrane and released as EVs by membrane fusion or projected to adjacent cells through actin tails [26,27].

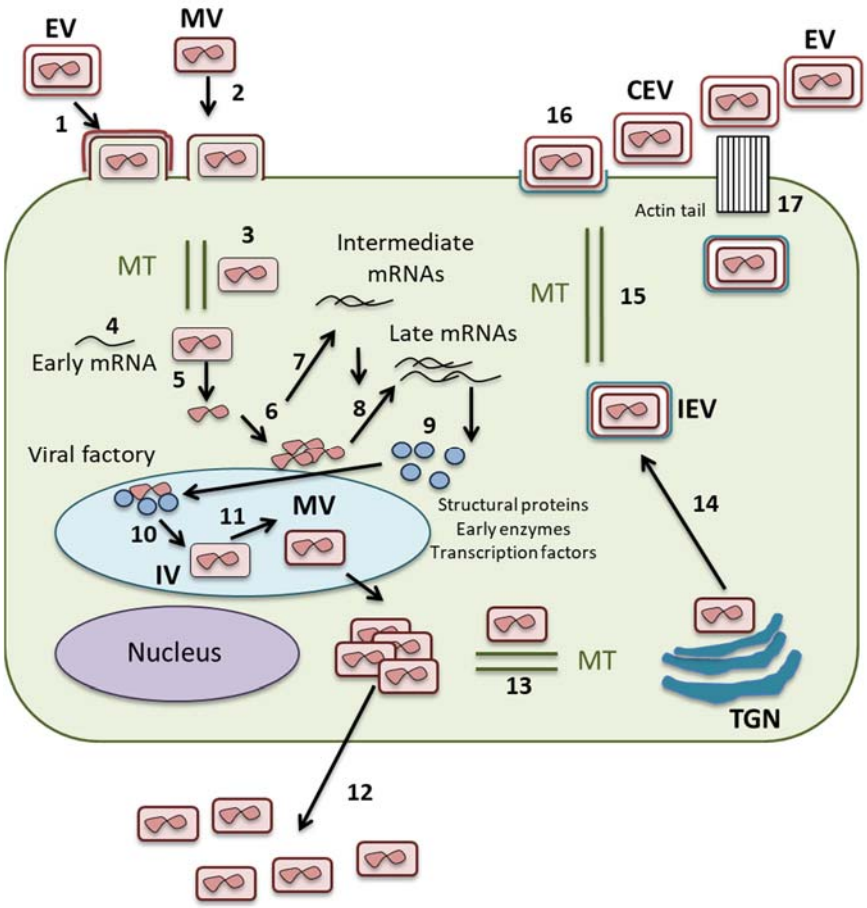

Figure 3. Overview of the VACV life cycle. Enveloped virions (EV, 1) and mature virions (MV, 2) bind to and enter the cell, releasing the core into the cytoplasm. The core is translocated (3) by microtubules (MT) deeper into the cell to a perinuclear site. Production of early mRNAs (4) leads to uncoating of the core, releasing of the genome (5) and following replication of the viral genome (6), the production of intermediate (7) and late mRNAs (8). These mRNAs are translated into structural proteins and early gene transcription machinery (9). Within the viral factories, a single genome interacts with the early transcription machinery plus structural proteins and these are assembled within membrane crescents to form immature virions (IV, 10). The IV undergoes nucleoprotein condensation and proteolytic cleavages of structural proteins to form the MV (11). Many MVs build up in the cell and are released upon cell lysis (12). However, a small proportion undergo further morphogenesis, transported on MT to sites of wrapping (13) by the trans-Golgi network (TGN) or early endosomes, wrapped by a double membrane to form intracellular enveloped virions (IEV, 14). IEVs are transported to the cell surface on MT (15) where the outer membrane fuses with the plasma membrane (16) to form cell-associated enveloped virions (CEV) on the cell surface. Actin polymerisation beneath the CEV forms actin tails (17), driving CEV towards neighbouring cells or releasing EVs that can infect either neighbouring or distant cells. Adapted from [27].

1.1.4. Effect of VACV on host cells

VACV induces early changes in cell morphology, adhesion properties and metabolism that eventually results in death of infected cells. These changes are called cytopathic effects and include inhibition of host protein synthesis, alterations to the extracellular matrix and adhesion properties, microtubules modification and cell rounding, and virus-induced cell motility.

1.1.4.1. Innate immune response to VACV

Like other viruses, VACV infection of mammalian cells is sensed by pattern recognition receptors (PRRs) and leads to an innate immune response that restricts virus replication and induces an adaptive immunity that finally gets rid of infection. To counteract this immune response and prevent virus elimination, VACV encoded numerous immune modulators that block several pathways of the innate immune system, including complement, macrophages, natural killer (NK) cells, and soluble mediators such as interferons (IFNs), other cytokines and chemokines [28,29]. Among these VACV immune modulators is of relevant importance the immune modulation of IFN, a group of secreted glycoproteins with potent antiviral effects. The IFN response is initiated upon sensing of viral pathogen-associated molecular patterns (PAMPs) by host cell PRRs, including Toll-like receptors (TLRs), retinoic acid inducible gene I (RIG-I)-like receptors (RLRs), such as RIG-I and melanoma differentiation antigen 5 (MDA-5) (that detect foreign cytoplasmic RNA) and putative cytosolic dsDNA sensors [30]. Engagement of PRRs induces signalling cascades that culminate in the activation of transcription factors (TFs), such as IFN-regulatory factors (IRF) 3 and IRF7, nuclear factor (NF)-κB and activator protein 1 (AP-1), their translocation into the nucleus and transcription of genes encoding type I IFNs (notably IFN-β), cytokines and chemokines [30]. IFNs are secreted from the cell and engage their cognate receptor on the same cell (autocrine signalling) or neighbouring cells (paracrine signalling), and thereby initiate the Janus kinase (JAK)/signal transducer and activator of transcription (STAT) signalling cascades, that activates transcription of IFN-stimulated genes (ISGs) by binding to IFN-stimulated response elements (ISREs) present in the promoters of these genes. IFN induces the coordinated expression of several hundred ISGs, and some ISGs products encode PPRs as well as TFs, feeding an amplification loop resulting in the generation of an anti-viral state in the cells. Other ISGs encode proteins with direct anti-viral activity that catalyse cytoskeletal remodelling, trigger apoptosis, induce shut-down of protein synthesis, stimulate the expression of major histocompatibility complex (MHC) class I molecules on the surface of the cell and elicit more pro-inflammatory cytokines [30].

VACV is able to inhibit the IFN response at multiple levels: a) secreting proteins from the infected cell, called decoy IFN receptors, that capture IFNs in solution or on the cell surface to prevent engagement of IFN receptors by IFNs; b) blocking signal transduction induced by IFNs when binding to their receptors within the JAK/STAT pathway; c) inhibiting IFN-induced antiviral proteins such as Mx proteins, protein kinase R (PKR) and 2'-5'-oligoadenylate synthase (OAS); and d) restricting the production of IFN. VACV blocks the IFN induction by minimizing the production of PAMPs, such as dsRNA, or its recognition by PRRs; inhibiting host protein synthesis; and by blocking the PRR-induced signalling pathways that activate TFs leading to IFN induction, such as IRF3 and NF-κB signalling pathways [28,29] (Fig. 4).

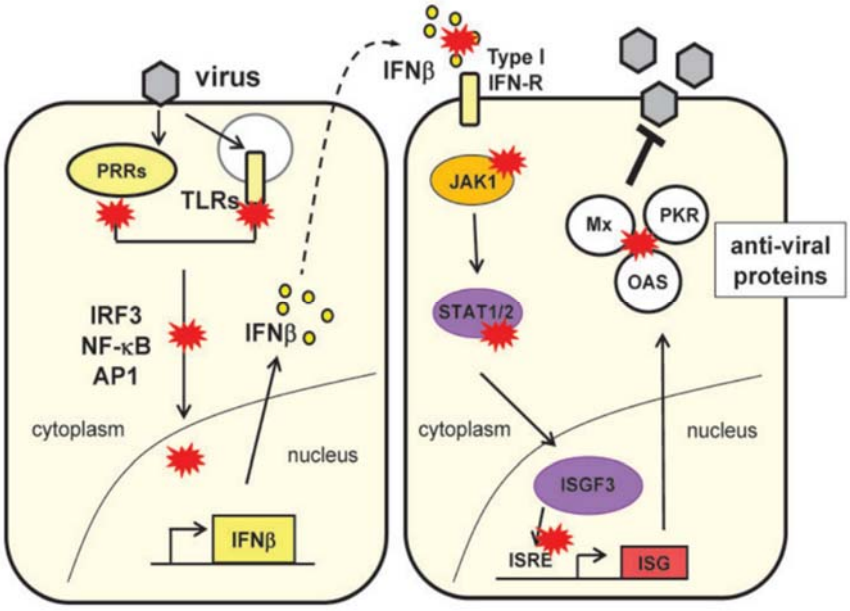

Figure 4. VACV antagonism of IFN signalling pathway. VACV is sensed by PRRs within the cytosol or in endosomes triggering signal cascades that lead to activation of TFs NF-kB, IRF3, IRF7 and AP-1. TFs enter the nucleus and stimulate transcription of the IFN-β gene that is then secreted from the cell and binds IFN receptors (IFN-R) on the same or adjacent cells triggering the activation of the JAK/STAT pathway. As result, the IFN-stimulated gene factor 3 (ISGF3) complex is assembled in the nucleus and, finally, leads the transcription of hundreds of antiviral ISGs, such as Mx proteins, PKR and OAS. The positions at which some VACV proteins can inhibit the production or action of IFN are shown by red stars. Adapted from [28].

1.1.4.2. Adaptive immune responses to VACV

1.1.4.2.1. Humoral responses

Antibodies (Abs) secreted by B cells in response to VACV infection are very important to clear the infection. Anti-VACV Abs can bind directly to VACV particles, causing aggregation and inhibiting virus binding and entry to cells, initiate complement-mediated lysis or opsonisation, or bind to infected cells, leading to Ab-dependent cell-mediated cytotoxicity (ADCC). The anti-VACV Ab response is primarily $CD4^+$ T cell-dependent [31] and is predominantly of an IgG2a isotype [32]. IgM appears by 7 days post-infection (p.i.)

and IgG by day 14 [33] and Ab levels peak around 6 weeks p.i. [34,35] and can be maintained for more than 3 months [35,36] in mouse models. Vaccination studies in humans demonstrate that a strong Ab response is elicited after primary vaccination. Abs are not detected before day 10 post-vaccination [37,38] but are apparent by day 13/14 [39] and Ab levels continue to rise until approximately day 28 [39,40]. Re-vaccination elicits a more rapid Ab response, with Ab levels peaking approximately day 14, considerably earlier than after primary immunisation and, furthermore, re-vaccination also boosts previous Ab levels [37,39,40]. Ab levels decrease slowly to a steady level but are long-lived, being maintained up to 50 years post-vaccination [41,42].

1.1.4.2.2. Cellular responses

In mice, both $CD4^+$ and $CD8^+$ T cell responses are elicited following VACV infection [31]. A kinetic analysis of infection shows that VACV induces a potent primary $CD8^+$ T cell response as well as long-term memory responses *in vivo* [43]. As early as day 5 p.i., an IFN-γ positive $CD8^+$ T cell response is detected and peaked at day 7, with 30% of $CD8^+$ T cells in the spleen being VACV-specific. There is also a strong cytotoxic T cell response by day 7 [43]. The $CD4^+$ T cell response displayed similar kinetics to that of $CD8^+$ T cells but at lower frequencies [43]. The response peaked at day 7 p.i., with 3% of the $CD4^+$ T cell being VACV-specific. When compared to $CD8^+$ T cells, a higher percentage of $CD4^+$ T cells produced IL-2, demonstrating an increased proliferative response compared to the $CD8^+$ T cell compartment. This is consistent with $CD4^+$ T cells acting as T helper cells. Although the response declines by approximately 90% by day 30, it is maintained for over 300 days [43]. In humans, strong $CD4^+$ and $CD8^+$ T cell responses are elicited following smallpox vaccination. In general, $CD8^+$ T cell responses are of a greater magnitude (2- to 4-fold higher) after immunisation [44,45], but $CD4^+$ T cell responses are maintained for a greater length of time at higher frequencies [41,44,45]. VACV-specific $CD4^+$ T cells are detected in the majority (82-100%) of individuals vaccinated up to 75 years previously, unlike $CD8^+$ T cell responses [41,44].

1.2. Modified vaccinia virus Ankara (MVA)

MVA was developed by the attenuation of the Turkish smallpox vaccine Chorioallontoic VACV Ankara (CVA) after more than 570 serial passages in chicken embryo fibroblast (CEF) cells [46]. The process involved the loss of about 30 kbp of genetic components mainly from the left and right terminal regions of the genome, involving genes non-essential for replication, for example, those responsible for host immune modulations [47]. The resulting MVA virus has limited replication ability in mammalian cell types but produces early and late viral proteins as in permissive cells [48], although there is a block in virion assembly, avoiding the cell-to-cell spread of the

virus [49,50]. The safety of MVA as a vaccine vector was established when used for smallpox vaccination by the Bavarian State Vaccine Institute in extensive clinical trials in Germany in more than 120,000 individuals until 1980, without any serious adverse events reported [51].

1.2.1. Recombinant MVA as vaccine vector

Recombinant MVA vectors have played an important role as vaccine candidates against several infectious diseases and cancer [52–56], because they combine the safety of a killed virus vaccine, due to their impaired replication capacity in mammalian cells, with the immunogenicity of a live virus vaccine. The great efficacy of recombinant MVA vectors in developing antigen-specific immune responses is due to the expression gene products within cells that are efficiently presented by both MHC class I and class II molecules, leading to the activation of $CD4^+$ and $CD8^+$ T cells, and to the induction of robust anti-viral responses, as happen with other VACV strains (see section 1.1.4.), that make MVA acts as an adjuvant itself [57,58].

There are also several characteristics that make recombinant MVA vectors excellent vaccine candidates: a) the packing flexibility of the genome, which allows the insertion of up to 25 kbp of foreign DNA without loss of infectivity, b) the lack of persistence or genomic integration in the host due to their cytoplasmic replication, c) the ability to induce both antibody and cytotoxic T cell immune responses against the heterologous antigens with long-lasting immunity after a single inoculation, d) the stability of freeze-dried vaccine, e) its ease of manufacture and administration and f) the low prevalence of anti-vector immunity in the global population due to the interruption of smallpox vaccination after the WHO declared its eradication in 1980 [52–56].

1.2.2. Enhancing MVA vaccine vector immunogenicity

Despite the good safety and immunogenicity profiles exhibited by recombinant MVA vectors, novel optimized and more efficient MVA vaccine vectors able to induce an enhanced magnitude, breadth, polyfunctionality, and durability of the immune responses to exogenously expressed antigens are desirable. Thus, several strategies have been developed to enhance the immunogenicity and efficacy of the MVA-based vaccine candidates [59], such as:

1.2.2.1. The use of optimized prime/boost immunization protocols

One of the most commonplace methods of immunization designed to improve the immune responses generated by MVA-based vaccines is to follow a multiple dose prime/boost strategy. The use of heterologous prime/boost protocols that combine an MVA vector (either as prime or as boost agent) with other vaccine agent such as DNA

[60–63], protein [64,65], virus-like particles (VLPs) [66], or other recombinant viral vectors, like adenovirus (Ad) or vesicular stomatitis virus (VSV) [67,68], are shown to improve the antigen-specific immune responses in different animal models. Furthermore, the use of heterologous prime/boost protocols including MVA vector have also demonstrated in human clinical trials to be able to induce potent T and B cell responses against various pathogens as, for example, human immunodeficiency virus (HIV)-1 [69–71], hepatitis C virus (HCV) [72], *Plasmodium falciparum* (the causative agent of malaria) [73,74], Ebolavirus (EBOV) [75], and respiratory syncytial virus (RSV) [76].

1.2.2.2. Enhance the virus promoter strength

It has been shown that the levels of the heterologous antigens expressed (and placed under the control of a VACV promoter) from poxvirus vectors correlates with the magnitude of the antigen-specific immune responses in mice [77]; and timing of antigen expression also influence the type (T $CD4^+$ or $CD8^+$), quantity, quality and durability of the antigen-specific immune responses [78]. Thus, the optimization of the virus promoter strength is an ideal strategy to increase the expression of the heterologous antigens at very early times p.i. [78–81]. Moreover, since the efficiency with which an antigen is processed and presented on the surface of infected cells influences its recognition [82], the timing of expression of heterologous antigens from the MVA vector is very important to induce robust antigen-specific T cell immune responses [78]. Considering that immunodominance is defined as the phenomenon whereby only a small fraction of all of the possible epitopes from a particular pathogen elicits an specific immune response [83], it is possible to modulate such immunodominance hierarchy changing the timing and the quantity of antigen production [84]. In fact, it has been described that in VACV 90% of the most recognized antigens by $CD8^+$ T cells were ranked in the top of 50% in terms of mRNA expression [85], and there is a positive correlation between viral gene expression and immunodominance hierarchy after a second immunization due to a mechanism of cross-competition between T cells specific for early and late viral epitopes [86]. Traditional VACV promoters with both early and/or late activity have been used to direct the expression of foreign antigens to ensure that adequate expression levels are present at the appropriate time for induction of strong antigen-specific immune responses [87]. However, novel VACV promoters able to improve the expression and immunogenicity of the foreign antigens are needed. Thus, the search for novel potent VACV promoters has been expanding through different approaches such as designing *in silico* based on early and late consensus motifs observed in native poxvirus promoters, generating hybrid early-late synthetic promoters, using tandem promoters present

naturally in VACV, or designing new potent promoters by using bioinformatic analysis [87].

1.2.2.2.1. The new synthetic Late-Early Optimized VACV promoter LEO160

Among the different novel synthetic VACV promoters studied, the new synthetic Late-Early Optimized (LEO)160 promoter, designed by using bioinformatic analysis (Fig. 5), is of particular interest to this work. This promoter significantly enhance the expression levels of the foreign antigen *in vitro*, correlating with an *in vivo* enhancement in the antigen-specific T cell immune responses [88,89].

Figure 5. Scheme of the synthetic LEO160 promoter. Late promoter element (29 nucleotides; green); early promoter motif (15 nucleotides; red), and a 160-nucleotide spacer (consisting in several multicloning sites; black) are shown. The nucleotide sequence of the different motifs of the promoter is indicated on the right. Adapted from [88].

1.2.2.3. Deletion of MVA immunomodulatory genes

In order to improve the host immune responses to vaccination, one of the strategies is the deletion of MVA genes that are involved in the modulation of host immunity [29,57]. This strategy has been extensively developed during the last years with the generation of several MVA-based vaccine candidates against HIV/acquired immune deficiency syndrome (AIDS) containing deletions in single or multiple MVA immunomodulatory genes that antagonize host anti-viral immune responses. The overall results obtained from preclinical studies in immunized mice [90–94], and non-human primates [95,96] showed a significant immunological benefit with an enhancement in the immunogenicity against HIV-1 antigens when compared with their parental MVA-based vaccines without deletions. For example, a single deletion of the MVA *C6L* gene, encoding an inhibitor of the type I IFN signalling pathway, in the genome of an MVA-based vaccine candidate against HIV/AIDS expressing several HIV-1 antigens (termed MVA-B) enhanced the overall HIV-1-specific immune responses, with an increase in the magnitude, polyfunctionality, and durability of HIV-1-specific $CD4^+$ and $CD8^+$ T cell responses [91]. Moreover, responses against HIV-1 antigens were further enhanced when MVA *C6L* and *K7R* genes, encoding type I IFN inhibitors, were deleted in combination in the genome of MVA-B [93]. Furthermore, based on those results on MVA-based vaccine candidates against HIV/AIDS lacking MVA immunomodulatory genes,

novel optimized recombinant MVA vectors lacking the MVA immunosuppressive genes *C6L*, *K7R*, and *A46R* and expressing chikungunya virus (CHIKV) or EBOV antigens have been generated, induced potent antigen-specific B and T cell immune responses in immunized mice and protected against challenge with the corresponding viral pathogen in susceptible mouse models [97,98].

However, MVA still contains several genes with unknown, known or suggested immunomodulatory functions, which could be deleted in order to try to increase the immune responses against the heterologous antigens expressed by the MVA-based vaccine candidates. Among them, the *A40R* gene, encoding a C-lectin membrane protein with an unknown function is of relevant importance to this work.

1.2.2.3.1. VACV *A40R* gene

The VACV *A40R* gene from Western Reserve (WR) strain encoded a type II membrane glycoprotein (A40) that is expressed early during infection and form higher molecular mass complexes under non-reducing conditions [99]. A40 protein is expressed on the cell surface but is not incorporated into intracellular MVs or extracellular EVs [99]. Moreover, although the role of A40 protein is still unknown, it shares amino acid similarity (about 20%) to the complementarity determining region (CDR) domain of C-type animal lectins, such as the rat Clr-b, the NKG2 proteins, CD94 and DC-SIGN [99]. C-type lectins are a group of Ca^{2+}-dependent (C-type) carbohydrate-binding (lectin) proteins that are very important in pathogen recognition and immunity [100]. MVA A40 protein (MVA *152R* gene) is identical to WR A40 protein from amino acid residues 1 to 154, but the last five residues of WR A40 protein are replaced with 14 unrelated residues in the MVA A40 protein.

It has been described that the deletion of *A40R* gene attenuates VACV strain WR, following intradermal inoculation of mice, showing that A40 has a role in virulence [101]. On the other hand, other studies affirmed that A40 is an early protein that is quantitatively sumoylated (a stably and infection-independent addition of a 20-kDa size peptide termed SUMO-1 that is mediated by cellular components) to prevent its own aggregation and allows the sumoylated protein to associate with the viral replication sites [102,103]. The small amount of non-modified A40 protein may play a putative role in the VACV life cycle joining the cytosolic side of the rough endoplasmic reticulum (ER) and inducing the proper apposition of several ER cisternae before they fuse to generate the ER envelope that surround the viral replication sites [103]. However, the role of the sumoylated A40 protein still remains unclear, although it was suggested that it could be involved in the process of replication itself or in the late transcription that is known to occur at VACV

replication sites [103]; in that case VACV *A40R* gene would be essential for VACV life cycle.

1.2.2.4. Optimize the foreign heterologous antigen

Another approach to improve the immunogenicity of MVA-based vaccine candidates is the optimization of the expressed foreign antigen, for example by human codon optimization (a widely used strategy) or by antigen rational design. There are various strategies to optimize the heterologous antigen expression, for example: to insert an N-terminal signal peptide in the transgene in order to increase the antigen expression and secretion [104,105], or to engineer the transgene to produce the heterologous protein in a certain form or conformation, such as being a released form, remaining intracellular, or with an specific ternary or quaternary structure, such as the case of VLPs [98,106–108]. Moreover, in the last few years, a great number of novel optimizations in the HIV-1 envelope (Env) protein have been developed, searching mainly the generation of more native-like Env trimer antigens able to induce higher levels of broadly neutralizing antibodies (bNAbs) against HIV-1 [108–112], and some of these novel HIV-1 Env immunogens have been inserted in MVA vectors with promising results [108–110].

Of particular interest in this Thesis is the HIV-1 and Zika virus (ZIKV) immunogen optimization. On the one hand, in our laboratory, an MVA-based vaccine candidate against HIV/AIDS (termed MVA-B) expressing HIV-1 gp120 (engineered to be produced as a cell-released product) and Gag-Pol-Nef (GPN, as an intracellular polyprotein) antigens from clade B, has been previously generated in order to improve the antibody and T cell immune responses, respectively [113]. Mice immunized with MVA-B have shown good levels of HIV-1-specific T cellular and humoral immune responses [91–93,113,114]. Importantly, MVA-B have shown a good immunological behaviour in prophylactic and therapeutic phase I clinical trials [115–121] reinforcing its use as a promising HIV/AIDS vaccine candidate. On the other hand, in many vaccines against several flavivirus, including ZIKV, the immunogen is optimized by the co-expression of the ZIKV premembrane (prM) and envelope (E) structural proteins in order to form and secrete VLPs. These VLPs resemble the virus structure and are able to elicit excellent immune responses [122–126].

The aim of this doctoral Thesis is the generation of novel optimized MVA-based vaccine candidates by using one or more of the approaches described above to enhance the immunogenicity against two viral pathogens, such as HIV-1 and ZIKV.

1.3. HIV/AIDS

Human immunodeficiency virus (HIV) was discovered as the causal agent of acquired immune deficiency syndrome (AIDS) in 1983 [127]. HIV is a lentivirus that belong to

Retroviridae, a unique family of viruses that uses a reverse transcriptase (RT) enzyme to produce DNA from the positive sense single-stranded RNA (ssRNA) genome that they carry within [128,129]. AIDS is a condition in which progressive failure of the immune system allows life-threatening opportunistic infections and cancers to thrive. In most cases, HIV is transmitted person-to-person by contaminated blood or body fluids. Vertical transmission can also occur from an infected mother to her infant during pregnancy, during childbirth by exposure to her blood or vaginal fluids, and through breast milk.

The HIV virion consists in an enveloped particle of about 100 nm in diameter. The cone-shaped core includes two copies of the positive sense single-stranded RNA genome, the enzymes RT, integrase (IN) and protease (PR), some minor proteins, and the major core protein [130] (Fig. 6a). The HIV genome has 9.2 kbp in length and encodes 15 viral proteins. From the 5'- to 3'-ends of the genome are found the Gag (for group-specific antigen), Pol (for polymerase), and Env (for envelope glycoprotein) genes (Fig. 6b). The Gag gene encodes a polyprotein precursor, Pr55Gag, that is cleaved by the PR to the mature Gag proteins matrix (also known as MA or p17), capsid (CA or p24), nucleocapsid (NC or p7), and p6, a non-structural protein involved in viral assembly and release. Furthermore, two spacer peptides, p1 and p2, are also generated upon Pr55Gag processing. The Pol-encoded enzymes are initially synthesized as part of a large polyprotein precursor, Pr160GagPol, whose synthesis results from a rare frameshifting event during Pr55Gag translation. The individual Pol-encoded enzymes, PR, RT, and IN, are cleaved from the Pr160GagPol precursor by the viral PR. The Env glycoproteins are also synthesized as a polyprotein precursor, gp160, that is processed by the cellular furin protease during Env trafficking to the cell surface, unlike the Gag and Pol precursors, which are cleaved by the viral PR. The gp160 precursor processing results in the generation of the surface Env glycoprotein gp120 and the transmembrane glycoprotein gp41. The gp120 protein contains the determinants that interact with the CD4 receptor and coreceptors in the cell surface, while gp41 anchors the gp120/gp41 complex in the membrane, and contains domains that are critical for catalyzing the membrane fusion reaction between viral and host lipid bilayers during virus entry. In addition to the Gag, Pol, and Env genes, HIV-1 also encodes a number of regulatory and accessory proteins. Tat is critical for transcription from the HIV-1 long terminal repeat (LTR) and Rev plays a major role in the transport of viral RNAs from the nucleus to the cytoplasm. Vpu, Vif, Vpr and Nef have been termed "accessory" or "auxiliary" proteins to reflect the fact that they are not required for virus replication but are needed for correct virion formation [130,131] (Fig. 6).

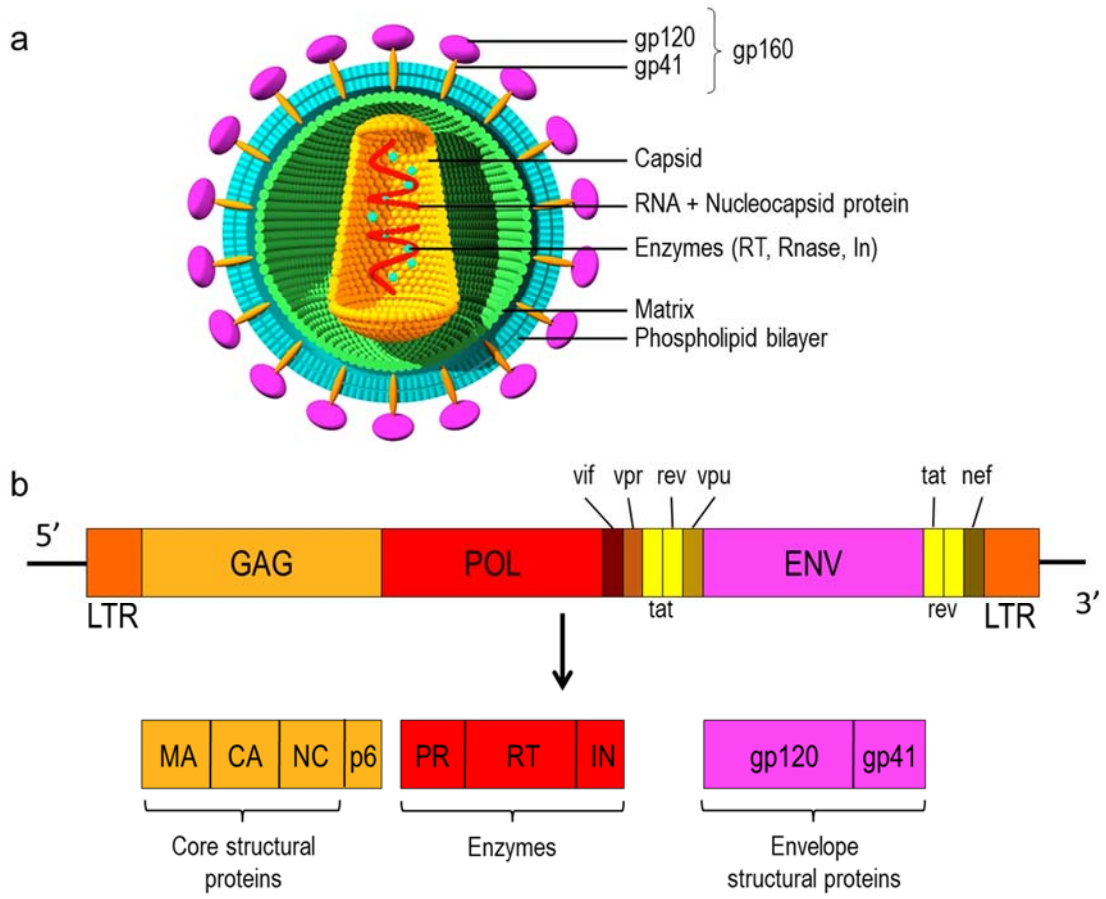

Figure 6. HIV structure and genome organization. (a) Representation of the HIV virion structure, showing the two copies of the positive sense single-stranded RNA genome and the rest of proteins. The size of the virion is about 100 nm. Enveloped structural proteins gp120 and gp41; core structural proteins Capsid, Nucleocapsid and Matrix; Enzymes (RT, RNAse and IN), RNA and phospholipid bilayer are indicated. (b) Scheme of the HIV genome and its processing to render the different viral proteins, including core structural proteins (MA, CA, NC and p6), enzymes (PR, RT and IN), envelope structural proteins (gp120 and gp41), and various regulatory proteins and elements (vif, vpr, tat, rev, vpu and nef). LTR: long terminal repeat. Adapted from www.cronodon.com

HIV is classified into two groups: i) HIV-1, which is responsible for the majority of the widespread AIDS pandemic, and ii) HIV-2, which is the mild or less virulent version confined to specific regions of West Africa. There is only a 40-60% homology at the nucleic acid and amino acid level between HIV-1 and HIV-2, being HIV-2 more closely related to a simian retrovirus, simian immunodeficiency virus (SIV), with which it shares about 75% nucleic acid sequence homology. The HIV-1 virus shows high genetic diversity owing largely to the error-prone RT enzyme, the selective immune pressure from the host and the replication process (including recombination events and the high turnover rate of the virus) [132]. In general, HIV-1 is grouped into three phylogenetic forms: main or "M" (which is responsible for the majority of the infections), outlier or "O" and non-M/O or "N". The M phylogenetic form is further classified into nine subtypes or

clades (A, B, C, D, F, G, H, J and K) and, into different circulating recombinant forms (CRFs) and several unique recombinant forms (URFs), derived from recombination between viruses of different subtypes, [133,134].

1.3.1. HIV/AIDS epidemiology and impact on public health

The AIDS pandemic caused by the HIV-1 has spread worldwide, with high impact and severity in human health, since its first description in 1981. The number of new infections and deaths caused by AIDS are increasing each year, and is particularly dramatic in developing and undeveloped countries. According to United Nations Programme on HIV/AIDS (UNAIDS) in 2017 there were approximately 36.9 million people worldwide living with HIV/AIDS, and it is estimated that 1.8 million persons became newly infected worldwide each year, with about 5,000 new infections per day (1% are children under 15 years). In 2017, 940,000 people died from AIDS-related illnesses worldwide (442 in Spain).

In the last years a great advance in antiretroviral therapy (ART) has been achieved but, in 2017, only 41% of people living with HIV-1 were accessing ART. Without treatment, average survival time after infection with HIV-1 is estimated to be 9 to 11 years, depending on the HIV-1 subtype. HIV-1 diversity impacts virtually every aspect of the HIV/AIDS pandemic, including disease progression and transmission, pathogenesis, vaccine development, immune response and escape and response to ART and drug resistance [130]. The different HIV-1 subtypes and recombinants have also distinct global distribution patterns and among them, clade B is the most disseminated variant, being the causative agent in approximately 11% of all cases of HIV/AIDS worldwide. HIV-1 clade B emerged in Kinshasa (Democratic Republic of Congo, Africa) and was then introduced through the Caribbean into the United States of America (USA), where the incidence of HIV-1 clade B infection increased exponentially in the population. Then, the virus disseminated and became established in other regions, including Europe, Asia, Latin America, and Australia [130].

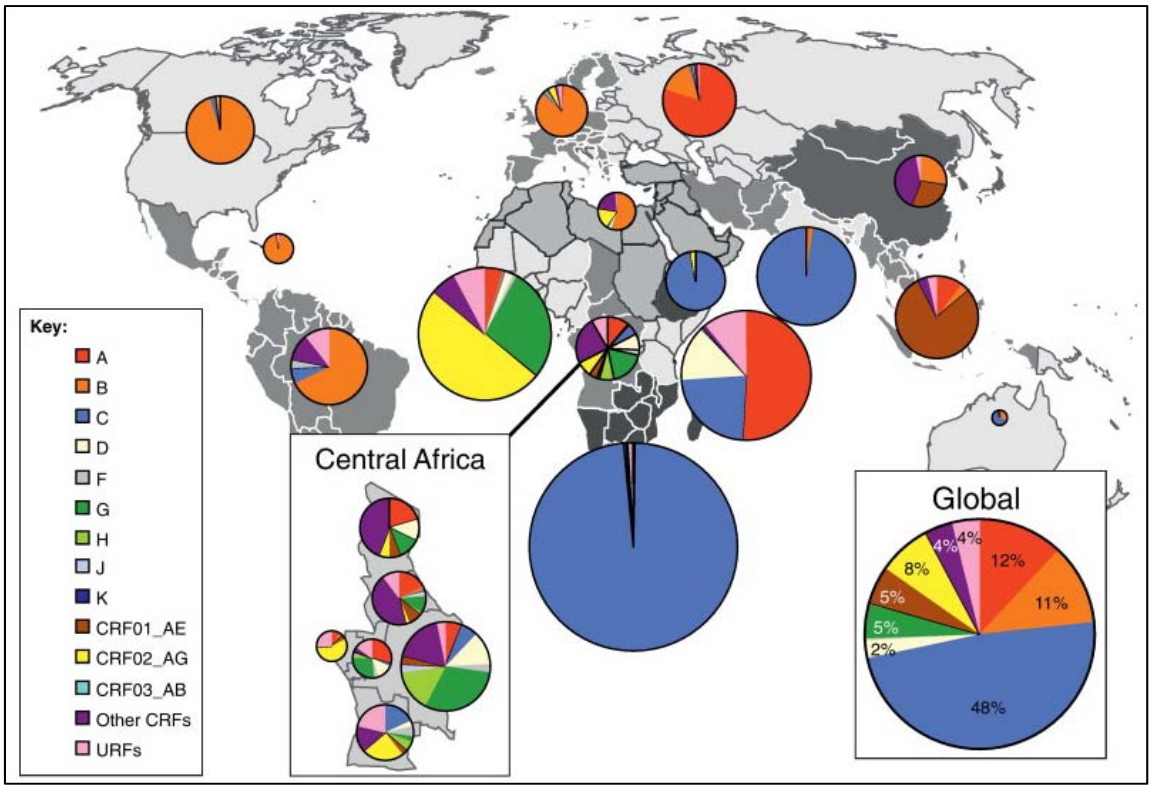

Figure 7. Geographic distribution of HIV-1 subtypes and recombinants. HIV-1 subtypes (A, B, C, D, F, G, H, J, and K), circulating recombinant forms (CRFs) (CRF01_AE, CRF02_AG, CRF03_AB, and other CRFs) and unique recombinant forms (URFs) are represented by a different colour. The size of the pie charts corresponds to the relative number of people living with HIV/AIDS in that particular region. Each pie chart showed the proportion of the different HIV-1 subtypes or viral recombinants circulating in that particular region. HIV-1 clade B represents the 11% of the global infections, and the majority of all the HIV-1 infections in Europe and the Americas. Adapted from [133].

1.3.2. HIV/AIDS vaccine development

While ART (more than 30 antiretroviral drugs are available at this moment) has drastically decreased the number of deaths associated to HIV/AIDS and a containment of global transmission simultaneously with a survival increase in HIV-1-infected individuals is reported [135], an effective vaccine able to prevent HIV-1 infection is a global health priority and the only way to eradicate the disease.

The main facts that make difficult the development of an efficacious vaccine against HIV/AIDS include: the rapid establishment of hard to clear infections, the integration of the HIV-1 genome into the host genome favouring the formation of latent viral reservoirs, the high mutation rate of the viral RT that makes HIV-1 population exist as a collection of closely related viral genomes known as quasispecies, the high diversity and structure of the envelope glycoprotein that limits the ability to elicit bnAbs, and the tropism of the virus for $CD4^+$ T cells facilitating infection, spread, and persistence [136].

Six HIV-1 vaccine efficacy phase IIb or III clinical trials have been conducted until now, targeting the different arms of the immune response, humoral and cellular systems, through distinct approaches (Table 1). However, five of them failed and showed no protection. Only the phase III RV144 “Thai Trial”, using four priming injections of a recombinant canarypox vector vaccine expressing Env from subtypes B/E and Gag/Pro from subtype B (ALVAC-HIV) plus two booster injections of a recombinant glycoprotein 120 subunit vaccine from subtypes B/E (AIDSVAX B/E), reach a modest vaccine efficacy of 31,2% of protection [137]. For the first time an HIV/AIDS showed some degree of protection.

Trial Name	Phase	Year	Participants	Vaccine	Immune Response	Efficacy
AIDSVAX B/E (VAX003)	III	1999-2003	2546	Env gp120 (B/E)	Humoral	Abs. No protection
AIDSVAX B/B (VAX004)	III	1998-2003	5417	Env gp120 (B/B)	Humoral	Abs. No protection
HVTN502 (STEP)	IIb	2004-2007	3000	MRKAd5 Gag-Pol-Nef	Cellular	Stopped T cell pressure
HVTN503 (Phambili)	IIb	2007	801	MRKAd5 Gag-Pol-Nef (B)	Cellular	Stopped T cell pressure
RV144	III	2003-2006	16402	ALVAC-HIV + AIDVAX B/ E rgp120	Cellular + Humoral	31.2% protection
HVTN505	IIb	2009-2017	504	DNA, rAd5 (A, B, C)	Cellular + Humoral	No protection

Table 1. HIV/AIDS human efficacy phase IIb and III clinical trials completed. Ad5 = Human Adenovirus 5; HVTN = HIV Vaccine Trials Network; MRK = Merck; r = recombinant form.

Although modest, the reduced infection risk achieved by the RV144 phase III clinical trial demonstrated the need of inducing both arms of the immune system, humoral and cellular, to obtain an effective vaccine against HIV/AIDS. The overall information obtained from all these trials, supports that vaccine protocols based on just viral vectors or heterologous viral vector prime/protein boost protocols appearing to perform better than multi-dose protein-based vaccines [136,138]. Moreover, the RV144 results highlighted the use of poxvirus vectors as promising HIV/AIDS vaccine candidates. Thus, novel optimized poxvirus-based vaccines against HIV/AIDS are desirable.

1.4. Zika virus

Zika virus (ZIKV) is a mosquito-borne virus from the family *Flaviviridae* and the genus *Flavivirus* [139], closely related with other mosquito-borne viruses with public health importance such as Japanese encephalitis virus (JEV), West Nile virus (WNV), dengue

virus (DENV), and yellow fever virus (YFV). The viral particle has 50 nm in diameter and contains an inner nucleocapsid composed of a linear positive sense, single-stranded RNA genome (of approximately 11 kbp in length) and multiple copies of the viral capsid (C) protein and an outer host cell-derived lipid bilayer bearing 180 copies each of two proteins: the viral membrane (M) protein [a cleavage product of the prM protein) and the E protein [140,141] (Fig. 8). The ORF encodes a large polyprotein of 3,423 amino acids which is cleaved by viral and cellular proteases into 10 individual proteins: three structural proteins located at the N-terminal region that form the infectious virion (C, prM/M, and E), and seven non-structural proteins, located at the C-terminal region, which are involved in viral replication (NS1, NS2A, NS2B, NS3, NS4A, NS4B, and NS5) [140,141] (Fig. 8). ZIKV E protein is the major protein involved in receptor binding and fusion, and data from ZIKV-infected patients indicate that is the main target of the majority of neutralizing Abs [142].

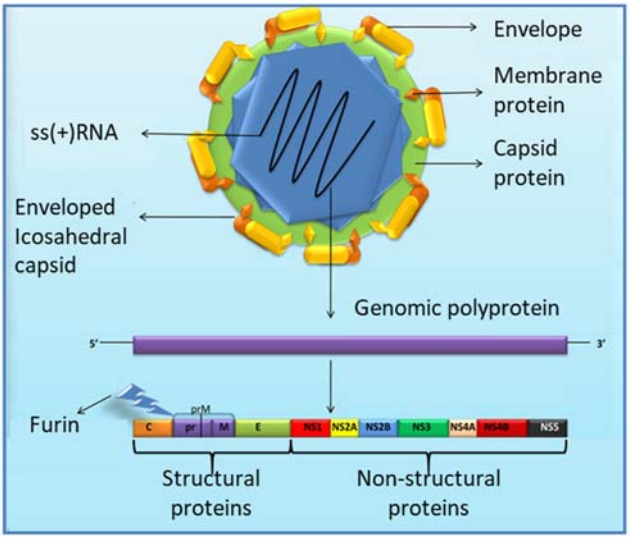

Figure 8. ZIKV structure and genome organization. ZIKV is an enveloped, icosahedral virus whose capsid has around 50 nm in diameter. Virions contain a linear single-stranded positive sense RNA genome [ss(+)RNA] inside an inner nucleocapsid formed by the capsid protein. The envelope, membrane protein and capsid protein are also indicated. Below the virion, the genomic polyprotein and its processing is represented. The ss(+)RNA encodes a large polyprotein that is cleaved by viral and cellular proteases into 10 individual proteins: three structural proteins, located at the N-terminal region, that form the infectious virion (C, prM/M, and E), and seven non-structural proteins, located at the C-terminal region, that are involved in viral replication (NS1, NS2A, NS2B, NS3, NS4A, NS4B, and NS5). Adapted from [143].

1.4.1. ZIKV epidemiology and impact on public health

ZIKV is transmitted to humans primarily through the bite of infected mosquitoes from genus *Aedes*, mainly by *A. albopictus* and *A. aegypti*, both widely distributed throughout the tropical and subtropical regions of the world, with the habitat of *A. albopictus* extending further into cool temperate regions [140,141]. Furthermore, ZIKV can also be

transmitted from mother to child during pregnancy or spread through sexual contact, breastfeeding, or blood transfusion [140,141]. The multiple modes of ZIKV transmission make it difficult to develop control strategies against the pathogen.

ZIKV was discovered in Uganda in 1947, but was confined for the first 60 years to an equatorial zone across Africa and Asia [140,141]. However, in 2007 a ZIKV outbreak emerged in Yap Island, in the Western Pacific Ocean, and between 2013-2014 a second larger outbreak spread eastward to French Polynesia and other Pacific Islands. Finally the virus reached Latin America in 2015, and disseminated further to North America in 2016, with 500,000–1,500,000 suspected cases of ZIKV infection reported in the Americas, and more than 4,300 cases of microcephaly [144]. As a consequence, the WHO declared the Public Health Emergency of International Concern from 1 February to 18 November 2016. Actually, ZIKV is circulating in the Americas, Southeast Asia, and the Pacific Islands, and represents a potential pandemic threat [140,141] (Fig. 9). In addition, since early 2015, there have been an increasing number of travel-related imported ZIKV cases in non-endemic countries and it is predicted that a large portion of the tropical and sub-tropical regions of the globe will have suitable environmental conditions for ZIKV mosquito transmission. Thus, there is currently a high risk of introducing and establishing new autochthonous transmission in these areas [140,141].

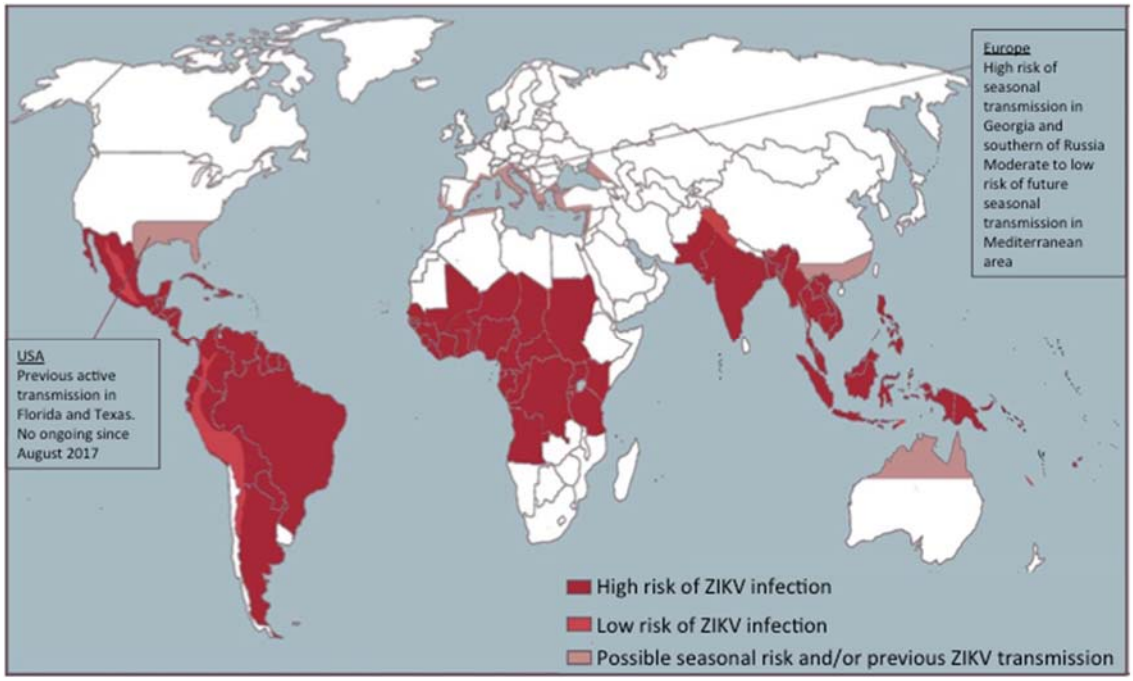

Figure 9. Map of high- and low-risk areas for ZIKV infection. The risk areas for ZIKV infection and transmission are shown in different colours. ZIKV has spread to 84 countries in the Americas, Africa and Asia. South and Southeast Asia and Oceania are at high risk for future outbreaks and, despite the decreasing trend of ZIKV infection in the Americas, seasonal transmission comprises a possible threat in southern parts of North America and also in China and Europe. Adapted from [145].

In most cases ZIKV infection causes no symptoms or only a mild self-limiting illness, but recent epidemiological studies derived from outbreaks in 2007 and 2015-2016 linked ZIKV infection to a rising number of concerning severe neurological diseases, including Guillain-Barré syndrome (GBS) and microcephaly in neonates that were exposed *in utero* [140,141]. In addition, it is now accepted that a wide range of severe congenital conditions (such as brain calcifications, arthrogryposis, ophthalmologic alterations, spinal deformities, among others) are develop as a result of *in utero* ZIKV exposure [146,147].

Until this moment, there are no antiviral treatments available to control ZIKV infection. However, a great labor has been made to search for antiviral candidates. Different strategies and methodologies have been used, from testing specific compounds with known antiviral activity in other virus models, to libraries composed of hundreds of bioactive molecules (many of them already approved for human), and several molecules targeting viral and cellular components (including nucleoside analogues, nucleoside synthesis inhibitors, drugs targeting viral enzymes, anticancer and anti-inflammatory molecules, antibiotics, antiparasitics, among others) have been tested [148], but none of them have been approved for use in ZIKV infection until now.

1.4.2. ZIKV vaccine development

The development of a safe and efficacious vaccine against ZIKV is critical given the rapid dissemination of the virus and the severe neurological and teratogenic sequelae associated with ZIKV infection [140]. The success previously obtained using vaccines against related flaviviruses such as JEV, YFV, and tick-borne encephalitis (TBEV), have demonstrated that recombinant vaccines expressing the viral E protein were able to induce antibody responses that correlate with complete protection [149,150]. Thus, following a similar design, in recent years several vaccine candidates against ZIKV have been developed, and some of them entered in phase I or II clinical trials [151,152]. However, there are no approved vaccines to prevent ZIKV infection. These vaccine candidates include various technologies and approaches, such as inactivated ZIKV, recombinant viral vectors, DNA plasmid vaccines, mRNA-based vaccines, and peptide-based vaccines; with most of them based on the whole inactivated organism or in vectored expression of prM and E structural proteins, as occurred with other flaviviral vaccines [151,152].

OBJECTIVES

2. OBJECTIVES

Due to the relevance of the poxvirus vector MVA as a vaccine candidate against several infectious diseases, there is a major interest in the optimization of this vector to achieve the most effective control of pathogens. Thus, the objectives of the Thesis are aimed at the immunological optimization of MVA-based vaccine candidates against HIV/AIDS by enhancing VACV promoter strength and by deleting immunosuppressive MVA genes. Additionally, these modifications were applied to a novel optimized MVA vector to generate a vaccine against ZIKV with the aim to demonstrate whether efficacy was obtained after challenge with ZIKV in a mouse model of disease.

The specific objectives are:

1) Generate and characterize the immunogenicity of a novel MVA vector containing an optimized stronger VACV promoter that controls the expression of a model antigen, HIV-1 gp120 protein.

2) Improve the immunogenicity of the HIV/AIDS vaccine candidate MVA-B by deleting the MVA *A40R* gene and define the immunomodulatory role of the A40 protein.

3) Develop a novel optimized MVA-based vaccine candidate against ZIKV (MVA-ZIKV) expressing the structural prM and E proteins and producing virus-like particles. Define the immunogenicity and efficacy of MVA-ZIKV in immunized mice.

MATERIALS AND METHODS

3. MATERIALS AND METHODS

3.1. Materials

3.1.1. Cell lines

The following cell lines have been used in this work:

- CEF: Primary chicken embryo fibroblast cells obtained from pathogen-free 11-day-old eggs (MSD, Salamanca, Spain).
- DF-1: Spontaneously immortalized CEF cell line (ATCC® CCRL-12203™).
- HeLa: Immortalized human epithelial cervix adenocarcinoma cells (ATCC® CCL-2™).
- Vero cells: Kidney epithelial cell line from African green monkey (ATCC® CCCL-81™).
- THP-1: Human monocytic cell line (ATCC® TIB-202™).

3.1.2. Culture media

CEF, DF-1 and HeLa cells were grown in Dulbecco´s modified Eagle medium (DMEM, Gibco) supplemented with non-essential amino acids (0.1 mM, Sigma-Aldrich), L-Glutamine (2 mM, Merck), streptomycin (100 µg/ml, Sigma-Aldrich), penicillin (100 U/ml, Sigma-Aldrich), fungizone (0.5 µg/ml, Gibco), gentamycin (0.05 µg/ml, Sigma-Aldrich) and 10% of heat-inactivated fetal calf serum (FCS, Gibco) for CEF and DF-1 cells or 10% newborn calf serum (NCS, Sigma-Aldrich) for HeLa cells. For virus infections DMEM-2% FCS or DMEM-2% NCS was used after the virus adsorption.

Vero cells were grown in Eagle's minimal essential medium (EMEM) and 5% heat-inactivated fetal bovine serum (FBS, Linus), as previously described [153].

THP-1 cells were grown in Roswell Park Memorial Institute (RPMI-1640, Gibco) medium supplemented with HEPES pH 7.4 (10 mM, Merck), β-mercaptoethanol (10 µM, Sigma-Aldrich), L-glutamine (2 mM, Merck) and 10% FCS.

DMEM-Hi glucose medium (Sigma-Aldrich), supplemented with 4500 mg/l glucose and sodium bicarbonate, and without L-glutamine and sodium pyruvate was used for virus infections where proteins in the supernatant were quantified.

All the cells were maintained at 37ºC in a humidified air atmosphere with 5% carbon dioxide (CO_2) and 95% humidity.

3.1.3. Bacteria

Escherichia coli bacterial strains DH5α (CNB) or DH10β (New England Biolabs) were used for bacterial transformations, in the generation of clones during the construction of recombinant plasmid DNAs. In all these cases, the media used for growing the bacteria was Luria-Bertani (LB) containing 1% bacto-tryptone (BD Biosciences), 1% NaCl

(Sigma-Aldrich) and 0.5% yeast extract (BD Biosciences) at pH 7 [154], in the presence of 100 µg/ml of the selection antibiotic ampicillin (Roche).

3.1.4. Oligonucleotides

The following oligonucleotides have been used in this work:

Oligonucleotide	Sequence (5´→ 3´)	Template
Oligonucleotides used for check mycoplasma contamination		
Myc A (F)	GGCGAATGGGTGAGTAACACG	Mycoplasma genome
Myc B (R)	CGGATAACGCTGCGACCTATG	Mycoplasma genome
Oligonucleotides used for amplify and/or sequence the MVA genome		
TK-L (F)	TGATTAGTTTGATGCGATTC	TK left flank
TK-R (R)	TGTCCTTGATACGGCAG	TK right flank
HA-2 (F)	GATCCGCATCATCGGTGG	HA left flank
HA-MVA (R)	TGACACGATTACCAATAC	HA right flank
Oligonucleotides used for generation of plasmid pGem-RG-ΔA40R and characterization of MVA-B ΔA40R		
LFA40R-AatII-F	ACGTTTGACGTCATAGAAAAATATAA	*A40R* left flank
LFA40R-XbaI-R	TACACCGCACGACAATGAACAAACAT	*A40R* left flank
LF'A40R-EcoRI-F	ACGTTTGAAGTCATAGAAAAATATAA	*A40R* left flank
LFA40R-ClaI-R	TACACCGCACGACAATGAACAAACAT	*A40R* left flank
RFA40R-ClaI-F	AGAAAAAATAAATATCGCGTACCG	*A40R* right flank
RFA40R-BamHI-R	CCATGAGGATCCAGTAAAATTAACAG	*A40R* right flank
Oligonucleotides used for generation of plasmid pHA-A40R and characterization of MVA-B ΔA40R-rev		
LFA40R-XmaI-F	TCCCCCCGGGATGAACAAACATAAGAC	*A40R* gene right flank
RFA40R-SacII-R	AGGCCGCGGTTATTTTTTTCTAAAACACTC	*A40R* gene right flank
Oligonucleotides used for MVA-LEO160-gp120 characterization		
$gp120_{BX08}$-F	ATGGACCGCGCCAAGCTGCTGCTG	$HIV\text{-}1_{BX08}$ gp120 (Env)
$gp120_{BX08}$-R	TCAGCGCTTCTCGCGCTGCACCACCCTCCT	$HIV\text{-}1_{BX08}$ gp120 (Env)
$gp120_{BX08}$-intF1	ACAGCAGCAGCGGCAAGGAG	$HIV\text{-}1_{BX08}$ gp120 (Env)
$gp120_{BX08}$-intR1	GCCCACCTCCTGCCACATGTTGAT	$HIV\text{-}1_{BX08}$ gp120 (Env)
$gp120_{BX08}$-intR2	GCAGCAGCAGCAGCAGCAGC	$HIV\text{-}1_{BX08}$ gp120 (Env)
$gp120_{BX08}$-intR4	TGTCGTAGGCCTTGGCGTCGG	$HIV\text{-}1_{BX08}$ gp120 (Env)
Oligonucleotides used for MVA-ZIKV characterization		
ZIKV-F	GCTAGCGCCACCATG	ZIKV insert (prM-E)
ZIKV-R	CAGGATCATTTAAATAGATCTATGCATTCAGGCGGACACGGCGGTGC	ZIKV insert (prM-E)

ZIKV-F (new)	GAGCTAGCTCGAGTTTAAACTGCAGGT CGACGCCACCATGGGAGCCGATAC	ZIKV insert (prM-E)
ZIKV-R (new)	CAGGATCATTTAAATAGATCTATGCATT CAGGCGGACACGGCGGTGC	ZIKV insert (prM-E)
ZIKV-intF1	GTCCTACAGCCTGTGTACCGCCGC	ZIKV insert (prM-E)
ZIKV-intR1	ACGGCCATCTGAGCTG	ZIKV insert (prM-E)
ZIKV-intR2	TGGTGGGAAGCTGATGGCCTCGCCGG	ZIKV insert (prM-E)
Oligonucleotides used for quantitative Real-Time RT-PCR		
$gp120_{BX08}$ sense	GGCGAGTTCTTCTACTGCAAC	HIV-1_{BX08} gp120 (Env)
$gp120_{BX08}$ antisense	CCTCGCTGTTGGTCTCGT	HIV-1_{BX08} gp120 (Env)
ZIKV sense	AARTACACATACCARAACAAAGTGGT	ZIKV NS5
ZIKV antisense	TCCRCTCCCYCTYTGGTCTTG	ZIKV NS5
E3L sense	CGGAGCTGTACACCATAGCA	VACV *E3L*
E3L antisense	TATTGACGAGCGTTCTGACG	VACV *E3L*
chGAPDH sense	ATCAAGAGGGTAGTGAAGGCTGCT	Chicken GAPDH
chGAPDH antisense	TCAAAGGTGGAGGAATGGCTGTCA	Chicken GAPDH
HPRT sense	GAACGTCTTGCTCGAGATGTG	Human HPRT
HPRT antisense	CCAGCAGGTCAGCAAAGAATT	Human HPRT
IFNβ sense	GATTCATCTAGCACTGGCTGG	Human IFNβ
IFNβ antisense	CTTCAGGTAATGCAGAATCC	Human IFNβ
IFIT1 sense	TTGCCTGGATGTATTACCAC	Human IFIT1
IFIT1 antisense	GCTTCTTGCAAATGTTCTCC	Human IFIT1
IFIT2 sense	ACAAGGCCATCCACCACTTTAT	Human IFIT2
IFIT2 antisense	CCCAGCAATTCAGGTGTTAACA	Human IFIT2
MDA-5 sense	GTGCATGGAGGAGGAACTGT	Human MDA-5 (IFIH1)
MDA-5 antisense	GTTATTCTCCATGCCCCAGA	Human MDA-5 (IFIH1)
TNFα sense	CACCACTTCGAAACCTGGGA	Human TNFα
TNFα antisense	CACTTCACTGTGCAGGCCAC	Human TNFα
MIP-1α sense	TGGTCAGTCCTTTCTTGG	Human MIP-1α (CCL3)
MIP-1α antisense	GCAGAGGAGGACAGCAAG	Human MIP-1α (CCL3)
RANTES sense	CGCTGTCATCCTCATTGCTA	Human RANTES (CCL5)
RANTES antisense	GCACTTGCCACTGGTGTAGA	Human RANTES (CCL5)
RIG-I sense	AGGAAAACTGGCCCAAAACT	Human RIG-I (DDX58)
RIG-I antisense	TTTCCCCTTTTGTCCTTGTG	Human RIG-I (DDX58)

Table 2. Oligonucleotides used in the present work. F=Forward, R=Reverse. Y = T or C, R = A or G. GAPDH=Glyceraldehyde-3-phosphate dehydrogenase gene. HPRT=Hypoxanthine phosphoribosyl transferase gene. IFNβ=Interferon beta gene. IFIT1=Interferon induced protein with tetratricopeptide repeats-1 gene. IFIT2=Interferon induced protein with tetratricopeptide repeats-2 gene. MDA-5 (IFIH1)=Melanoma differentiation-associated protein-5 gene (Interferon induced with helicase C domain-1). TNFα=Tumour necrosis factor alpha gene. MIP-1α (CCL3)=Macrophage inflammatory

protein-1 alpha gene (Chemokine C-motif ligand-3). RANTES (CCL5)=Regulated upon activation normal T cell expressed and secreted (Chemokine C-motif ligand-5). RIG-I (DDX58)=Retinoic acid inducible gene-I (DEAD box helicase-58).

3.1.5. Antibodies

The antibodies used in this work are described in the table below:

Antibody	Characteristics	Source
Primary Antibodies		
Rabbit α WR	Polyclonal, against proteins from the VACV WR strain	CNB
Rabbit α E3	Polyclonal, against VACV E3 protein	CNB
Rabbit α β-actin	Monoclonal, against cellular β-actin	Cell Signaling
Rabbit α gp120	Polyclonal, against HIV-1 gp120 protein	CNB
Rabbit α gag p24	Polyclonal, against HIV-1 p24 protein	CNB
Mouse α E	Monoclonal, against ZIKV envelope protein	BioFront Tech
Rabbit α prM	Polyclonal, against ZIKV prM protein	GeneTex
Rabbit α Calnexin	Polyclonal, against cellular calnexin	Enzo Life Sciences
Secondary Antibodies		
Goat α Rabbit-HRP	Polyclonal, against rabbit IgG, conjugated with horseradish peroxidase (HRP)	Sigma-Aldrich
Goat α Mouse-HRP	Polyclonal, against mouse IgG, conjugated with horseradish peroxidase (HRP)	Sigma-Aldrich
Goat α Human-HRP	Polyclonal, against human IgG, conjugated with horseradish peroxidase (HRP)	Sigma-Aldrich
Conjugated Antibodies (Immunofluorescence)		
Goat α Rabbit-Alexa 488	Polyclonal, against rabbit IgG, conjugated with Alexa Fluor® 488	ThermoFisher
Goat α Rabbit-Alexa 594	Polyclonal, against rabbit IgG, conjugated with Alexa Fluor® 594	ThermoFisher
Goat α Mouse-Alexa 488	Polyclonal, against mouse IgG, conjugated with Alexa Fluor® 488	ThermoFisher
Conjugated Antibodies (Flow Cytometry)		
Rat α Mouse CD107a-FITC	Monoclonal, against mouse CD107a conjugated with FITC (Fluorescein), Clone 1D4B	BD Biosciences
Hamster α Mouse CD3e-PE-CF594	Monoclonal, against mouse CD3e conjugated with PE-CF594, Clone 145-2C11	BD Biosciences
Rat α Mouse CD4-PECy7	Monoclonal, against mouse CD4 conjugated with PECy7, Clone RM4-5	BD Biosciences
Rat α Mouse CD8a-V500	Monoclonal, against mouse CD8a, conjugated with V500, Clone 53-6.7	BD Biosciences
Rat α Mouse CD127-PerCPCy5.5	Monoclonal, against mouse CD127 conjugated with PerCPCyanine5.5, Clone A7R34	eBioscience

Rat α Mouse CD62L-Alexa700	Monoclonal, against mouse CD62L conjugated with Alexa Fluor 700, Clone MEL-14	BD Biosciences
Rat α Mouse CD4-APC-Cy7	Monoclonal, against mouse CD4, conjugated with APC-Cy7, Clone GK1.5	BD Biosciences
Rat α Mouse IL-2-APC	Monoclonal, against mouse IL-2, conjugated with APC, Clone JES6-5H4	BD Biosciences
Rat α Mouse IFNγ-PECy7	Monoclonal, against mouse IFNγ, conjugated with PECy7, Clone XMG1.2	BD Biosciences
Rat α Mouse TNFα-PE	Monoclonal, against mouse TNFα, conjugated with PE, Clone MP6-XT22	eBioscience
Rat α Mouse CD4-Alexa700	Monoclonal, against mouse CD4, conjugated with Alexa Fluor700, Clone RM4-5	BD Biosciences
Rat α Mouse CD44-PECy5	Monoclonal, against mouse CD44, conjugated with PECy5, Clone IM7	BioLegend
Armenian Hamster α Mouse CD154(CD40L)-Biotin	Monoclonal, against mouse CD154(CD40L), conjugated with Biotin, Clone MR1	BD Biosciences
Mouse α Biotin-FITC	Monoclonal, against Biotin (Avidin, conjugated with FITC), Clone SB58c	Southern Biotech
Rat α Mouse CXCR5-PE-CF594	Monoclonal, against mouse CXCR5, conjugated with PE-CF594, Clone 2G8	BD Biosciences
Rat α Mouse IL-4-Alexa Fluor 488	Monoclonal, against mouse IL-4, conjugated with Alexa Fluor 488, Clone 11B11	BD Biosciences
Rat α Mouse IL-21-APC	Monoclonal, against mouse IL-21, conjugated with APC, Clone FFA21	eBioscience
Armenian Hamster α Mouse PD1(CD279)-APC-eFluor780	Monoclonal, against mouse CD279 (PD1), conjugated with APC-eFluor780, Clone J43	eBioscience
Rat α Mouse CD16/CD32 (Fc block)	Monoclonal, against mouse CD16/CD32,Clone 2.46	BD Biosciences

Table 3. Antibodies used in the present work. α= anti.

3.1.6. Peptides and proteins

3.1.6.1. Peptides

Different peptide pools were used in the ICS assays:

- HIV-1 peptide pools, with each purified peptide at 1 mg/ml per vial, were provided by BEI Resources (National Institute of Allergy and Infectious Disease, National Institutes of Health, USA). The peptides covered the Env, Gag, Pol, and Nef proteins present in the consensus sequence of HIV-1 clade B as consecutive 15-mers overlapping by 11 amino acids. The HIV-1_{BX08} gp120 protein was spanned by the Env-1 (60 peptides) and Env-2 (61 peptides) pools. The HIV-1_{IIIB}GPN fusion protein was spanned by the following pools: Gag-1 (55 peptides), Gag-2 (50 peptides), GPN-1 (56 peptides), GPN-2 (56 peptides), GPN-3 (56 peptides) and GPN-4 (56 peptides). For immunological analysis we grouped the peptides in three main pools: Env, Gag and GPN. The Env-pool

comprises Env-1 + Env-2; Gag-pool comprises Gag-1 + Gag-2; and GPN-pool comprises GPN-1 + GPN-2 + GPN-3 + GPN-4.

- A ZIKV envelope (E) peptide pool of the ZIKV PRVABC59 strain (GenPept: AMZ03556), with each purified peptide at 1 mg/ml per vial, was obtained through BEI Resources (National Institute of Allergy and Infectious Disease, National Institutes of Health, USA). The peptides spanned the entire ZIKV E protein as consecutive 15-mers overlapping by 12 amino acids. The ZIKV-E pool comprises ZIKV-E1 (54 peptides), ZIKV-E2 (55 peptides) and ZIKV-E3 (55 peptides).

3.1.6.2. Proteins

The HIV-1 gp120 envelope protein from isolate Bx08 (750µg/µl, CNB) was used for Enzyme Linked Immunosorbent Assays (ELISAs)..

3.1.7. Plasmids

3.1.7.1. Plasmid transfer vectors used for the generation of MVA recombinant viruses

Plasmid transfer vectors were used for the insertion of a heterologous sequence or the deletion of a VACV gene in the MVA genome. Cells were first infected with the parental MVA virus and then transfected with these plasmids. After that, the recombinant MVA viruses were selected after consecutive plaque purification steps.

3.1.7.1.1. Plasmid transfer vector used for the deletion of MVA *A40R* gene in the MVA-B genome: pGem-RG-ΔA40R wm

The plasmid transfer vector pGem-RG-ΔA40R wm contains: the right flanking region of the MVA *A40R* gene*,* the gene for dsRed2 fluorescent marker, the left flanking region of the MVA *A40R* gene*,* the gene for red-shifted green fluorescent protein (rsGFP) fluorescent marker, another left flanking region of the MVA *A40R* gene*,* and the ampicillin gene used for the bacterial selection (Fig. 10). It was used for the generation of the MVA-B ΔA40R deletion mutant by homologous recombination between the flanking regions of the MVA *A40R* gene during the infection/transfection process. The letters “wm” stand for “without markers”, indicating that the final recombinant virus lacks the markers used for its selection, dsRed2 and rsGFP. The plasmid transfer vector pGem-RG-ΔA40R wm was obtained by sequential cloning of MVA *A40R* flanking sequences into plasmid pGem-Red2-GFP wm (termed pGem-RG wm) (4,540 bp), whose generation was previously described [92]. The MVA-B genome was used as the template to amplify by PCR the left flank of the *A40R* gene (352 bp) with oligonucleotides LFA40R-AatII-F and LFA40R-XbaI-R (containing *AatII* and *XbaI* restriction sites, respectively) (see Table 2). The left flank was digested with *AatII* and *XbaI* and cloned into plasmid pGem-RG wm, which

had previously been digested with the same restriction enzymes, to generate plasmid pGem-RG-LFsA40R wm (4,859 bp). Then, the repeated left flank of the *A40R* gene (352 bp) was amplified by PCR from the MVA-B genome with oligonucleotides LF′A40R-EcoRI-F and LF′A40R-ClaI-R (containing *EcoRI* and *ClaI* restriction sites, respectively) (see Table 2), digested with *EcoRI* and *ClaI*, and inserted into *EcoRI*/*ClaI*-digested pGem-RG-LFsA40R wm to generate plasmid pGem-RG-LFdA40R wm (5,170 bp). Finally, the right flank of the *A40R* gene (372 bp) was amplified by PCR from the MVA-B genome with oligonucleotides RFA40R-ClaI-F and RFA40R-BamHI-R (containing *ClaI* and *BamHI* restriction sites, respectively) (see Table 2), digested with *ClaI* and *BamHI*, and inserted into *ClaI*/*BamHI*-digested pGem-RG-LFdA40R wm plasmid. The resulting plasmid transfer vector generated was termed pGem-RG-A40R wm (5,512 bp), and its correct construction was confirmed by DNA sequence analysis.

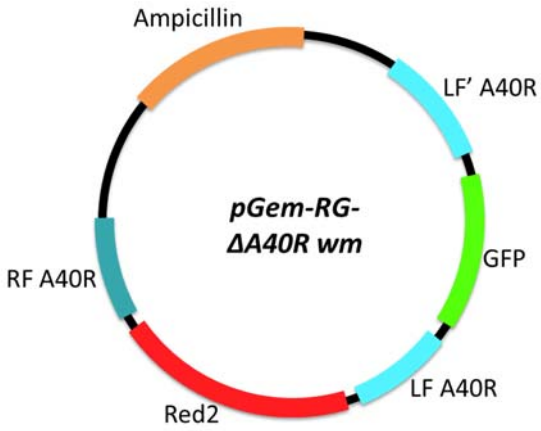

Figure 10. Scheme of pGem-RG-ΔA40R wm plasmid transfer vector. Contains: the right flanking region of the MVA *A40R* gene (RF A40R), the dsRed2 fluorescent marker gene (Red2), the left flanking region of the MVA *A40R* gene (LF A40R), the rsGFP fluorescent marker gene (GFP), another left flanking region of the MVA *A40R* gene (LF'A40R), and the ampicillin gene used for the bacterial selection.

3.1.7.1.2. Plasmid transfer vectors used for the insertion of heterologous DNA in the MVA backbone

These plasmid transfer vectors contains: the left flanking region of the MVA thymidine kinase (TK) or hemagglutinin (HA) genes, the β-galactosidase (β-gal) or β-glucuronidase (β-gus) genes (as selectable markers), the repeated left flanking region of the MVA TK or HA genes, the corresponding heterologous sequence under the control of a synthetic VACV promoter and cloned into a multiple cloning site (MCS), the right flanking region of the MVA TK or HA genes and the ampicillin gene used for the bacterial selection. The plasmid transfer vector used for the insertion of heterologous antigens in the MVA TK locus is termed pCyA, and its generation was previously described [155], and the plasmid

transfer vector used for the insertion of heterologous antigens in the MVA HA locus is termed pHA, and its generation was previously described [98] (Fig. 11).

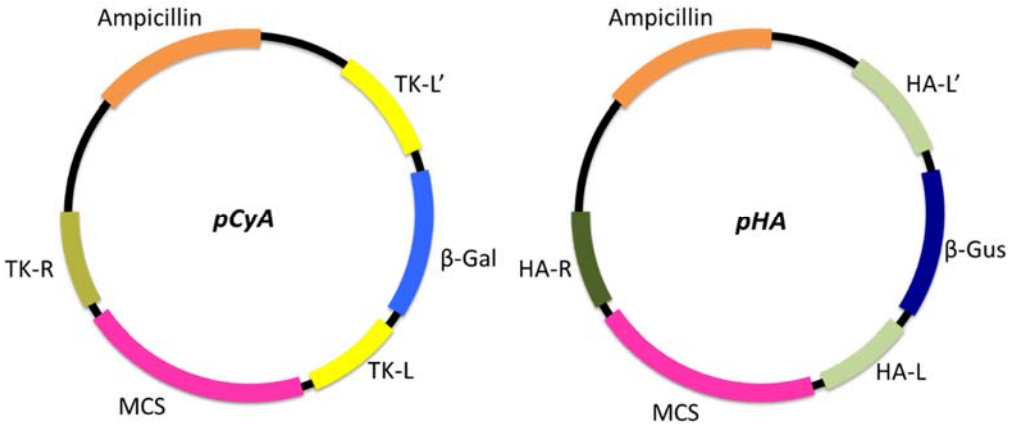

Figure 11. Scheme of the MVA insertional plasmids. Contains: the left flanking region of the MVA TK (TK-L) or HA (HA-L) genes, the β-gal or β-gus genes (as selectable markers), the repeated left flank of the MVA TK or HA genes, the multiple cloning site (MCS), the right flank of the MVA TK or HA genes, and the ampicillin gene used for the bacterial selection.

The plasmid transfer vectors constructed in this work to insert heterologous sequences in the MVA genome are:

- **pLZAW1-LEO160-gp120:** Used to generate the MVA-LEO160-gp120 recombinant virus. Directs the insertion of the HIV-1 gp120 sequence (clade B, isolate Bx08, GenBank accession number: GQ855765.1), under the control of the novel synthetic VACV LEO160 promoter into the TK locus of MVA. Obtained by inserting the HIV-1_{BX08} gp120 sequence into the pLZAW1-LEO160 plasmid [88] that contains the novel synthetic VACV LEO160 promoter by using GeneArt Subcloning and Plasmid Services (ThermoFischer Scientific). Contains the HIV-1_{BX08} gp120 sequence under the control of the novel synthetic VACV LEO160 promoter introduced in a MCS between the MVA TK-L and TK-R flanking regions, and the selectable marker genes for ampicillin and β-gal. The β-gal gene (LacZ) is inserted among two repetitions of the left TK flanking region, allowing their deletion from the final recombinant virus by homologous recombination after consecutive plaque purification steps. The resulting plasmid pLZAW1-LEO160-gp120 (9,217 bp) was confirmed by DNA sequence analysis.
- **pHA-A40R:** Used for the insertion of the MVA *A40R* gene into the VACV HA locus of the MVA-B ΔA40R recombinant virus to generate the MVA-B ΔA40R-rev revertant virus. To construct the plasmid transfer vector pHA-A40R (7,126 bp), the MVA *A40R* gene (526 bp) was amplified by PCR from the MVA-B genome with oligonucleotides

LFA40R-XmaI-F and RFA40R-SacII-R (containing *XmaI* and *SacII* restriction sites, respectively) (see Table 2), digested with *XmaI* and *SacII* restriction enzymes, and then inserted into the *XmaI*/*SacII*-digested pHA plasmid (6,600 bp) [98]. Thus, pHA-A40R contains the MVA *A40R* gene under the control of the viral sE/L promoter introduced in an MCS between the MVA HA-L and HA-R flanking regions, and the selectable marker genes for ampicillin and β-gus. The β-gus gene is inserted among two repetitions of the left HA flanking region, allowing their deletion from the final recombinant virus by homologous recombination after consecutive plaque purification steps. The resulting plasmid pHA-A40R was confirmed by DNA sequence analysis.

- **pLEOLZ-ZIKV:** Used to generate the MVA-ZIKV recombinant virus. Directs the insertion of the ZIKV cassette under the control of the novel synthetic VACV LEO160 promoter into the TK locus of MVA ΔC6L/K7R/A46R-GFP. Initially, the ZIKV cassette comprising the ZIKV precursor membrane (prM) and envelope (E) structural genes, preceded by the last 18 amino acids of the C-terminal hydrophobic stretch of the C protein (that acts as a signal peptide for the proper translocation of the prM protein into the lumen of the ER) (isolate Z1106033, GenBank accession number: KU312312) was chemically synthesized and codon optimized for human cell expression and then was subcloning into the pCyA plasmid transfer vector [155] by GeneArt Subcloning and Plasmid Services (ThermoFischer Scientific), to generate the plasmid transfer vector termed pCyA-ZIKV. Then, pLEOLZ-ZIKV plasmid was obtained by amplifying the ZIKV cassette from the pCyA-ZIKV plasmid with oligonucleotides ZIKV-F (new) and ZIKV-R (new) (see Table 2) and subcloning it into the pLEOLZ plasmid, previously digested with *PstI* and *BglII* restriction enzymes, using the Gibson Assembly method [156]. The plasmid transfer vector pLEOLZ was obtained substituting the VACV E/L promoter presented in the pCyA plasmid for the LEO160 promoter [88] by using GeneArt Subcloning and Plasmid Services (ThermoFischer Scientific). The resulting plasmid pLEOLZ-ZIKV (9,657 bp) was confirmed by DNA sequence analysis.

3.1.7.2. Plasmids used for vaccination

The various plasmid DNAs used for vaccination are:

- **pcDNA3.0(+) (Invitrogen):** Mammalian expression vector used as such for vaccination and also for the insertion of heterologous antigens described below. The plasmid contains an MCS after the cytomegalovirus (CMV) promoter and an ampicillin resistance gene for selection.

- **pCMV (Invitrogen):** Mammalian expression vector used as such for vaccination and also for the insertion of heterologous antigens described below. The plasmid contains a MCS after the CMV promoter and a kanamycin resistance gene for selection.
- **pCMV-gp120$_{BX08}$:** Plasmid expressing the HIV-1gp120$_{BX08}$ protein. Kindly provided by Sanofi-Pasteur. Used for prime vaccination in heterologous prime/boost protocols.
- **pCMV-GPN$_{IIIB}$:** Plasmid expressing the GPN$_{IIIB}$ polyprotein. Previously described in [113]. Used for prime vaccination in heterologous prime/boost protocols.

3.1.8. Viruses

3.1.8.1. MVA viruses

VACV used in this work are based on the parental highly attenuated MVA strain and are detailed as follows:

- **MVA-WT:** Attenuated MVA wild-type (WT) strain, kindly provided by Dr. G. Sutter (University of Munich, Germany). It was obtained from the CVA strain after 586 serial passages in CEF cells [46], and was used as the parental virus for the generation of several recombinant MVA vectors and as a vector control in mice immunization protocols.
- **MVA-B:** MVA containing the HIV-1 gp120 antigen (clade B, isolate Bx08) and the GPN polyprotein (clade B, isolate IIIB) inserted into the TK locus [113].
- **MVA-GFP:** MVA recombinant virus containing the GFP gene into the TK locus [88]. Used as parental virus for the generation of MVA-LEO160-gp120.
- **MVA ΔC6L/K7R/A46R-GFP:** MVA recombinant virus containing the GFP gene into the TK locus and lacking the immunomodulatory VACV genes *C6L*, *K7R*, and *A46R* [97]. Used as parental virus for the generation of MVA-ZIKV.
- **MVA-B ΔA40R:** MVA containing the HIV-1 gp120 antigen (clade B, isolate Bx08) and the GPN polyprotein (clade B, isolate IIIB) inserted into the TK locus and lacking the MVA *A40R* gene. MVA-B ΔA40R was generated using MVA-B as parental virus and pGem-RG-A40R wm as the plasmid transfer vector employing an infection/transfection protocol (see section 3.2.4.2).
- **MVA-B ΔA40R-rev:** MVA-B ΔA40R containing the MVA *A40R* gene inserted into the HA locus. MVA-B ΔA40R-rev was generated using MVA-B ΔA40R as parental virus and pHA-A40R as the plasmid transfer vector employing an infection/transfection protocol (see section 3.2.4.2).
- **MVA-LEO160-gp120:** MVA containing the HIV-1 gp120 antigen (clade B, isolate Bx08) inserted into the TK locus and placed under the control of the synthetic VACV LEO160 promoter. MVA-LEO160-gp120 was generated using MVA-GFP as parental

virus and pLEO160-gp120 as the plasmid transfer vector employing an infection/transfection protocol (see section 3.2.4.2).

- **MVA-ZIKV:** MVA containing the ZIKV prM and E structural genes preceded by a signal peptide (isolate Z1106033, derived from an Asian lineage virus, isolated from a patient in Suriname at the onset of the late-2015 expansion of the virus in the Americas; GenBank accession number: KU312312) [157],. The ZIKV genes were inserted into the TK locus and the parental MVA contains deletions in the immunomodulatory VACV genes *C6L*, *K7R*, and *A46R* [97]. MVA-ZIKV was constructed using MVA ΔC6L/K7R/A46R-GFP as parental virus and pLEOLZ-ZIKV as a plasmid transfer vector employing an infection/transfection protocol.

3.1.8.2. ZIKV viruses

ZIKV PA259459 strain was used for the MVA-ZIKV challenge study. ZIKV PA259459 and ZIKV FSS13025 strains were used for performing the plaque reduction neutralization (PRNT) assays. Both ZIKV strains were isolated from an infected human in Panama in 2015 and in Cambodia in 2010, respectively. Both ZIKV strains were propagated using Vero cells and titrated in semisolid agarose medium, as previously described [158].

3.1.9. Animals/mice

Female Balb/cOlaHsd mice (6 to 8 weeks old) used for immunogenicity assays were purchased from Envigo Laboratories and stored in the animal facility of the CNB (Madrid, Spain). The immunogenicity animal studies were approved by the Ethical Committee of Animal Experimentation (CEEA) of the CNB (Madrid, Spain) and by the Division of Animal Protection of the Comunidad de Madrid (PROEX 331/14) and were conducted at the CNB.

IFNAR$^{-/-}$ mice (6 weeks old) used for the ZIKV efficacy assay were kindly provided by Javier Ortego, Centro de Investigación en Sanidad Animal (CISA)- Instituto Nacional de Investigación y Tecnología Agraria y Alimentaria (INIA). The efficacy animal study was approved by the CEEA of Instituto Nacional de Investigación y Tecnología Agraria y Alimentaria (INIA, Madrid, Spain) and by the Division of Animal Protection of the Comunidad de Madrid (PROEX 187/17) and were conducted in the biosafety level 3 laboratory at CISA-INIA (Madrid, Spain).

All animal procedures were conformed to international guidelines and to the Spanish law under the Royal Decree (RD 53/2013). Animals were maintained and handled according to the recommendations of the CNB-CSIC and CISA-INIA institutional Ethics Committees.

3.1.10. Buffers

The following buffers have been used in the present work:

- PBS 1X: NaCl 137 mM, KCl 2.7 mM, Na_2PO_4 8 mM and KH_2PO_4 1.5 mM.

- PBS staining: PBS 1X, BSA 0.5%, FCS 1%, sodium azide 0.0065% and EDTA 2 mM.

- IB Buffer: PBS 1X, FCS 2% and EDTA 2mM

- Protein loading buffer (Laemmli 1X): Tris-HCl 50 mM pH 6.8, Sodium dodecyl sulfate (SDS) 2%, β-mercaptoethanol 5%, glycerol 10% and bromophenol blue 0.012%.

- DNA loading buffer: Xylene-cyanol 0.25%, glycerol 30% and bromophenol blue 0.25%.

- Electrophoresis buffer for Sodium dodecyl sulfate polyacrylamide gel Electrophoresis (SDS-PAGE): Tris 25 mM, glycine 192 mM and SDS 0.1%.

- Transfer buffer for SDS-PAGE: Tris 25 mM, glycine 192 mM and methanol 20%, pH 8.3.

- TBE: Tris-Borate 90 mM pH 8.3 and EDTA 2 mM.

- Proteinase K buffer: Tris-HCl 50 mM pH 8.0, EDTA 100 mM, NaCl 100 mM and SDS 1%.

3.2. Methods

3.2.1. RNA manipulation techniques

Total RNA was isolated using the RNeasy Kit (Qiagen GmbH, Hilden, Germany), according to the manufacturer's recommendations. RNA and DNA concentrations were measured using a NanoDrop® ND-1000 full-spectrum spectrophotometer (Thermo Scientific).

Reverse transcription of up to 1000 ng of RNA to cDNA was performed with the QuantiTect reverse transcription Kit (Qiagen GmbH, Hilden, Germany), according to the manufacturer's recommendations.

3.2.1.1. Quantitative real-time RT-PCR

Up to 20 ng of cDNA template and 0.6 mM of the corresponding oligonucleotides in 10 µl of RNase water were mixed with the same volume of Power SYBR green PCR Master Mix (ThermoFisher Scientific), following manufacturer's recommendations. Quantitative PCR protocol, performed with a 7500 Real-Time PCR system (Applied Biosystems), consisted of two initial steps of 2 min at 50°C and 10 min at 95°C, followed by 40 cycles of 15 seconds at 95°C and 1 min at 60°C. Specific gene expression was represented relative to the expression of the cellular HPRT gene and/or the VACV *E3L* gene in arbitrary units (A.U.) using the $2^{-\Delta\Delta Ct}$ method [159]

3.2.2. DNA manipulation techniques

3.2.2.1. PCR

DNA amplification using PCR was carried out for the molecular cloning of genes of interest into a plasmid backbone or to check the insertion/deletion of genes in the MVA backbone. In all cases, about 10-50 ng of template DNA was used along with 0.4 mM of the corresponding oligonucleotides, 1–2.5 units of Phusion® High Fidelity polymerase (NewEngland Biolabs) with its corresponding buffer and 0.2 mM of each of the four deoxyribose nucleoside triphosphates (dNTPs) (Roche Diagnostics GmbH). Annealing temperature and extension time varied depending on the reaction conditions (melting temperature of the oligonucleotides and length of the target fragment, respectively). The reactions were carried out in a VeritiTM 96-well thermocycler (Applied Biosystems).

3.2.2.2. DNA detection

DNA fragments were mixed with SYBR Safe 1% (Conda), as binding dye, loaded in 1% agarose gel, separated though electrophoresis and, finally, detected using a GEL Doc 2000 UV Transilluminator System (Bio-Rad).

3.2.2.3. Cloning DNA fragments into a plasmid vector

Cloning of inserts into plasmid vectors to generate pGem-RG-ΔA40R wm and pHA-A40R plasmid transfer vectors were carried out using standard molecular cloning procedures described in [154].

Gibson Assembly Master Mix (New England Biolabs) protocol was used, according to manufacturer´s instructions, for pLEOLZ-ZIKV plasmid construction.

In the case of pLAZW1-LEO160-gp120, pLEOLZ and pCyA-ZIKV, cloning processes were performed by GeneArt Subcloning and Plasmid Services (Thermo Fisher Scientific).

3.2.2.4. DNA purification

Purification of DNA fragments amplified by PCR or extracted from agarose gels was carried out using the Wizard genomic DNA purification Kit (Promega) following manufacturer´s instructions.

Plasmid DNA purification during the molecular cloning process was performed using the standard alkaline lysis protocols [154] from 2 ml of cultures of positive bacterial clones. Larger quantities of purified plasmid DNA (for use in transfections and generation of other plasmid vectors through molecular cloning) were obtained using the Plasmid Maxi Kit (Qiagen) following manufacturer´s protocol. Plasmid DNAs used in *in vivo* experiments were purified using the Endofree Plasmid Mega Kit (Qiagen) following manufacturer´s instructions.

Purification of genomic DNA from infected cells was performed as follows: when infected cells exhibited extensive cytopathic effect, the monolayer was recovered and centrifuged (3000 rpm for 5 min) and the pellet was stored at -20ºC until use. For DNA extraction, the pellet was thawed, resuspended in Tris-HCl 50 mM pH 8.0 and 200 µg/ml of Proteinase K (Roche) was added in its corresponding buffer, followed by 1 hour (h) of incubation at 55ºC. Next, 40 µg/ml of RNase A (PanReac AppliChem) was added and incubated at 37ºC for 30 min. Then, saturated NaCl was added, the mixture was centrifuged (13,000 rpm for 10 min at 4ºC), the supernatant was collected and mixed with isopropanol (1:0.7 v/v ratio) and centrifuged (10,000 rpm for 10 min at room temperature, RT). The precipitated DNA was allowed to dry and was then resuspended in 30 µl of sterile distilled H_2O. The concentration of the purified DNA was measured using NanoDrop (Thermo Scientific, USA). The DNA thus obtained was used to check for the correct insertion/deletion of the gene of interest using PCR and sequencing.

3.2.3. Protein manipulation techniques

3.2.3.1. Electrophoresis and Western blotting

Protein samples from cell extracts were analyzed using one dimensional electrophoresis on polyacrylamide gels in the presence of SDS according to the standard protocols described previously [154]. The percentage of acrylamide in the gels varied according to the molecular weight of the proteins of interest. The samples were prepared with loading buffers (Laemmli 1X-β-mercaptoethanol) and denatured at 95ºC for 10 min prior to loading. The manufacturer´s protocol from Mini Trans-Blot® Cell (Bio-Rad) was followed for the transfer of protein samples from the electrophoretic gels to nitrocellulose membranes (GE Healthcare). The nitrocellulose membrane and filter papers (Whattman-3MM®) were moistened in transfer buffer and mounted in the transfer system with the nitrocellulose membrane. The transfer was carried out at 200-400 mA during 50 min. The successful transfer was verified using Ponceau staining (0.2% Ponceau in 3% TCA; Sigma-Aldrich). The nitrocellulose membrane was then blocked in 5% skimmed milk solution prepared in PBS-1X-0.05% Tween20 (Sigma-Aldrich) (PBS-T) at RT for 1 h with subtle agitation. The corresponding primary antibodies, prepared at the desire dilution in the blocking buffer, were used for overnight incubation of the membrane at 4ºC. Following four washes with PBS-T, the membrane was incubated with the proper secondary antibody (appropriate dilutions were prepared in the same blocking buffer) for 60 min at RT and later washed four times with PBS-T. The membranes were revealed using the ECL western blotting detection reagent (Amersham) according to the manufacturer´s instructions and detected in a ChemiDoc™ Imaging System (Bio-Rad).

3.2.3.2. Protein quantification by Enzyme Linked Immunosorbent Assay (ELISA)

To quantify the protein secreted to supernatants from infected cells, 100 mm diameter culture dishes (Falcon) of HeLa cells were infected with MVA recombinant viruses and incubated with 12 ml of DMEM-Hi glucose medium (Sigma-Aldrich) for different periods of time at 37ºC. Then, supernatants were centrifuged at 1500 rpm for 5 min to clarify them and concentrated using Amicon® Ultra-15 Centrifugal Filters (Millipore). Next, 96-well plates (NUNC MaxiSorp™, Thermo Fisher Scientific) were coated with concentrated supernatants and, at the same time, with serial dilutions (in PBS) of the purified protein of interest at known concentrations in order to have a standard curve. Plates were incubated at 4ºC overnight and, the next day, blocked for 1 h with 5% skimmed milk prepared in PBS-T, following by three washes with PBS-T. Next, an appropriate dilution of the antibody of interest was prepared in PBS-T and added to the protein coated plates for 90 min at RT. Then, the plates were washed three times again with PBS-T and 1/1000 dilution of the corresponding secondary antibody was added to the wells and incubated for 1 h at RT. Finally, after another washing step, the plates were developed by adding 100 µl of 3,3',5,5' Tetramethylbenzidine (TMB) substrate (Sigma-Aldrich) and the reaction was stopped by adding 50 µl of 1 M H_2SO_4. The absorbance was read at 450 nm.

3.2.3.3. Confocal immunofluorescence

Microscope cover glasses of 12 mm diameter (Marienfield) were put in 24-well plates and then HeLa cells were seeded. Next day, infections were performed at 0,5 PFU/ml for 18-24 h in cells grown at 80% confluency. Cell membranes and Golgi were labeled using Wheat Germ Agglutinin (WGA) probe (conjugated to the red fluorescent dye Alexa Fluor® 555) (ThermoFisher) for 20 min at 37ºC. Then, cells were fixed with 4% paraformaldehyde for 15 min at RT and incubated for 15 min at RT with NH_4Cl 0.05 M in order to quench fluorescence. Next, the plates were washed twice with PBS and cells were blocked with PBS-10% FCS or blocked and permeabilized with PBS-0.05% saponin-10% FCS for 30-60 min at RT. The corresponding primary antibodies (see section 3.1.5) were incubated in PBS-5% FCS (non-permeabilized samples) or in PBS-0.05% saponin-5% FCS (permeabilized samples) for 2 h or 24 h at 4ºC. Then, cells were washed twice with PBS and blocked again before incubation with the corresponding secondary antibodies (see section 3.1.5) for 1 h at RT. After three washes with PBS, 4′,6′-diamidino-2-phenylindole (DAPI) (Sigma-Aldrich) was used for 15 min at RT to stain the cell nuclei. Following three more washes with PBS plus one wash with distilled water, cover glasses were mounted in 76x26mm microscope slides (Menzel-Glaser) using

ProLong™ Gold Antifade Mountant (ThermoFisher). Images of sections of the cells were taken with a Leica TCS SP5 microscope and processed using LAS X Core software (Leica Microsystems) with the assistance of Silvia Gutiérrez and Ana Oña from the CNB Confocal Immunofluorescence Service.

3.2.3.4. Virus-like particles (VLPs) purification

Supernatants obtained from cells infected with MVA-ZIKV were collected and concentrated by ultracentrifugation through a 20% sucrose (Merck) cushion at 25,000 rpm for 2 h at 4ºC in a Beckmann SW28 rotor. Then, the pellet was resuspended in 1 ml of PBS 1X and loaded into a 20–60% w/v sucrose gradient and ultracentrifuged at 35,000 rpm for 18 h at 4ºC in a Beckmann SW41 rotor. Fractions of 500 µl were taken and the amount of protein and sucrose density was analysed by refractometry. The fraction with higher amount of protein was then dialysed through a 0.025-µm-pore-size membrane filter (Merck Millipore) for 12 h at RT to eliminate sucrose and inorganic salts.

3.2.3.5. Electron microscopy

Electron microscopy of ZIKV VLP samples obtained as indicated in section 3.2.3.4 was performed with the assistance of Cristina Patiño from the CNB Electron Microscopy Service. Briefly, 20 µl of the purified VLP sample was adsorbed to carbon-coated collodion films mounted on 400-mesh/inch nickel grids (Aname) and then stained with 2% uranyl acetate (Aname) for 30 s at RT. For immunogold technique, after the adsorption, grids were incubated with the primary antibody, M α ZIKV E (BioFront Tech, diluted 1:20 in PBS-1%BSA) for 15 min at RT, and then washed four times with PBS1x for 2 min. After blocking with PBS-1%BSA for 5 min, grids were incubated with an anti-IgG secondary antibody coupled to 10-nm colloidal gold beads (GAM Au 10 nm, BBInternational; diluted 1:40 in PBS-1%BSA) for 15 min at RT. Finally, grids were washed 5 times with PBS1x for 1 min and 3 times in distilled water for 1 min before being stained with 2% uranyl acetate (Aname) for 30 s at RT. Pictures were taken using a transmission electron microscope (JEOL JEM-1011) equipped with an ES1000W Erlangshen charge-coupled-device (CCD) camera (Gatan Inc.) at an acceleration voltage of 40 to 100 kV.

3.2.4. Viral protocols

3.2.4.1. Infections

All the viruses were stocked at -80ºC and thawed in a 37ºC bath before their use. Once thawed, the viruses were vortexed, sonicated (three cycles of 10 second sonication with a 10 s pause using the S-3000-010 Misonix Sonicator (Misonix Inc) and vortexed again before use them to infect cells. The proper multiplicity of infection (MOI) of virus

was then mixed with the minimum volume of DMEM (without serum) and added to cover the cell monolayer. After 1 h of adsorption at 37ºC the inoculum was removed and fresh DMEM-2%FCS medium with was added. The time that the different infections were maintained varied with the objective of the infection, an also did the way the cells were harvested.

3.2.4.2. Generation of MVA recombinant viruses

To generate the MVA recombinant viruses an standardized infection/transfection protocol was performed [160], with some modifications. DF-1 cells grown to 70-80% confluency in a 60-mm plate (Nunc) were infected at 0.01 PFU/cell with the MVA parental virus. At the mean time a DNA-Lipofectamine 2000 (ThermoFisher) mixture was made by mixing up to 10 µg of the corresponding plasmid transfer vector with the proper volume (1.5 µl/µg DNA) of lipofectamine 2000 reagent (Invitrogen) in OPTIMEM (Gibco) during 20 min at RT. After 1 h of virus adsorption, the inoculum was removed, the cells were washed twice with OPTIMEM and incubated with 1 ml of the mixture DNA-lipofectamine for 4-6 h at 37ºC with 5% CO_2. Then, the mix was removed, cells were washed twice with OPTIMEM and then were incubated with DMEM-2% FCS at 37ºC with 5% CO_2. The cells were harvested when extensive cytopathic effect was observed, centrifuged (1500 rpm for 5 min), resuspended in 500 µl of DMEM and lysed using three freeze-thaw cycles. The viral extract obtained was sonicated before use, as described previously. Next, DF-1 cells grown in 6-well plates (Nunc) were infected for 1 h with serial dilutions of this virus extract and then 3 ml of 1:1 agar (1.4%)-DMEM 2X-4% FCS was added and incubated at 37ºC with 5% CO_2. In the cases of plasmid transfer vectors containing β-Gal [161,162] or β-Gus as selectable markers [161,162], at 48 hours post-infection (h.p.i) 1.2 mg/ml of 5-bromo-4-chloro-3-indolyl-β-D-galactopyranoside (X-Gal, Sigma-Aldrich) or 0.8 mg/ml of 5-bromo-4-chloro-3-indolyl-beta-D-glucuronic acid (β-Gus, Sigma-Aldrich) in 1 ml of agar (1.4%)-DMEM 2X-4%FCS (1:1) were added. After 24 h, those plaques that corresponded to the MVA recombinant viruses became blue and were picked and resuspended in 500 µl of DMEM. The process of blue plaque selection was repeated three times followed by three more rounds of selection of plaques without colour, corresponding to those viruses that have lost the selection marker gene (Fig. 12a).

On the other hand, in the case of the plasmid transfer vectors containing dsRed2 (red) and rsGFP (green) fluorescent markers, red/green or green fluorescent plaques were first picked (corresponding to the recombinant viruses) resuspended in 500 µl of DMEM and used as inoculum for further rounds of purification in DF-1 cells. The purification process of red/green plaque selection was repeated twice, followed by two more rounds

of green plaque selection, and two rounds of selection of plaques without colour (Fig. 12b).

Finally, in both cases, the isolated MVA recombinant viruses obtained were used to generate the first intermediate stock (referred to as “P1 stock”) that was then successive scale up to generate the master seed virus or working stock (referred to as “P2 stock”).

On the other hand, in the case of the plasmid transfer vector with dsRed2 (red) and rsGFP (green) fluorescent markers, red/green or green fluorescent plaques corresponding to the recombinant viruses were picked, resuspended in 0.5 ml of DMEM and used as inoculum for further rounds of purification in DF-1 cells. The purification process of red/green plaque selection was repeated twice followed by two more rounds of green plaque selection and two of plaques without colour (Fig. 11b).

Finally, in both cases, the isolated recombinant viruses obtained were used to generate the first intermediate stock (referred to as “P1 stock”) that was then successive scale up to generate the master seed virus or working stock (referred to as “P2 stock”).

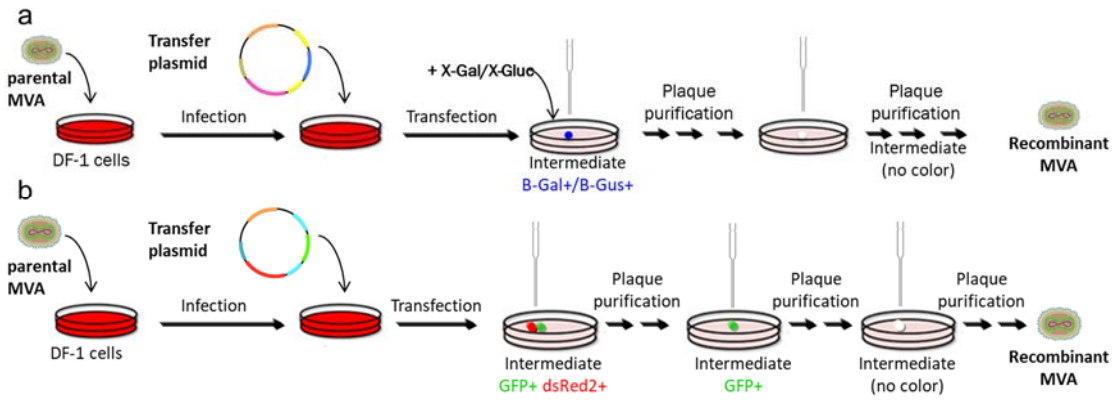

Figure 12. Generation of MVA recombinant viruses. (a) Using a plasmid transfer vector containing β-gal (LacZ) or β-gus genes as selectable markers. After infection/transfection in DF-1 cells, three rounds of plaque purification were performed selecting blue plaques (β-gal$^+$ or β-gus$^+$), followed by another three rounds selecting plaques without colour (no marker) to finally generate the MVA recombinant virus. **(b)** Using a plasmid transfer vector with dsRed2 and rsGFP as selectable markers. After infection/transfection in DF-1 cells, two rounds of plaque purification were performed selecting red/green plaques (dsRed2$^+$, GFP$^+$), followed by two rounds selecting green plaques (GFP$^+$), and two rounds selecting plaques without colour (no marker) to finally generate the MVA recombinant virus.

3.2.4.3. MVA characterization

Biological characterization of MVA recombinant viruses was carried out *in vitro* using the P2 stock and is detailed as follows:

- The correct insertion/deletion of the corresponding genes in the resulting MVA recombinant viruses and their purity was checked by PCR and DNA sequencing, while the correct expression of the corresponding heterologous antigens was confirmed by using Western blotting.

- Virus titrations were carried out according to standard protocols previously described [163]. Briefly, 6-well plates of DF-1 cells were infected with serial dilutions of the virus. At 30-40 h.p.i., the medium was removed and the cells were fixed using 1:1 methanol-acetone mixture and the titer was determined using an immunostaining assay. Plates were incubated with rabbit anti-VACV polyclonal antibody (diluted 1:1,000 in PBS-3% FCS) during 1 h at RT; then washed three times with PBS 1X and incubated for 1 h at RT with goat anti-rabbit HRP-conjugated secondary antibody (diluted 1:1,000 in PBS-3% FCS). After one additional wash with PBS 1X, the plates were revealed using 3,3′-diaminobenzidine tetrahydrochloride (DAB; Sigma-Aldrich), as HRP substrate, with hydrogen peroxide (30%, Sigma-Aldrich) and nickel sulphate ($NiSO_4$, 3%, Sigma-Aldrich). The plaques were counted and the viral titer was referred as PFU/ml (Fig.13).

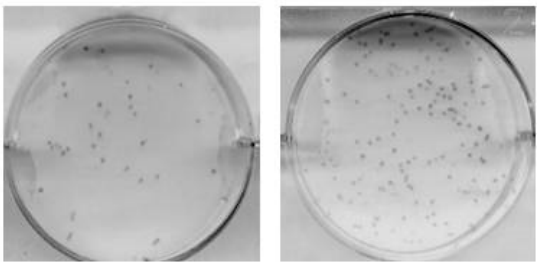

Figure 13. Immunostaining titration of MVA in DF-1 cells. DF-1 cells were infected with serial dilutions of MVA. After 30-40 h.p.i. cells were fixed and an immunostaining assay was performed using anti-VACV polyclonal antibody (diluted 1:1,000) as primary antibody, and goat anti-rabbit HRP-conjugated (diluted 1:1,000) as secondary antibody. The plates were revealed using 3,3′-diaminobenzidine tetrahydrochloride (DAB) as HRP substrate, with hydrogen peroxide (30%) and nickel sulphate ($NiSO_4$). The plaques (dark dots) were counted and the viral titer expressed as PFU/ml.

- To study the virus growth profile, DF-1 cells were seeded on 12-well plates and then infected at 0.01 PFU/cell with the corresponding viruses for 1 h at 37ºC, following which the inoculum was removed and DMEM-2% FCS was added. At various h.p.i. (0, 24, 48, 72 and 96 h.p.i.), the infected cells were recovered and lysed through three freeze-thaw cycles and sonication. The infectious virus was determined using the titration techniques described above.

3.2.4.4. Virus purification

Purification of recombinant MVA viruses through sucrose (Merk) gradient was carried out using previously described methods [164–166]. Briefly, CEF cells were infected at 0.01 PFU/cell with the corresponding viruses. When cytopathic effect was achieved, cells were harvested, centrifuged (2,000 rpm for 10 min at 4ºC) and the pellet was washed once with PBS 1X and resuspended in Tris-HCl 10 mM pH 9.0. Next, two cycles of sonication/centrifugation (three 10 second pulses/1,800 rpm for 5 min) were performed. The supernatant from each cycle was centrifuged (20,000 rpm for 60 min at 4ºC, in SW28

rotor (Beckman) over a 36% sucrose cushion in 10 mM Tris-HCl pH 9.0. The pellet obtained was recovered and centrifuged over another sucrose cushion under the same conditions. The purified virus was resuspended in 10 mM Tris-HCl pH 9.0 and was titrated and checked for contamination (bacteria in LB agar plate, fungi in blood agar plate and mycoplasma through PCR), and stored in small aliquots at -80ºC until further use.

3.2.4.5. ZIKV viral titer measurement

ZIKV viral titers present in serum samples from immunized mice were determined on Vero cells grown in EMEM-5% FBS. Serum samples were serially 10-fold diluted and 200 µl were added on Vero cell monolayers grown in 24-well plates. After 4 h of virus adsorption at 37°C, cells were overlaid with 3,2% of carboxymethylcellulose medium containing 10% FBS and incubated at 37°C for 7 days. Then, cells were stained with 1% amido black staining solution (Sigma-Aldrich), dried at RT and the plaques were counted.

On the other hand, ZIKV RNA was automatically extracted from serum samples using QIAmp® Viral RNA Mini Kit (Qiagen) and a QIAcube apparatus (Qiagen). The amount of viral RNA was determined by real-time fluorogenic RT-PCR in a Rotorgene 3000 equipment (Corbett Research) using the High Scriptolls-Quantimix Easy probes kit (Biotools) and a primer set (ZIKV sense and ZIKV antisense, see Table 2) and probe (6-carboxyfluorescein-CTYAGACCAGCTGAAR-Black Berry Quencher) specific for ZIKV [167]. Genomic equivalents to PFU/ml were calculated by comparison with 10-fold serial dilutions of ZIKV RNA extracted from previously titrated samples. The amount of ZIKV infectious particles in serum samples from infected mice was also determined by titration of 10-fold dilutions of serum samples in Vero cells grown in semisolid agarose medium.

3.2.5. Immunizations and immunological methods

3.2.5.1. Animal/mouse immunizations

Two different immunization protocols were carried out in order to assay the immunogenicity or efficacy of the different vaccine candidates: i) homologous prime/boost regimen, that involved the injection 1 or 2 x 10^7 PFU of MVA virus per mouse given via intra-peritoneal; and ii) heterologous prime/boost regimen, that involved the injection of 100 µg of DNA per mouse given via intra-muscular route and 1 or 2 x 10^7 PFU of MVA virus per mouse given via intra-peritoneal. All inoculum preparations were made in endotoxin-free PBS (Gibco). At the end of each immunization study, the corresponding animals were sacrificed using CO_2. The following samples were extracted from the animals to analyze the antigen-specific immune responses:

- **Blood.** Peripheral blood was extracted directly from the heart, or alternatively from cheek bleeding, of the mice, incubated 1 h at 37ºC and stocked overnight at 4ºC. Then, to obtain the serum, coagulated whole blood samples were centrifuged at 3,600 rpm for 20 min at 4ºC.
- **Spleen.** Once extracted from mice, spleens were homogenized mashing them through 40 µm cell strainers (Falcon) and then, red blood cells were lysed with NH_4Cl 0.1M. Pelleted cells, after removing fat tissue, were final passed through a Falcon® 40 µm pore size cell strainer to obtain a uniform single-cell suspension.
- **Popliteal draining lymph nodes.** Once extracted from mice, lymph nodes were homogenized and passed through a Falcon® 40 µm pore size cell strainer to obtain a uniform single-cell suspension.

3.2.5.2. Intracellular cytokine staining (ICS)

- **Analysis of antigen-specific T cell responses**

Antigen-specific T cell responses were analyzed by flow cytometry and ICS using previously described protocols [90,91,93,97]. Briefly, $4x10^6$ splenocytes were stimulated with 5 µg/ml of specific (HIV-1 or ZIKV) peptides (see section 3.1.6.1.) along with 1 µl/ml GolgiPlug (BD Biosciences), anti-CD107a-FITC (BD Biosciences, diluted 1/300), Protein Transport Inhibitor BD GolgiPlug (BFA, 1X; BD Biosciences) and monensin (1X; eBioscience), using RPMI-10% FCS for 6 h at 37ºC in a 96-well plate. Next, live cells were stained for cellular viability using the LIVE/DEAD Fixable Violet Dead Cell Stain Kit (ThermoFisher) for 20 min at 4ºC. Then, after being washed twice with IB buffer, cells were stained for the surface markers using 50 µl of the corresponding antibodies CD3-PE-CF594, CD4-APC-Cy7, CD8-V500, CD127-PerCPCy5.5 and CD62L-Alexa700 diluted following manufacturer's instructions for 20 min at 4ºC. After being washed again two times with IB buffer, splenocytes were fixed and permeabilized with BD Cytofix/Cytoperm™ solution Kit (BD Biosciences) for 20 min at 4ºC and rested overnight in IB buffer. The day after, cells were washed with Permwash 1X (BD Biosciences) and the Fc receptors were blocked with 25 µl of anti CD16/CD32 (FcBlock) antibody diluted 1:1000 in Permwash 1X for 5 min at 4ºC. Finally, the cells were stained intracellularly for cytokines using 25 µl of intracellular antibodies IFN-γ-PE-Cy7, IL-2-APC and TNF-α-PE (diluted following manufacturer's instructions) for 20 min at 4ºC and washed then twice in IB buffer after loaded them in 200 µl of IB buffer after being passed through a GALLIOS flow cytometer (Beckman Coulter). Data analysis was carried out using FlowJo software (Tree Star. Inc).

- **Analysis of T follicular helper (Tfh) responses**

For the analysis of Tfh response, 1-4x10^6 splenocytes were stimulated with 5 µg/ml of Env peptide pools and/or 0.5 µg/ml of Env gp120 protein along with 1 µl/ml GolgiPlug (BD Biosciences), anti-CD154(CD40L)-Biotin/Avidin-PE, BFA (1X; BD Biosciences) and monensin (1X; eBioscience), using RPMI 1640 media (10% FCS) for 6 h in a 96-well plate at 37ºC. Next, live cells were stained using Fixable Viability Stain (FVS) 520 (BD Biosciences) for 20 min at 4ºC and then. Then, after being washed twice with IB buffer, cells were stained for the surface markers using 50 µl of the corresponding antibodies CD4-Alexa 700, PD1(CD279)-APC-Efluor780 and CD8-V500 diluted following manufacturer's instructions for 20 min at 4ºC. After being washed again two times with IB buffer, splenocytes were fixed and permeabilized with BD Cytofix/Cytoperm™ solution Kit (BD Biosciences) for 20 min at 4ºC and rested overnight in IB buffer. The day after, cells were washed with Permwash 1X (BD Biosciences) and the Fc receptors were blocked with 25 µl of anti CD16/CD32 (FcBlock) antibody diluted 1:1000 in Permwash 1X for 5 min at 4ºC. Finally, the cells were stained intracellularly for cytokines using 25 µl of intracellular antibodies IL-4-FITC, IFNγ-PECy7 and IL-21-APC (diluted following manufacturer's instructions) for 20 min at 4ºC and washed then twice in IB buffer after loaded them in 200 µl of IB buffer after being passed through a GALLIOS flow cytometer (Beckman Coulter). Data analysis was carried out using FlowJo software (Tree Star. Inc).

3.2.5.3. Antibody measurement by ELISA

To analyze the antibody levels in the serum of immunized animals, ELISA assays were performed. 96-well plates (NUNC MaxiSorp™, Thermo Fisher Scientific) were coated with 2 µg/ml of the corresponding purified protein (see section 3.1.6.2) in PBS and incubated at 4ºC overnight. The next day, the plates were blocked for 2 h at RT with 5% skimmed milk prepared in PBS-0,05%Tween20. Next, the plates were washed three times with PBS-0,05%Tween20, and 50µl of serial dilutions of the serum samples diluted in PBS-0,05% Tween20-1% skimmed milk were added. After 1.5 h of incubation at RT, the plates were washed three times with PBS-0,05%Tween20 and incubated with 50 µl of the appropriate anti-IgG antibody conjugated with HRP (diluted 1:1000 in PBS-0,05% Tween20-1% skimmed milk) for 1 h at RT. Finally, after another washing step, the plates were developed by adding 100 µl of TMB substrate (Sigma) and the reaction was stopped by adding 50 µl of 1 M H_2SO_4. The absorbance was read using a EZ Read 400 microplate reader (Biochrom) at 450 nm.

3.2.5.4. Plaque reduction neutralization (PRNT) assay

Titers of neutralizing antibodies against ZIKV present in the sera of immunize mice were determined by a PRNT assay using Vero cells, as previously described [168].

Briefly, heat-inactivated pooled serum samples were diluted in EMEM and filtered through 0.22 µm filters. Neutralization was performed by incubating a fixed amount (100 PFU of PA259459 or FSS13025 ZIKV strains) with two-fold serial dilutions of each serum (starting from 1:20) for 1 h at 37ºC. Then, the mixture was adsorbed for 1 h to subconfluent Vero cell monolayers grown in 6-well plates. After virus adsorption, culture medium was removed and cells, overlaid with semisolid agarose medium, were incubated for 72 h, fixed, and stained with 0.5% crystal violet solution (Sigma-Aldrich) in methanol (Merck). Titers of neutralizing antibodies were expressed as the reciprocal of the serum dilution that inhibited plaque formation by 50% ($PRNT_{50}$) or 90% ($PRNT_{90}$), relative to samples incubated with negative control sera.

3.2.6. Statistical methods

Student's T test was used for protein and antibody measurement to establish the differences between two groups.

For statistical analysis of cytokine/chemokine expression, one-way analysis of variance (ANOVA) with Tukey's honestly significant difference (HSD) *post hoc* tests was applied.

The statistical significance of neutralization measurements ($PRNT_{90}$) in Balb/c sera from immunized mice was determined by an unpaired t-test, and in $IFNAR^{-/-}$ mice by an ANOVA analysis applying Bonferroni's correction for multiple comparisons. The statistical significance of viremia was also determined by an ANOVA analysis applying Bonferroni's correction for multiple comparisons.

Statistical analysis of the ICS data was realized as previously described [92,169], using an approach that corrects measurements for the medium response (RPMI), with calculation of confidence intervals and P values. Only antigen response values significantly larger than the corresponding RPMI values are represented. Background values were subtracted from all values used to allow analysis of proportionate representation of responses.

RESULTS

4. RESULTS

4.1. An MVA vector expressing HIV-1 envelope gp120 protein under the control of a potent VACV promoter as a promising strategy in HIV/AIDS vaccine design

One of the main approaches to improve the MVA immunogenicity focuses on optimizing poxviral promoters that drive the expression of the heterologous antigens encoded within the recombinant MVA vector genome. In our laboratory, it has previously been described a novel optimized VACV synthetic promoter, LEO160, that was able to increase in immunized mice the specific $CD4^+$ and $CD8^+$ T cell memory immune responses elicited by the MVA-LACK vaccine candidate against the *Leishmania* homologue of activated C kinase (LACK) antigen, an intracellular antigen, due to a very early times of expression of the heterologous antigen [88]. Therefore, in this Thesis the first modification to be introduced into the MVA genome to enhance the expression and immunogenicity of a selected foreign antigen is the optimization of the virus promoter strength.

4.1.1. Generation and *in vitro* characterization of MVA-LEO160-gp120

Thus, to study if this novel LEO160 promoter was also able to increase the expression levels and the immune responses of a soluble antigen, such as the HIV-1 gp120 protein, in comparison with the HIV/AIDS vaccine candidate MVA-B that expresses HIV-1 gp120 under the VACV sE/L promoter [113], a novel MVA vector expressing the HIV-1 envelope gp120 protein (clade B, isolate Bx08) under the control of the synthetic VACV LEO160 promoter was generated (termed MVA-LEO160-gp120), as described in Materials and Methods (Fig. 14). Briefly, the HIV-1 $gp120_{BX08}$ gene was subcloned downstream of the LEO160 promoter in the VACV insertional pLZAW1 plasmid transfer vector, to generate the plasmid transfer vector pLZAW1-LEO160-gp120, which contains the LacZ gene for transient selection of the insertion, and it was used to generate the MVA-LEO160-gp120 recombinant virus following standard procedures (see Materials and Methods, section 3.2.4.2).

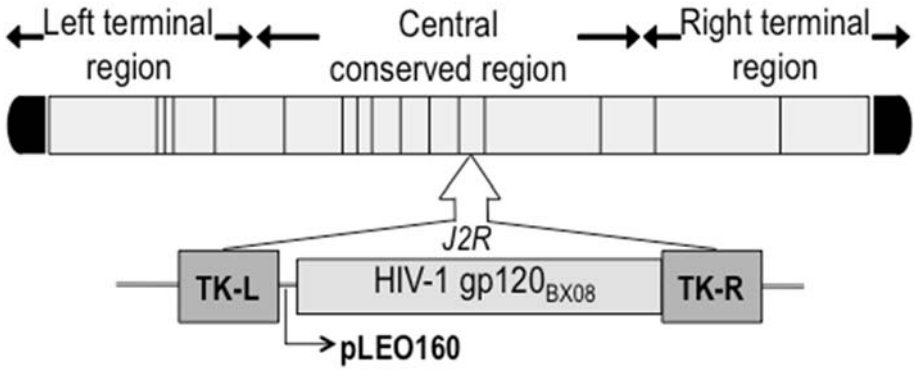

Figure 14. Scheme of the MVA-LEO160-gp120 genome map. The central conserved region and the variable left and right terminal regions are shown. The HIV-1 gp120 gene (from the clade B isolate Bx08) placed under the control of the LEO160 virus promoter and inserted within the MVA TK viral locus (*J2R* gene) is indicated. TK-L= TK left flanking region, TK-R= TK right flanking region. The LEO160 promoter nucleotide sequence is included in Fig. 5 (section 1.2.2.2.1.).

The correct presence of the VACV LEO160 promoter and the HIV-1 gp120 gene in the MVA-LEO160-gp120 recombinant virus was analyzed by PCR using oligonucleotides annealing in the VACV TK-flanking regions (Fig. 15a), and was also confirmed by DNA sequencing (data not shown). The virus growth kinetics in cultured permissive chicken DF-1 cells of the novel MVA-LEO160-gp120 recombinant virus and MVA-B (used as control) were similar (Fig. 15b), proving that the insertion of the VACV LEO160 promoter and the HIV-1 gp120 gene does not relapse MVA vector replication under permissive conditions. The correct expression of the heterologous HIV-1 gp120 protein was studied by Western blot in cell extracts from DF-1 cells, mock infected or infected with MVA-LEO-160-gp120, MVA-B, or MVA-WT using a specific rabbit polyclonal anti-gp120 antibody. The results demonstrated that MVA-LEO160-gp120 correctly expressed the HIV-1 gp120 protein (Fig. 15c). Moreover, to ensure that the encoded HIV-1 gp120 protein is stably expressed from the MVA genome and its expression can be maintained though long-time passages, MVA-LEO160-gp120 was grown in DF-1 cells infected at low MOI for 9 consecutive passages (Fig. 15d) and at passage 9, 28 individual virus plaques were isolated (Fig. 15e). The expression of the HIV-1 gp120 protein was determined in cell extracts by Western blot, revealing that MVA-LEO160-gp120 efficiently expresses the HIV-1 gp120 protein at all passages (Fig. 15d) and that 100% of the plaques at passage 9 correctly expressed the HIV-1gp120 protein (Fig. 15e), demonstrating the high genetic stability of MVA-LEO160-gp120).

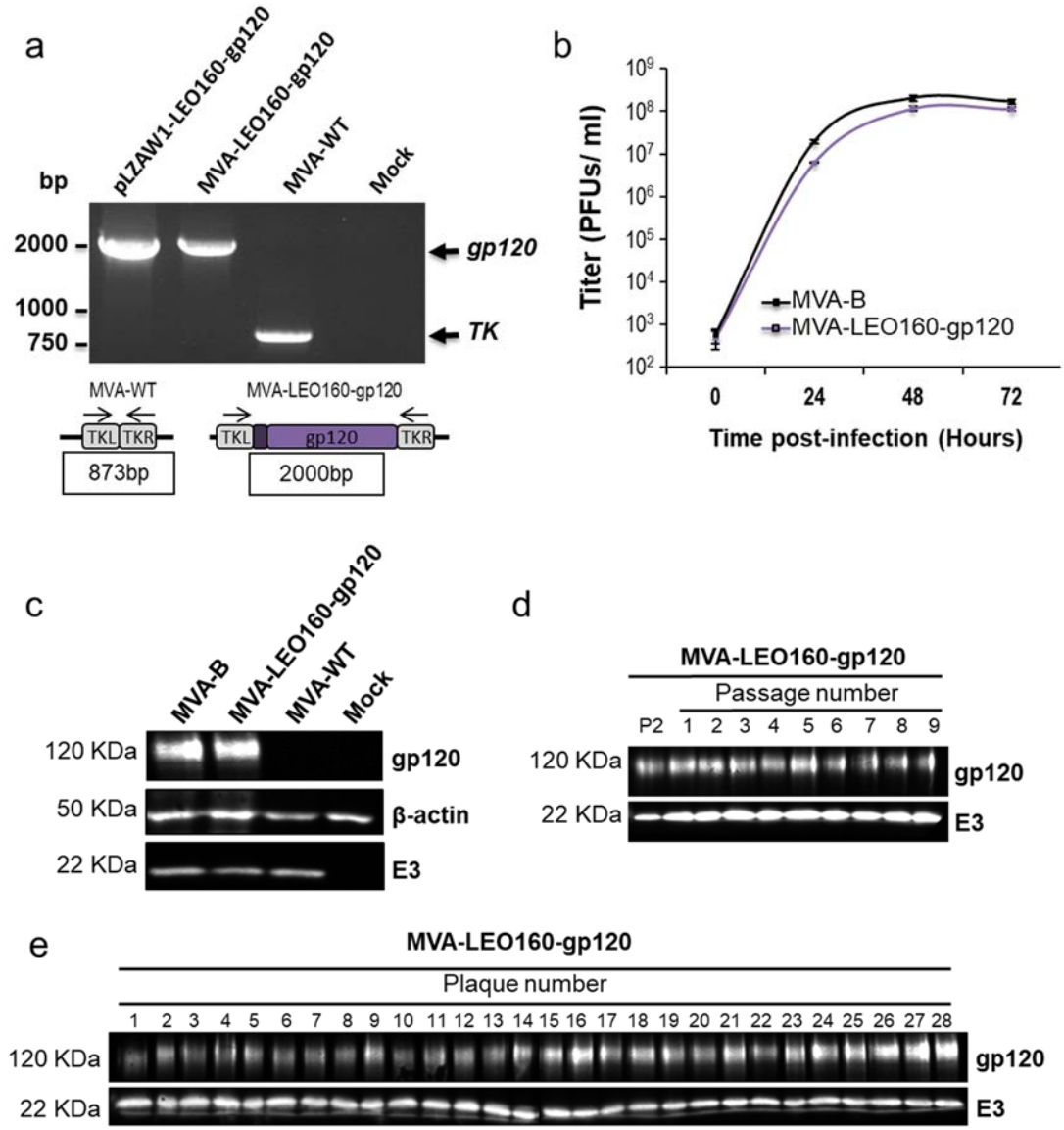

Figure 15. ***In vitro*** **characterization of MVA-LEO160-gp120. (a)** PCR analysis of MVA *TK locus*. Viral DNA was extracted from DF-1 cells mock infected or infected at 5 PFU/cell with MVA-WT, or MVA-LEO160-gp120. DNA from pLZAW1-LEO160-gp120 plasmid transfer vector was used as positive control for LEO160-gp120 insert. Primers spanning the TK locus-flanking regions were used for PCR analysis of the LEO160-gp120 transgene inserted within the TK locus. DNA products corresponding to the MVA TK gene and the gp120 insertion are indicated on the right. Molecular size markers (1-kb ladder) with the corresponding sizes (base pairs) are indicated on the left. PCR amplification schemes are placed below. **(b)** Viral growth kinetics. Monolayers of permissive DF-1 cells were infected at 0.01 PFU/cell with MVA-B or MVA-LEO160-gp120. At different times post-infection (0, 24, 48, and 72 h.p.i.) cells were collected and virus titers in cell lysates were quantified by plaque immunostaining assay with anti-VACV antibodies. The mean ± standard deviations of two independent experiments are shown. **(c)** Expression of HIV-1 gp120 protein. Western blot analysis of the HIV-1 gp120 protein detected in cells extracts of DF-1 cells mock infected or infected with MVA-B, MVA-LEO160-gp120, or MVA-WT, using a polyclonal anti-gp120 antibody (1: 3,000, CNB). Antibodies against VACV E3 (1:1,000, CNB) and β-actin (1:1,000, Cell Signaling) were used as viral and cellular loading controls, respectively. The proteins detected are indicated on the right and the protein molecular weight (in kDa) is indicated on the left. **(d and e)** Stability of MVA-LEO160-gp120. MVA-

LEO160-gp120 (P2 stock) was continuously grown in DF-1 cells to passage 9 and at passage 9, 28 individual plaques were picked. Virus stocks from each passage **(d)** and from the 28 individual plaques at passage 9 **(e)** were used to infect cells and the expression of HIV-1 gp120 protein was determined by Western blotting. Rabbit anti-VACV E3 protein antibody was used as a VACV loading control. The proteins detected are indicated on the right and the protein molecular weight (in kDa) is indicated on the left.

4.1.2. MVA-LEO160-gp120 increases the expression and cell release of HIV-1 envelope gp120 antigen

To determine whether MVA-LEO160-gp120 could enhance the expression levels of HIV-1 gp120, in comparison to MVA-B, DF-1 (permissive) and HeLa (non-permissive) cells were infected with MVA-B and MVA-LEO160-gp120 at a MOI of 5 PFU/cell for 2 h, 4 h, 6 h and 24 h. Then, total RNA was isolated and mRNA levels of HIV-1 gp120 were determined by quantitative RT-PCR. The results showed that MVA-LEO160-gp120 significantly increased HIV-1 gp120 transcription compared to MVA-B at all times analyzed (Fig. 16), in both cell types, DF-1 (Fig. 16a) and HeLa cells (Fig. 16b). Noticeable are the differences observed in mRNA levels at early times post infection, highlighting the robust increase in gene expression achieved by the LEO160 promoter.

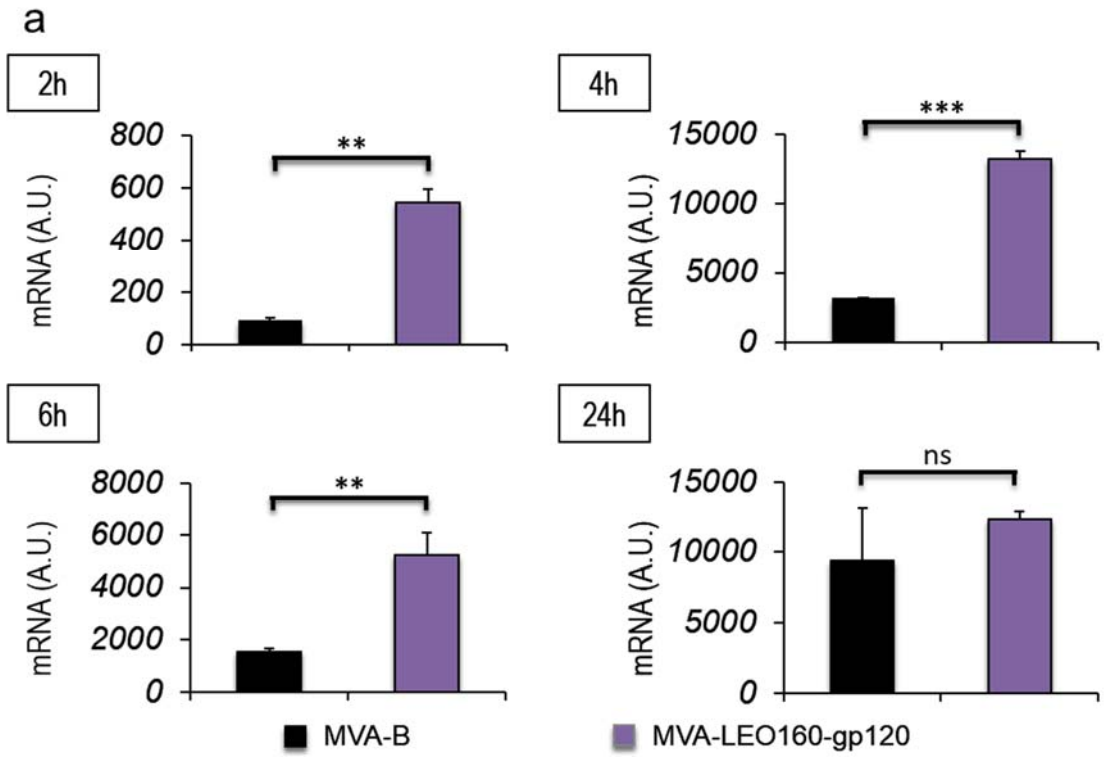

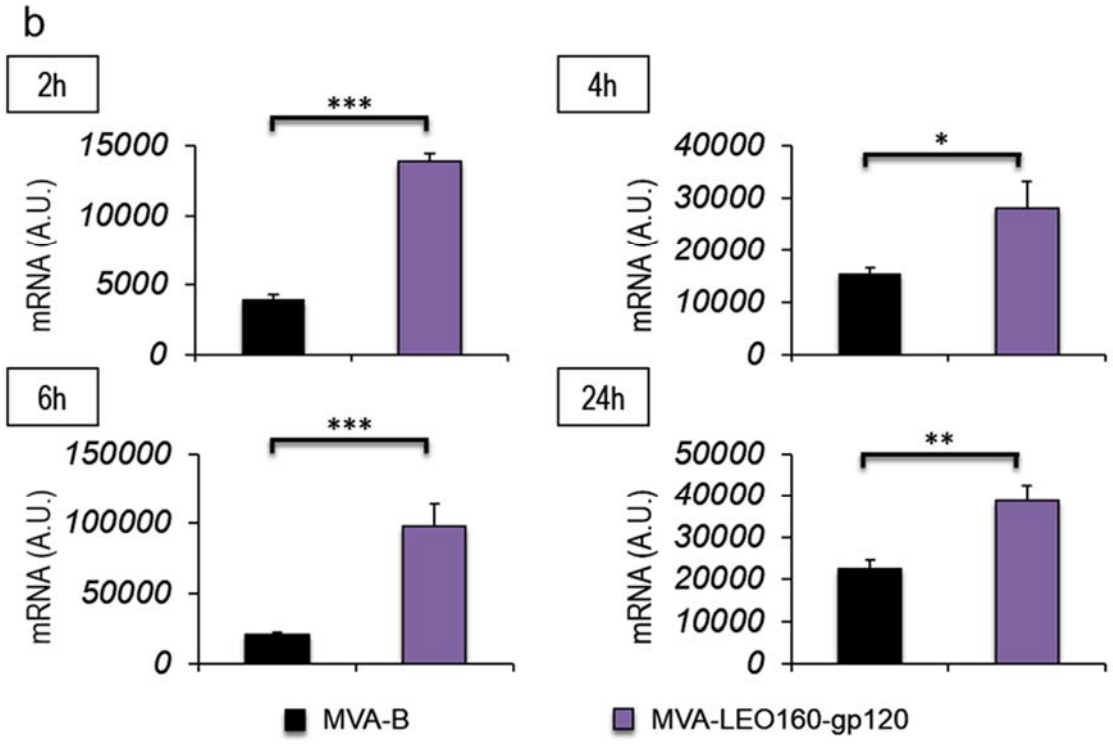

Figure 16. MVA-LEO160-gp120 enhances the mRNA levels of HIV-1 gp120, compared to MVA-B. (a) DF-1 (permissive) or **(b)** HeLa (non-permissive) cells were mock infected or infected with MVA-B, or MVA-LEO160-gp120 at 5 PFU/cell. At 2, 4, 6 and 24 h.p.i., RNA was extracted, and HIV-1 gp120 expression was analyzed by real-time qRT-PCR. Results are expressed as the ratio of HIV-1 gp120 to endogenous HPRT mRNA levels. A.U.= arbitrary units. P values indicate significant response differences between MVA-B and MVA-LEO160-gp120 at the same hour (*, $p<0.05$; **, $p<0.005$, ***, $p<0.001$). Data are means ± standard deviations of triplicate samples from one experiment and are representative of two independent experiments in each cell type.

In order to compare the HIV-1 gp120 protein expression between MVA-B and MVA-LEO160-gp120, total protein was extracted at different time points (2, 4, 6 and 24 h) from HeLa cells infected at 5 PFU/cell with MVA-B or MVA-LEO160-gp120. Equal amounts of protein were loaded on SDS-PAGE and the HIV-1 gp120 protein levels were detected by Western blot (Fig. 17). The results showed that MVA-LEO160-gp120 increased the expression levels of HIV-1 gp120 protein, compared with MVA-B (Fig. 17a). Furthermore, the band intensity was quantified using Image Lab software and the expression of HIV-1 gp120 protein was normalized to VACV E3 protein (VACV constitutive early protein) to show that the difference in heterologous antigen expression was the result of distinct promoter strengths, and not to different virus infective capacities. The results showed that MVA-LEO160-gp120 induced a significantly increased gp120 production compared with MVA-B at all time points analyzed (Fig. 17b), correlating with the previous results of mRNA levels (Fig. 16).

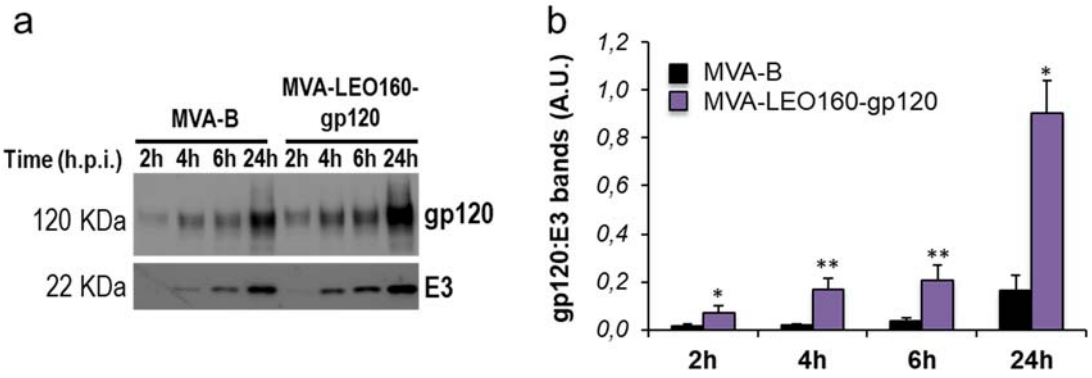

Figure 17. ***In vitro*** **HIV-1 gp120 expression driven by LEO160 promoter. (a)** HIV-1 gp120 expression in HeLa cells infected at 5 PFU/cell with MVA-B or MVA-LEO160-gp120 at 2, 4, 6 and 24 h.p.i. VACV E3 was used as a VACV loading control. **(b)** Bars showed the ratio of HIV-1 gp120 protein to VACV E3, after quantification of the corresponding band intensities represented in panel a, using Image Lab software. A.U. values showed the mean ± SEM of two independent experiments. (*, $p<0.05$; **, $p<0.005$).

To further analyze whether there were differences in cell released of soluble HIV-1 gp120 protein to the extracellular medium, supernatants derived from HeLa cells infected with MVA-B or MVA-LEO160-gp120 were collected at early times post-infection (2 and 4 h) and concentrated using Amicon® Ultra-15 Centrifugal Filters (Millipore). The total amount of HIV-1 gp120 protein present in the supernatants was quantified by ELISA using a standard curve of purified HIV-1 $gp120_{BX08}$ protein. The results showed that MVA-LEO160-gp120 released more soluble HIV-1 gp120 to the extracellular medium than MVA-B at early times post-infection (Fig. 18). At later times post-infection (6 and 24 h) there were no significant differences between MVA-LEO160-gp120 and MVA-B in the total amount of HIV-1 gp120 protein released to the supernatant (data not shown).

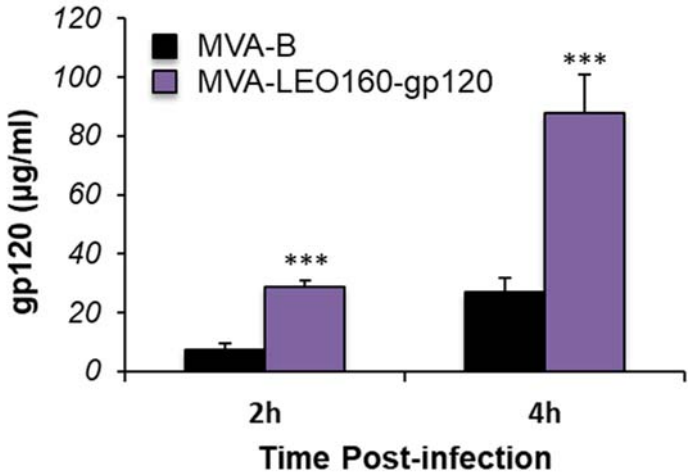

Figure 18. MVA-LEO160-gp120 releases more HIV-1 gp120 protein to the extracellular medium than MVA-B. Hela cells were infected with MVA-B or MVA-LEO160-gp120 at 5 PFU/cell for 2 and 4 h. Next, supernatants were concentrated and the amount of HIV-1 gp120 protein was determined by ELISA. Data are means ± standard deviations of

duplicate samples from one experiment and are representative of two independent experiments. (***, p<0.001).

These *in vitro* results with virus-infected cells of different origins (chicken and human) confirmed that the VACV LEO160 promoter positively enhances the expression of the antigen HIV-1 gp120.

4.1.3. MVA-LEO160-gp120 increases the magnitude of Env-specific T cell immune responses in mice

To determine whether the increased HIV-1 gp120 early expression observed *in vitro* in cells infected with MVA-LEO160-gp120 could drive an enhancement in the Env-specific T cell responses *in vivo*, the HIV-1 Env-specific $CD4^+$ and $CD8^+$ T cell immune responses induced in mice immunized with MVA-B and MVA-LEO160-gp120 were analyzed. A DNA prime/MVA boost immunization protocol, in which mice received 100 µg of DNA prime by intramuscular (i.m.) route and 14 days later were boosted with 2 x 107 PFU of MVA viruses by intraperitoneal (i.p.) route, was used; as this protocol amplifies the levels of T and B cell responses compared to the homologous MVA prime/MVA boost immunization [113,170]. Animals primed with sham DNA (DNA-ϕ) and boosted with non-recombinant MVA-WT were used as a control group. Adaptive Env-specific $CD4^+$ and $CD8^+$ T cell immune responses elicited by the different immunization groups (DNA-gp120/MVA-B, DNA-gp120MVA-LEO160-gp120, and DNA-ϕ/MVA-WT) were measured 10 days after the boost by ICS assay, after the stimulation of splenocytes with a pool of Env peptides that spanned the HIV-1 gp120 from an HIV-1 clade B consensus sequence (Fig. 19).

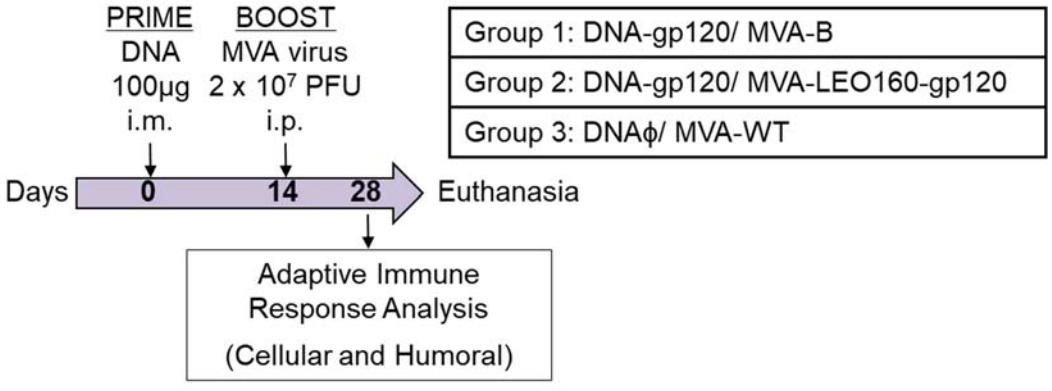

Figure 19. Immunization schedule. Groups of 6–8-week-old female mice (*n* = 5) received 100 µg of DNA prime by intramuscular (i.m.) route; 14 days later, the animals were boosted with 2 x 10^7 PFU of MVA viruses by intraperitoneal (i.p.) route. At 14 days post-boost, mice were sacrificed, and the spleens were processed for ICS assay and sera harvested for ELISA to measure the cellular and humoral adaptive immune responses against HIV-1 Env, respectively.

The magnitude of the total HIV-1 Env-specific $CD4^+$ (Fig. 20a) and $CD8^+$ (Fig. 20b) T cell adaptive immune responses (determined as the sum of the individual responses producing IFN-γ, TNF-α, and/or IL-2 cytokines, as well as the expression of CD107a on the surface of activated T cells as an indirect marker of cytotoxicity) was significantly greater in the DNA-gp120/MVA-LEO160-gp120 immunization group than in DNA-gp120/MVA-B, with both vaccinated groups triggering an overall Env-specific immune response mediated mainly by $CD8^+$ T cells (Fig. 20a and 20b).

Furthermore, the quality of the Env-specific T cell adaptive immune responses was characterized in part by the pattern of cytokine production and its cytotoxic potential. Thus, on the basis of the production of CD107a, IFN-γ, TNF-α, and IL-2 from HIV-1 Env-specific $CD4^+$ and $CD8^+$ T cells, 15 different HIV-1 Env-specific $CD4^+$ and $CD8^+$ T cell populations could be identified (Fig. 20c and 20d). As shown in Fig. 20c (pie charts), Env-specific $CD4^+$ T cell responses were similarly polyfunctional in both vaccinated groups, with around 80% of the $CD4^+$ T cells exhibiting 2 or more functions. $CD4^+$ T cells producing CD107a-IFN-γ-TNF-α-IL-2, CD107a-TNF-α-IL-2 or IFN-γ-TNF-α-IL-2 were the most induced populations elicited by both vaccinated groups, but DNA-gp120/MVA-LEO160-gp120 induced a significantly greater percentage of these major populations than DNA-gp120/MVA-B (Fig. 20c, bars). On the other hand, as shown in Fig. 20d (pie charts), DNA-gp120/MVA-B and DNA-gp120/MVA-LEO160-gp120 have a similar polyfunctional profile of Env-specific $CD8^+$ T cell responses, with 85% and 87% of the $CD8^+$ T cells exhibiting 2 or more functions, respectively. $CD8^+$ T cells producing CD107a-IFN-γ-TNF-α was the most abundant population elicited by both vaccinated groups, but once again DNA-gp120/MVA-LEO160-gp120 induced a significantly greater increase in the percentage of this population, and others, than DNA-gp120/MVA-B (Fig. 20d, bars).

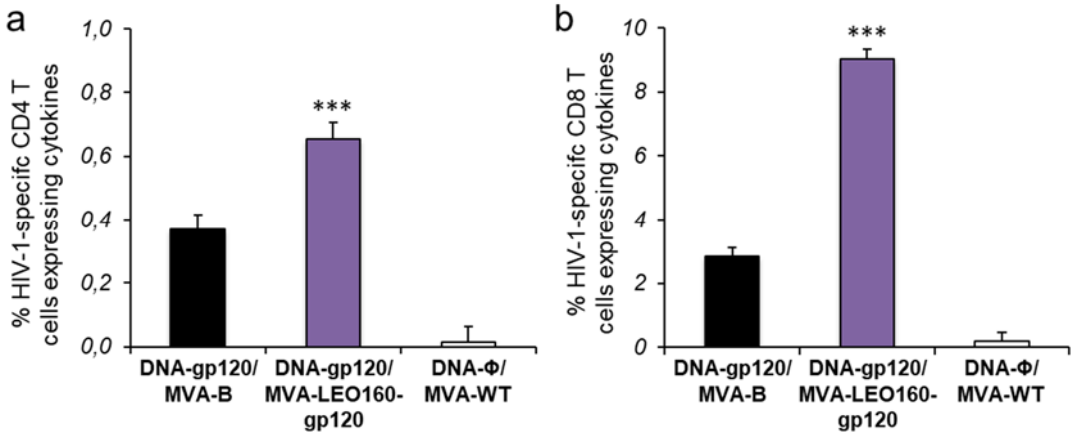

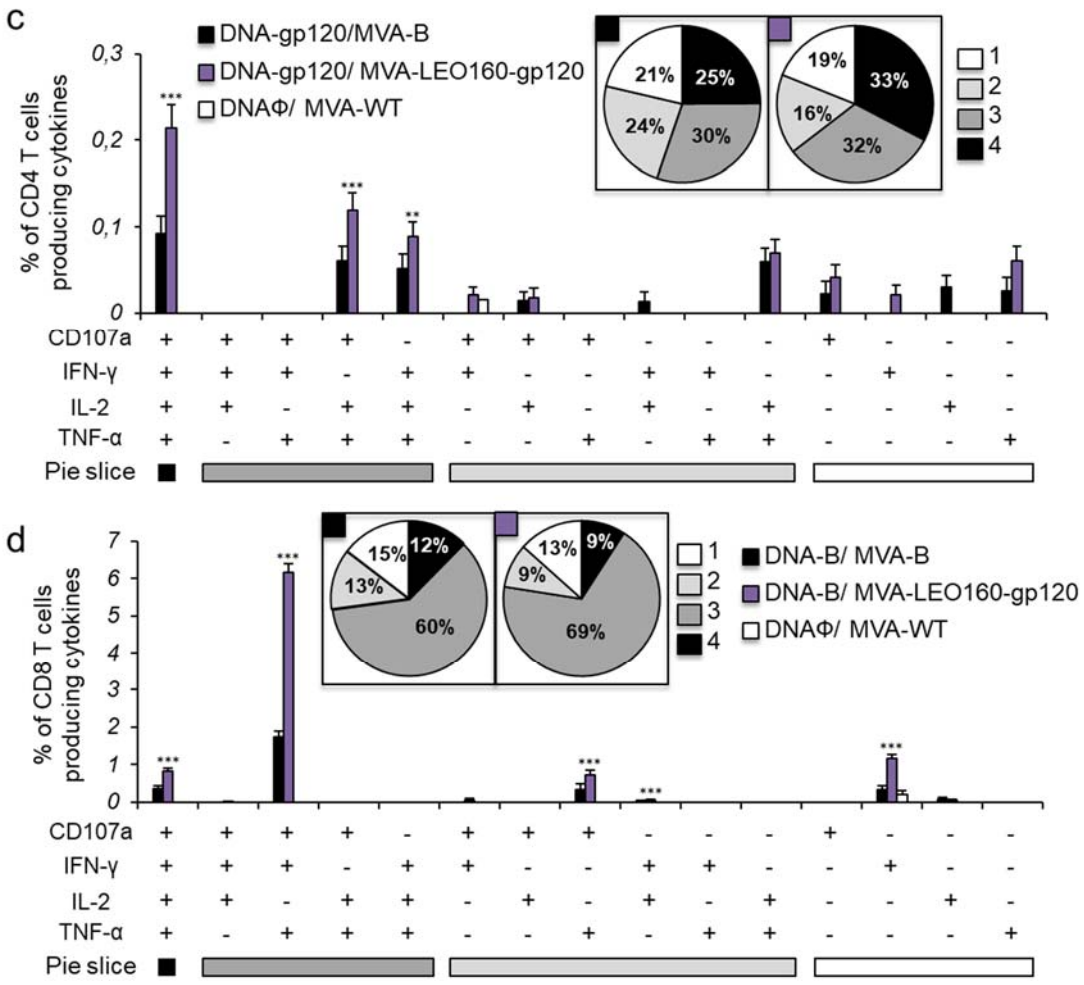

Figure 20. Immunization with DNA-gp120/MVA-LEO160-gp120 enhances the magnitude of HIV-1 Env-specific CD4⁺ and CD8⁺ T cell adaptive immune responses. Splenocytes were collected from mice (n=5 per group) immunized with DNA-φ/MVA-WT, DNA-gp120/MVA-B or DNA-gp120/MVA-LEO160-gp120, 10 days after the last immunization. Next, HIV-1 Env-specific CD4⁺ and CD8⁺ T cell adaptive immune responses triggered by the different immunization groups were measured by ICS assay following the stimulation of splenocytes with an Env peptide pool (comprising Env-1 + Env-2 + Env-3 peptide pools). Values from unstimulated controls were subtracted in all cases. P values indicate significant response differences between the DNA-gp120/MVA-B and DNA-gp120/MVA-LEO160-gp120 immunization groups (**, p<0.005; ***, P<0.001). **(a and b)** Overall percentages of Env-specific CD4⁺ **(a)** and CD8⁺ **(b)** T cells. The values represent the sum of the percentages of T cells producing CD107a and/or IFN-γ and/or TNF-α and/or IL-2 against the Env peptide pool. **(c and d)** Polyfunctional profiles of Env-specific CD4⁺ **(c)** and CD8⁺ **(b)** T cells. All of the possible combinations of responses are shown on the x axis, while the percentages of T cells producing CD107a and/or IFN-γ and/or TNF-α and/or IL-2 against the Env peptide pool are shown on the y axis. Responses are grouped and colour coded on the basis of the number of functions (4, 3, 2, or 1). The pie charts summarize the data. Each slice corresponds to the proportion of the total Env-specific CD4⁺ and CD8⁺ T cells exhibiting 1, 2, 3, or 4 functions (CD107a and/or IFN-γ and/or TNF-α and/or IL-2).

4.1.4. MVA-LEO160-gp120 enhances the magnitude of Env-specific T cells with an effector memory phenotype

It has been described that HIV-1-specific T cells of a mature effector memory phenotype are more frequently detectable in HIV-1 controllers than in HIV-1 progressors [171–173]. Thus, next we determined the memory phenotype of HIV-1 Env-specific $CD4^+$ and $CD8^+$ T cells by measuring the expression of the CD127 and CD62L surface markers, which allow the definition of the different memory subpopulations: T central memory (TCM, $CD127^+/CD62L^+$), T effector memory (TEM, $CD127^+/CD62L^-$), and T effector (TE, $CD127^-/CD62L^-$) cells [174], and determined as the sum of the individual responses producing CD107a, IFN-γ, TNF-α, and/or IL-2 obtained for the Env peptide pool (Fig. 21). The results showed that in both vaccinated groups, Env-specific $CD4^+$ and $CD8^+$ T cells were mainly of the TEM phenotype, followed by the TE phenotype. However, immunization with DNA-gp120/MVA-LEO160-gp120 induced a significantly greater increase in the percentage of Env-specific $CD4^+$ and $CD8^+$ TEM and TE cells than immunization with DNA-gp120/MVA-B (Fig. 21).

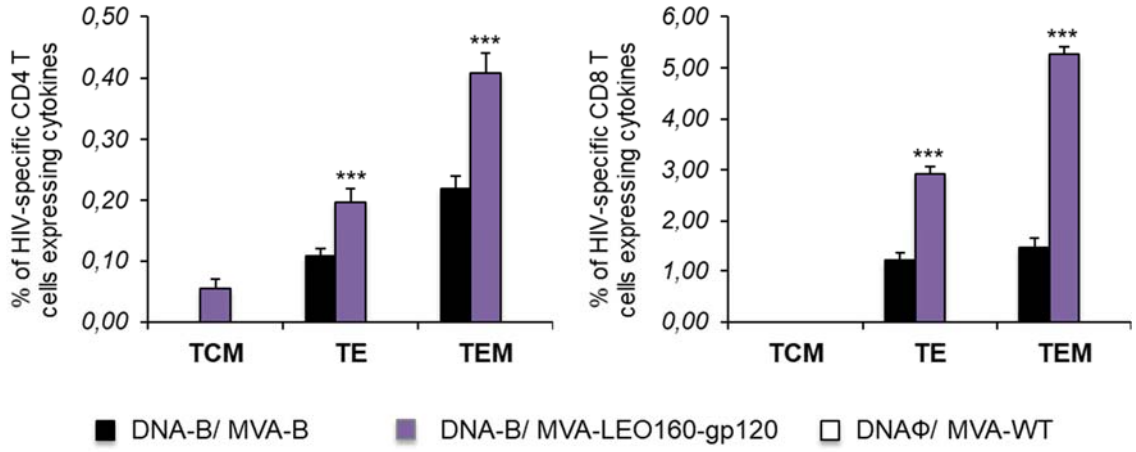

Figure 21. Phenotypic profile of Env-specific $CD4^+$ and $CD8^+$ T cells. Percentages of TCM, TEM, and TE HIV-1 Env-specific $CD4^+$ and $CD8^+$ T cells producing CD107a and/or IFN-γ and/or TNF-α and/or IL-2 against Env peptide pool 10 days after the last immunization, in the adaptive phase. Values from unstimulated controls were subtracted in all cases. P values indicate significant response differences between the DNA-gp120/MVA-B and DNA-gp120/MVA-LEO160-gp120 immunization groups (***, $p<0.001$).

4.1.5. MVA-LEO160-gp120 increases the magnitude of Env-specific $CD4^+$ T follicular helper (Tfh) cell responses

The development of HIV-1 bNAbs has been previously correlated with the frequency and quality of $CD4^+$ T follicular helper (Tfh) cells [175,176]. This subpopulation of T helper cells is involved in the development and sustaining of germinal center (GC) interactions, an essential crosstalk that promotes the generation of long-lived high affinity humoral immunity. Since, the interaction between Tfh and B cells is mediated both by cell-

associated and soluble factors, including CD40L (CD154), ICOS, IL-21, IL-10 and IL-4 [177], the HIV-1 Env-specific response of this specific cellular subset was studied in the spleen of immunized mice at 10 days after the last immunization. Thus, splenocytes were non-stimulated (RPMI) or stimulated *ex vivo* for 6 h with $gp120_{Bx08}$ protein plus Env peptide pool. Frequencies of total $CD4^+$ T cells with Tfh phenotype ($CXCR5^+$, $PD1^+$) were significantly higher in animals immunized with DNA-gp120/MVA-LEO160-gp120 than in those immunized with DNA-gp120/MVA-B; in both cases the frequencies were lower than in animals of control group DNA-ϕ/MVA-WT (Fig. 22a). Afterwards, the HIV-1 Env-specific Tfh response was evaluated by quantifying the $CD4^+$ Tfh cells that produced CD40L and/or IL-21 and/or IL-4 and/or IFN-γ. Since about 70% of the $CD4^+$ Tfh cells obtained in the non-stimulated (RPMI) or stimulated (with the $gp120_{Bx08}$ protein plus the Env peptide pool) conditions were positive for IL-21, whereas in the $CD4^+$ non-Tfh population only 2% of the cells were IL-21^+, the Env-specific Tfh response was finally established by analyzing the percentage of $CD4^+$ Tfh cells that produced IFN-γ and/or IL-4 and/or CD154 after stimulation, in comparison with non-stimulated cells (Fig. 22b). The results showed that the magnitude of the HIV-1 Env-specific Tfh response induced by animals immunized with DNA-gp120/MVA-LEO160-gp120 was significantly higher than in animals immunized with DNA-gp120/MVA-B (Fig. 22b).

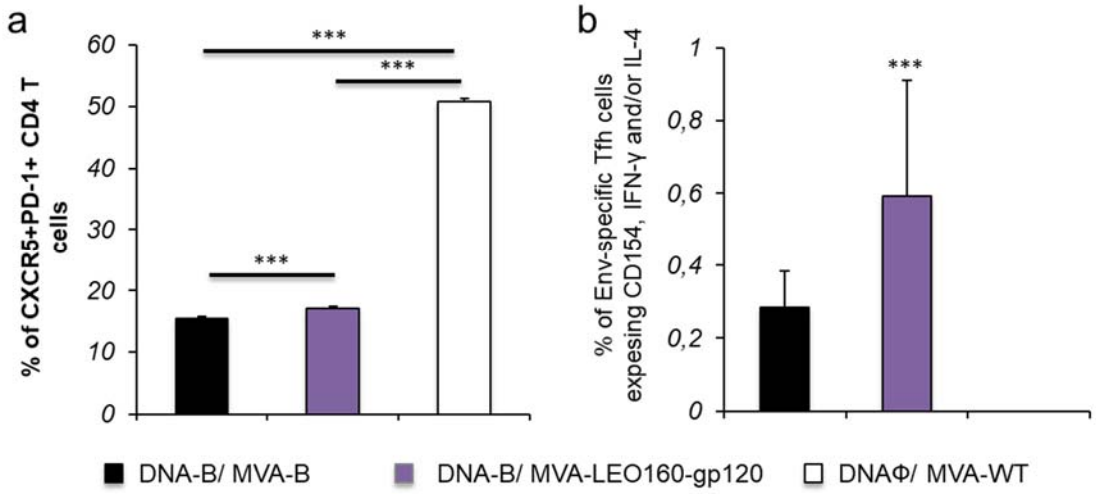

Figure 22. Env-specific Tfh cell immune responses. Mice (n=5) were immunized with DNA-gp120/MVA-B, DNA-gp120/MVA-LEO160-gp120 or DNA-φ/MVA-WT. At 10 days after the last immunization, Env-specific $CD4^+$ Tfh cell immune response was studied in splenocytes. **(a)** Magnitude of the $CD4^+$ T cells with Tfh phenotype ($CXCR5^+$, $PD1^+$) measured by ICS assay in non-stimulated (RPMI) splenocytes. All the data are background-subtracted (***, $p < 0.001$). **(b)** Magnitude of the Env-specific $CD4^+$ Tfh cells. The total value in each group represents the sum of the percentages of $CD4^+$ Tfh cells producing IFN-γ and/or IL-4 and/or CD40L against $gp120_{BX08}$ protein plus Env peptide pool. Data are background (RPMI)-subtracted.

4.1.6. MVA-LEO160-gp120 enhances the levels of antibodies against HIV-1 gp120

Since both the cellular and humoral arms of the immune system are thought to be necessary to control HIV-1 infection [178], the humoral responses elicited after immunization with DNA-gp120/MVA-B and DNA-gp120/MVA-LEO160-gp120 were also analyzed, quantifying by ELISA the total IgG levels of antibodies against HIV-1 Env protein (clade B, isolate Bx08) in pooled sera obtained from mice 10 days postboost (Fig. 23). The results showed that DNA-gp120/MVA-LEO160-gp120 elicited significantly higher levels of total IgG anti-gp120 antibodies than DNA-gp120/MVA-B.

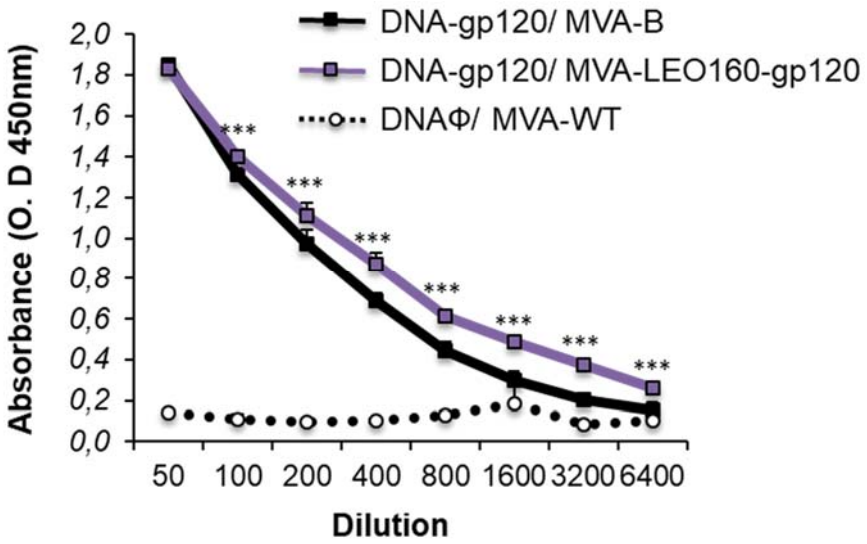

Figure 23. Humoral immune responses elicited by DNA-gp120/MVA-B and DNA-gp120/MVA-LEO160-gp120 against HIV-1 gp120 protein. Levels of Env-specific total IgG binding antibodies were measured by ELISA in pooled sera from mice immunized with DNA-gp120/MVA-B, DNA-gp120/MVA-LEO160-gp120 or DNA-φ/MVA-WT (n=5) 10 days after the last immunization. Mean absorbance values (measured at 450 nm) and standard deviations of duplicate pooled serum dilutions are represented. P values indicate significant differences in antibody levels between the DNA-gp120/MVA-B and DNA-gp120/MVA-LEO160-gp120 immunization groups at each serum dilution (***, $p<0.001$).

4.2. Improving the immunogenicity of the HIV/AIDS vaccine candidate MVA-B by deletion of the MVA *A40R* gene: Immune regulatory role of MVA A40 protein

MVA vectors have the advantage as vaccine candidates to induce a potent innate immune response that makes them act as an adjuvant itself [57,58]. Although MVA strain has lost several genes during its evolution in cell culture, it still contains numerous immunomodulatory genes, commonly located in the variable left and right terminal regions, some of which still have an unknown function [57]. Thus, one of the most promising strategies to improve the immunogenicity of the MVA vectors is the deletion of one or more immunomodulatory genes [59]. One of these genes, the MVA *A40R* gene, is located at the right terminal region of the MVA genome and has amino acid similarity to the CDR domain of C-type animal lectins, fact that suggest an immunomodulatory role that, nonetheless, is still not proved. Therefore, in this Thesis the second modification to be introduced into the MVA genome to enhance the immunogenicity of selected foreign antigens is the deletion of the suggested immunomodulatory MVA A40*R gene*.

4.2.1. Generation and *in vitro* characterization of MVA-B ΔA40R

To determine whether the VACV gene *A40R* might have an immunomodulatory role that, in turn, could influence the immunogenicity profile of antigens delivered from a poxvirus vector, we deleted *A40R* from the HIV/AIDS vaccine candidate MVA-B (expressing HIV-1 Env, Gag, Pol, and Nef antigens from clade B) [113], generating the MVA-B deletion mutant termed MVA-B ΔA40R (see Materials and Methods) (Fig. 24).

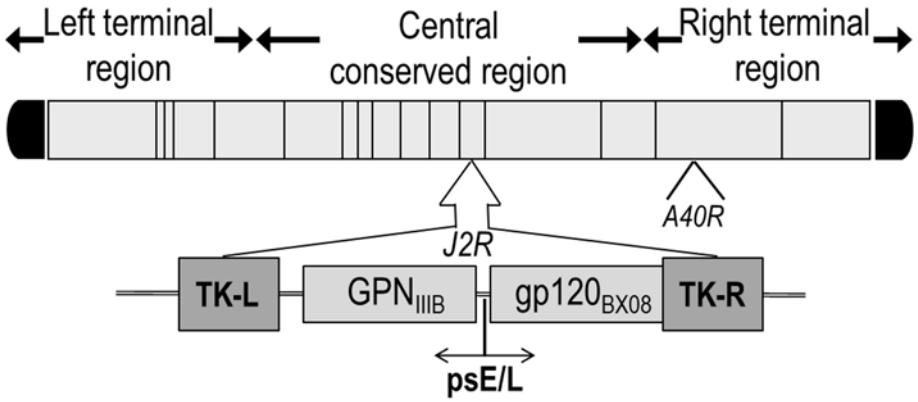

Figure 24. Scheme of the MVA-B ΔA40R genome map. The central conserved region, and the left and right terminal regions are shown. The deleted *A40R* gene is indicated. The HIV-1 GPN (from isolate IIIB) and gp120 (from isolate BX08) clade B sequences driven by the VACV sE/L promoter inserted within the TK viral locus (*J2R*) are indicated. TK-L= TK left flanking region, TK-R= TK right flanking region. Adapted from [179].

The correct presence of the HIV-1 antigens and the proper occurrence of the *A40R* deletion was confirmed by PCR of the VACV TK and *A40R* viral loci (Fig. 25a and 25b,

respectively), and was also validated by DNA sequencing (data not shown). Analysis by Western blotting demonstrated that MVA-B ΔA40R expressed HIV-1_{BX08} gp120 and HIV-1_{IIIB} GPN antigens similarly as the parental MVA-B (Fig. 25c). Moreover, the growth kinetics of parental MVA-B and deletion mutant MVA-B ΔA40R in cultured permissive DF-1 cells were similar (Fig. 25d), confirming that the MVA A40 protein is not required for MVA replication.

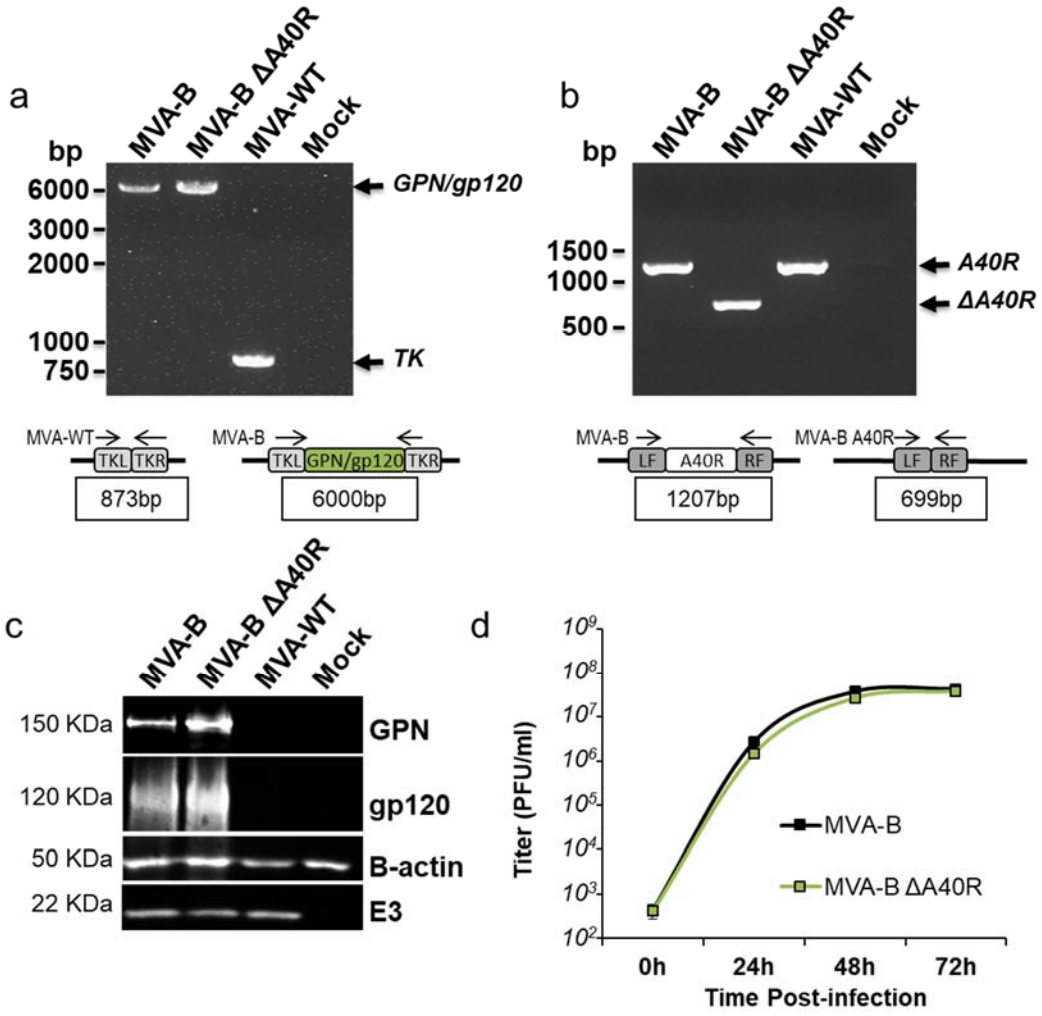

Figure 25. Generation and *in vitro* characterization of MVA-B ΔA40R. PCR analysis of the MVA TK **(a)** and *A40R* **(b)** loci. Viral DNA was extracted from DF-1 cells mock infected or infected at 5 PFU/cell with MVA-WT, MVA-B, or MVA-B ΔA40R. Primers spanning TK and *A40R* flanking regions were used for PCR analysis of the TK and *A40R* loci, respectively. DNA products corresponding to the parental virus (WT) and the *A40R* deletion mutant are indicated on the right. Molecular size markers (1-kb ladder) with the corresponding sizes (base pairs) are indicated on the left. PCR amplification schemes are placed below. **(c)** Expression of HIV-1_{BX08} gp120 and HIV-1_{IIIB}GPN proteins. DF-1 cells were mock infected or infected at 5 PFU/cell with MVA-WT, MVA-B, or MVA-B ΔA40R. At 24 h.p.i., cells were lysed in Laemmli buffer, fractionated by 8% SDS-PAGE, and analyzed by Western blotting with rabbit polyclonal anti-gp120 antibody or polyclonal anti-gag p24 serum. A rabbit anti-β-actin antibody was used as a protein loading control. Rabbit anti-VACV early E3 protein antibody was used as a VACV loading control. The proteins detected are indicated on the right and the protein molecular weight (in kDa) is indicated

on the left. **(d)** Viral growth kinetics in DF-1 cells. DF-1 cells were infected at 0.01 PFU/cell with MVA-B or MVA-B ΔA40R. At different times (0, 24, 48, and 72 h.p.i.) cells were collected and virus titers of cell lysates were quantified by plaque immunostaining assay with anti-VACV antibodies. The mean and standard deviations of two independent experiments is shown.

4.2.2. Deletion of MVA *A40R* gene enhances the MVA-B innate immune responses in human macrophages

The production of type I IFN, pro-inflammatory cytokines and chemokines is an important initial step in the induction of antiviral immunity [57,180]. Thus, to study whether MVA A40 protein impact on innate immune responses, human THP-1 macrophages were mock infected or infected for 3 and 6 h with MVA-WT, MVA-B, and MVA-B ΔA40R at 5 PFU/cell, and analyzed by quantitative real-time RT-PCR the mRNA expression levels of type I IFN (IFN-β), type I IFN-induced genes (IFIT1 and IFIT2), the viral dsRNA sensor MDA-5, the proinflammatory cytokine TNF-α, and the chemokine MIP-1α. The results showed that, compared to parental MVA-B, MVA-B ΔA40R significantly upregulated the mRNA levels of IFN-β, IFIT1, IFIT2, MDA-5, and MIP-1α, but does not affect the mRNA expression of TNF-α (Fig. 26), showing an enhancement in the innate immune responses. The enhanced mRNA values of MVA-WT over MVA-B vectors is likely due to some suppressive effect exerted by the expressed HIV-1 proteins [181]. These results suggested an immunosuppressive function of MVA A40 protein.

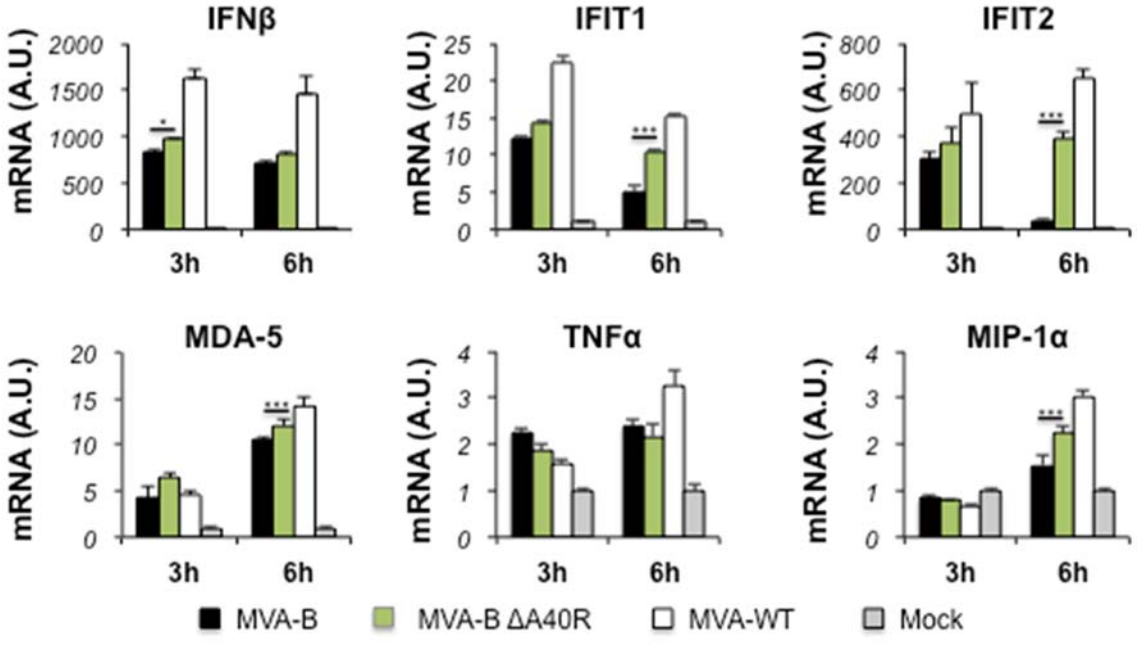

Figure 26. MVA-B ΔA40R upregulates the levels of type I IFN, proinflammatory cytokines and chemokine expression, compared to parental MVA-B. Human THP-1 macrophages were mock infected or infected with MVA-WT, MVA-B, or MVA-B ΔA40R at 5 PFU/cell. At 3 and 6 h.p.i., RNA was extracted, and IFN-β, IFIT1, IFIT2, MDA-5, TNF-α, MIP-1α, and HPRT mRNA levels were analyzed by RT-PCR. Results are expressed as the

ratio of the gene of interest to HPRT mRNA levels. A.U., arbitrary units. P values indicate significant response differences between the MVA-B and MVA-B ΔA40R at the same hour (*, $p<0.05$; ***, $p<0.001$). Data are means ± standard deviations of triplicate samples from one experiment and are representative of two independent experiments.

4.2.3. MVA-B ΔA40R increases the magnitude of HIV-1-specific T cell adaptive immune responses

Given the apparent immunosuppressive role of the VACV A40 protein in impairing the innate immune responses in human macrophages, we next asked whether deletion of VACV *A40R* from MVA-B could have an impact on the immunogenicity of the vector. Therefore, to study *in vivo* the effect of the *A40R* deletion on the HIV-1-specific T cellular immunogenicity elicited by the HIV/AIDS vaccine candidate MVA-B, we next analyzed the HIV-1-specific $CD4^+$ and $CD8^+$ T cell immune responses induced by MVA-B ΔA40R in Balb/c mice immunized with a DNA prime/MVA boost immunization protocol, as this protocol amplifies the levels of T and B cell responses, while the homologous MVA prime/MVA boost immunization triggers lower responses [113,170]. Mice received 100 µg of DNA prime by i.m. route and 14 days later were boosted with 2 x 107 PFU of MVA viruses by i.p. route. Animals primed with sham DNA (DNA-ϕ) and boosted with non-recombinant MVA-WT were used as a control group.,. Adaptive HIV-1-specific $CD4^+$ and $CD8^+$ T cell immune responses elicited by the different immunization groups (DNA-B/MVA-B, DNA-B/MVA-B ΔA40R, and DNA-ϕ/MVA-WT) were measured 10 days post-boost by ICS assay, after the stimulation of splenocytes with pools of peptides (Env, Gag, and GPN peptide pools) that spanned the HIV-1 Env, Gag, Pol, and Nef antigens from an HIV-1 clade B consensus sequence.

The magnitude of the total HIV-1-specific $CD4^+$ and $CD8^+$ T cell adaptive immune responses (determined as the sum of the individual responses producing IFN-γ, TNF-α, and/or IL-2 cytokines, as well as the expression of CD107a on the surface of activated T cells as an indirect marker of cytotoxicity; obtained for the Env, Gag, and GPN peptide pools) was significantly greater in the DNA-B/MVA-B ΔA40R immunization group than in DNA-B/MVA-B (2.3 and 1.4-fold times higher, respectively), with both vaccinated groups triggering an overall HIV-1-specific immune response mediated mainly by $CD8^+$ T cells (91% and 95%, respectively) (Fig. 27a).

The pattern of HIV-1-specific T cell adaptive immune responses showed that $CD4^+$ and $CD8^+$ T cell responses were directed mainly against the Env pool in both vaccinated groups, with $CD8^+$ T cell responses broadly distributed among Env, Gag, and GPN (Fig. 27b). However, DNA-B/MVA-B ΔA40R significantly enhanced the magnitude of Env-specific $CD4^+$ T cell responses and Env- and GPN-specific $CD8^+$ T cell responses (Fig. 27b). Moreover, HIV-1-specific $CD4^+$ T cells producing IFN-γ, TNF-α or IL-2 and HIV-1-

specific CD8⁺ T cells producing CD107a or IFN-γ were the most induced populations in both vaccinated groups, with DNA-B/MVA-B ΔA40R inducing a significantly greater magnitude of those populations (data not shown).

Furthermore, the quality of the HIV-1-specific T cell adaptive immune response was characterized in part by the pattern of cytokine production and its cytotoxic potential. Thus, on the basis of the production of CD107a, IFN-γ, TNF-α, and IL-2 from HIV-1-specific CD4⁺ and CD8⁺ T cells, 15 different HIV-1-specific CD4⁺ and CD8⁺ T cell populations could be identified (Fig. 27c and 27d). As shown in Fig. 27c (pie charts), HIV-1-specific CD4⁺ T cell responses were similarly polyfunctional in both vaccinated groups, with around 90% of the CD4⁺ T cells exhibiting 2 or more functions. CD4⁺ T cells producing CD107a-IFN-γ-TNF-α-IL-2, and IFN-γ-TNF-α-IL-2 were the most induced populations elicited by both vaccinated groups, with DNA-B/MVA-B ΔA40R inducing a significantly greater percentage of most of the CD4⁺ T cells exhibiting 4, 3, 2, or 1 functions than DNA-B/MVA-B (Fig. 27c, bars). On the other hand, as shown in Fig. 27d (pie charts), DNA-B/MVA-B and DNA-B/MVA-B ΔA40R have a similar polyfunctional profile of HIV-1-specific CD8⁺ T cell responses, with 80% and 83% of the CD8⁺ T cells exhibiting 2 or more functions, respectively. CD8⁺ T cells producing CD107a-IFN-γ-TNF-α, and CD107a-IFN-γ were the most abundant populations elicited by both vaccinated groups, with DNA-B/MVA-B ΔA40R inducing, once again, a significantly greater increase in the percentage of those populations than DNA-B/MVA-B (Fig. 27d, bars).

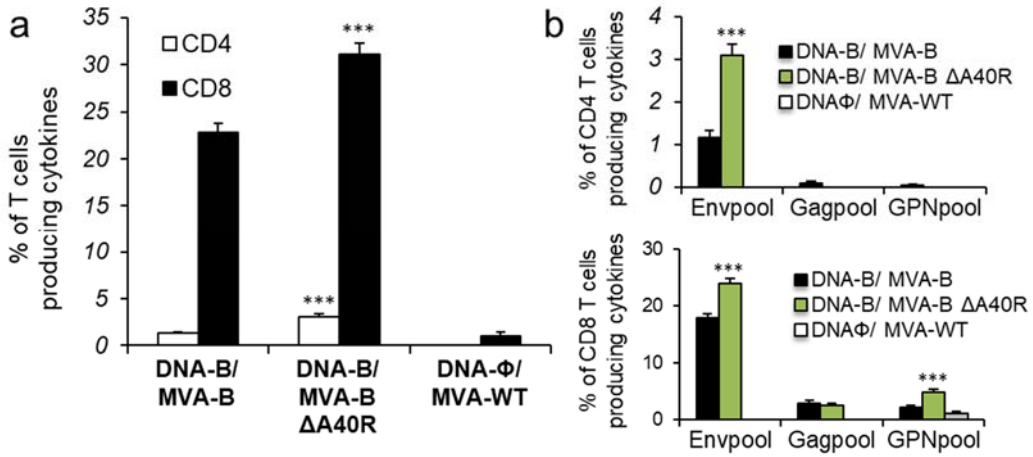

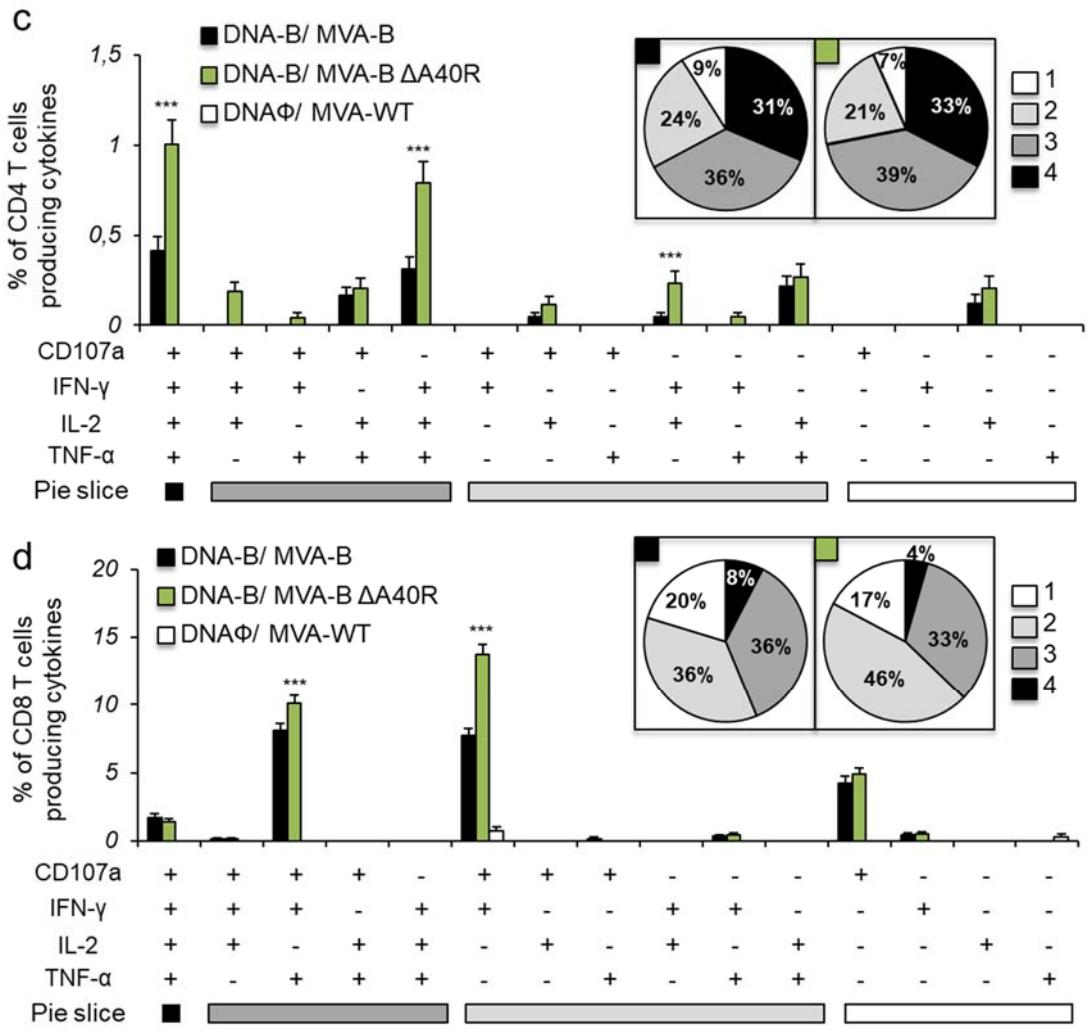

Figure 27. Immunization with MVA-B ΔA40R enhances the magnitude of HIV-1-specific CD4⁺ and CD8⁺ T cell adaptive immune responses. Splenocytes were collected from mice (n=4 per group) immunized with DNA-φ/MVA-WT, DNA-B/MVA-B or DNA-B/MVA-B ΔA40R 10 days after the last immunization. Next, HIV-1-specific CD4⁺ and CD8⁺ T cell adaptive immune responses triggered by the different immunization groups were measured by ICS assay following the stimulation of splenocytes with different HIV-1 peptide pools (Env, Gag, and GPN). Values from unstimulated controls were subtracted in all cases. P values indicate significant response differences between the DNA-B/MVA-B ΔA40R and DNA-B/MVA-B immunization groups (***, p<0.001). Data are from one experiment representative of three independent experiments. **(a)** Overall percentages of HIV-1-specific CD4⁺ and CD8⁺ T cells. The values represent the sum of the percentages of T cells producing CD107a and/or IFN-γ and/or TNF-α and/or IL-2 against Env, Gag, and GPN peptide pools. **(b)** Percentages of Env, Gag, and GPN HIV-1-specific CD4⁺ and CD8⁺ T cells. Frequencies represent the sum of the percentages of T cells producing CD107a and/or IFN-γ and/or TNF-α and/or IL-2 against Env, Gag, or GPN peptide pools. **(c and d)** Polyfunctional profiles of HIV-1-specific CD4⁺ **(c)** and CD8⁺ **(d)** T cells. All of the possible combinations of responses are shown on the x axis, while the percentages of T cells producing CD107a and/or IFN-γ and/or TNF-α and/or IL-2 against Env, Gag, and GPN peptide pools are shown on the y axis. Responses are grouped and colour coded on the basis of the number of functions (4, 3, 2, or 1). The pie charts summarize the data. Each slice corresponds to the proportion of the total HIV-1-specific CD4⁺ and CD8⁺ T cells

exhibiting 1, 2, 3, or 4 functions (CD107a and/or IFN-γ and/or TNF-α and/or IL-2) within the total HIV-1-specific $CD4^+$ and $CD8^+$ T cells.

4.2.4. MVA-B ΔA40R improves HIV-1-specific T cell memory immune responses

Memory T cell responses might be critical for protection against HIV-1 infection [182–185], and the durability of a vaccine-induced T cell response is an important feature since long-term protection is a requirement for prophylactic vaccination. Thus, we next analyzed the HIV-1-specific T cell memory immune responses elicited by the different immunization groups 53 days after the boost, following the same ICS assay described in the adaptive phase.

Similar to the results obtained in the adaptive phase, the magnitude of the total HIV-1-specific $CD4^+$ and $CD8^+$ T cell memory immune responses was again significantly greater in the DNA-B/MVA-B ΔA40R immunization group than in DNA-B/MVA-B (2- and 2-fold times higher, respectively), with both vaccinated groups triggering an overall HIV-1-specific immune response mediated mainly by $CD8^+$ T cells (Fig. 28a).

The pattern of HIV-1-specific T cell memory immune responses showed that $CD4^+$ and $CD8^+$ T cell responses were directed mainly against the Env pool in both vaccinated groups, with both $CD4^+$ and $CD8^+$ T cell responses broadly distributed among Env, Gag, and GPN (Fig. 28b). However, DNA-B/MVA-B ΔA40R significantly enhanced the magnitude of Env- and GPN-specific $CD4^+$ T cell memory responses and Env-, Gag- and GPN-specific $CD8^+$ T cell memory responses (Fig. 28b). Furthermore, HIV-1-specific $CD4^+$ T memory cells producing TNF-α or IL-2 and HIV-1-specific $CD8^+$ T memory cells producing CD107a, IFN-γ, or TNF-α were the most induced populations in both vaccinated groups, with DNA-B/MVA-B ΔA40R inducing a significantly greater magnitude of those populations (data not shown).

The quality of the HIV-1-specific $CD4^+$ and $CD8^+$ T cell memory immune responses was characterized as described above (section 4.2.3.) (Fig. 28c and 28d). HIV-1-specific $CD4^+$ T cell memory responses were more polyfunctional in the group immunized with DNA-B/MVA-B ΔA40R than in DNA-B/MVA-B, with 77% and 49% of the $CD4^+$ T cells exhibiting 2 or more functions, respectively (Fig. 28c, pie charts). $CD4^+$ T cells producing CD107a-IFN-γ-TNF-α-IL-2, IFN-γ-TNF-α-IL-2, and CD107a-IFN-γ-TNF-α were the most induced populations elicited by both vaccinated groups, with DNA-B/MVA-B ΔA40R inducing a significantly greater percentage of these populations (Fig. 28c, bars). On the other hand, as shown in Fig. 28d (pie charts), HIV-1-specific $CD8^+$ T cell memory responses were also more polyfunctional in the group immunized with DNA-B/MVA-B ΔA40R than in DNA-B/MVA-B, with 93% and 88% of the $CD8^+$ T cells exhibiting 2 or

more functions, respectively. CD8⁺ T cells producing CD107a-IFN-γ-TNF-α-IL-2, CD107a-IFN-γ-TNF-α and CD107a-IFN-γ were the most abundant populations elicited by both vaccinated groups, with DNA-B/MVA-B ΔA40R, once again, inducing a significantly greater increase in the percentage of those populations than DNA-B/MVA-B (Fig. 28d, bars).

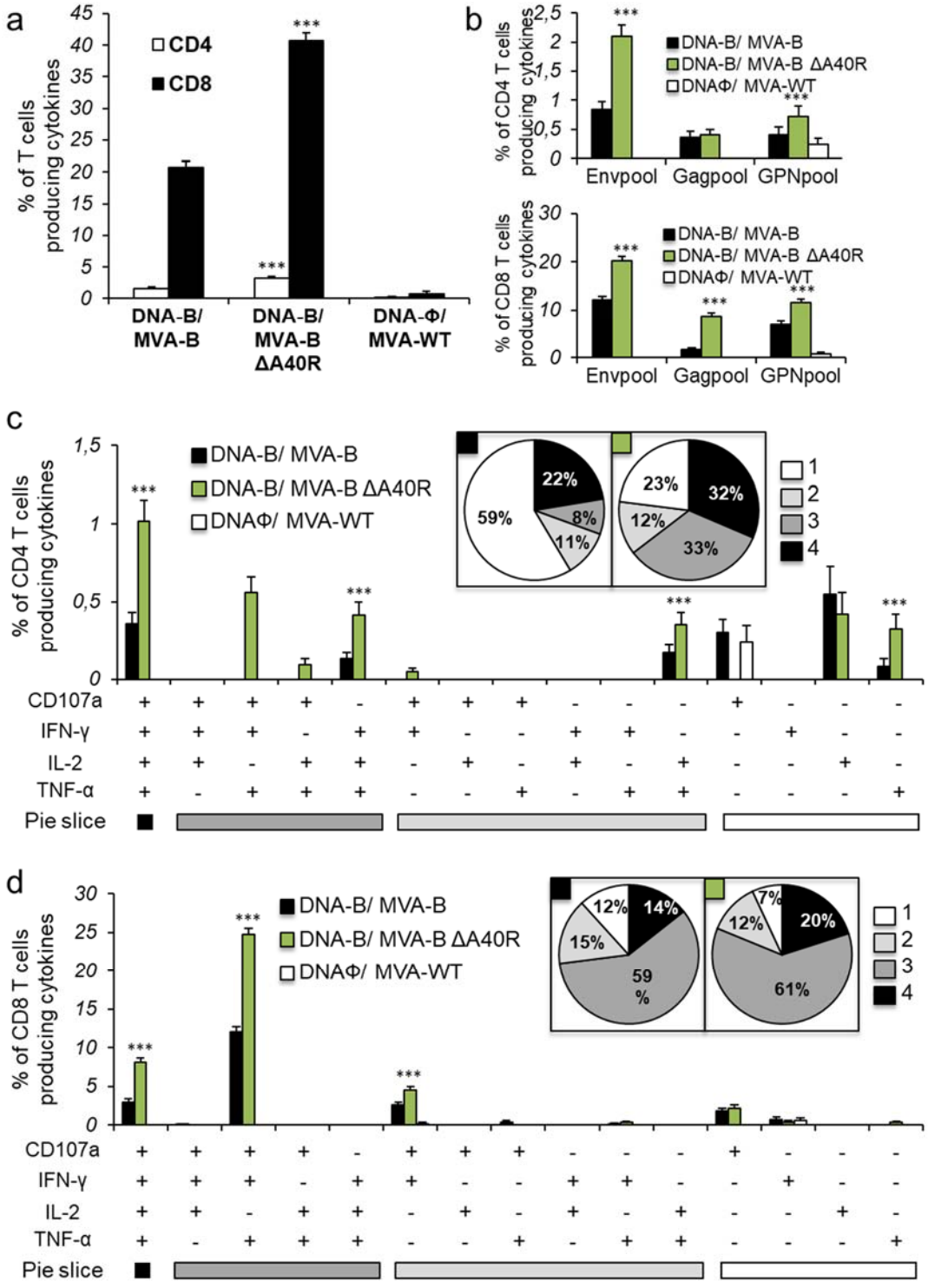

Figure 28. Immunization with MVA-B ΔA40R enhances the magnitude of HIV-1-specific CD4⁺ and CD8⁺ T cell memory immune responses. Splenocytes were collected

from mice (n=4 per group) immunized with DNA-φ/MVA-WT, DNA-B/MVA-B or DNA-B/MVA-B ΔA40R 53 days after the last immunization. Next, HIV-1-specific $CD4^+$ and $CD8^+$ T cell memory immune responses triggered by the different immunization groups were measured by ICS assay as described in the legend to Fig. 27. Values from unstimulated controls were subtracted in all cases. P values indicate significant response differences between the DNA-B/MVA-B ΔA40R and DNA-B/MVA-B immunization groups (***, $p<0.001$). Data are from one experiment representative of two independent experiments. **(a)** Overall percentages of HIV-1-specific $CD4^+$ and $CD8^+$ T cells. The values represent the sum of the percentages of T cells producing CD107a and/or IFN-γ and/or TNF-α and/or IL-2 against Env, Gag, and GPN peptide pools. **(b)** Percentages of Env, Gag, and GPN HIV-1-specific $CD4^+$ and $CD8^+$ T cells. Frequencies represent the sum of the percentages of T cells producing CD107a and/or IFN-γ and/or TNF-α and/or IL-2 against Env, Gag, or GPN peptide pools. **(c and d)** Polyfunctional profiles of HIV-1-specific $CD4^+$ **(c)** and $CD8^+$ **(d)** T cells. All of the possible combinations of responses are shown on the x axis, while the percentages of T cells producing CD107a and/or IFN-γ and/or TNF-α and/or IL-2 against Env, Gag, and GPN peptide pools are shown on the y axis. Responses are grouped and colour coded on the basis of the number of functions (4, 3, 2, or 1). The pie charts summarize the data. Each slice corresponds to the proportion of the total HIV-1-specific $CD4^+$ and $CD8^+$ T cells exhibiting 1, 2, 3, or 4 functions (CD107a and/or IFN-γ and/or TNF-α and/or IL-2) within the total HIV-1-specific $CD4^+$ and $CD8^+$ T cells.

4.2.5. MVA-B ΔA40R enhances HIV-1-specific T cells with an effector memory phenotype in the adaptive and memory phases

It has been described that HIV-1-specific T cells of mature effector memory phenotype are more frequently detectable in HIV-1 controllers than in HIV-1 progressors [171–173]. Thus, next we determined the phenotype of the adaptive and memory HIV-1-specific $CD4^+$ and $CD8^+$ T cells by measuring the expression of the CD127 and CD62L surface markers, which allow the definition of the different memory subpopulations: T central memory (TCM, $CD127^+/CD62L^+$), T effector memory (TEM, $CD127^+/CD62L^-$), and T effector (TE, $CD127^-/CD62L^-$) cells [174], and determined as the sum of the individual responses producing CD107a, IFN-γ, TNF-α, and/or IL-2 obtained for the Env, Gag, and GPN peptide pools (Fig. 29). The results showed that in both vaccinated groups, adaptive and memory HIV-1-specific $CD4^+$ and $CD8^+$ T cells were mainly of the TEM phenotype, followed by the TE phenotype. However, immunization with DNA-B/MVA-B ΔA40R induced a significantly greater increase in the percentage of adaptive and memory HIV-1-specific $CD4^+$ and $CD8^+$ TEM and TE cells (Fig. 29a and 29b). Representative flow cytometry plots of memory HIV-1-specific $CD8^+$ T cells against Env, Gag, and GPN peptide pools are shown in Fig. 29c.

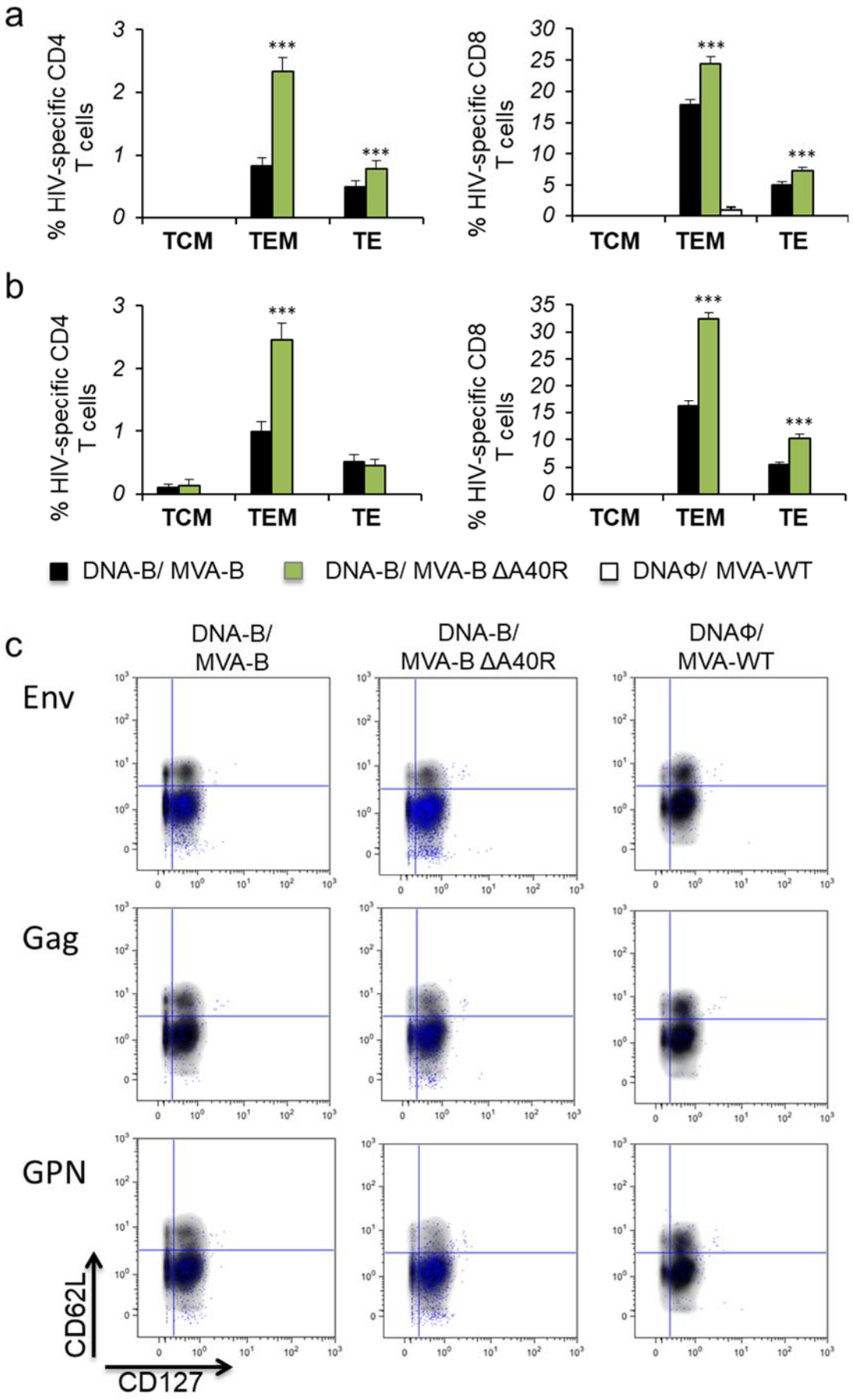
a
% HIV-specific CD4 T cells
% HIV-specific CD8 T cells
***
TCM
TEM
TE
b
DNA-B/ MVA-B
DNA-B/ MVA-B ΔA40R
DNAΦ/ MVA-WT
c
DNA-B/ MVA-B
DNA-B/ MVA-B ΔA40R
DNAΦ/ MVA-WT
Env
Gag
GPN
CD62L
CD127

Figure 29. Phenotypic profile of adaptive and memory HIV-1-specific CD4⁺ and CD8⁺ T cells. Percentages of TCM, TEM, and TE HIV-1-specific CD4⁺ and CD8⁺ T cells producing CD107a and/or IFN-γ and/or TNF-α and/or IL-2 against Env, Gag, and GPN peptide pools in the adaptive **(a)** and memory **(b)** phases. Values from unstimulated controls were subtracted in all cases. P values indicate significant response differences between the DNA-B/MVA-B ΔA40R and DNA-B/MVA-B immunization groups (***, p<0.001). **(c)** Representative flow cytometry phenotypic profile plots of memory HIV-1-specific CD8⁺ T cell responses against Env, Gag, and GPN peptide pools.

4.2.6. MVA-B ΔA40R enhances the levels of antibodies against HIV-1 gp120

Since cells infected with MVA-B release monomeric gp120 [113], and both the cellular and humoral arms of the immune system are thought to be necessary to control HIV-1 infection [178], we next analyzed the humoral immune responses elicited after immunization with DNA-B/MVA-B and DNA-B/MVA-B ΔA40R, quantifying by ELISA the total IgG and subclass IgG1, IgG2a, and IgG3 levels of antibodies against HIV-1 Env (clade B, isolate Bx08) in pooled sera obtained from mice 10 and 53 days postboost (Fig. 30). The results showed that DNA-B/MVA-B ΔA40R elicited significantly higher levels of total IgG anti-gp120 antibodies than DNA-B/MVA-B, in the adaptive and memory phases (Fig. 30a). Furthermore, the analysis of the IgG subtypes showed that DNA-B/MVA-B ΔA40R induced significantly higher levels of IgG1, IgG2a, and IgG3 anti-gp120 antibodies than DNA-B/MVA-B (Fig. 30b), with IgG1 levels higher than IgG3 and IgG2a levels, indicating a Th2 response.

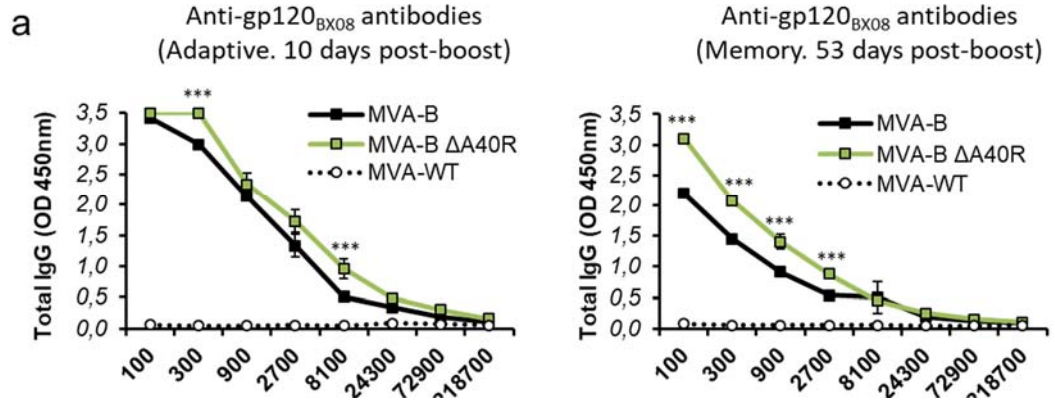

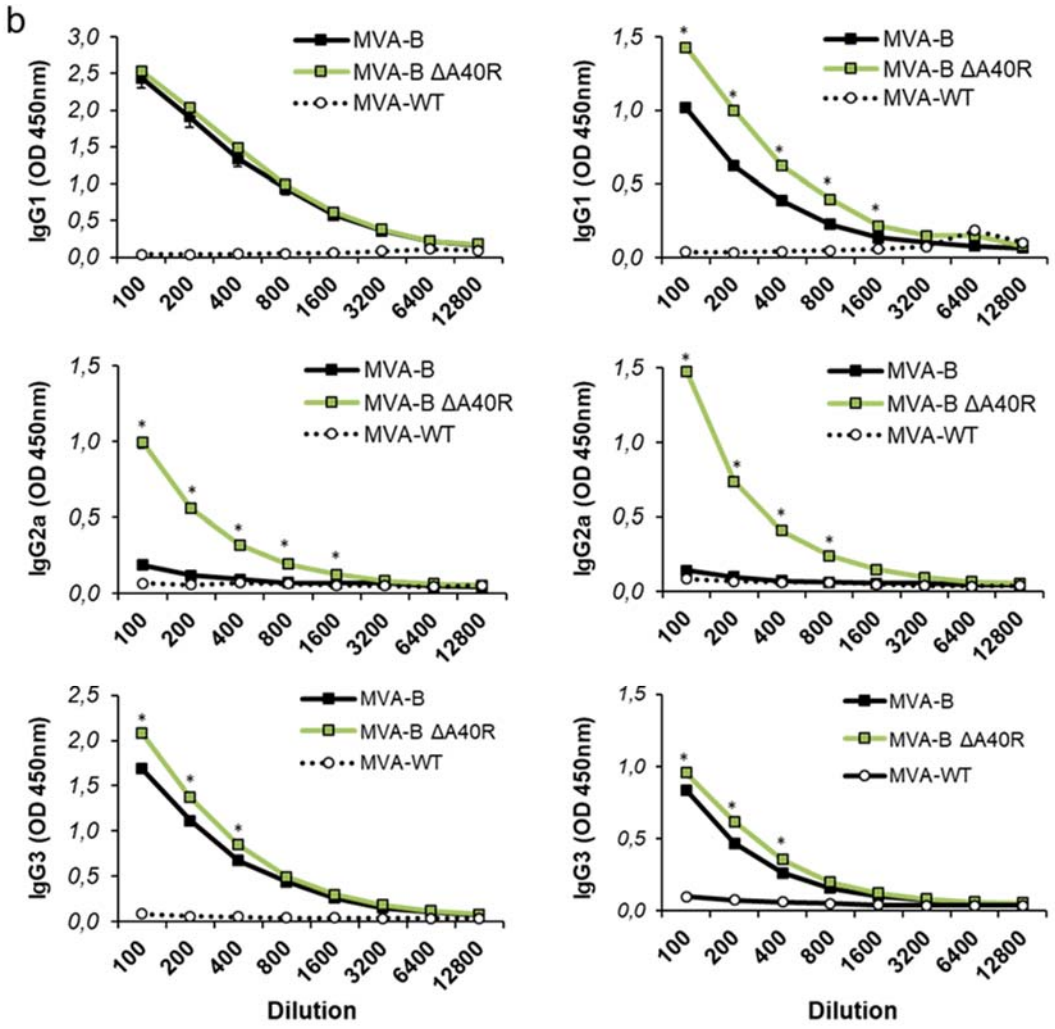

Figure 30. Humoral immune responses elicited by MVA-B and MVA-B ΔA40R against HIV-1 gp120 protein. Levels of gp120-specific total IgG **(a)**, and isotypes IgG1, IgG2a, and IgG3 **(b)** binding antibodies were measured by ELISA in pooled sera from mice immunized with DNA-B/MVA-B, DNA-B/MVA-B ΔA40R B or DNA-φ/MVA-WT (n=4, at each time point) 10 days (left panels) or 53 days (right panels) after the last immunization. Mean absorbance values (measured at 450 nm) and standard deviations of duplicate pooled serum dilutions are presented. P values indicate significant differences in antibody levels between the DNA-B/MVA-B and DNA-B/MVA-B ΔA40R immunization groups (*, $p<0.05$; ***, $p<0.001$) at each dilution. Data are from one experiment representative of three independent experiments.

4.2.7. Generation of a revertant MVA-B ΔA40R-rev virus expressing high levels of MVA A40 protein

To further confirm the immunosuppressive role of the MVA A40 protein and to ensure that any phenotypic difference seen with MVA-B ΔA40R was not due to mutations elsewhere in the virus genome, a revertant virus termed MVA-B ΔA40R-rev was constructed by reinserting the MVA *A40R* gene into the VACV HA locus (VACV *A56R* gene) of the MVA-B ΔA40R virus, and placed the *A40R* gene under the control of the VACV sE/L promoter. We selected this synthetic promoter due to the inability to detect

the A40 protein expression, by confocal immunofluorescence and Western blot, from its own promoter in MVA-infected cells using two different anti-A40 antibodies (generously provided by Drs. Geoffrey L. Smith and Jacomine Krijnse-Locker).

PCR analysis with primers annealing within HA flanking regions confirmed the correct reintroduction of the *A40R* gene in MVA-B ΔA40R (Fig. 31a), which was further confirmed by DNA sequencing (data not shown). Furthermore, the growth kinetics of MVA-B ΔA40R-rev in cultured permissive DF-1 cells was similar to that of MVA-B and MVA-B ΔA40R, confirming that the reintroduction of the MVA *A40R* gene does not affect MVA replication (Fig. 31b).

Next, the study of the VACV *A40R* mRNA expression by quantitative real-time RT-PCR showed that, while the deletion mutant MVA-B ΔA40R does not express *A40R* mRNA, MVA-WT, MVA-B and revertant MVA-B ΔA40R-rev viruses expressed VACV *A40R* mRNA (Fig. 31c). Interestingly, MVA-B ΔA40R-rev expressed the highest levels of VACV *A40R* mRNA (7.5-, and 5-fold higher than MVA-WT or MVA-B, at 3 and 6 h.p.i., respectively) (Fig. 31c), probably due to the stronger effect of the VACV sE/L promoter, in comparison with the natural *A40R* virus promoter. This higher expression of VACV *A40R* mRNA triggered by MVA-B ΔA40R-rev correlated with higher levels of VACV A40 protein (Fig. 31d). The presence of two bands in the western blot using the anti-A40 antibody is compatible with different post-translational modifications, being the upper band compatible with the full-length glycosylated A40 protein. Expression of A40 protein from cells infected with MVA-B or MVA-WT was not detected by Western blotting, indicating low levels of A40 protein expression under regulation of its natural promoter.

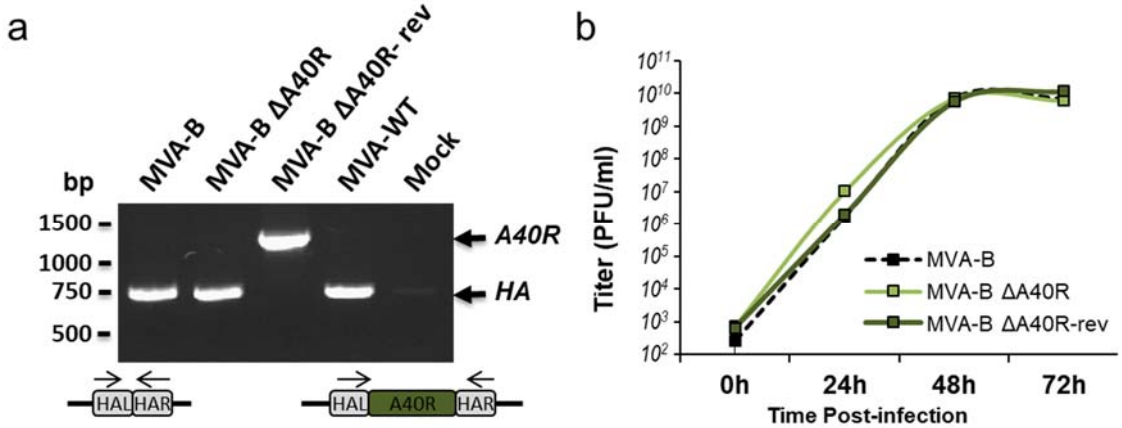

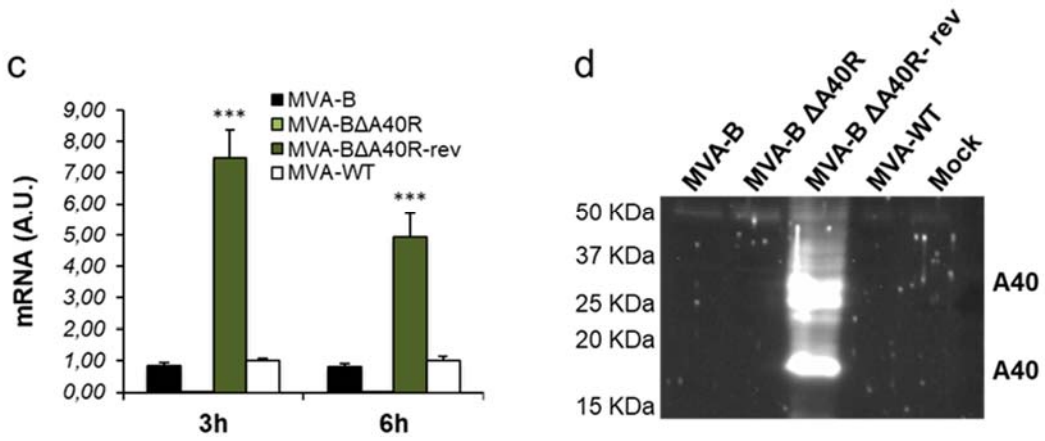

Figure 31. Generation and *in vitro* characterization of MVA-B ΔA40R-rev virus. (a) PCR analysis of the *HA* locus. Viral DNA was extracted from DF-1 cells mock infected or infected at 5 PFU/cell with MVA-WT, MVA-B, MVA-B ΔA40R, or MVA-B ΔA40R-rev. Primers spanning *HA* flanking regions were used for PCR analysis of the *HA* locus. DNA products corresponding to the parental virus (WT) HA gen without or with the insertion of the *A40R* gene are indicated on the right. Molecular size markers (1-kb ladder) with the corresponding sizes (base pairs) are indicated on the left. PCR amplification schemes are placed below. **(b)** Viral growth kinetics in DF-1 cells. DF-1 cells were infected at 0.01 PFU/cell with MVA-B, MVA-B ΔA40R, or MVA-B ΔA40R-rev. At different times (0, 24, 48, and 72 h.p.i.) cells were collected and virus titers of cell lysates were quantified by plaque immunostaining assay with anti-VACV antibodies. **(c)** mRNA levels of VACV *A40R* gene. Human THP-1 macrophages were mock infected or infected with MVA-WT, MVA-B, MVA-B ΔA40R or MVA-B ΔA40R-rev at 5 PFU/cell. At 3 and 6 h.p.i., RNA was extracted, and VACV *A40R* and *E3L* mRNA levels were analyzed by RT-PCR. Results are expressed as the ratio of the VACV *A40R* gene to *E3L* mRNA levels. A.U. arbitrary units. P values indicate significant response differences between the different viruses at the same hour (***, $p<0.001$). Data are means ± standard deviations of duplicate samples from one experiment and are representative of two independent experiments. **(d)** Expression of VACV A40 protein. DF-1 cells were mock infected or infected at 5 PFU/cell with MVA-WT, MVA-B, MVA-B ΔA40R, or MVA-B ΔA40R-rev. At 24 h.p.i. cells were lysed in Laemmli buffer, fractionated by 8% SDS-PAGE, and analyzed by Western blotting with rabbit polyclonal anti-A40 antibody. On the right is indicated the position of the VACV A40 protein. The sizes (in kDa) of standards (Precision Plus protein standards; Bio-Rad Laboratories) are indicated on the left.

Previous studies reported that VACV WR A40 protein is expressed at the cell surface [99]. Thus, the expression and intracellular localization of the VACV MVA A40 protein expressed by MVA-B ΔA40R-rev was next studied by confocal immunofluorescence microscopy in non-permissive HeLa cells. Therefore, cells were infected with MVA-B, MVA-B ΔA40R and MVA-B ΔA40R-rev for 18 h and then non-permeabilized or permeabilized fixed cells were stained with a polyclonal antibody against VACV A40 protein and the specific WGA probe to label the cell surface and Golgi reticulum (Fig. 32). The results showed that in non-permeabilized cells A40 protein (in green) was expressed in cells infected with MVA-B ΔA40R-rev and, as expected, co-localized with the cell membrane, whereas it was not detected in cells infected with MVA-B and MVA-

B ΔA40R (Fig. 32a). On the other hand, in permeabilized cells A40 protein (in green) was expressed in cells infected with MVA-B ΔA40R-rev with a diffused cytoplasmic pattern; and again, no detection of A40 protein was observed in cells infected with MVA-B and MVA-B ΔA40R (Fig. 32b).

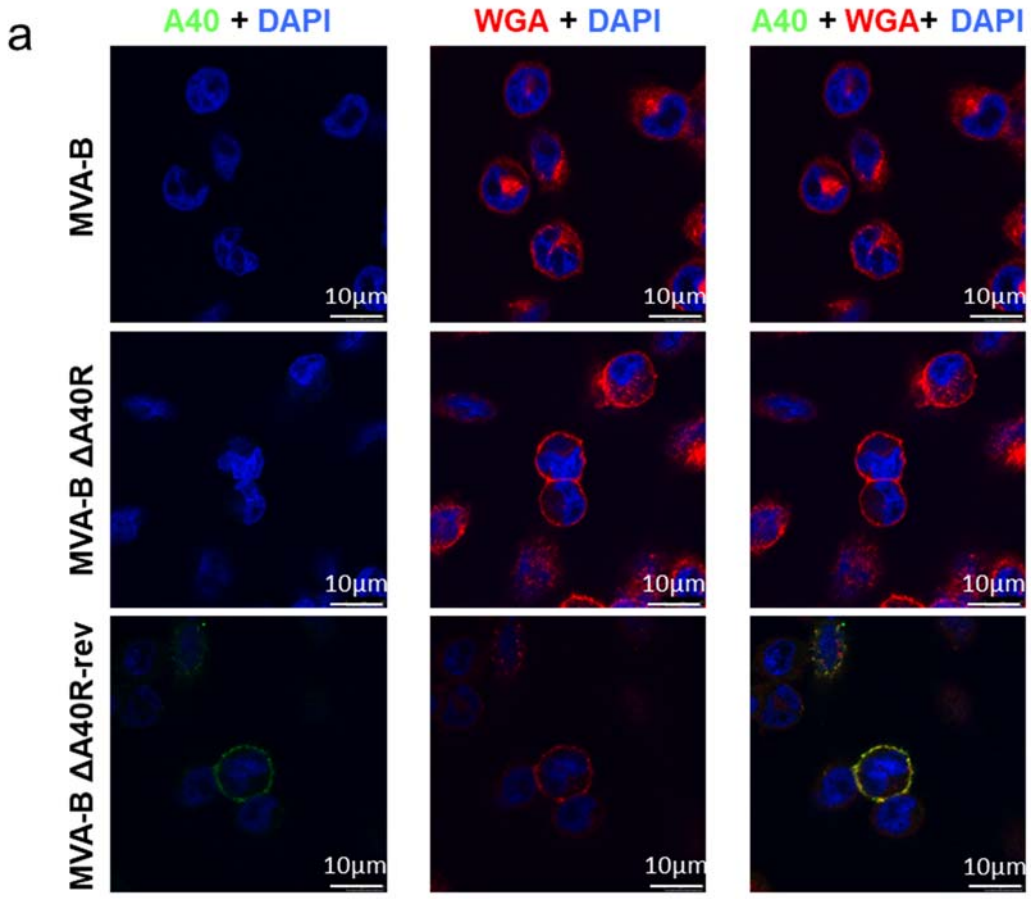

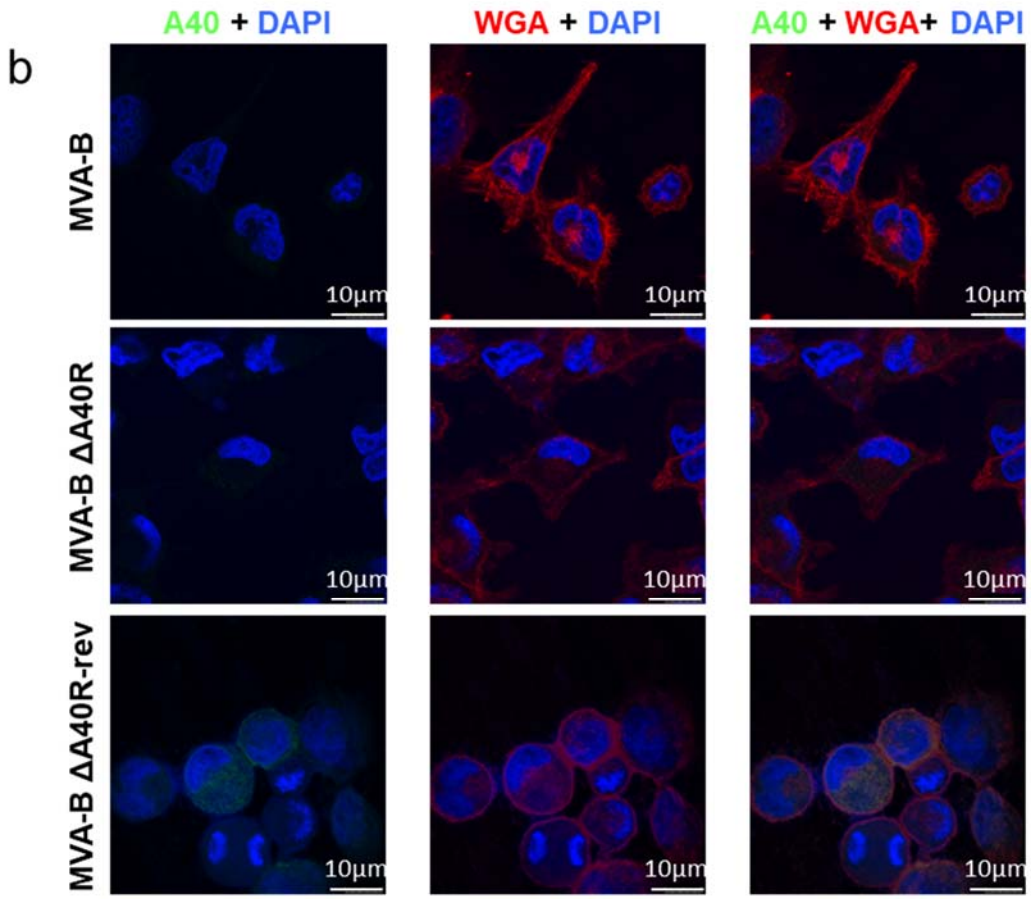

Figure 32. Immunofluorescence of A40 protein. HeLa cells were infected at 0.5 PFU/cell with MVA-B, MVA-B ΔA40R and MVA-B ΔA40R-rev and at 18 h.p.i. non-permeabilized **(a)** or permeabilized **(b)** fixed cells were stained with WGA probe conjugated to the fluorescent dye Alexa Fluor 594 (red) and a rabbit anti-A40 polyclonal antibody further detected with an anti-rabbit secondary antibody conjugated with the fluorochrome Alexa Fluor 488 (green). Cell nuclei were stained using DAPI (blue). Scale bar: 10 µm.

Moreover, expression analysis by quantitative real-time RT-PCR showed that MVA-B ΔA40R-rev expressed similar levels of HIV-1_{BX08} gp120 mRNA (relative gp120:HPRT expression levels) than MVA-B and MVA-B ΔA40R (Fig. 33a). Furthermore, analysis by Western blotting showed that MVA-B ΔA40R-rev expressed similar HIV-1_{BX08} gp120 and HIV-1_{IIIB} GPN protein levels than MVA-B and MVA-B ΔA40R (Fig. 33b). These results confirmed that the expression of HIV-1 antigens was not modified because of the reintroduction and overexpression of the MVA *A40R* gene.

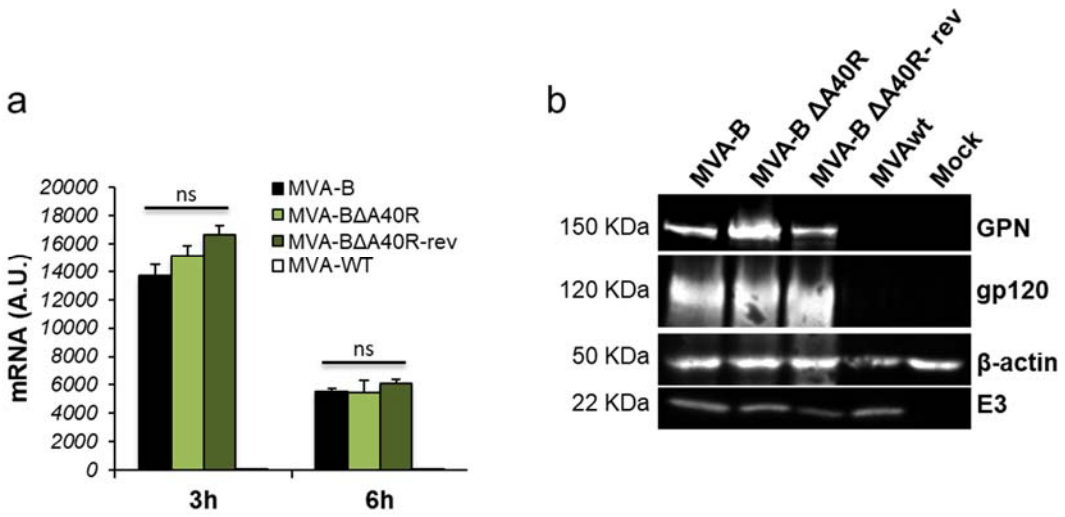

Figure 33. HIV-1 antigens expression. (a) mRNA levels of HIV-1_{BX08} gp120 gene. Human THP-1 macrophages were mock infected or infected with MVA-WT, MVA-B, MVA-B ΔA40R, or MVA-B ΔA40R-rev at 5 PFU/cell. At 3 and 6 h.p.i., RNA was extracted, and HIV-1_{BX08} gp120 and endogenous HPRT mRNA levels were analyzed by RT-PCR. Results are expressed as the ratio of the HIV-1_{BX08} gp120 gene to HPRT mRNA levels. A.U., arbitrary units. Data are means ± standard deviations of duplicate samples from one experiment and are representative of two independent experiments. **(b)** Expression of HIV-1_{BX08} gp120 and HIV-1_{IIIB}GPN proteins. DF-1 cells were mock infected or infected at 5 PFU/cell with MVA-WT, MVA-B, MVA-B ΔA40R, or MVA-B ΔA40R-rev. At 24 h.p.i., cells were lysed in Laemmli buffer, fractionated by 8% SDS-PAGE, and analyzed by Western blotting with rabbit polyclonal anti-gp120 antibody or rabbit anti-gag p24 serum. Rabbit anti-β-actin antibody was used as a protein loading control. Rabbit anti-VACV early E3 protein antibody was used as a VACV loading control. The proteins detected are indicated on the right and the protein molecular weight (in kDa) is indicated on the left.

4.2.8. Reintroduction of MVA *A40R* gene in MVA-B ΔA40R inhibits innate immune responses *in vitro*

Next, to confirm whether the reintroduction of VACV *A40R* gene in MVA-B ΔA40R restores the previously enhancement in type I IFN innate immune responses (see Fig. 26) and to further demonstrate the immunosuppressive role of VACV A40 protein, we infected human THP-1 macrophages for 3 h and 6 h with MVA-WT, MVA-B, MVA-B ΔA40R, and MVA-B ΔA40R-rev at 5 PFU/cell, and analyzed by quantitative real-time RT-PCR the mRNA expression levels of the innate immune related genes affected previously by the VACV *A40R* deletion, such as IFN-β, IFIT1, IFIT2, MDA-5, and MIP-1α (see Fig. 26). Interestingly, the results showed that, compared to parental MVA-B ΔA40R and MVA-B, MVA-B ΔA40R-rev significantly downregulated the mRNA levels of IFN-β, IFIT1, IFIT2, MDA-5, RIG-I, and MIP-1α (Fig. 34). Moreover, MVA-B ΔA40R-rev downregulated the mRNA levels of others genes not affected by the deletion of VACV *A40R* gene in MVA-B ΔA40R, such as TNFα and RANTES, while it does not affect the mRNA expression of the endogenous cellular gene HPRT (Fig. 34). These results

confirm the immunosuppressive role of the VACV A40 protein, and strongly suggest that acts by blocking the type I IFN pathway.

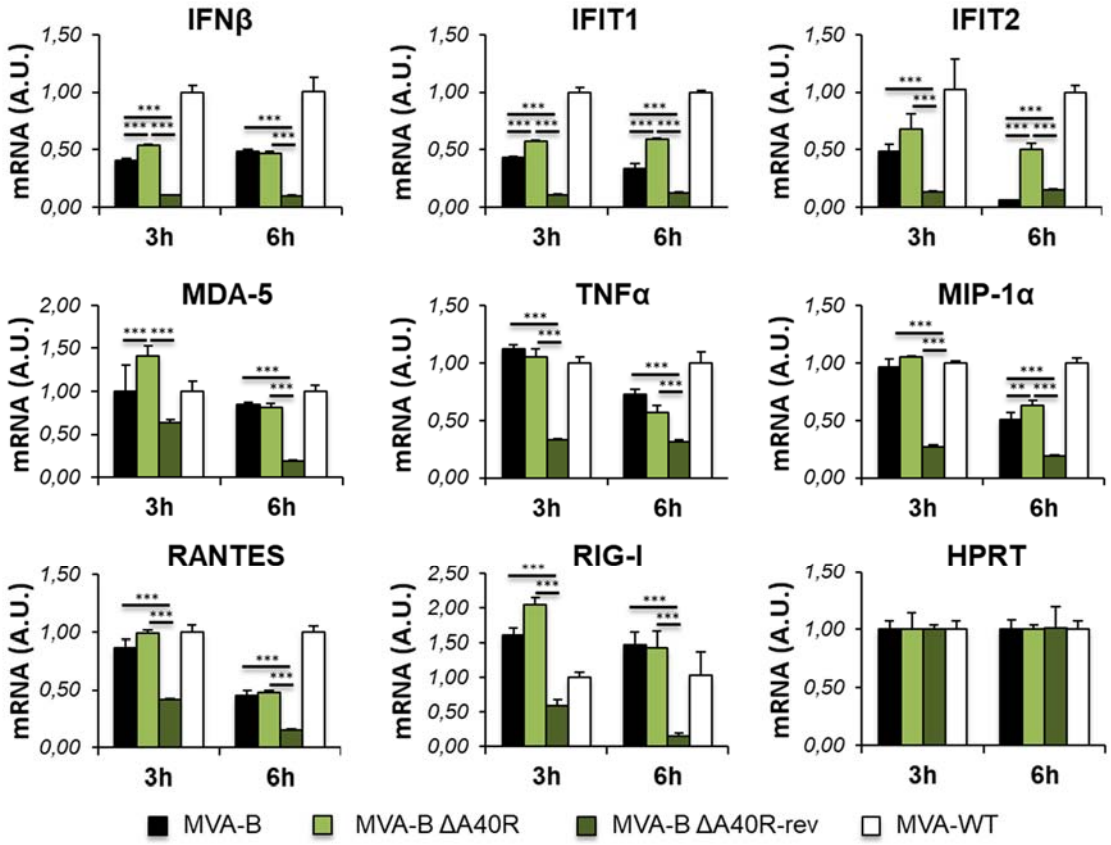

Figure 34. MVA-B ΔA40R-rev downregulated the mRNA levels of type I IFN, proinflammatory cytokines and chemokines. Human THP-1 macrophages were mock infected or infected with MVA-WT, MVA-B, MVA-B ΔA40R, or MVA-B ΔA40R-rev at 5 PFU/cell. At 3 and 6 h.p.i., RNA was extracted, and IFN-β, IFIT1, IFIT2, MDA-5, TNF-α, MIP-1α, RANTES, RIG-1, HPRT and VACV *E3L* mRNA levels were analyzed by RT-PCR. Results are expressed as the ratio of the gene of interest to VACV *E3L* mRNA levels. A.U., arbitrary units. P values indicate significant response differences between MVA-B, MVA-B ΔA40R, and MVA-B ΔA40R-rev at the same hour (**, $p<0.005$; ***, $p<0.001$). Data are means ± standard deviations of triplicate samples from one experiment and are representative of two independent experiments.

4.2.9. Reintroduction of MVA *A40R* gene in MVA-B ΔA40R impairs adaptive HIV-1-specific CD4⁺ T cell immune responses

Next, to know whether the reintroduction of VACV *A40R* gene in MVA-B ΔA40R could restore HIV-1-specific T cell immunogenicity (see Figs. 27 and 28), we analyzed the adaptive HIV-1-specific $CD4^+$ and $CD8^+$ T cell immune responses induced by MVA-B ΔA40R-rev in mice at 10 days after the last immunization, following the same DNA prime/MVA boost immunization protocol described before (see section 4.2.3).. The magnitude of the total HIV-1-specific $CD4^+$ T cell adaptive immune responses induced by the DNA-B/MVA-B ΔA40R-rev immunization group was similar to that induced by the

DNA-B/MVA-B group, but significantly lower than that induced by DNA-B/MVA-B ΔA40R (Fig. 35a), confirming that the reintroduction of VACV *A40R* gene in MVA-B ΔA40R restores the magnitude of the adaptive HIV-1 specific CD4⁺ T cell immune responses. The pattern of HIV-1-specific CD4⁺ T cell adaptive immune responses was similar in all immunization groups, being mainly directed against the Env pool (Fig. 35b, upper panel), with DNA-B/MVA-B ΔA40R-rev group restoring the Env-specific CD4⁺ T cell immune responses to levels similar to those induced by DNA-B/MVA-B. The polyfunctionality of HIV-1-specific CD4⁺ T cell adaptive immune responses was also similar in all immunization groups, with 84-90% of the CD4⁺ T cells exhibiting 2 or more functions (Fig. 35c).

However, the magnitude of the total HIV-1-specific CD8⁺ T cell adaptive immune responses induced by DNA-B/MVA-B ΔA40R-rev was similar to that induced by DNA-B/MVA-B ΔA40R (Fig. 35a). The pattern of HIV-1-specific CD8⁺ T cell adaptive immune responses was similar in all immunization groups, being mainly directed against the Env pool, followed by Gag and GPN (Fig. 35b, lower panel). In detail, DNA-B/MVA-B ΔA40R-rev induced similar or higher levels of Env- and GPN-specific CD8⁺ T cells than DNA-B/MVA-B ΔA40R immunization group, and restores the Gag-specific CD8⁺ T cell immune responses to levels similar to those induced by DNA-B/MVA-B (Fig. 35b, lower panel). The polyfunctionality of HIV-1-specific CD8⁺ T cell adaptive immune responses was also similar in all immunization groups, with around 50-60% of the CD8⁺ T cells exhibiting 2 or more functions (Fig. 35d).

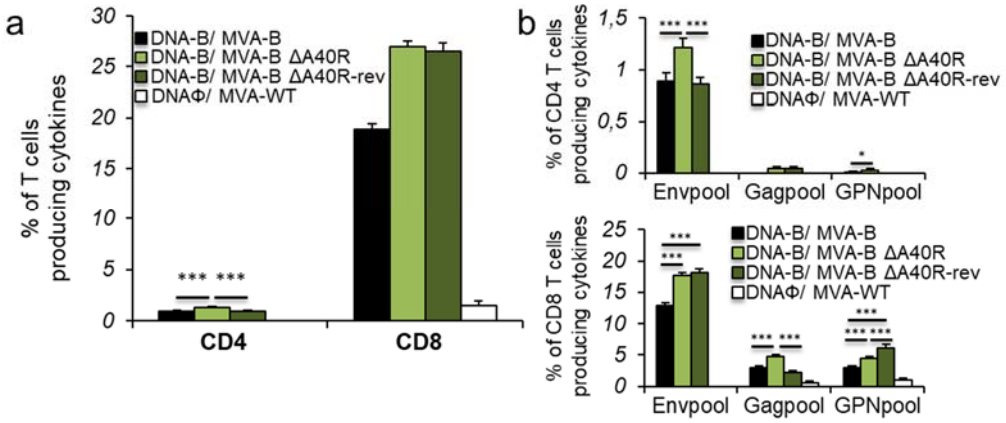

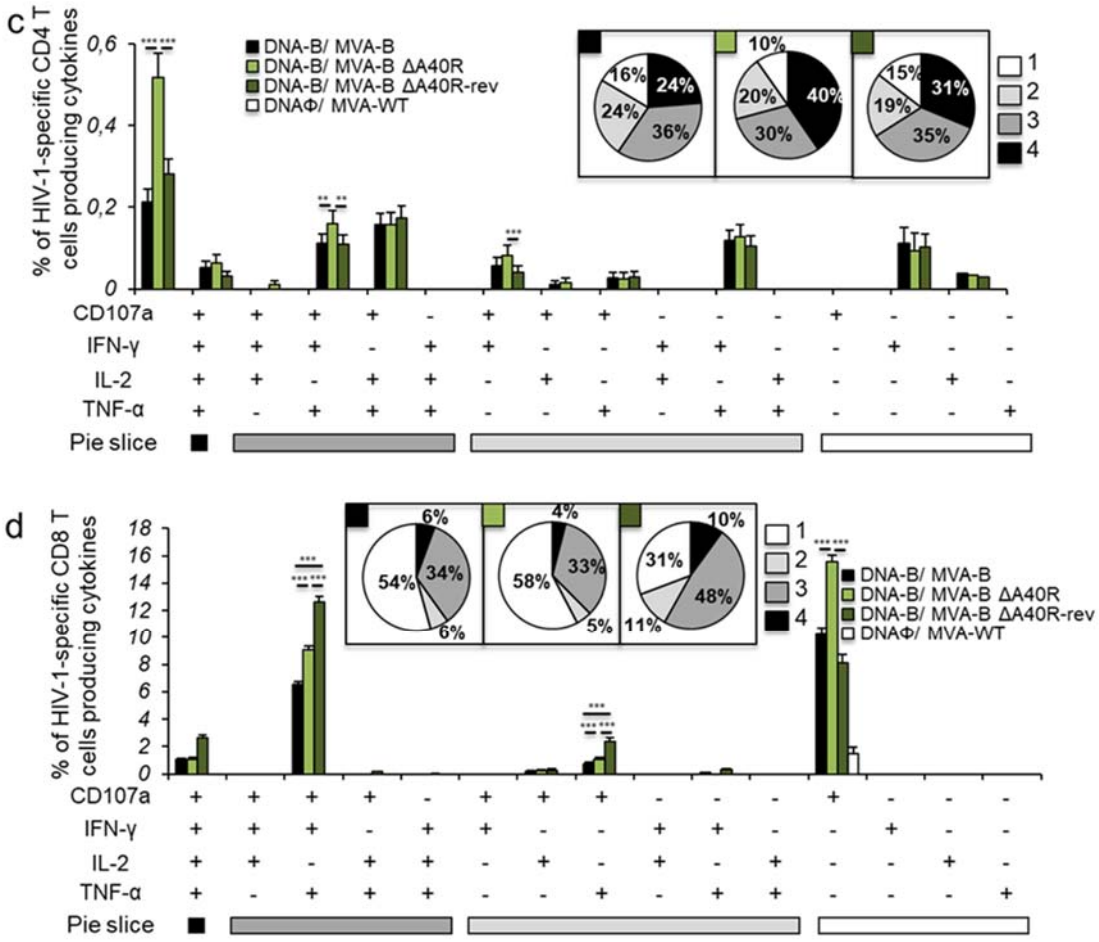

Figure 35. Immunization with MVA-B ΔA40R-rev impairs the magnitude of HIV-1-specific T cell adaptive immune responses. Splenocytes were collected from mice (n=4 per group) immunized with DNA-B/MVA-B, DNA-B/MVA-B ΔA40R, DNA-B/MVA-B ΔA40R-rev or DNA-φ/MVA-WT, 10 days after the last immunization. Next, HIV-1-specific T cell adaptive immune responses triggered by the different immunization groups were measured by ICS assay as described in the legend to Fig. 27. Values from unstimulated controls were subtracted in all cases. P values indicate significant response differences between immunization groups (**, p<0.005; ***, p<0.001). **(a)** Overall percentages of HIV-1-specific $CD4^+$ and $CD8^+$ T cells. The values represent the sum of the percentages of T cells producing CD107a and/or IFN-γ and/or TNF-α and/or IL-2 against Env, Gag, and GPN peptide pools. **(b)** Percentages of Env, Gag, and GPN HIV-1-specific $CD4^+$ (upper panel) and $CD8^+$ (lower panel) T cells. Frequencies represent the sum of the percentages of T cells producing CD107a and/or IFN-γ and/or TNF-α and/or IL-2 against Env, Gag, or GPN peptide pools. **(c and d)** Polyfunctional profiles of HIV-1-specific $CD4^+$ **(c)** and $CD8^+$ **(d)** T cells. All of the possible combinations of responses are shown on the x axis, while the percentages of T cells producing CD107a and/or IFN-γ and/or TNF-α and/or IL-2 against Env, Gag, and GPN peptide pools are shown on the y axis. Responses are grouped and color coded on the basis of the number of functions (4, 3, 2, or 1). The pie charts summarize the data. Each slice corresponds to the proportion of the total HIV-1-specific $CD4^+$ or $CD8^+$ T cells exhibiting 1, 2, 3, or 4 functions (CD107a and/or IFN-γ and/or TNF-α and/or IL-2) within the total HIV-1-specific $CD4^+$ or $CD8^+$ T cells

4.3. A vaccine based on an MVA vector expressing ZIKV structural proteins controls ZIKV replication in mice

After confirm that the HIV-1-specific immune responses were improved by modifying promoter strength or by deleting immunomodulatory VACV genes in MVA vaccine candidates against HIV/AIDS, the next step was to prove whether these modifications could be applied to novel MVA vectors against other viral diseases and can confer an advantage as candidate vaccines. Thus, ZIKV pathogen was selected, as it is responsible for severe human disease, particularly in new-borns due to microcephaly, and because the efficacy of vaccination against a ZIKV challenge can be demonstrated in a mouse model.

4.3.1. Generation and *in vitro* characterization of MVA-ZIKV

An optimized MVA-based vaccine candidate encoding for the ZIKV prM-E structural genes (termed MVA-ZIKV) that could activate the ZIKV-specific B and T cell immune responses was designed and generated (Fig. 36). ZIKV prM-E structural genes of the ZIKV isolate Z1106033 (Suriname; the most contemporary American isolate available at the time this work was initiated) [157], were inserted into the VACV TK locus of an optimized parental MVA (termed MVA-Δ-GFP) containing deletions in the VACV immunomodulatory genes *C6L*, *K7R*, and *A46R* [97,98]. Furthermore, the expression of the ZIKV antigens was placed under the control of the transcriptional novel optimized synthetic LEO160 promoter [88,89] (see the Results section 4.1 and Materials and Methods) (Fig. 36).

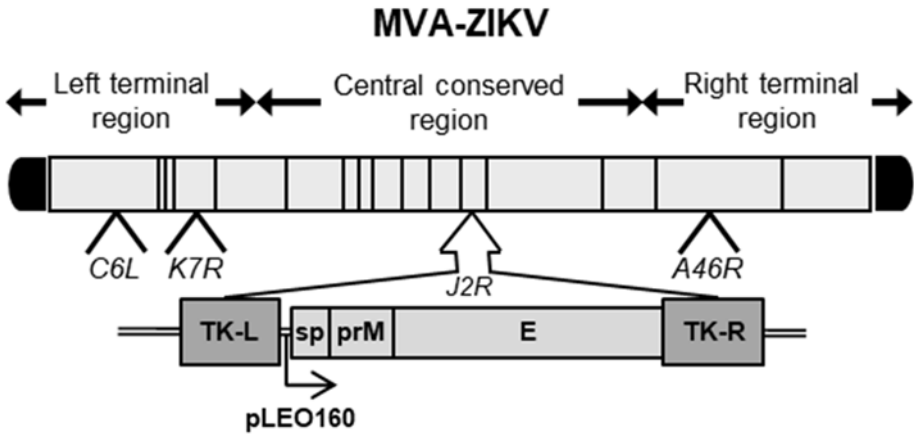

Figure 36. Scheme of the MVA-ZIKV genome map. The ZIKV signal peptide (sp) following by the ZIKV prM-E structural genes (isolate Z1106033) are driven by the novel VACV synthetic pLEO160 promoter and are inserted within the VACV TK viral locus (J2R). The deleted VACV *C6L*, *K7R*, and *A46R* genes are indicated. TK-L= TK left flanking region, TK-R= TK right flanking region.

The correct generation of MVA-ZIKV was analyzed by PCR using oligonucleotides annealing in the VACV TK-flanking regions that demonstrated the proper insertion of the ZIKV prM-E structural genes within the genome of MVA-ZIKV, with no parental MVA virus contamination (Fig. 37a). Moreover, the correct nucleotide sequence of the ZIKV prM-E genes inserted in the VACV TK locus was further confirmed by DNA sequencing (data not shown).

To demonstrate that MVA-ZIKV constitutively expresses and correctly processes the ZIKV prM-E polyprotein into prM and E structural proteins, we performed a Western blot analysis of cell extracts from MVA-infective permissive chicken DF-1 cells, mock infected or infected with MVA-ZIKV, parental MVA-Δ-GFP, or attenuated MVA-WT using specific antibodies that recognize the ZIKV prM and E proteins. The results proved that MVA-ZIKV correctly expressed the ZIKV prM-E polyprotein that was properly processed leading to the ZIKV prM and E proteins of expected molecular sizes (Fig. 37b). The presence of two bands in the western blot using the anti-ZIKV E antibody is compatible with the production of different ZIKV E protein species that differ in post-translational modification [186], being the upper band compatible with the full-length glycosylated E protein.

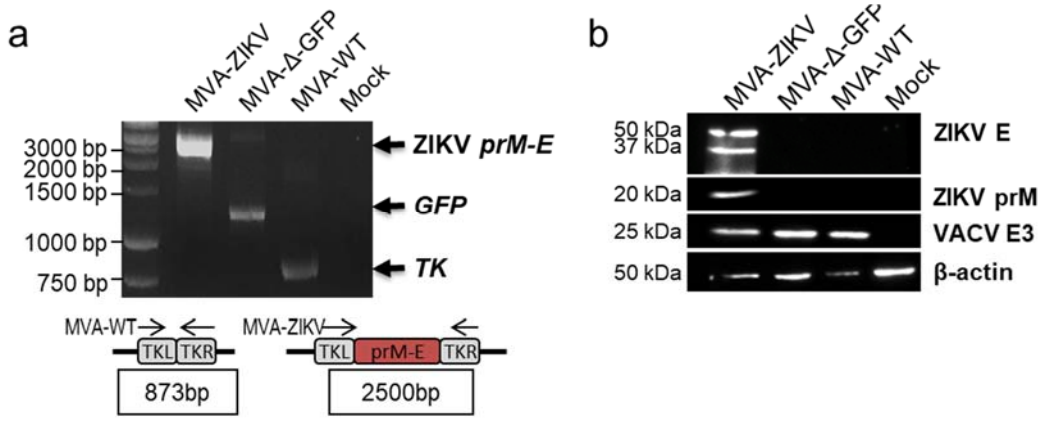

Figure 37. Generation and *in vitro* characterization of MVA-ZIKV. (a) PCR analysis of the VACV TK locus. Viral DNA was extracted from DF-1 cells mock infected or infected at 5 PFU/cell with MVA-ZIKV, MVA-Δ-GFP, or MVA-WT. Primers spanning the TK locus-flanking regions were used for PCR analysis of the ZIKV genes inserted within the TK locus. DNA products are indicated on the right and a molecular size marker (1-kb ladder) with the corresponding sizes (base pairs) is indicated on the left. PCR amplification schemes are placed below. **(b)** Expression of ZIKV prM and E proteins. DF-1 cells were mock infected or infected at 5 PFU/cell with MVA-ZIKV, MVA-Δ-GFP, or MVA-WT. At 24 h.p.i., cells were lysed, fractionated by 8% SDS-PAGE, and analyzed by Western blotting. The proteins detected are indicated on the right and the protein molecular weight (in kDa) is indicated on the left.

To analyze whether expression of ZIKV prM-E structural proteins affects MVA replication in cell culture, we evaluated the growth kinetics of MVA-ZIKV and MVA-WT in permissive DF-1 cells. Both viruses had a similar kinetics of viral growth (Fig. 38),

demonstrating that the constitutive expression of ZIKV prM-E structural proteins does not weaken MVA vector replication under permissive conditions. Moreover, similarly to parental MVA-WT and, as expected, MVA-ZIKV is a viral vector that does not replicate in human HeLa cells (Fig. 38).

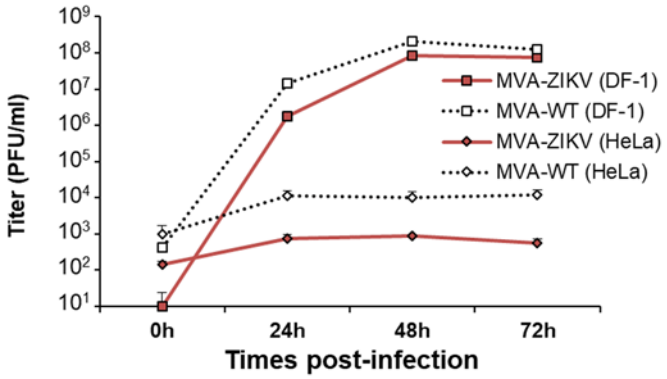

Figure 38. Viral growth kinetics of MVA-ZIKV. Monolayers of permissive DF-1 or non-permissive HeLa cells were infected at 0.01 PFU/cell with MVA-WT or MVA-ZIKV. At different times postinfection (0, 24, 48, and 72 h.p.i.), virus titers in cell lysates were quantified by a plaque immunostaining assay. The mean and standard deviations of two independent experiments is shown.

Next, to ensure that MVA-ZIKV is stable and the insert can be maintained in the viral genome without the loss of the sequence encoding the ZIKV prM-E structural genes, MVA-ZIKV was grown in DF-1 cells infected at low MOI for 9 successive passages, and expression of the ZIKV prM and E proteins was determined by Western blotting (Fig. 39a). The results revealed that MVA-ZIKV efficiently expresses the ZIKV prM and E proteins after consecutive passages. Moreover, analysis by Western blot of the expression of the ZIKV E protein in 24 individual plaques isolated from MVA-ZIKV at passage 9 showed that 100% of the plaques correctly expressed the ZIKV E protein (Fig. 39b), demonstrating the high genetic stability of MVA-ZIKV.

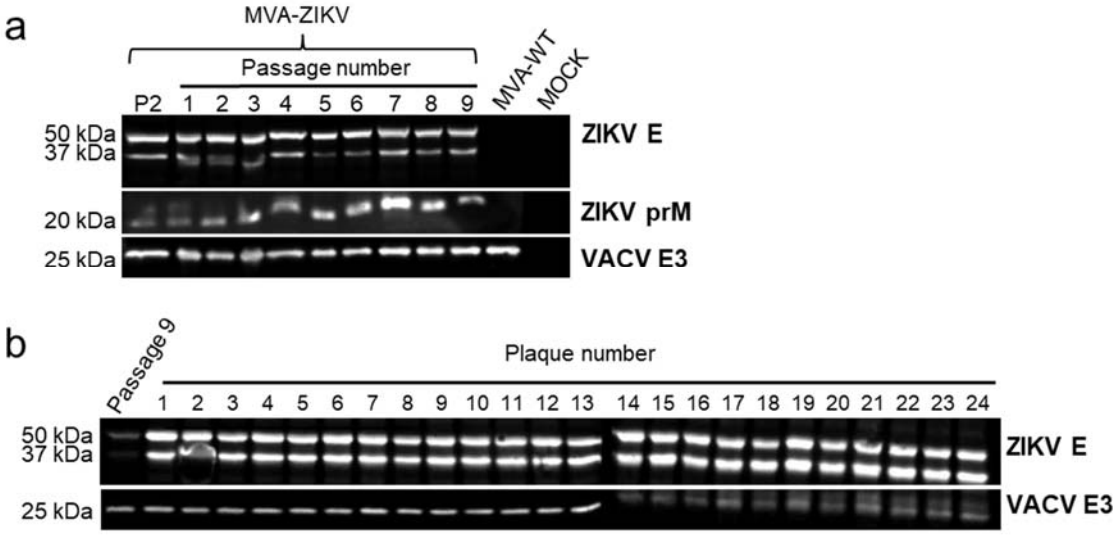

Figure 39. Stability of MVA-ZIKV. MVA-ZIKV (P2 stock) was continuously grown in DF-1 cells to passage 9 **(a)** and at passage 9, 24 individual plaques were picked **(b)**. Virus stocks from each passage and from the 24 individual plaques were used to infect cells and the expression of ZIKV prM and E proteins was determined by Western blotting in cell extracts. Rabbit anti-VACV E3 protein antibody was used as a VACV loading control. The proteins detected are indicated on the right and the protein molecular weight (in kDa) is indicated on the left.

Flavivirus prM and E proteins are synthesized at the ER [187]. Thus, the expression and intracellular localization of the ZIKV E protein expressed by MVA-ZIKV was studied by confocal immunofluorescence microscopy in non-permissive HeLa cells infected with MVA-ZIKV and MVA-WT using an antibody against ZIKV E protein and a specific antibody to detect ER (anti-Calnexin). The results showed that at 24 h.p.i. ZIKV E protein (in green) was highly expressed from MVA-ZIKV-infected cells and, as expected, co-localized with the ER (Fig. 40a, right panel). Moreover, to determine whether ZIKV E protein could be detected on the cell surface, HeLa cells were infected with MVA-ZIKV and permeabilized and non-permeabilized cells were analyzed by confocal immunofluorescence microscopy using an antibody against ZIKV E protein and the WGA probe to label the surface of fixed cells (Fig. 40b). While the infected-cell membrane was well observed using the WGA probe, labeling of ZIKV E protein was not detected. These results indicate that, as expected, the ZIKV E protein is not present on the surface of infected cells, and suggest that is release to the medium.

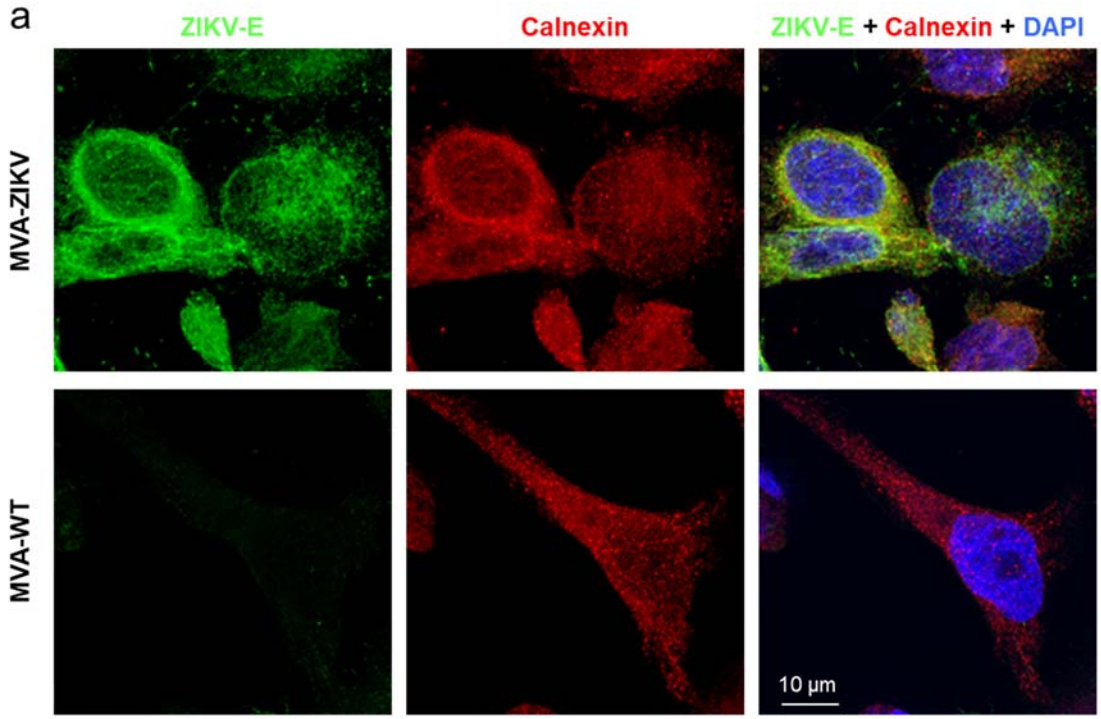

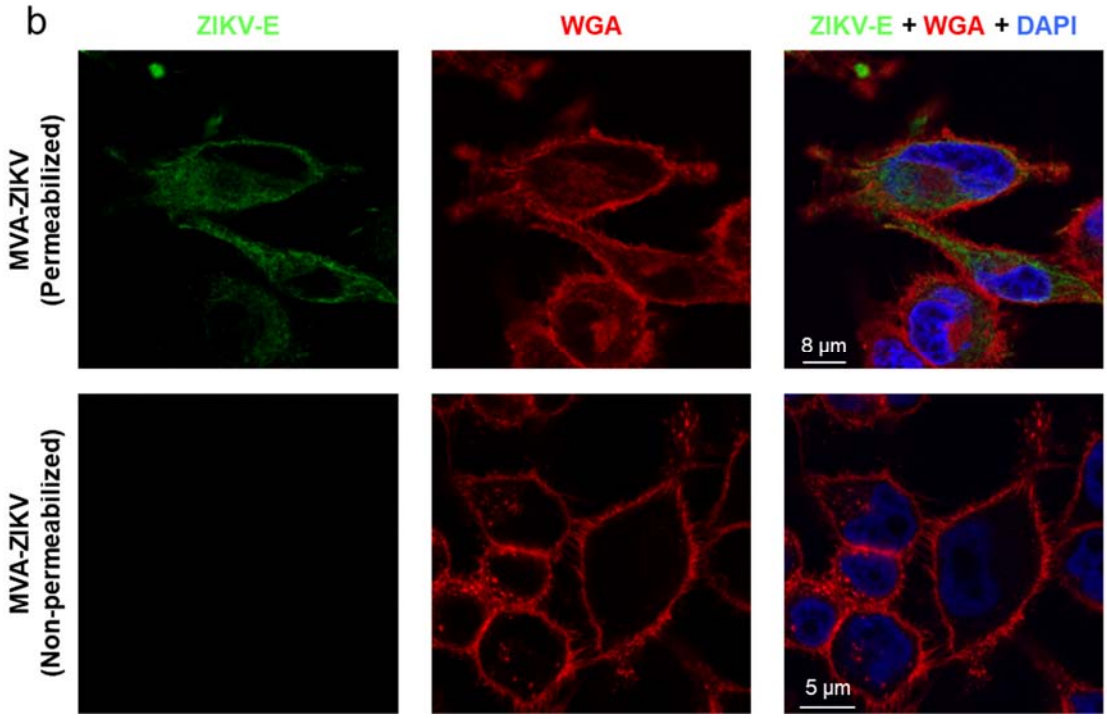

Figure 40. Immunofluorescence analysis of the expression of ZIKV E protein by MVA-ZIKV. (a) Detection of ZIKV E protein in the ER. HeLa cells were infected at 0.5 PFU/cell with MVA-ZIKV or MVA-WT for 24 h. Then, permeabilized cells were labeled with an anti-ZIKV E monoclonal mouse antibody and an anti-calnexin antibody. Anti-ZIKV E was detected with a mouse secondary antibody conjugated with the fluorochrome Alexa Fluor 488 (green). Anti-calnexin was detected with a rabbit secondary antibody conjugated with Alexa Fluor 594 (red). Cell nuclei were stained using DAPI (blue). The degree of co-localization of E and calnexin proteins is shown on the right by the yellow color. Scale bar: 10 µm. **(b)** Immunofluorescence analysis of ZIKV E protein in the cell membrane. HeLa cells were infected at 0.5 PFU/cell with MVA-ZIKV and at 24 h permebilized (upper panels) or non-permebilized (lower panels) fixed cells were stained with WGA probe conjugated to the fluorescent dye Alexa Fluor 594 (red) and a mouse monoclonal anti-ZIKV E antibody further detected with a mouse secondary antibody conjugated with the fluorochrome Alexa Fluor 488 (green). Cell nuclei were stained using DAPI (blue). Scale bars: 5 µm and 8 µm..

4.3.2. MVA-ZIKV produced VLPs

It has been described that coexpression of flaviviral prM and E proteins results in the production of VLPs [also termed subviral particles (SVPs)] [186,188–191]. Thus, to test whether MVA-ZIKV could form VLPs, we investigated their presence in the supernatant of infected cells. Therefore, HeLa cells were infected with MVA-ZIKV and MVA-WT and at 18 h.p.i., supernatants were concentrated by pelleting through a 20% sucrose cushion. The analysis by western blot of the concentrated supernatants demonstrated the presence of ZIKV M and E proteins, confirming their release to the medium (Fig. 41a). Moreover, the detection of a mature M protein suggests that fully-assembled VLPs could be produced (Fig. 41a).

Thus, next we loaded the concentrated supernatants into a 20-60% w/v sucrose gradient and after ultracentrifugation, fractions were taken and the amount of protein and sucrose density was analyzed (Fig. 41b). A single peak of protein, determined by measurement of the absorbance of each fraction at 280 nm, exhibited a density about 1.18 g/cm^3 (42% of sucrose) estimated by refractometry analysis. This value is comparable to that exhibited by other VLPs from different flaviviruses [192–195].

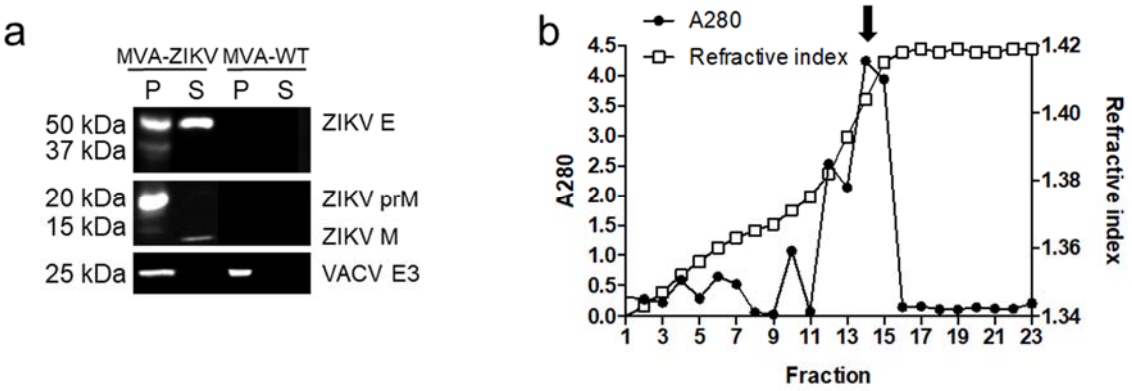

Figure 41. ZIKV VLPs purification. (a) Western blot analysis of the ZIKV proteins detected in cells extracts (P) or in supernatants (S) concentrated through a 20% sucrose cushion and derived from HeLa cells infected with MVA-ZIKV or MVA-WT. The proteins detected are indicated on the right and the protein molecular weight (in kDa) is indicated on the left **(b)** Amount of protein and sucrose density in fractions obtained after ultracentrifugation of MVA-ZIKV-concentrated supernatants loaded into a 20–60% w/v sucrose gradient. The amount of protein in each fraction was determined by spectrophotometry measuring the absorbance at 280 nm (A280). The sucrose density in each fraction was determined by refractometry. Arrow indicates the fraction (14) analyzed by electron microscopy.

The protein peak fraction was then analyzed by negative staining and transmission electron microscopy to evaluate whether VLPs were observed (Fig. 42a). The results showed that MVA-ZIKV formed smooth spherical particles of similar size (around 50 nm) and morphology than ZIKV VLPs produced by other ZIKV vaccines expressing prM-E genes [186,188,191,196] (Fig. 42a). Immunogold electron microscopy demonstrated the presence of ZIKV E protein on the surface of these structures, confirming that these particles were ZIKV VLPs (Fig. 42b).

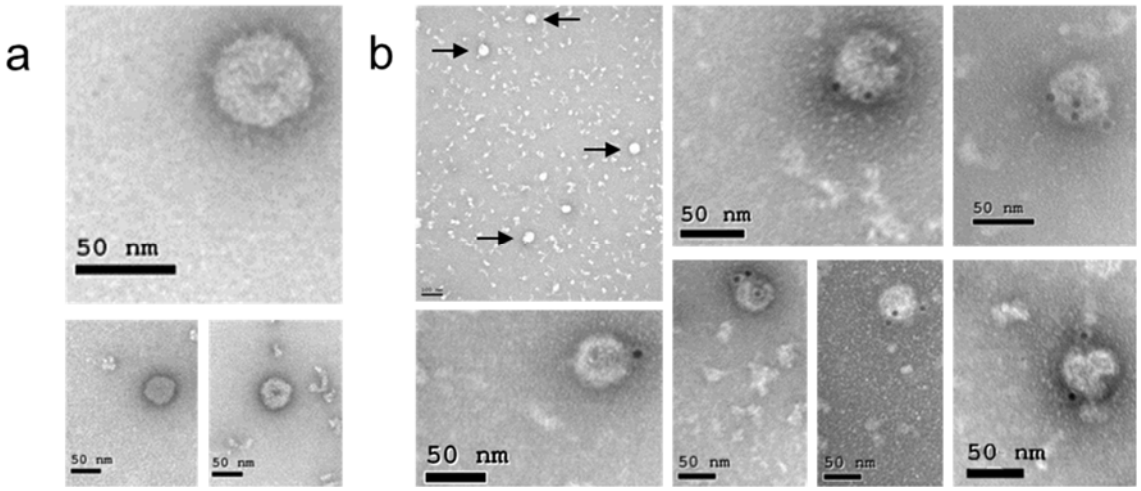

Figure 42. Detection by electron microscopy of VLPs produced by MVA-ZIKV. Negative-stained **(a)** or anti ZIKV E immunogold-stained **(b)** transmission electron microscopy images of purified ZIKV VLPs contained in the fraction 14 of the MVA-ZIKV gradient shown in Fig. 41b. Arrows indicate the VLPs detected in a lower magnification image of the immunogold-stained assay. Scale bar: 50 nm or 100nm.

4.3.3. MVA-ZIKV is highly immunogenic in immunocompetent mice

Neutralizing antibodies against ZIKV are critical to control ZIKV infection [197–199]. Thus, to evaluate the ability of MVA-ZIKV to induce neutralizing antibodies against ZIKV, we determined the PRNT against ZIKV in serum samples obtained at 10 days post-boost from Balb/c mice immunized with MVA-ZIKV or MVA-WT (negative control group), following a homologous MVA prime/MVA boost immunization protocol in which mice were immunized with 1 × 107 PFUs of MVA-WT or MVA-ZIKV by the i.p. route and two weeks later received a second dose of 2 × 107 PFUs of MVA-WT or MVA-ZIKV. The results showed that individual serum obtained from mice immunized with MVA-ZIKV neutralized ZIKV (PA259459 strain, from Panama) in a dilution-dependent manner (Fig. 43a), compared to serum from MVA-WT-immunized animals where no neutralization was observed. The elicited mean-value antibody titers induced by MVA-ZIKV neutralized 90% of ZIKV ($PRNT_{90}$) at a dilution of 1/50 (Fig. 43b).

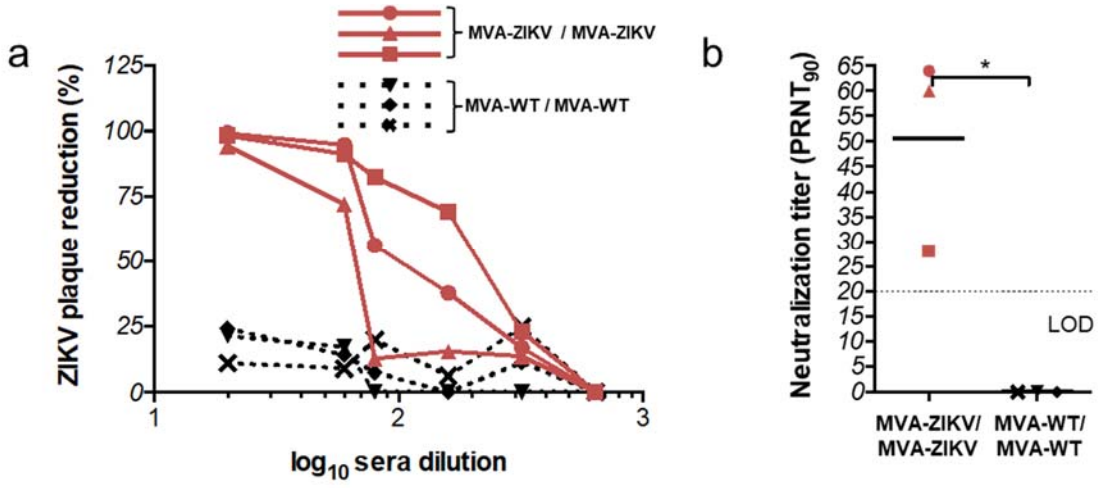

Figure 43. Induction of neutralizing antibodies by MVA-ZIKV in immunocompetent mice. Balb/c mice were immunized with MVA-ZIKV/MVA-ZIKV or MVA-WT/MVA-WT and 10 days after the last immunization ZIKV-specific humoral immune responses were analyzed (see Materials and Methods). **(a)** Percentage of ZIKV plaque reduction. Data represent the percentage of ZIKV plaque reduction, determined by a PRNT assay, from each individual serum sample at different serial dilutions. **(b)** ZIKV-neutralizing antibody titers. Data represent the reciprocal of the serum dilution that inhibited plaque formation by 90% ($PRNT_{90}$), relative to samples incubated with negative control sera. Dashed line indicates the limit of detection (LOD) of the neutralization assay (1/20 dilution). The statistically significant difference between both groups is indicated (*, $p< 0.05$).

Although the specificity of $CD8^+$ T cell responses varies among ZIKV strains, $CD8^+$ T cells might play a protective role against ZIKV infection [200–203]. Therefore, to investigate in detail the capability of MVA-ZIKV to stimulate T cellular immune responses against ZIKV, we next evaluated the ZIKV-specific T cell immune responses elicited by MVA-ZIKV in Balb/c mice immunized following a homologous prime/boost immunization protocol. ZIKV E-specific $CD4^+$ and $CD8^+$ T cell immune responses induced by MVA-WT/MVA-WT and MVA-ZIKV/MVA-ZIKV immunization groups were measured at 10 days post-boost by an ICS assay, after the stimulation of splenocytes with ZIKV-specific peptide pools spanning the entire ZIKV E protein. The results showed that immunization with MVA-ZIKV stimulated robust ZIKV-E-specific $CD8^+$ T cell immune responses (determined as the percentage of ZIKV E-specific $CD8^+$ T cells producing IFN-γ, TNF-α, and/or IL-2 cytokines, as well as the expression of CD107a on the surface of activated T cells as an indirect marker of cytotoxicity) (Fig. 44a). MVA-ZIKV elicited total ZIKV-specific immune responses mediated mostly by $CD8^+$ T cells, with very low levels of ZIKV-specific $CD4^+$ T cells (Fig. 44a). ZIKV-specific $CD8^+$ T cells produced mainly CD107a, followed by similar levels of IFN-γ and TNF-α, and to a minor extent IL-2 (Fig. 44b).

The quality of the ZIKV-specific T cell immune response was defined by the pattern of cytokine production (IFN-γ, TNF-α, and/or IL-2) and its cytotoxic potential (CD107a).

Thus, the most representative ZIKV-specific CD8⁺ T cell populations induced by MVA-ZIKV were those producing CD107a + IFN-γ + TNF-α (triple), CD107a + IFN-γ (double) and CD107a (single), with a high polyfunctional pattern represented by 57% of CD8⁺ T cells having two, three, or four functions (Fig. 44c).

Moreover, we also determined the phenotype of the ZIKV-specific CD8⁺ T cells by evaluating the presence of CD127 and CD62L surface markers, which define memory subpopulations: T central memory (TCM; CD127⁺/CD62L⁺), T effector memory (TEM; CD127⁺/CD62L⁻), and T effector (TE; CD127⁻/CD62L⁻) T cells [174]. The results showed that immunization with MVA-ZIKV induced ZIKV-specific CD8⁺ T cells with a phenotype of TEM (70%) and TE (30%) (Fig. 44d).

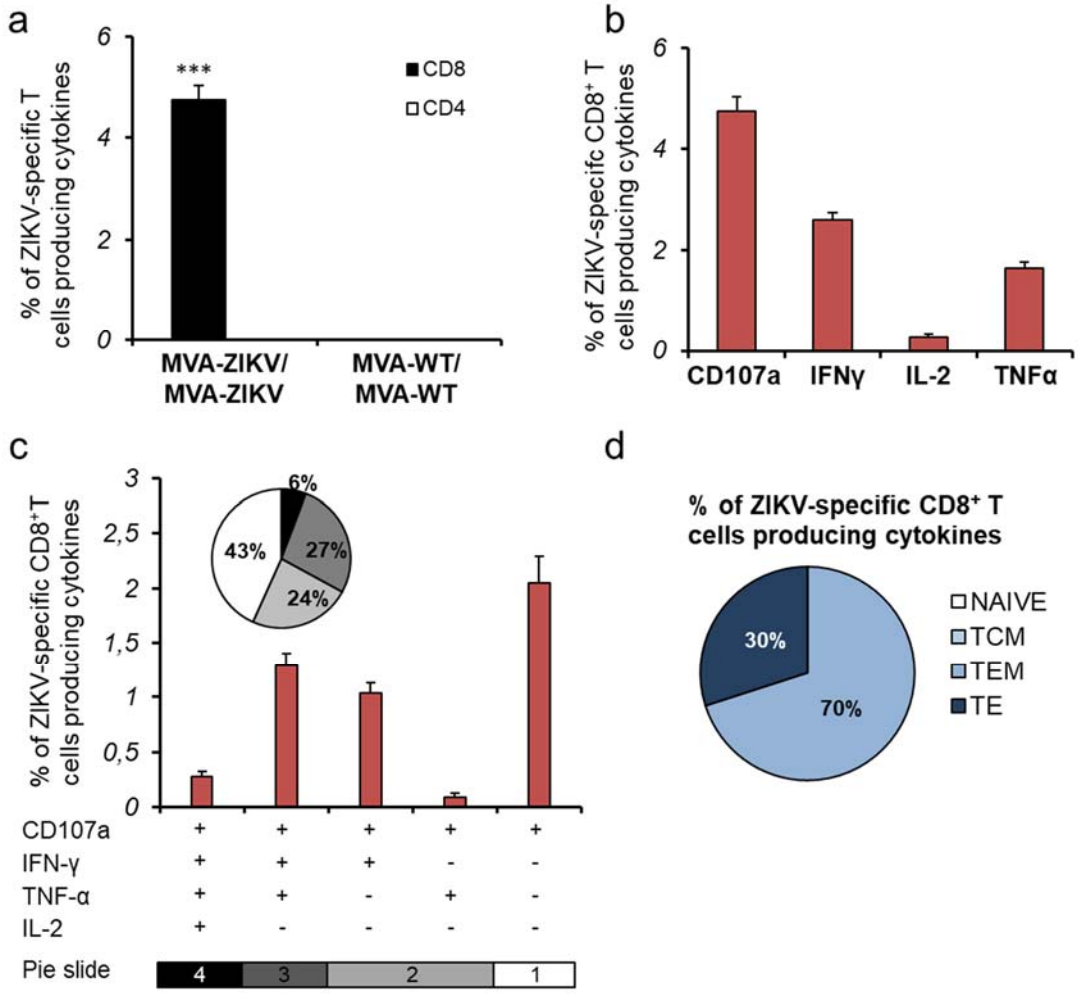

Figure 44. MVA-ZIKV induced robust CD8⁺ T cell responses in mice. Balb/c mice were immunized as in Fig. 43. **(a)** Overall magnitude of ZIKV-specific CD4⁺ and CD8⁺ T cells. The values represent the sums of the percentages of T cells producing CD107a and/or IFN-γ and/or TNF-α and/or IL-2 against the ZIKV E protein peptide pool. P values indicate significantly higher responses in comparison of MVA-ZIKV/MVA-ZIKV to MVA-WT/MVA-WT (***, p< 0.001). **(b)** Pattern of ZIKV-specific CD8⁺ T cell immune responses in MVA-ZIKV-vaccinated mice. Frequencies were calculated by reporting the number of CD8⁺ T cells producing CD107a, IFN-γ, TNF-α or IL-2. **(c)** Polyfunctional profile of ZIKV-specific CD8⁺ T cell immune responses in MVA-ZIKV-vaccinated mice. Those T cell populations

with a positive response are shown on the x axis, while the percentages of $CD8^+$ T cells producing CD107a and/or IFN-γ and/or TNF-α and/or IL-2 against the ZIKV E peptide pool are shown on the y axis. Responses are grouped and coded on the basis of the number of functions (4, 3, 2, or 1). The pie charts summarize the data, with each slice corresponding to the proportion of ZIKV-specific $CD8^+$ T cells exhibiting one, two, three, or four functions within the total population of ZIKV-specific $CD8^+$ T cells. **(d)** Phenotypic profile of ZIKV-specific $CD8^+$ T cells in MVA-ZIKV-vaccinated mice. CD127 and CD62L expression was used to identify naive, TCM, TEM and TE subpopulations. Each slice corresponds to the proportion of each ZIKV-specific $CD8^+$ T cell subpopulations within the total ZIKV-specific $CD8^+$ T cells producing CD107a and/or IFN-γ and/or TNF-α and/or IL-2.

4.3.4. MVA-ZIKV controls viral replication in a challenged mouse model

The efficacy of MVA-ZIKV as a vaccine candidate against ZIKV was studied in mice deficient in the α/β interferon receptor ($IFNAR^{-/-}$), a suitable susceptible mouse model for ZIKV [204,205]. Thus, six weeks old $IFNAR^{-/-}$ mice were immunized by i.p. route with MVA-ZIKV (one or two doses) or MVA-WT (one dose; use as a control), at days 0 and/or 14. At day 28 mice were challenged with 10^4 PFUs of ZIKV (PA259459 strain, from Panama). Blood was obtained at days 13 and 27 (before prime) to analyze the neutralizing antibodies in sera, and 2 and 3 days after virus challenge to analyze viremia (Fig. 45).

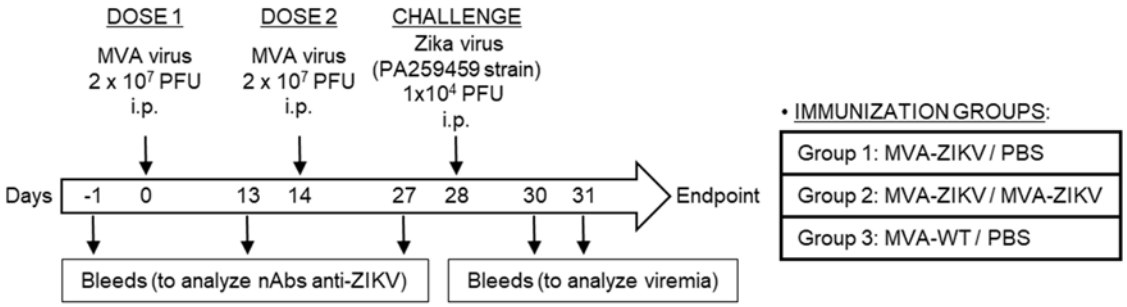

Figure 45. Inoculation scheme of the efficacy study of MVA-ZIKV. Groups of $IFNAR^{-/-}$ mice (n=10 mice/group) were immunized with 2 x 10^7 PFUs of MVA-WT (one dose, at day 0) or MVA-ZIKV (one or two doses, at days 0 and 14, respectively) by the i.p. route. Twenty eight days after the first immunization, mice were challenged with 10^4 PFUs of ZIKV (PA259459, strain Panama) via the i.p. route. Mice were bleed at day 13, 27, 30 and 31 to measure anti-ZIKV neutralizing antibody titers or viremia.

The results showed that one or two doses of MVA-ZIKV elicited good neutralizing antibody titers against ZIKV PA259459 strain, with a second dose significantly increasing the ZIKV neutralization titer ($PRNT_{90}$) to around 110 (Fig. 46a). Furthermore, neutralization of another ZIKV strain from the Asian lineage (FSS13025, Cambodia 2010) using serum samples obtained after two doses of the MVA-ZIKV vaccine showed similar results ($PRNT_{90}$ 149 ± 77), confirming that the elicited neutralizing antibodies could also neutralize other ZIKV strains. Next, the MVA-ZIKV efficacy was analyzed in immunized mice after challenge with ZIKV. Intraperitoneal infection of adult $IFNAR^{-/-}$ mice (10 weeks old) with the ZIKV American strain PA259459 did not induce severe body

weight loss or mortality, but induced viremia (Fig. 46b, c). Along this line, the MVA-ZIKV efficacy, defined as the capacity to control ZIKV replication, was evaluated at days 2 and 3 post-challenge determining in serum ZIKV viremia by quantitative RT-PCR (Fig. 46b) and presence of ZIKV infectious virus by plaque assay (Fig. 46c). The results showed that MVA-ZIKV-vaccinated mice control ZIKV replication as index of significant reduction in levels of ZIKV RNA (Fig. 46b) and of infectious virus (Fig. 46c), compared to the control group MVA-WT. One or two doses of MVA-ZIKV reduced the ZIKV viremia and infectious virus by 2.5-4 logs, while MVA-WT-immunized mice developed ZIKV infection, with high levels of ZIKV RNA and of infectious virus that peaked at day 2 post-challenge (Fig. 46b and c).

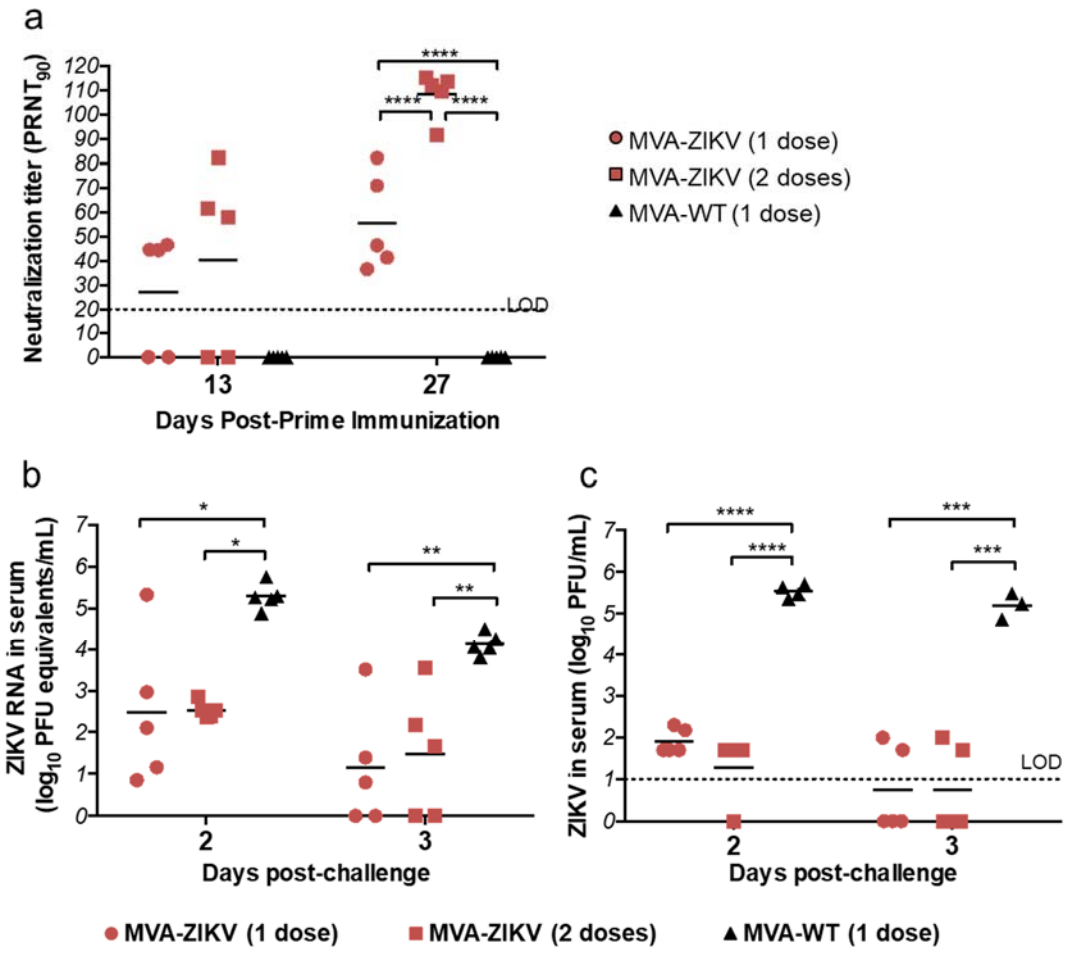

Figure 46. Efficacy of MVA-ZIKV in immunocompromised susceptible IFNAR$^{-/-}$ mice. **(a)** ZIKV-neutralizing antibody titers ($PRNT_{90}$) detected at 13 and 27 days post-prime immunization in sera (n=5) of animals immunized with one dose of MVA-WT or one or two doses of MVA-ZIKV. Titers of neutralizing antibodies against ZIKV PA259459 strain were determined by a PRNT assay and are expressed as the reciprocal of the serum dilution that inhibited plaque formation by 90% ($PRNT_{90}$), relative to samples incubated with negative control sera (from day 1 pre-prime). Dashed line indicates the limit of detection (LOD) of the neutralization assay (1/20 dilution). The statistically significant difference between the groups is indicated (****, p< 0.0001). **(b)** ZIKV RNA viremia after challenge. Blood samples were collected at days 2 (n = 5) or 3 (n = 5) post-challenge, and ZIKV RNA

viremia was analyzed by quantitative real-time PCR (PFU equivalents/ml). Graph shows mean with each point representing an individual mouse. P values indicate significantly higher responses between the different groups (*, $p< 0.05$; **, $p< 0.005$). **(c)** ZIKV infectious virus after challenge. Blood samples were collected at days 2 (n=5) or 3 (n=5) post-challenge, and ZIKV infectious virus was analyzed by a plaque assay (PFUs/ml). Graph shows mean with each point representing an individual mouse. P values indicate significantly higher responses between the different groups (***, $p< 0.001$, ****, $p< 0.0001$).

DISCUSSION

5. DISCUSSION

The aim of this Thesis is to improve the immunogenicity of the poxvirus MVA vector through several specific genetic modifications, such as enhancing virus promoter strength; deletion of immunomodulatory VACV genes; and optimizing antigen presentation. These modifications have been introduced in MVA vectors expressing HIV-1 antigens in order to prove in mouse models an improved HIV-1-specific immunogenicity. Furthermore, to demonstrate efficacy of some of these vectors, we have tested the ability of an optimized MVA vector lacking three VACV immunomodulatory genes and with a stronger virus promoter, for its capacity to induce in mice immunogenicity (T cell and neutralizing antibody responses) and protection against a human emerging pathogen, ZIKV.

The highly attenuated MVA poxvirus strain has several characteristics that make it an excellent vector to be use as a vaccine, such as: 1) it can insert up to 25 kpb of foreign DNA without loss of infectivity, thanks to the high packing flexibility of its genome; 2) it express high levels of the inserted heterologous antigen(s); 3) it has an exclusively cytoplasmic replication, which impede persistence in host cells or genomic integration; 4) it can induce both antibody and cytotoxic T cell immune responses against the heterologous antigen(s) with long-lasting immunity after a single inoculation; 5) it is stable when manufactured as freeze-dried vaccine; 6) it is relatively easy and cheap to produce and transport; and 7) it has the advantage over other vector-based vaccines, such as adenovirus, of a low prevalence of anti-VACV antibodies in the global population as the smallpox vaccination was interrupted following its eradication in 1980 [55,56,206]. Moreover, MVA recombinant vaccines combined the safety of a killed virus vaccine, due to their impaired replication capacity in human cells, with the immunogenicity of a live virus vaccine, through a great ability to induce antigen-specific immune responses due to the expression of gene products within the cells that are efficiently presented by both MHC class I and class II pathways, leading to potent activation of antigen-specific $CD4^+$ and $CD8^+$ T cells, and induction of robust humoral responses [55,56,206]. All these advantages make recombinant MVA vectors important vaccine candidates against several infectious diseases and cancer [52–56]. Nonetheless, more efficient and optimized MVA vector-based vaccines able to enhance antigen-specific T cellular and humoral immunogenicity are desirable [59].

5.1. Novel optimized MVA-based vaccine candidates against HIV/AIDS

Many recombinant poxvirus vectors (such as MVA, NYVAC, canarypox, and folwpox viruses) expressing different HIV-1 antigens have been widely used in several human clinical trials in the last few years, proving that they are safe and immunogenic, inducing HIV-1-specific cellular and humoral immune responses [55,62,207–209]. In fact, the recombinant canarypox vector vaccine ALVAC-HIV, expressing Env from subtypes B/E and Gag/Pro from subtype B combined with recombinant gp120 subunit vaccine from subtypes B/E (AIDSVAX B/E) is actually the only effective HIV/AIDS vaccine candidate, which showed a 31.2% protective effect in the RV144 phase III clinical trial [137].

A number of prophylactic and therapeutic HIV-1 vaccines at different stages of development are currently in the HIV/AIDS pipeline. Among them, various MVA-based vaccine candidates have been tested in human clinical trials, both as a single immunogen (such as the HIV/AIDS vaccine candidate MVA-B, generated in our laboratory), or in combination with other vaccine vectors, reinforcing the value of MVA vectors as vaccine candidates against HIV/AIDS (Table 4).

Vaccine	Trial number	Phase	Characteristics	Reference
Recombinant MVA vectors as single immunogen				
MVA-B (Env_{BX08}/GPN_{IIIB})	NCT00679497	I	Safe, well tolerated and elicited strong and durable T cell and antibody responses.	[115–121]
MVA Mosaic HIV	NTC02218125	I	Safe and well tolerated. Cellular and humoral cross-clade immune responses.	[210]
Recombinant MVA vectors in combination with different immunogens				
Ad26 Mosaic HIV prime. Ad26 Mosaic HIV or MVA Mosaic HIV and/or clade C gp140/aluminum phosphate boost	NCT02315703	I/II	Robust immune responses	[211]
DNA-HIV (Env_{CN54}/GPN_{ZM6}) prime. MVA-C/$rgp140_{CN54}$/GLA-AF adjuvant boost	NCT01922284	I	Potent cellular immune responses. No impact on the magnitude of CN54gp140-specific systemic antibody responses.	[212]
Ad35-GRIN/MVA.HIVconsv with/without pSG2. HIVconsv DNA with/without electroporation	NTC02099994	I/II	Well tolerated. Robust CD8+ T-cell responses to many normally subdominant epitopes	[213]
DNA Nat-B env or DNA CON-S env or DNA Mosaic env prime, MVA-CMDR boost	NCT02296541	I	Safe and immunogenic. Neutralizing antibodies in peripheral, moderate ADCC activity.	[214]
LIPO-5 or MVA HIV-B or DNA-GTU®-Multi HIV B prime and Lipo-5 or MVA HIV-B boost	NCT02038842	I/II	Safe and immunogenic. HIV-specific sustained $CD8^+$ and $CD4^+$ T-cell responses.	ClinicalTrials.gov

Table 4. Clinical trials in the HIV/AIDS pipeline that include MVA vectors. GRIN= Gag/RT/IN/Nef. MVA-CMDR= recombinant MVA-HIV vaccine expressing env/gag/pol inserts derived from a CRF01_AE HIV-1 isolate. LIPO-5= mixture of 5 HIV-lipopeptides. Adapted from [215].

However, besides the proved suitability of MVA recombinant vectors as vaccine candidates against HIV/AIDS, the efficacy elicited by these candidates in human clinical trials is still modest, and the immunogenicity against HIV-1 antigens limited. Thus, more efficient and optimized MVA-based HIV/AIDS vaccines able to enhance HIV-1-specific cellular and humoral immunogenicity are desirable [59]. In this Thesis we have applied two promising strategies to enhance the immunogenicity of MVA-based vaccines against HIV/AIDS:

5.1.1. Enhancing VACV promoter strength: Generation of MVA-LEO160-gp120

One of the approaches more recently applied to increase the immunogenicity of MVA recombinant vectors is the use of stronger VACV promoters to enhance the expression of foreign antigen(s) inserted in the MVA genome [59,87]. Poxviral promoters contains different sequence motifs that can be classified into early, intermediate, and late, depending on the expression timing during poxvirus infection [22,23]. The modification of the promoter sequence is an excellent approach to control transgene expression; for example, some have both early and late elements, allowing their ORFs or recombinant antigens to be expressed early in the virus infection and late after the viral genome replication. In the last few years, a number of poxviral promoters have been tested in recombinant MVA vectors, to increase recombinant antigen expression and, potentially, enhance antigen-specific immune responses [77,78,88,89,216,217]. Among them, one of the most promising is the novel synthetic VACV LEO promoter, which was previously designed in our laboratory using bioinformatic approaches and contains a late motif followed by an optimized immediate-early motif that allowed the transcriptional control of a heterologous antigen. The LEO promoter enhanced GFP expression and the magnitude of GFP-specific $CD8^+$ T cells in immunized mice [89]. Further improvement of the LEO promoter was achieved by elongating from 38 to 160 nucleotides the spacer sequence between the promoter elements and the transgene transcriptional start site (termed LEO160 promoter), thus improving antigen-specific memory $CD4^+$ and $CD8^+$ T cell responses in immunized mice, as tested with GFP or the *Leishmania* antigen LACK [88]. Thus, considering the strength of the LEO160 promoter in inducing better early expression of the intracellular GFP and LACK antigens, and improving antigen-specific cellular immune responses in immunized mice, this promoter modification was introduced in the context of an MVA-based

HIV/AIDS vaccine candidate. Therefore, the first genetic modification introduced in the genome of the MVA vector during this Thesis was the insertion of the novel VACV optimized LEO160 promoter to try to enhance the expression and immunogenicity of the HIV-1 gp120 antigen from clade B. The recombinant virus MVA-LEO160-gp120 was generated to define the role of the LEO160 promoter strength in the early expression and secretion of the soluble HIV-1 gp120 antigen, and to test whether gp120-specific cellular and humoral immune responses could be enhanced.

When a new promoter or insertion site is inserted within any viral vector the demonstration of the genetic stability of the transgenes should be tested, because several reports have suggested that the promoter used and/or the insertion site could affect the stability of the recombinant transgene [218–220]. Although genetic stability data were absent in previous LEO promoter reports [88,89], here the high genetic stability of MVA-LEO160-gp120 is demonstrated through long-term passages in cell culture showing high levels of expression of the HIV-1 gp120 antigen during all the passages.

The temporal expression of HIV-1 gp120 under the control of the LEO160 promoter was studied and the results showed that the mRNA transcription levels of HIV-1 gp120 and the total HIV-1 gp120 protein production in cells infected with MVA-LEO160-gp120 was significantly upregulated at all times studied compared with cells infected with the HIV/AIDS vaccine candidate MVA-B, that express simultaneously the HIV-1_{IIIB} GPN as an intracellular polyprotein and HIV-1_{BX08} gp120 as a cell-released product from HIV-1 clade B isolates under the control of the widely used sE/L promoter [221]. These results confirm the previous results obtained by [88,89], and are in agreement with various recent studies reporting that new early promoters increase the expression of heterologous antigen under their transcriptional control [78,216,217], when compared to the early and late p7.5 promoter (p7.5), one of the first VACV promoters described [222], and to the widely used synthetic VACV sE/L promoter [221].

Moreover, the analysis of the HIV-1 gp120 secretion to the extracellular media showed a significant enhancement at early times post-infection in cells infected with MVA-LEO160-gp120, compared to MVA-B-infected cells; confirming that the LEO160 promoter can also enhance the cell release of a soluble antigen, such as HIV-1 gp120.

Few comparative studies have reported about the choice of transgene promoter or insertion site and heterologous antigen secretion *in vitro* from poxviral vectors, but some reports have associate an increase in the secretion of an MVA transgene with an enhanced transgene-specific immune responses [104]. Thus, next to determine whether the enhanced levels of HIV-1 gp120 expressed by MVA-LEO160-gp120 observed in

cultured cells could correlate with an increased magnitude of HIV-1-specific T cellular and humoral immune responses *in vivo*, a DNA-gp120 prime/MVA boost immunization protocol was performed in mice, as this regimen has been stablished to increase the antigen-specific T cell and humoral immune responses over homologous immunization vectors [113,170]. Compared to DNA-gp120/MVA-B, DNA-gp120/MVA-LEO160-gp120 significantly enhanced the magnitude of the adaptive HIV-1 gp120-specific $CD4^+$ and $CD8^+$ T cell immune responses. Similar results were obtained using a homologous MVA/MVA immunization regimen but, as expected, the elicited HIV-1 gp120-specific $CD4^+$ and $CD8^+$ T cell responses magnitudes were lower (data not shown). Apart from the results obtained from previous reports of our lab with the novel LEO promoter, many other reports confirmed a positive correlation between enhanced early expression triggered by MVA vectors and increased T cellular immunogenicity [77,78,216,218]. In particular, a previous report of MVA recombinants expressing either enhanced GFP or chicken ovalbumin, each under the control of a hybrid early-late promoter (pHyb) compared with the widely used 7.5 and sE/L promoters, have demonstrated that a stronger immediate-early neoantigen expression by a poxviral vector results in superior induction of neoantigen-specific $CD8^+$ T cell responses [78], and were able to stimulate potent recall responses after repeated boosters providing an advantage in the context of homologous vaccination regimes and immunotherapy [216]. Furthermore, in the field of MVA-based HIV/AIDS vaccine candidates, a previous report has already correlated a 4 to 7-fold enhanced expression of HIV-1 Env antigen driven by the stronger mH5 promoter with a significant increase in Env-specific $CD4^+$ (1 to 2-fold) and $CD8^+$ T (3 to 5-fold) cell responses [77]. This results are in agreement with the results obtained with the MVA-LEO160-gp120, in which an up to 9-fold increase expression of HIV-1 gp120 antigen correlate with a increase in Env-specific $CD4^+$ (1.5-fold) and $CD8^+$ T (3-fold) cell responses

The increase in HIV-1 gp120-specific $CD4^+$ and $CD8^+$ T cell responses obtained with the DNA-gp120/MVA-LEO160-gp120 immunization could be of relevant importance, because several studies indicate that the HIV-1-specific cellular response goes some way towards controlling HIV-1 infection, although it fails ultimately to deal with virus infection [223]. Vaccines that can stimulate both $CD4^+$ and $CD8^+$ T cell responses to HIV-1 may be able to control the virus early in infection before it causes major immune damage, as was demonstrated with the partially efficacy obtained in the RV144 trial [137].

Additionally, when evaluating the HIV-1-specific cellular immune responses, it is also important to consider the phenotype of the T cells elicited, because a fast acquisition of

TEM and TE phenotypes in the adaptive phase could be important in the development of the T cell memory responses and in the mounting of a more effective immunity during a primary pathogen encounter, as the presence of TEM cells has been correlated with protection in the macaque-simian immunodeficiency virus model [224,225]. In this Thesis, both immunization groups elicited mainly HIV-1 gp120-specific T cells of a TEM phenotype, followed by a TE phenotype; again, DNA-gp120/MVA-LEO160-gp120 significantly enhanced the magnitude of these T cell populations, which is a positive cell marker for HIV-1 protective responses.

Furthermore, it has been identified a $CD4^+$ T cell population, named Tfh cells, which is responsible for providing help to B cells [226]. Since then a deep research of this T cell subpopulation has been done in the context of HIV-1 infection and vaccine development [176]. Circulating HIV-1-specific $IL\text{-}21^+$ Tfh cells were found at higher frequencies in sera from participants in the partially protective ALVAC+AIDSVAX (RV144) HIV/AIDS clinical trial compared to the non-protective DNA+Ad5 clinical trial, thus correlating protective antibody responses with elevated percentages of this $CD4^+$ T cell subtype [227]. Moreover, in HIV-1-infected patients it has been reported a correlation between the frequencies of circulating Tfh cells and the induction of bNAbs [228], and in HIV-1 controllers higher percentages of circulating Tfh cells have been associated with the induction of HIV-1-specific antibodies in functional assays favouring preserved memory B cell responses [229]. Given the central role for the Tfh cell response in inducing protective responses against HIV-1, the percentages of total and HIV-1 gp120-specific Tfh cells elicited by the recombinant MVA-LEO160-gp120 in comparison with the MVA-B vaccine candidate were studied. The results obtained in immunized mice showed that the overall magnitude of HIV-1-gp120-specific Tfh cell response was significantly higher in splenocytes from animals receiving DNA-gp120/MVA-LEO160-gp120 immunization compared with the group immunized with DNA-gp120/MVA-B, disclosing the ability of the LEO160 promoter to increase also the HIV-1-gp120-specific response of this important cell subtype. These findings are in agreement with recent results from our laboratory that suggest that MVA-based vectors might represent an advantageous platform to potentially activate HIV-1-specific Tfh cell responses [108,230].

Although the positive correlation between the heterologous antigen expression in the MVA system and the improvement of the T cell (particularly $CD8^+$) responses has been well documented [77,78,88,216,218], none of these reports have found difference in the levels of neo-antigen-specific antibodies independently of the promoter used [216]. This result was attributed to the fact that during VACV infection the late and intermediate

genes have shown to be the preferred targets for antibody responses [79,80], but the factors that regulate and determine the antibody responses from MVA expressed genes are still not well defined. Here, when HIV-1-specific humoral immune responses elicited in serum samples from immunized animals were analysed by ELISA, the data revealed that DNA-gp120/MVA-LEO160-gp120 immunization protocol enhanced the levels of total IgG binding antibodies against HIV-1 gp120 protein compared to DNA-gp120/MVA-B. The more efficient production of anti-Env-specific antibodies seen may be due to the higher expression of HIV-1 Env in infected cells, as the modest but significant higher total IgG HIV-1 Env binding antibody levels observed in mice immunized with DNA-gp120/MVA-LEO160-gp120 is consistent with the higher levels of gp120 observed in MVA-LEO160-gp120-infected cells. Even though, it is suggested that in MVA immunizations antibodies are mainly induced against late poxviral antigens [231], here an enhancement in the antigen-specific antibody responses obtained by an early stronger transgene expression is shown. Although a previous report using a promoter optimization within the VACV replicative strain LC16m8 expressing HIV-1 Env found an increased production of anti-HIV-1 Env-specific antibodies when the stronger SFJ1-10 promoter was used, compared with the widely used p7.5 [217], this is the first time that this phenomenon is described for a recombinant MVA vector. Higher levels of total IgG in serum could be an important parameter associated with the protective effect induced by HIV/AIDS vaccine candidates, because studies on the RV144 vaccine regimen revealed that the protection against HIV-1 infection was directly correlated with the level of IgG antibodies specific for the HIV-1 gp120 V1V2 region [137,232].

In summary, the results obtained demonstrate how VACV promoter strength modification can be use to enhance the levels of HIV-1 gp120 soluble protein in cells infected with an MVA vector. *In vivo*, the magnitude of the HIV-1 gp120-specific $CD4^+$ and $CD8^+$ T cell immune responses and the levels of anti-gp120 antibodies were also increased, demonstrating the enhanced immune properties of this promoter. Thus, based on its capacity to increase heterologous antigen expression *in vitro* and antigen-specific $CD4^+$ and $CD8^+$ T cell responses *in vivo*, the novel synthetic VACV LEO160 promoter is a promising prototype to be used in the design of novel future poxvirus-based vaccine vectors.

5.1.2. Deletion of an expected immunomodulatory MVA gene: Generation of MVA-B ΔA40R

Another promising strategy developed to enhance the immune response induced by MVA vectors, is the removal of one or more VACV immunomodulatory genes that are still present in the MVA genome [28,29,57]. Several recombinant MVA vectors

expressing HIV-1 antigens and containing deletions in different immunomodulatory VACV genes have been generated, and were able to enhance the immune responses to HIV-1 antigens in animal models [90–94,96,233].

Therefore, the second genetic modification introduced in the genome of the MVA vector during this Thesis was the deletion of the VACV *A40R* gene, a C-type lectin homolog whose immunomodulatory role was previously not known. The role of the VACV gene *A40R* is controversial. On one hand, several studies from Dr. G.L. Smith group reported that the VACV WR *A40R* gene encodes a type II membrane glycoprotein that shares amino acid similarity to the CDR domain of C-type lectins (including NK cell receptors, the human IgE receptor and CD69) and it is expressed early during infection on the cell surface, but is not incorporated into IMVs or EEVs [99]. C-type lectins are key players in pathogen recognition and innate immunity [100], and, in this regard, the A40 protein might have a role in interfering the host response to infection. Moreover, the localization of A40 protein at the cell surface suggest that it may modulate the immune response interacting at the plasma membrane level with signaling pathways and/or with other cells, but there is no evidence for any of these interactions. Interestingly, deletion of VACV *A40R* gene from the VACV WR strain, showed a modest attenuation after intradermal inoculation of mice, which could perhaps reflect an immunomodulatory role for this protein [101]. On the other hand, other reports affirmed that VACV A40 is an early protein that is partially SUMO-1-modified and associated with the viral “mini-nuclei” [103]. Although the small amount of non-sumoylated A40 protein might have a role in the VACV life cycle joining the cytosolic side of the ER and inducing the proper apposition of several ER cisternae before their fusion to generate the ER envelope that surrounds the viral replication sites, the role that sumoylated A40 protein could play in the VACV life cycle still remains unknown. Other options are that A40 protein could participate in the process of replication itself or in the late transcription happening at VACV replication sites, becoming A40 essential for VACV life cycle [102]. However, nothing was previously known about the immune function of this VACV gene.

Consequently, to evaluate whether the VACV A40 protein has an immunomodulatory role an MVA recombinant vector lacking the VACV *A40R* gene was generated from the HIV/AIDS vaccine candidate MVA-B (termed MVA-B ΔA40R). The results showed that *A40R* deletion has no effect on virus growth, demonstrating that VACV *A40R* gene is not essential for VACV life cycle, differing on what was suggested by others [102].

As the loss of immunomodulatory genes in the MVA backbone impairs the innate immune response to this vector [90,93,94], the first step to elucidate the supposed

immunomodulatory role of the MVA *A40R* gene was to study the innate immune responses in THP-1 human macrophages infected with MVA-WT, parental MVA-B and MVA-B ΔA40R deletion mutant. The results showed that, compared to parental MVA-B, MVA-B ΔA40R significantly enhanced the expression of several genes involved in the type I IFN signaling pathway such as IFN-β, IFIT1, IFIT2, as well as the pro-inflammatory chemokine MIP-1α and the viral dsRNA sensor MDA-5, suggesting that MVA A40 protein could have an immunomodulatory role blocking innate immune responses during virus infection. Moreover, since it has been described that innate immune responses play a critical role in the control and resolution of HIV-1 infection, providing signals for the efficient priming of the adaptive branch of immune response [234]; these results could prove and advantage of this recombinant vector as HIV/AIDS vaccine candidate.

To further define whether VACV A40 could impair the immune system *in vivo*, a DNA prime/MVA boost immunization protocol was performed in mice to compare adaptive and memory immune responses to HIV-1 antigens induced by parental MVA-B and the deletion mutant MVA-B ΔA40R. Results showed that DNA-B/MVA-B ΔA40R immunization group significantly enhanced the magnitude of the overall adaptive and memory HIV-1-specific $CD4^+$ and $CD8^+$ T cells producing CD107a, IFN-γ, TNF-α, and/or IL-2 compared to DNA-B/MVA-B. These results further suggest the immunosuppressive role of VACV A40 protein, as deletions of well-known immunosuppressive VACV genes from MVA or NYVAC vectors expressing HIV-1 antigens behave similarly [90,91,237,238,92–96,233,235,236]. Furthermore, both immunization groups elicited an adaptive and memory HIV-1-specific T cell immune response with a similar polyfunctional profile and mainly with TEM and to a lesser extent TE phenotypes. However, again MVA-B ΔA40R significantly enhanced the magnitude of those populations, an important and relevant feature because the presence of TEM has been correlated with protection in the macaque-simian immunodeficiency virus model [224,225], as we stated previously in the promoter optimization discussion section. Moreover, adaptive and memory $CD4^+$ T cell immune responses were directed mainly against Env in both immunization groups. However, in contrast to other MVA-B deletion mutants previously characterized (with deletions in *C6L*, *C6L-K7R* and *A41L-B16R* MVA genes), where a pattern of GPN-specific $CD8^+$ T cell immune responses was mainly induced [91–93], MVA-B ΔA40R triggered $CD8^+$ T cell immune responses preferentially directed against Env, similarly as the MVA-B deletion mutant lacking the N2L gene, encoding for a nuclear inhibitor of IRF3 [90]. The biological relevance of this T cell immune shift is not known.

The analysis of the gp120-specific humoral immune responses at the adaptive and memory phases showed that DNA-B/MVA-B ΔA40R immunization induced higher levels of total IgG, IgG1, IgG2a, and IgG3 anti-gp120 antibodies than DNA-B/MVA-B. This enhancement may be mediated by the increases in innate immune responses and, as discussed before, it could be a positive immune parameter, as it has been described that IgG avidity and ADCC activity inversely correlated with infection indicating that these antibodies could have contributed to the observed protection in the RV144 phase III clinical trial [232].

To finally demonstrate that the *in vivo* effects triggered by MVA-B ΔA40R in immunized mice were due to the deletion of the MVA *A40R* gene, and to confirm the previously suggested immunosuppressive role exerted by the MVA *A40R* gene, a revertant virus, termed MVA-B ΔA40R-rev, was generated by reintroducing the MVA *A40R* gene into the MVA HA locus of MVA-B ΔA40R under the transcriptional control of the sE/L virus promoter. The MVA-B ΔA40R-rev expressed the MVA *A40R* gene at higher mRNA levels (7-fold) than MVA-B or MVA-WT, which subsequently allowed to amplify the signal of the A40 protein during virus infection. In the MVA-B or MVA-WT viruses the protein levels of A40 were very low since the rabbit polyclonal antibody anti-A40 used could not detect the A40 protein by Western blot, while in MVA-B ΔA40R-rev-infected cells A40 protein was readily detected. For these experiments, we used the same antibody that was described in the first report of the A40 protein from the WR strain [99]. The Western blot with this anti-A40 antibody detected three major bands at 18, 28 and 35 kDa. It has been suggested that the 18 kDa form correspond with the unglycosylated A40 protein whereas the 28 and 35 kDa forms (together with a 38 kDa form that was not detected here) correspond with the N- and O-linked glycosylated forms of A40 [99]. The over-expression of A40 by MVA-B ΔA40R-rev provided also the means to follow the subcellular localization of the A40 protein. The immunofluorescence analysis of MVA-B ΔA40R-rev-infected HeLa cells detected the A40 protein at the cell surface membrane in non-permeabilized cells, and as punctuate cytoplasmic structures in permeabilized cells that appear to colocalize with the Golgi network and exocytic vesicles. These results were similar to the results obtained previously by the group of G.L. Smith [99] and reinforce the membrane localization of A40 protein, in contrast to what stated the group of Jacomine Krijnse-Locker [103].

Importantly, the qRT-PCR experiments showed that mRNA levels of IFN-β, IFIT1, IFIT2, MDA-5, and MIP-1α in MVA-B ΔA40R-rev–infected human THP-1 macrophages were lower than those induced by MVA-B ΔA40R or MVA-B. Interestingly, MVA-B ΔA40R-rev was able to impair the mRNA levels of other cytokines that were not affected

by the deletion of the *A40R* gene in the recombinant MVA-B ΔA40R, such as TNFα and RANTES, and the viral sensor RIG-I; but other constitutive cellular gene, HPRT, and the heterologous gp120 gene mRNA levels were not affected, suggesting that A40 only blocks innate immune sensing genes. The clear decrease in the levels of cytokines and chemokines induced by the revertant virus MVA-B ΔA40R-rev, expressing high mRNA levels of VACV *A40R* gene and of A40 protein, confirm their immunosuppressive function. However, at what level of the innate signaling pathways acts the A40 protein is still unknown, although the results suggest that blocks the type I IFN signaling pathway.

Moreover, the enhancing effect on adaptive HIV-1 specific $CD4^+$ T cell immune responses observed in mice immunized with MVA-B ΔA40R was restored to levels similar to MVA-B when the MVA *A40R* gene was reintroduced in the MVA-B ΔA40R backbone, confirming *in vivo* the immunosuppressive function of VACV A40 protein. However, this phenomenon was not observed for the HIV-1 specific $CD8^+$ T cell immune responses, where MVA-B ΔA40R and MVA-B ΔA40R-rev induced similar levels. This could be explained by the over-expression of the A40 in the MVA-B ΔA40R-rev recombinant virus, as shown in *in vitro* experiments from the impact on cytokine mRNA levels elicited by over-expression of A40R gene, and/or by the abrogation of the MVA HA gene (*A56R*) when *A40R* was re-inserted in this locus. The HA protein is not an essential VACV protein, but contributions of HA to VACV virulence have not been fully elucidated. In fact, a vector lacking the VACV HA gene (*A56R*) (along with a series of other gene deletions) resulted in virus attenuation and was able to reduce the size of breast cancer tumors in a nude mouse model when compared with the parental virus without HA deletion [239].

Overall, these findings revealed the immunomodulatory role of *A40R*, proving that its deletion or over-expression from the MVA-B vector modulates cytokine expression in infected macrophages and alters the magnitude and quality of adaptive and memory HIV-1-specific $CD4^+$ and $CD8^+$ T cell immune responses, as well as the gp120-specific humoral immune responses. Thus, as it is provided in this thesis, the MVA *A40R* gene plays an immunomodulatory function acting at various levels, with its deletion enhancing innate, adaptive and memory HIV-specific immune responses, while its overexpression has a negative effect on innate and adaptive $CD4^+$ T cell immune responses, being less effective over $CD8^+$ T cell responses. There was also some effect of A40 protein over humoral responses. All these results together with the membrane localization in infected cells and the significant similarity of A40 to C-type lectins like NKG2A and DC-SIGN, suggest that the immune function of A40R could be exerted by: 1) mimicking native host

lectins, or 2) modulating recognition of VACV-infected cells by cells of the immune system and, consequently, interrupting host immune responses to the viral infection.

In summary, the consequence of deleting the *A40R* gene in the HIV-1 vaccine candidate MVA-B is an enhancement of the immunogenicity of this vector, hence, we have established an important strategy for the optimization of MVA vectors as vaccines.

5.2. Immunogenicity and efficacy of an optimized MVA-based vaccine candidate against ZIKV: MVA-ZIKV

The promising results obtained previously with the use of the novel strong LEO160 promoter or the deletion of an immunomodulatory VACV gene in the context of an MVA-based vaccine against HIV/AIDS showed that these strategies could be successfully applied for the design of future novel MVA-based vaccine candidates against HIV/AIDS or other infectious diseases. Thus, in the third part of this Thesis a novel MVA-based vaccine candidate against ZIKV, lacking several immunomodulatory VACV genes (*C6L*, K7R, and *A46R*), and expressing under the control of the stronger VACV LEO160 promoter the ZIKV prM and E antigens optimized to be released and assembled as VLPs (a third genetic improvement) was generated. The aim of this study was to demonstrate that the immune responses induced in an animal model following vaccination correlate with protection after a challenge in the context of an emerging viral disease different from HIV/AIDS.

ZIKV is an important emerging flavivirus transmitted by infected mosquitoes from the genus *Aedes* that can cause severe complications in humans. The virus has caused recent outbreaks of the disease worldwide and their future expansion to novel geographical areas is highly possible [140,141]. Although several ZIKV vaccine candidates have been generated using different strategies [151,152], actually no licensed vaccine exists. These vaccines have been tested in animals in preclinical trials and in early phase I or II human clinical trials, but although they are immunogenic many of them required numerous immunizations, have high costs of manufacturing or require the use of chemical adjuvants. Therefore, novel strategies are necessary to achieve potent and long-lasting protective immune responses, with less immunizations, better safety profile, and lower costs of vaccine production. An ideal ZIKV vaccine should 1) be safe, especially for women of child-bearing age; 2) be stable and cost effective to manufacture, as ZIKV is endemic in developing countries; 3) avoid the addition of chemical adjuvants to minimize associated-risks; 4) be effective against all circulating ZIKV strains; and 5) be able to induce a rapid onset of protective levels of neutralizing anti-ZIKV antibodies as well as T cell responses to control the replication of the virus.

MVA-ZIKV possesses many of the characteristics needed for an ideal vaccine against ZIKV. MVA-ZIKV is replication competent in avian cells but replication deficient in human cells, making it safe for humans, including immunocompromised individuals, children and elderly. Moreover, a recent study in pregnant macaques immunized with an MVA vector showed no adverse or teratogenic effects [240], opening the possibility of its use in pregnant women, which could be highly relevant in ZIKV vaccination because of severe sequelae of ZIKV infection during pregnancy. Additionally, as it has been discussed above, MVA vectors induce strong innate responses during vaccination acting itself as an adjuvant [57] and eliminating the need of other chemical adjuvants, thus minimizing reactogenicity and adverse effects caused by these synthetic substances [241,242], and promoting a better activation of the immune system [180]. Furthermore, MVA vaccines can be produced easily in primary avian cells, the most common cells used in the good manufacturing practice of MVA lots, and the cost of production and manufacture is low, which is of relevant importance in developing countries, the more affected with the ZIKV epidemic. Therefore, the use of an MVA vector expressing ZIKV antigens, such as the MVA-ZIKV reported here, is a promising approach against ZIKV. In addition, as mentioned before, the MVA-ZIKV vaccine candidate developed has a MVA genome more optimized than its parental MVA-WT, due to additional deletions in three MVA immunomodulatory genes (*C6L*, *K7R,* and *A46R*), whose deletion enhanced in immunized mice the HIV-1-specific cellular and humoral immune responses induced by a MVA vector expressing Env, Gag, Pol and Nef HIV-1 antigens [93]. Furthermore, one dose of a vaccine against CHIKV based on MVA with these three deletions and expressing CHIKV structural antigens (termed MVA-CHIKV) protected 100% of animals against CHIKV infection in mice and nonhuman primates [97,243]. Recently, this optimized MVA vector was used to generate MVA-based vaccines that protected against EBOV infection in a susceptible mouse model [98], reinforcing the use of this vaccine platform against emerging viruses, like CHIKV, EBOV and ZIKV.

The MVA-ZIKV vaccine candidate expresses the ZIKV prM and E structural genes of the ZIKV isolate Z1106033 (derived from an Asian lineage virus, isolated from a patient in Suriname). Although there are three main ZIKV lineages (East African, West African, and Asian-American) [244], up to date, only one ZIKV serotype has been established [190]. Thus, MVA-ZIKV vaccine should be potentially effective against different ZIKV strains, due to low heterogeneity between ZIKV lineages. In fact, the results demonstrated that elicited neutralizing antibodies from MVA-ZIKV were effective against a different ZIKV strain of the Asian lineage. The E protein is the main ZIKV protein involved in receptor binding and fusion, while the M protein is a small protein that is

hidden under the E protein layer [245,246]. The prM and E proteins are, together with the inactivated whole viruses, the flaviviral proteins more widely used as vaccine antigens showing an excellent capacity to protect against these family of virus, including ZIKV [151,152]. Recent studies comparing in mice and nonhuman primates the efficacy of diverse vectored-based vaccines against ZIKV, showed that live-attenuated adenoviral vectors are one of the most potent approaches, even in long-term studies [197,247,248]. Moreover, the combination of a robust humoral and cellular immune responses elicited by a adenovirus expressing prM-E ZIKV antigens were able to induce sterilizing protection against ZIKV infection in mice [249,250], which is very important for the vertical transmission because ZIKV seems to replicate more efficiently in fetal tissue, especially at earlier gestational stages [251]. These results confirm the advantage of live-attenuated recombinant vaccines, a case that can be extrapolated to the MVA-ZIKV vaccine developed here.

Another advantage of the MVA-ZIKV vaccine candidate is that it expresses high levels of ZIKV prM and E antigens, as observed by Western blot and/or immunofluorescence. This high expression is due to the presence in the MVA vector of the optimized strong VACV LEO160 promoter which suitability as approach to increase the antigen-specific immunogenicity has been discussed above in section 5.1.1 and demonstrated in previous reports [88]. As happened with the MVA-LEO160-gp120 recombinant vector, MVA-ZIKV is highly stable in cell culture, maintaining the expression of ZIKV antigens at least during 9 continuous passages at low MOI, with 100% of the plaques picked at passage 9 expressing the correct size ZIKV antigens.

The ZIKV E protein expressed by MVA-ZIKV co-localized with the ER (the place where prM-E protein is translocated to dimerize), supporting their correct subcellular localization. Furthermore, the apparent absence of the ZIKV E protein in the cell membrane of the MVA-ZIKV-infected cells suggests that the E protein is not exposed in the outer membrane but released to the medium. Moreover, we have detected the presence of the ZIKV E protein and the mature M protein in supernatants of cells infected with MVA-ZIKV, confirming their release to the medium. Remarkably, the analysis by immunogold electron microscopy of the purified supernatants demonstrated that MVA-ZIKV produced VLPs, similarly to other ZIKV and flavivirus vaccines expressing the prM-E genes [186,188,191,196].

The adaptive immune response against ZIKV plays an essential role in regulating ZIKV infection and preventing the spread of the virus to key organs, like the brain and testes [200,248], especially when type I IFN response is reduced, as in human ZIKV infection [252]. It has been described that neutralizing antibody titers higher than 10

correlated with protection after vaccination with most of the licensed flavivirus vaccines [253], and adoptive transfer studies suggest that vaccine-elicited antibodies, even at low titers, are sufficient for protection against ZIKV challenge in mice and nonhuman primates [197–199,254]. MVA-ZIKV induced after 2 doses and at 10-13 days post-boost, neutralizing antibody titers by PRNT50 higher than 200 in in immunocompetent Balb/c mice (data not shown). Similar levels of neutralizing antibody titers induced by a inactivated ZIKV vaccine were shown to conferred passive protection against virus replication in the AG129 mouse model [255]. The potent generation of neutralizing antibodies by MVA-ZIKV could be favored by the production of VLPs, which are efficiently recognized by the B cells [256], leading to an MHC-II upregulation that will promote the production of high levels of neutralizing antibodies against ZIKV. VLPs are highly immunogenic and therefore are very important to improve the ZIKV-specific immune responses *in vivo*, as it has been reported with VLPs from ZIKV or other viruses that induced high titers of neutralizing antibodies which correlate with protection [186,188,191,196,257].

Regarding the T cell response to ZIKV infection, to date relatively little is known. It has been recently shown that adoptive transfer of ZIKV-specific $CD8^+$ T cells prevented disease in immunocompromised susceptible mice, while $CD8^+$ T cell suppression increased susceptibility to ZIKV infection [200,202]. Moreover, ZIKV-specific $CD8^+$ T cells were shown to traffic to the brain, where they protected against not only ZIKV infection but also DENV infection [202]. Given the neurotropism of ZIKV and its presence in fetal brain tissues and cerebrospinal fluid in both humans and animal models [251,258], $CD8^+$ T cells may have a key role in clearing ZIKV from the central nervous system (CNS) and, thus, in preventing or mitigating neurological complications. A recent study in pregnant macaques infected with ZIKV and then treated with a cocktail of ZIKV-neutralizing human monoclonal antibodies (mAbs) at the peak of viremia, showed that while the mAbs can be effective in clearing the virus from the maternal sera of treated nonhuman primates, it is not sufficient to fully stop vertical transmission [259]. This finding suggest the importance of $CD8^+$ T cell immune response against ZIKV infection, especially when the immune system integrity is compromised, as during pregnancy [260]. These results suggest that a vaccine eliciting ZIKV-specific $CD8^+$ T cell responses could contribute effectively at preventing disease and clearing the virus from the CNS. Up to now only few vaccine candidates have described the induction of ZIKV-specific T cell responses towards E protein; reporting mainly a modest activation [197,198,248,261], except for one adenoviral vectored vaccine candidate expressing ZIKV M-E antigens that elicited a robust cellular response after only one dose, although

the magnitude of the response was very dependent of the dose [250]. MVA-ZIKV using to vaccinate immunocompetent mice, was able to induce potent and polyfunctional ZIKV-specific $CD8^+$ T cell immune responses, as natural ZIKV infection does [202], indicating that MVA-ZIKV could be a promising vaccine candidate against ZIKV. On the other hand, the low $CD4^+$ T cell response that we observed was consistent with a report where appearance of $CD4^+$ T cell responses in ZIKV-infected rhesus monkeys was not found until production of antibodies and $CD8^+$ T cell responses, at 2 weeks post-infection [262].

Next, to analyze whether the potent T cell and humoral antibody responses achieved by MVA-ZIKV correlate with protection against ZIKV infection, a type I IFN receptor-knockout mouse model ($IFNAR^{-/-}$) was used to perform efficacy assays, as current immunocompetent mouse models for ZIKV are not susceptible to viremia or lethal outcome. $IFNAR^{-/-}$ mice are extensively used as a challenge model for ZIKV vaccine candidates [204,205]. As it happened in immunocompetent Balb/c mice, $IFNAR^{-/-}$ mice immunized with one or two doses of MVA-ZIKV produced good titers of ZIKV-neutralizing antibodies (against ZIKV PA259459 strain or against other isolates such as FSS13025) and controlled ZIKV viral replication after a challenge with live ZIKV PA259459 strain Panama, representative of the circulating virus during the American epidemic. After the challenge, $IFNAR^{-/-}$ mice (10 weeks old at the moment of challenge) did not loss body weight or have mortality during 15 days post-challenge. This results are consistent with data obtained in adult $IFNAR^{-/-}$ mice (10-11 weeks old) challenged with other ZIKV strains belonging to the same genetic lineage than PA259459 strain that did not develop disease and had higher survival rates than young mice challenged with the same ZIKV strain [204,205,263–265]. Accordingly, this non-lethal challenge model was selected for the evaluation of vaccine efficacy because it resembles better the ZIKV infection in humans, which usually provokes a mild disease that does not result fatal.

The control of ZIKV infection obtained after administration of one or two doses of MVA-ZIKV was in the range between 2.5 and 4 log virus reduction, highlighting the efficacy of the vaccine. We do not know the contribution of B and T cell responses in the control of ZIKV infection in this mouse model. However, considering the potent ZIKV-specific $CD8^+$ T cellular immunogenicity and humoral immune responses induced by MVA-ZIKV in the immunocompetent mouse model, we suggest that in a similar way, neutralizing antibodies and $CD8^+$ T cells should both contribute to the effective reduction of viral load observed in $IFNAR^{-/-}$ mice and this vaccine would be an effective approach to protect against ZIKV. Further studies will be needed to define in this system the independent role of B and T cell responses elicited by MVA-ZIKV in virus protection. Remarkably, the fact that MVA-ZIKV induced antibodies that can neutralize other ZIKV

strain (FSS13025, Cambodia 2010), the high homology among ZIKV structural proteins from different isolates and the existence of only one ZIKV serotype [190] support that the protection observed could be likely extended to other different ZIKV strains.

In summary, a novel and promising ZIKV vaccine candidate named MVA-ZIKV was successfully developed. MVA-ZIKV was able to produce VLPs and induced in mice ZIKV-specific neutralizing antibodies and a potent $CD8^+$ T cell immune response, being strongly effective in reducing ZIKV viremia after a challenge with ZIKV.

Overall this Thesis show that poxviral vectors, and in particular MVA, are promising vaccine candidates against a wide range of pathogens, including HIV-1 and ZIKV, because they are able to elicit balanced antigen-specific cellular and humoral immune responses to counteract the infection. The several genetic modifications introduced in the MVA vector (enhancing promoter strength, deleting immunomodulatory viral genes and optimizing the expression of genes from selected pathogens), reinforce the idea that development of novel optimized MVA vectors is the way to follow in order to improve the immunogenicity and efficacy of these vectors as vaccines.

CONCLUSIONS

6. CONCLUSIONS

1) The MVA-LEO160-gp120 recombinant virus, containing the HIV-1 gp120 gene under the control of the novel synthetic VACV LEO160 promoter, triggered in infected cells higher HIV-1 gp120 mRNA and protein levels than clinical vaccine candidate MVA-B.

2) Mice immunized with DNA-gp120/MVA-LEO160-gp120 induced an enhancement in the Env-specific $CD4^+$ and $CD8^+$ T cell and Tfh immune responses, and in the levels of total IgG binding antibodies against gp120, in comparison to DNA-gp120/MVA-B. These results revealed the strength of the novel synthetic VACV LEO160 promoter and confirmed a positively correlation of an increased *in vitro* HIV-1 gp120 expression with an *in vivo* enhancement of Env-specific T cell and humoral immune responses.

3) The MVA-B ΔA40R deletion mutant, lacking the MVA *A40R* gene from the HIV/AIDS vaccine candidate MVA-B, triggered in infected human macrophages an enhancement in the innate immune responses, in comparison to parental MVA-B, suggesting an immunosuppressive role of the MVA A40 protein.

4) Mice immunized with DNA-B/MVA-B ΔA40R induced an increase in the magnitude of adaptive and memory HIV-1-specific $CD4^+$ and $CD8^+$ T cell immune responses and in the levels of antibodies against HIV-1 gp120, in comparison to DNA-B/MVA-B, reinforcing the suggested immunosuppressive role of the MVA *A40R* gene.

5) A revertant virus, termed MVA-B ΔA40R-rev, constructed by reinserting the MVA *A40R* gene into the HA locus of the MVA-B ΔA40R genome, and placed under the control of a VACV synthetic early/late promoter expressed high mRNA and protein A40 levels. In infected human macrophages, MVA-B ΔA40R-rev significantly reduced the mRNA levels of several innate immune related genes, confirming the immunosuppressive role of the MVA A40 protein, and strongly suggesting that acts blocking the type I IFN pathway.

6) Mice immunized with DNA-B/MVA-B ΔA40R-rev induced lower levels of adaptive HIV-1-specific $CD4^+$ T cell immune responses than DNA-B/MVA-B ΔA40R, and similar to parental DNA-B/MVA-B regimen, confirming the immunosuppressive role *in vivo* of the MVA A40 protein.

7) A novel vaccine candidate against ZIKV, termed MVA-ZIKV, based on an optimized MVA vector lacking three VACV immunomodulatory genes (*C6L*, *K7R,* and *A46R*) and containing the ZIKV structural prM and E genes under the control of the stronger synthetic VACV LEO160 promoter was successfully generated. MVA-ZIKV correctly expressed and processed the ZIKV structural prM and E proteins that were assembled as VLPs, being released from the infected cells.

8) In immunocompetent mice immunized with an MVA-ZIKV/MVA-ZIKV prime/boost regimen, robust ZIKV-specific $CD8^+$ T cell immune responses and high levels of neutralizing antibodies were induced.

9) In an immunocompromised susceptible mice model, MVA-ZIKV was able to control ZIKV infection after administration of one or two doses; supporting the advantage of optimized recombinant MVA-based vaccines against emerging diseases, such as Zika.

CONCLUSIONES

7. CONCLUSIONES

1) El virus recombinante MVA-LEO160-gp120, que contiene el gen gp120 del VIH-1 bajo el control del nuevo promotor sintético LEO160del VACV indujo en células infectadas mayores niveles de ARNm y de proteína de gp120 del VIH-1 que el candidato vacunal clínico MVA-B.

2) Ratones inmunizados con DNA-gp120/MVA-LEO160-gp120 indujeron un aumento en las respuestas inmunitarias de células T $CD4^+$ y $CD8^+$ y de Tfh específicas frente a Env y en los niveles de anticuerpos IgG de unión a gp120, en comparación con DNA-gp120/MVA-B. Estos resultados revelaron la potencia del nuevo promotor sintético LEO160 del VACV y confirmaron una correlación positiva entre una mayor expresión *in vitro* de gp120 del VIH-1 con un aumento *in vivo* de las respuestas inmunitarias de células T y humorales específicas frente a Env.

3) El mutante de deleción MVA-B ΔA40R, que carece del gen *A40R* del MVA en el candidato vacunal MVA-B frente a VIH/SIDA, indujo en macrófagos humanos infectados un aumento de las respuestas inmunitarias innatas en comparación con el parental MVA-B, sugiriendo un papel inmunosupresor de la proteína A40 del MVA.

4) Ratones inmunizados con DNA-B/MVA-B ΔA40R indujeron un incremento en la magnitud de las respuestas inmunitarias de células T $CD4^+$ y $CD8^+$ específicas frente a VIH-1 en fase adaptativa y de memoria, y en los niveles de anticuerpos frente a gp120 del VIH-1, en comparación con DNA-B/MVA-B, reforzando el papel inmunosupresor sugerido del gen A40R del MVA.

5) Un virus revertiente, denominado MVA-B ΔA40R-rev, generado mediante la reinserción del gen *A40R* del MVA en el locus *HA* del genoma de MVA-B ΔA40R, y situado bajo el control del promotor sintético temprano/tardío del VACV, expresó altos niveles de ARNm y proteína de A40. En macrófagos humanos infectados, MVA-B ΔA40R-rev redujo significativamente los niveles de ARNm de varios genes relacionados con la inmunidad innata, confirmando el papel inmunosupresor de la proteína A40 del MVA, y sugiriendo fuertemente que actúa bloqueando la ruta del IFN tipo I.

6) Ratones inmunizados con DNA-B/MVA-B ΔA40R-rev indujeron menores niveles de respuestas inmunitarias de células T $CD4^+$ específicas frente a VIH-1 que DNA-B/MVA-B ΔA40R, y similares al régimen parental DNA-B/MVA-B, confirmando el papel inmunosupresor *in vivo* de la proteína A40 del MVA.

7) Se generó satisfactoriamente un nuevo candidato vacunal frente al ZIKV, denominado MVA-ZIKV, basado en un vector MVA optimizado que carece de tres genes inmunomoduladores del VACV (*C6L*, *K7R* y *A46R*) y que contiene los genes estructurales prM y E del ZIKV bajo el control del potente promotor sintético LEO160 del

VACV. MVA-ZIKV expresó y procesó correctamente las proteínas estructurales prM y E del ZIKV que se ensamblaron como VLPs, liberándose de las células infectadas.

8) En ratones inmunocompetentes inmunizados con un régimen *prime/boost* MVA-ZIKV/MVA-ZIKV se indujeron respuestas inmunitarias robustas de células T $CD8^+$ específicas frente a ZIKV y altos niveles de anticuerpos neutralizantes.

9) En un modelo inmunocomprometido susceptible de ratones, MVA-ZIKV fue capaz de controlar la infección por ZIKV después de la administración de una o dos dosis, apoyando la ventaja de vacunas recombinantes optimizadas basadas en MVA frente a enfermedades emergentes, como Zika

REFERENCES

8. REFERENCES

1. Mercer AA (Andrew A., Schmidt A, Weber OF (2007) *Poxviruses*. Birkhäuser.
2. Panicali D, Paoletti E (1982) Construction of poxviruses as cloning vectors: insertion of the thymidine kinase gene from herpes simplex virus into the DNA of infectious vaccinia virus. *Proc Natl Acad Sci U S A* **79**: 4927–4931.
3. Mackett M, Smith GL, Moss B (1982) Vaccinia virus: a selectable eukaryotic cloning and expression vector. *Proc Natl Acad Sci U S A* **79**: 7415–7419.
4. Verardi PH, Titong A, Hagen CJ (2012) A vaccinia virus renaissance. *Hum Vaccin Immunother* **8**: 961–970.
5. Walsh SR, Dolin R (2011) Vaccinia viruses: Vaccines against smallpox and vectors against infectious diseases and tumors. *Expert Rev Vaccines* **10**: 1221–1240.
6. Jacobs BL, Langland JO, Kibler K V., Denzler KL, White SD, Holechek SA, Wong S, Huynh T, Baskin CR (2009) Vaccinia virus vaccines: Past, present and future. *Antiviral Res* **84**: 1–13.
7. Prow NA, Jimenez Martinez R, Hayball JD, Howley PM, Suhrbier A (2018) Poxvirus-based vector systems and the potential for multi-valent and multi-pathogen vaccines. *Expert Rev Vaccines* **17**: 925–934.
8. Sánchez-Sampedro L, Perdiguero B, Mejías-Pérez E, García-Arriaza J, Di Pilato M, Esteban M (2015) The evolution of poxvirus vaccines. *Viruses* **7**: 1726–1803.
9. Esteban M, Flores L, Holowczak JA (1977) Model for vaccinia virus DNA replication. *Virology* **83**: 467–473.
10. Goebel SJ, Johnson GP, Perkus ME, Davis SW, Winslow JP, Paoletti E (1990) The complete DNA sequence of vaccinia virus. *Virology* **179**: 247–266.
11. Moss B (2013) Poxvirus DNA replication. *Cold Spring Harb Perspect Biol* **5**: a010199–a010199.
12. Moss B (2007) Poxviridae: The viruses and their replication. In KNIPE, D. M. & HOWLEY PM (ed.), *Fields Virology* pp 2905–2946. Lippincott Williams & Wilkins, Philadelphia.
13. McFadden G (2005) Poxvirus tropism. *Nat Rev Microbiol* **3**: 201–213.
14. Smith GL, Vanderplasschen A, Law M (2002) The formation and function of extracellular enveloped vaccinia virus. *J Gen Virol* **83**: 2915–2931.
15. Cyrklaff M, Risco C, Fernandez JJ, Jimenez M V., Esteban M, Baumeister W, Carrascosa JL (2005) Cryo-electron tomography of vaccinia virus. *Proc Natl Acad Sci* **102**: 2772–2777.
16. Moss B (2012) Poxvirus cell entry: How many proteins does it take? *Viruses* **4**: 688–707.
17. Carter GC, Rodger G, Murphy BJ, Law M, Krauss O, Hollinshead M, Smith GL (2003) Vaccinia virus cores are transported on microtubules. *J Gen Virol* **84**: 2443–2458.
18. Sarov I, Joklik WK (1972) Characterization of intermediates in the uncoating of vaccinia virus DNA. *Virology* **50**: 593–602.
19. Esteban M, Soloski M, Cabrera C V, Holowczak JA (1979) Replication of vaccinia DNA and studies on the structure of the viral chromosome. *Cold Spring Harb Symp Quant Biol* **43**: 789–799.
20. Joklik WK, Becker Y (1964) The replication and coating of vaccinia DNA. *J Mol Biol* **10**: 452–474.
21. Esteban M, Metz DH (1973) Early virus protein synthesis in vaccinia virus-infected cells. *J Gen Virol* **19**: 201–206.
22. Assarsson E, Greenbaum JA, Sundström M, Schaffer L, Hammond JA, Pasquetto V, Oseroff C, Hendrickson RC, Lefkowitz EJ, Tscharke DC, et al. (2008) Kinetic analysis of a complete poxvirus transcriptome reveals an immediate-early class of genes. *Proc Natl Acad Sci U S A* **105**: 2140–2145.

23. Yang Z, Bruno DP, Martens CA, Porcella SF, Moss B (2010) Simultaneous high-resolution analysis of vaccinia virus and host cell transcriptomes by deep RNA sequencing. *Proc Natl Acad Sci U S A* **107**: 11513–11518.
24. Vos JC, Stunnenberg HG (1988) Derepression of a novel class of vaccinia virus genes upon DNA replication. *EMBO J* **7**: 3487–3492.
25. Rodriguez JR, Risco C, Carrascosa JL, Esteban M, Rodriguez D (1997) Characterization of early stages in vaccinia virus membrane biogenesis: implications of the 21-kilodalton protein and a newly identified 15-kilodalton envelope protein. *JVirol* **71**: 1821–1833.
26. Blasco R, Moss B (1991) Extracellular vaccinia virus formation and cell-to-cell virus transmission are prevented by deletion of the gene encoding the 37,000-Dalton outer envelope protein. *J Virol* **65**: 5910–5920.
27. Roberts KL, Smith GL (2008) Vaccinia virus morphogenesis and dissemination. *Trends Microbiol* **16**: 472–479.
28. Smith GL, Benfield CTO, Maluquer de Motes C, Mazzon M, Ember SWJ, Ferguson BJ, Sumner RP (2013) Vaccinia virus immune evasion: Mechanisms, virulence and immunogenicity. *J Gen Virol* **94**: 2367–2392.
29. Albarnaz JD, Torres AA, Smith GL (2018) Modulating vaccinia virus immunomodulators to improve immunological memory. *Viruses* **10**:.
30. Haller O, Kochs G, Weber F (2006) The interferon response circuit: Induction and suppression by pathogenic viruses. *Virology* **344**: 119–130.
31. Xu R, Johnson AJ, Liggitt D, Bevan MJ (2004) Cellular and humoral immunity against vaccinia virus infection of mice. *J Immunol* **172**: 6265–6271.
32. Fogg C, Lustig S, Whitbeck JC, Eisenberg RJ, Cohen GH, Moss B (2004) Protective immunity to vaccinia virus induced by vaccination with multiple recombinant outer membrane proteins of intracellular and extracellular virions. *J Virol* **78**: 10230–10237.
33. Spriggs MK, Koller BH, Sato T, Morrissey PJ, Fanslow WC, Smithies O, Voice RF, Widmer MB, Maliszewski CR (1992) Beta 2-microglobulin-, CD8+ T-cell-deficient mice survive inoculation with high doses of vaccinia virus and exhibit altered IgG responses. *Proc Natl Acad Sci U S A* **89**: 6070–6074.
34. Wyatt LS, Earl PL, Eller LA, Moss B (2004) Highly attenuated smallpox vaccine protects mice with and without immune deficiencies against pathogenic vaccinia virus challenge. *Proc Natl Acad Sci* **101**: 4590–4595.
35. Meseda CA, Garcia AD, Kumar A, Mayer AE, Manischewitz J, King LR, Golding H, Merchlinsky M, Weir JP (2005) Enhanced immunogenicity and protective effect conferred by vaccination with combinations of modified vaccinia virus Ankara and licensed smallpox vaccine Dryvax in a mouse model. *Virology* **339**: 164–175.
36. Coulibaly S, Brühl P, Mayrhofer J, Schmid K, Gerencer M, Falkner FG (2005) The nonreplicating smallpox candidate vaccines defective vaccinia Lister (dVV-L) and modified vaccinia Ankara (MVA) elicit robust long-term protection. *Virology* **341**: 91–101.
37. Mccarthy K, Downie AW, Bradley WH (1958) The antibody response in man following infection with viruses of the pox group: II. Antibody response following vaccination. *J Hyg (Lond)* **56**: 466–478.
38. McClain DJ, Harrison S, Yeager CL, Cruz J, Ennis FA, Gibbs P, Wright MS, Summers PL, Arthur JD, Graham JA (1997) Immunologic responses to vaccinia vaccines administered by different parenteral routes. *J Infect Dis* **175**: 756–763.
39. Greenberg RN, Kennedy JS, Clanton DJ, Plummer EA, Hague L, Cruz J, Ennis FA, Blackwelder WC, Hopkins RJ (2005) Safety and immunogenicity of new cell-cultured smallpox vaccine compared with calf-lymph derived vaccine: a blind, single-centre, randomised controlled trial. *Lancet* **365**: 398–409.
40. Frey SE, Newman FK, Yan L, Lottenbach KR, Belshe RB (2003) Response to Smallpox Vaccine in Persons Immunized in the Distant Past. *JAMA* **289**: 3295.

41. Hammarlund E, Lewis MW, Hansen SG, Strelow LI, Nelson JA, Sexton GJ, Hanifin JM, Slifka MK (2003) Duration of antiviral immunity after smallpox vaccination. *Nat Med* **9**: 1131–1137.
42. Putz MM, Alberini I, Midgley CM, Manini I, Montomoli E, Smith GL (2005) Prevalence of antibodies to Vaccinia virus after smallpox vaccination in Italy. *J Gen Virol* **86**: 2955–2960.
43. Harrington LE, Most R v. d., Whitton JL, Ahmed R (2002) Recombinant Vaccinia Virus-Induced T-Cell Immunity: Quantitation of the Response to the Virus Vector and the Foreign Epitope. *J Virol* **76**: 3329–3337.
44. Amara RR, Nigam P, Sharma S, Liu J, Bostik V (2004) Long-lived poxvirus immunity, robust CD4 help, and better persistence of CD4 than CD8 T cells. *J Virol* **78**: 3811–3816.
45. Rock MT, Yoder SM, Talbot TR, Edwards KM, Crowe, Jr. JE (2006) Cellular Immune Responses to Diluted and Undiluted Aventis Pasteur Smallpox Vaccine. *J Infect Dis* **194**: 435–443.
46. Mayr A, Stickl H, Müller HK, Danner K, Singer H (1978) The smallpox vaccination strain MVA: marker, genetic structure, experience gained with the parenteral vaccination and behavior in organisms with a debilitated defence mechanism . *Zentralbl Bakteriol B* **167**: 375–390.
47. Wyatt LS, Carroll MW, Czerny C-P, Merchlinsky M, Sisler JR, Moss B (1998) Marker Rescue of the Host Range Restriction Defects of Modified Vaccinia Virus Ankara. *Virology* **251**: 334–342.
48. Sutter G, Moss B (1992) Nonreplicating vaccinia vector efficiently expresses recombinant genes. *Proc Natl Acad Sci* **89**: 10847–10851.
49. Gallego-Gómez JC, Risco C, Rodríguez D, Cabezas P, Guerra S, Carrascosa JL, Esteban M (2003) Differences in virus-induced cell morphology and in virus maturation between MVA and other strains (WR, Ankara, and NYCBH) of vaccinia virus in infected human cells. *J Virol* **77**: 10606–10622.
50. Sancho MC, Schleich S, Griffiths G, Krijnse-Locker J (2002) The block in assembly of modified vaccinia virus Ankara in HeLa cells reveals new insights into vaccinia virus morphogenesis. *J Virol* **76**: 8318–8334.
51. Mahnel H, Mayr A (1994) Experiences with immunization against orthopox viruses of humans and animals using vaccine strain MVA. *Berl Munch Tierarztl Wochenschr* **107**: 253–256.
52. Gilbert SC (2013) Clinical development of Modified Vaccinia virus Ankara vaccines. *Vaccine* **31**: 4241–4246.
53. Gómez CE, Nájera JL, Krupa M, Perdiguero B, Esteban M (2011) MVA and NYVAC as vaccines against emergent infectious diseases and cancer. *Curr Gene Ther* **11**: 189–217.
54. Boukhebza H, Bellon N, Limacher JM, Inchauspé G (2012) Therapeutic vaccination to treat chronic infectious diseases: Current clinical developments using MVA-based vaccines. *Hum Vaccines Immunother* **8**: 1746–1757.
55. Gómez CE, Perdiguero B, García-Arriaza J, Esteban M (2013) Clinical applications of attenuated MVA poxvirus strain. *Expert Rev Vaccines* **12**: 1395–1416.
56. Volz A, Sutter G (2017) Modified Vaccinia Virus Ankara: History, Value in Basic Research, and Current Perspectives for Vaccine Development. In, *Advances in Virus Research* pp 187–243.
57. Price PJRR, Torres-Domínguez LE, Brandmüller C, Lehmann MH, Sutter G, Lehmann MH (2013) Modified vaccinia virus ankara: Innate immune activation and induction of cellular signalling. *Vaccine* **31**: 4231–4234.
58. Delaloye J, Roger T, Steiner-Tardivel QG, Le Roy D, Reymond MK, Akira S, Petrilli V, Gomez CE, Perdiguero B, Tschopp J, et al. (2009) Innate immune sensing of modified vaccinia virus Ankara (MVA) is mediated by TLR2-TLR6,

MDA-5 and the NALP3 inflammasome. *PLoS Pathog* **5**: e1000480.
59. García-Arriaza J, Esteban M (2014) *Enhancing poxvirus vectors vaccine immunogenicity*. Taylor & Francis.
60. Marín MQ, Pérez P, Ljungberg K, Sorzano CÓS, Gómez CE, Liljeström P, Esteban M, García-Arriaza J (2019) Potent Anti-Hepatitis C (HCV) T Cell Immune Responses Induced in Mice Vaccinated with DNA-launched RNA Replicons and MVA-HCV. *J Virol*.
61. Hinkula J, Petkov S, Ljungberg K, Hallengärd D, Bråve A, Isaguliants M, Falkeborn T, Sharma S, Liakina V, Robb M, et al. (2017) HIVIS-DNA or HIVISopt-DNA priming followed by CMDR vaccinia-based boosts induce both humoral and cellular murine immune responses to HIV. *Heliyon* **3**: e00339.
62. Chea LS, Amara RR (2017) *Immunogenicity and efficacy of DNA/MVA HIV vaccines in rhesus macaque models*. NIH Public Access.
63. Lorenzo G, López-Gil E, Ortego J, Brun A (2018) Efficacy of different DNA and MVA prime-boost vaccination regimens against a Rift Valley fever virus (RVFV) challenge in sheep 12 weeks following vaccination. *Vet Res* **49**: 21.
64. Shen X, Basu R, Sawant S, Beaumont D, Kwa SF, LaBranche C, Seaton KE, Yates NL, Montefiori DC, Ferrari G, et al. (2017) HIV-1 gp120 and Modified Vaccinia Virus Ankara (MVA) gp140 Boost Immunogens Increase Immunogenicity of a DNA/MVA HIV-1 Vaccine. *J Virol* **91**:.
65. Vijayan A, Mejías-Pérez E, Espinosa DA, Raman SC, Sorzano COS, Zavala F, Esteban M (2017) A Prime/Boost PfCS14K ^{M} /MVA-sPfCS ^{M} Vaccination Protocol Generates Robust CD8 $^{+}$ T Cell and Antibody Responses to Plasmodium falciparum Circumsporozoite Protein and Protects Mice against Malaria. *Clin Vaccine Immunol* **24**:.
66. Gangadhara S, Kwon Y-M, Jeeva S, Quan F-S, Wang B, Moss B, Compans R, Amara R, Jabbar M, Kang S-M (2017) Vaccination with Combination DNA and Virus-Like Particles Enhances Humoral and Cellular Immune Responses upon Boost with Recombinant Modified Vaccinia Virus Ankara Expressing Human Immunodeficiency Virus Envelope Proteins. *Vaccines* **5**: 52.
67. Biswas S, Dicks MDJ, Long CA, Remarque EJ, Siani L, Colloca S, Cottingham MG, Holder AA, Gilbert SC, Hill AVS, et al. (2011) Transgene optimization, immunogenicity and in vitro efficacy of viral vectored vaccines expressing two alleles of plasmodium falciparum AMA1. *PLoS One* **6**: e20977.
68. Van Rompay KKA, Abel K, Earl P, Kozlowski PA, Easlick J, Moore J, Buonocore-Buzzelli L, Schmidt KA, Wilson RL, Simon I, et al. (2010) Immunogenicity of viral vector, prime-boost SIV vaccine regimens in infant rhesus macaques: Attenuated vesicular stomatitis virus (VSV) and modified vaccinia Ankara (MVA) recombinant SIV vaccines compared to live-attenuated SIV. *Vaccine* **28**: 1481–1492.
69. Joachim A, Nilsson C, Aboud S, Bakari M, Lyamuya EF, Robb ML, Marovich MA, Earl P, Moss B, Ochsenbauer C, et al. (2015) Potent functional antibody responses elicited by HIV-I DNA priming and boosting with heterologous HIV-1 recombinant MVA in healthy tanzanian adults. *PLoS One* **10**: e0118486.
70. Gray GE, Mayer KH, Elizaga ML, Bekker L-G, Allen M, Morris L, Montefiori D, De Rosa SC, Sato A, Gu N, et al. (2016) Subtype C gp140 Vaccine Boosts Immune Responses Primed by the South African AIDS Vaccine Initiative DNA-C2 and MVA-C HIV Vaccines after More than a 2-Year Gap. *Clin Vaccine Immunol* **23**: 496–506.
71. Joachim A, Bauer A, Joseph S, Geldmacher C, Munseri PJ, Aboud S, Missanga M, Mann P, Wahren B, Ferrari G, et al. (2016) Boosting with subtype C CN54rgp140 protein adjuvanted with glucopyranosyl lipid adjuvant after priming with HIV-DNA and HIV-MVA is safe and enhances immune responses: A phase I trial. *PLoS One* **11**: e0155702.
72. Swadling L, Capone S, Antrobus RD, Brown A, Richardson R, Newell EW,

Halliday J, Kelly C, Bowen D, Fergusson J, et al. (2014) A human vaccine strategy based on chimpanzee adenoviral and MVA vectors that primes, boosts, and sustains functional HCV-specific T cell memory. *Sci Transl Med* **6**: 261ra153-261ra153.

73. Mensah VA, Gueye A, Ndiaye M, Edwards NJ, Wright D, Anagnostou NA, Syll M, Ndaw A, Abiola A, Bliss C, et al. (2016) Safety, Immunogenicity and Efficacy of Prime-Boost Vaccination with ChAd63 and MVA Encoding ME-TRAP against Plasmodium falciparum Infection in Adults in Senegal. *PLoS One* **11**: e0167951.
74. Venkatraman N, Anagnostou N, Bliss C, Bowyer G, Wright D, Lövgren-Bengtsson K, Roberts R, Poulton I, Lawrie A, Ewer K, et al. (2017) Safety and immunogenicity of heterologous prime-boost immunization with viral-vectored malaria vaccines adjuvanted with Matrix-M™. *Vaccine* **35**: 6208–6217.
75. Ewer K, Rampling T, Venkatraman N, Bowyer G, Wright D, Lambe T, Imoukhuede EB, Payne R, Fehling SK, Strecker T, et al. (2015) A Monovalent Chimpanzee Adenovirus Ebola Vaccine Boosted with MVA. *N Engl J Med* **374**: 1635–1646.
76. Green CA, Scarselli E, Sande CJ, Thompson AJ, De Lara CM, Taylor KS, Haworth K, Del Sorbo M, Angus B, Siani L, et al. (2015) Chimpanzee adenovirus- and MVA-vectored respiratory syncytial virus vaccine is safe and immunogenic in adults. *Sci Transl Med* **7**: 300ra126-300ra126.
77. Wyatt LS, Earl PL, Vogt J, Eller LA, Chandran D, Liu J, Robinson HL, Moss B (2008) Correlation of immunogenicities and in vitro expression levels of recombinant modified vaccinia virus Ankara HIV vaccines. *Vaccine* **26**: 486–493.
78. Baur K, Brinkmann K, Schweneker M, Pätzold J, Meisinger-Henschel C, Hermann J, Steigerwald R, Chaplin P, Suter M, Hausmann J (2010) Immediate-early expression of a recombinant antigen by modified vaccinia virus ankara breaks the immunodominance of strong vector-specific B8R antigen in acute and memory CD8 T-cell responses. *J Virol* **84**: 8743–8752.
79. Yang Z, Reynolds SE, Martens CA, Bruno DP, Porcella SF, Moss B (2011) Expression profiling of the intermediate and late stages of poxvirus replication. *J Virol* **85**: 9899–9908.
80. Moutaftsi M, Tscharke DC, Vaughan K, Koelle DM, Stern L, Calvo-Calle M, Ennis F, Terajima M, Sutter G, Crotty S, et al. (2010) Uncovering the interplay between CD8, CD4 and antibody responses to complex pathogens. *Future Microbiol* **5**: 221–239.
81. Moutaftsi M, Bui H-H, Peters B, Sidney J, Salek-Ardakani S, Oseroff C, Pasquetto V, Crotty S, Croft M, Lefkowitz EJ, et al. (2007) Vaccinia virus-specific CD4+ T cell responses target a set of antigens largely distinct from those targeted by CD8+ T cell responses. *J Immunol* **178**: 6814–6820.
82. Moutaftsi M, Salek-Ardakani S, Croft M, Peters B, Sidney J, Grey H, Sette A (2009) Correlates of protection efficacy induced by vaccinia virus-specific CD8+ T-cell epitopes in the murine intranasal challenge model. *Eur J Immunol* **39**: 717–722.
83. Pasquetto V, Bui H-H, Giannino R, Banh C, Mirza F, Sidney J, Oseroff C, Tscharke DC, Irvine K, Bennink JR, et al. (2005) HLA-A*0201, HLA-A*1101, and HLA-B*0702 transgenic mice recognize numerous poxvirus determinants from a wide variety of viral gene products. *J Immunol* **175**: 5504–5515.
84. Wilson EH, Hunter CA (2008) Immunodominance and Recognition of Intracellular Pathogens. *J Infect Dis* **198**: 1579–1581.
85. Sette A, Grey H, Oseroff C, Peters B, Moutaftsi M, Crotty S, Assarsson E, Greenbaum J, Kim Y, Kolla R, et al. (2009) Definition of epitopes and antigens recognized by vaccinia specific immune responses: their conservation in variola virus sequences, and use as a model system to study complex pathogens. *Vaccine* **27 Suppl 6**: G21-6.
86. Kastenmuller W, Gasteiger G, Gronau JH, Baier R, Ljapoci R, Busch DH, Drexler

l (2007) Cross-competition of CD8 + T cells shapes the immunodominance hierarchy during boost vaccination. *J Exp Med* **204**: 2187–2198.
87. Alharbi NK (2019) Poxviral promoters for improving the immunogenicity of MVA delivered vaccines. *Hum Vaccines Immunother* **15**: 203–209.
88. Di Pilato M, Sánchez-Sampedro L, Mejías-Pérez E, Sorzano CO, Esteban M, Mariano Esteban C, Sánchez-Sampedro L, Mejías-Pérez E, Sorzano COS, Esteban M (2015) Modification of promoter spacer length in vaccinia virus as a strategy to control the antigen expression. *J Gen Virol* **96**: 2360–2371.
89. Di Pilato M, Mejías-Pérez E, Gómez CE, Perdiguero B, Oscar C, Sorzano S, Esteban M, Di Pilato M, Mejias-Perez E, Gomez CE, et al. (2013) New vaccinia virus promoter as a potential candidate for future vaccines. *J Gen Virol* **94**: 2771–2776.
90. Garcia-Arriaza J, Gomez CE, Sorzano COS, Esteban M (2014) Deletion of the Vaccinia Virus N2L Gene Encoding an Inhibitor of IRF3 Improves the Immunogenicity of Modified Vaccinia Virus Ankara Expressing HIV-1 Antigens. *J Virol* **88**: 3392–3410.
91. García-Arriaza J, Nájera JL, Gómez CE, Tewabe N, Sorzano COS, Calandra T, Roger T, Esteban M (2011) A candidate HIV/AIDS vaccine (MVA-B) lacking vaccinia virus gene C6L enhances memory HIV-1-specific T-cell responses. *PLoS One* **6**: e24244.
92. García-Arriaza J, Nájera JL, Gómez CE, Sorzano COS, Esteban M (2010) Immunogenic profiling in mice of a HIV/AIDS vaccine candidate (MVA-B) expressing four HIV-1 antigens and potentiation by specific gene deletions. *PLoS One* **5**: e12395.
93. García-Arriaza J, Arnáez P, Gómez CE, Sorzano CÓS, Esteban M (2013) Improving Adaptive and Memory Immune Responses of an HIV/AIDS Vaccine Candidate MVA-B by Deletion of Vaccinia Virus Genes (C6L and K7R) Blocking Interferon Signaling Pathways. *PLoS One* **8**: e66894.
94. Perdiguero B, Gómez CE, Nájera JL, Sorzano COS, Delaloye J, González-Sanz R, Jiménez V, Roger T, Calandra T, Pantaleo G, et al. (2012) Deletion of the Viral Anti-Apoptotic Gene F1L in the HIV/AIDS Vaccine Candidate MVA-C Enhances Immune Responses against HIV-1 Antigens. *PLoS One* **7**: e48524.
95. Garber DA, O'Mara LA, Gangadhara S, McQuoid M, Zhang X, Zheng R, Gill K, Verma M, Yu T, Johnson B, et al. (2012) Deletion of Specific Immune-Modulatory Genes from Modified Vaccinia Virus Ankara-Based HIV Vaccines Engenders Improved Immunogenicity in Rhesus Macaques. *J Virol* **86**: 12605–12615.
96. Garber DA, O'Mara LA, Zhao J, Gangadhara S, An IC, Feinberg MB (2009) Expanding the repertoire of modified vaccinia Ankara-based vaccine vectors via genetic complementation strategies. *PLoS One* **4**: e5445.
97. García-Arriaza J, Cepeda V, Hallengärd D, Sorzano COSÓS, Kümmerer BM, Liljeström P, Esteban M, Garcia-Arriaza J, Cepeda V, Hallengard D, et al. (2014) A Novel Poxvirus-Based Vaccine, MVA-CHIKV, Is Highly Immunogenic and Protects Mice against Chikungunya Infection. *J Virol* **88**: 3527–3547.
98. Lázaro-Frías A, Gómez-Medina S, Sánchez-Sampedro L, Ljungberg K, Ustav M, Liljeström P, Muñoz-Fontela C, Esteban M, García-Arriaza J (2018) Distinct Immunogenicity and Efficacy of Poxvirus-based Vaccine Candidates against Ebola Virus expressing GP and VP40 Proteins. *J Virol* JVI.00363-18.
99. Wilcock D, Duncan SA, Traktman P, Zhang W-HH, Smith GL (1999) The vaccinia virus A4OR gene product is a nonstructural, type II membrane glycoprotein that is expressed at the cell surface. *J Gen Virol* **80 (Pt 8)**: 2137–2148.
100. Mayer S, Raulf M-K, Lepenies B (2017) C-type lectins: their network and roles in pathogen recognition and immunity. *Histochem Cell Biol* **147**: 223–237.
101. Tscharke DC, Reading PC, Smith GL (2002) *Dermal infection with vaccinia virus reveals roles for virus proteins not seen using other inoculation routes*.

102. Schramm B, Locker JK (2005) Cytoplasmic organization of POXvirus DNA replication. *Traffic* **6**: 839–846.
103. Palacios S, Perez L, Welsch S, Schleich S, Chmielarska K, Melchior F, Locker J (2005) Quantitative SUMO-1 modification of a vaccinia virus protein is required for its specific localization and prevents its self-association. *Mol Biol Cell* **16**: 2822–2835.
104. Kou Y, Xu Y, Zhao Z, Liu J, Wu Y, You Q, Wang L, Gao F, Cai L, Jiang C (2017) Tissue plasminogen activator (tPA) signal sequence enhances immunogenicity of MVA-based vaccine against tuberculosis. *Immunol Lett* **190**: 51–57.
105. Quinan BR, Flesch IEA, Pinho TMG, Coelho FM, Tscharke DC, da Fonseca FG (2014) An intact signal peptide on dengue virus E protein enhances immunogenicity for CD8+ T cells and antibody when expressed from modified vaccinia Ankara. *Vaccine* **32**: 2972–2979.
106. Schmeisser F, Adamo JE, Blumberg B, Friedman R, Muller J, Soto J, Weir JP (2012) Production and characterization of mammalian virus-like particles from modified vaccinia virus Ankara vectors expressing influenza H5N1 hemagglutinin and neuraminidase. *Vaccine* **30**: 3413–3422.
107. Schweneker M, Laimbacher AS, Zimmer G, Wagner S, Schraner EM, Wolferstätter M, Klingenberg M, Dirmeier U, Steigerwald R, Lauterbach H, et al. (2017) Recombinant Modified Vaccinia Virus Ankara Generating Ebola Virus-Like Particles. *J Virol* **91**:.
108. Perdiguero B, Sánchez-Corzo C, Sorzano COS, Saiz L, Mediavilla P, Esteban M, Gómez CE (2019) A Novel MVA-Based HIV Vaccine Candidate (MVA-gp145-GPN) Co-Expressing Clade C Membrane-Bound Trimeric gp145 Env and Gag-Induced Virus-Like Particles (VLPs) Triggered Broad and Multifunctional HIV-1-Specific T Cell and Antibody Responses. *Viruses* **11**: 160.
109. Capucci S, Wee EG, Schiffner T, LaBranche CC, Borthwick N, Cupo A, Dodd J, Dean H, Sattentau Q, Montefiori D, et al. (2017) HIV-1-neutralizing antibody induced by simian adenovirus- and poxvirus MVA-vectored BG505 native-like envelope trimers. *PLoS One* **12**: e0181886.
110. Iyer SS, Gangadhara S, Victor B, Shen X, Chen X, Nabi R, Kasturi SP, Sabula MJ, Labranche CC, Reddy PBJ, et al. (2016) Virus-Like Particles Displaying Trimeric Simian Immunodeficiency Virus (SIV) Envelope gp160 Enhance the Breadth of DNA/Modified Vaccinia Virus Ankara SIV Vaccine-Induced Antibody Responses in Rhesus Macaques. *J Virol* **90**: 8842–8854.
111. Jones AT, Chamcha V, Kesavardhana S, Shen X, Beaumont D, Das R, Wyatt LS, LaBranche CC, Stanfield-Oakley S, Ferrari G, et al. (2018) A Trimeric HIV-1 Envelope gp120 Immunogen Induces Potent and Broad Anti-V1V2 Loop Antibodies against HIV-1 in Rabbits and Rhesus Macaques. *J Virol* **92**:.
112. Torrents de la Peña A, Julien J-P, de Taeye SW, Garces F, Guttman M, Ozorowski G, Pritchard LK, Behrens A-J, Go EP, Burger JA, et al. (2017) Improving the Immunogenicity of Native-like HIV-1 Envelope Trimers by Hyperstabilization. *Cell Rep* **20**: 1805–1817.
113. Gómez CE, Nájera JL, Jiménez EP, Jiménez V, Wagner R, Graf M, Frachette M-J, Liljeström P, Pantaleo G, Esteban M (2007) Head-to-head comparison on the immunogenicity of two HIV/AIDS vaccine candidates based on the attenuated poxvirus strains MVA and NYVAC co-expressing in a single locus the HIV-1BX08 gp120 and HIV-1(IIIB) Gag-Pol-Nef proteins of clade B. *Vaccine* **25**: 2863–2885.
114. Gómez CE, Nájera JL, Sánchez R, Jiménez V, Esteban M (2009) Multimeric soluble CD40 ligand (sCD40L) efficiently enhances HIV specific cellular immune responses during DNA prime and boost with attenuated poxvirus vectors MVA and NYVAC expressing HIV antigens. *Vaccine* **27**: 3165–3174.
115. Rosás-Umbert M, Mothe B, Noguera-Julian M, Bellido R, Puertas MC, Carrillo J, Rodriguez C, Perez-Alvarez N, Cobarsí P, Gomez CE, et al. (2017) Virological

and immunological outcome of treatment interruption in HIV-1-infected subjects vaccinated with MVA-B. *PLoS One* **12**: e0184929.
116. García F, Bernaldo de Quirós JCL, Gómez CE, Perdiguero B, Nájera JL, Jiménez V, García-Arriaza J, Guardo AC, Pérez I, Díaz-Brito V, et al. (2011) Safety and immunogenicity of a modified pox vector-based HIV/AIDS vaccine candidate expressing Env, Gag, Pol and Nef proteins of HIV-1 subtype B (MVA-B) in healthy HIV-1-uninfected volunteers: A phase I clinical trial (RISVAC02). *Vaccine* **29**: 8309–8316.
117. Gómez CE, Nájera JL, Perdiguero B, García-Arriaza J, Sorzano COS, Jiménez V, González-Sanz R, Jiménez JL, Muñoz-Fernández MA, López Bernaldo de Quirós JC, et al. (2011) The HIV/AIDS Vaccine Candidate MVA-B Administered as a Single Immunogen in Humans Triggers Robust, Polyfunctional, and Selective Effector Memory T Cell Responses to HIV-1 Antigens. *J Virol* **85**: 11468–11478.
118. Guardo AC, Gómez CE, Díaz-Brito V, Pich J, Arnaiz JA, Perdiguero B, García-Arriaza J, González N, Sorzano COS, Jiménez L, et al. (2017) Safety and vaccine-induced HIV-1 immune responses in healthy volunteers following a late MVA-B boost 4 years after the last immunization. *PLoS One* **12**: e0186602.
119. Rallón N, Mothe B, Lopez Bernaldo de Quiros JC, Plana M, Ligos JM, Montoya MM, Muñoz-Fernández MA, Esteban M, Garcia F, Brander C, et al. (2016) Balance between activation and regulation of HIV-specific CD8+T-cell response after modified vaccinia Ankara B therapeutic vaccination. *AIDS* **30**: 553–562.
120. Gómez CE, Perdiguero B, García-Arriaza J, Cepeda V, Sánchez-Sorzano CÓ, Mothe B, Jiménez JL, Muñoz-Fernández MÁ, Gatell JM, López Bernaldo de Quirós JC, et al. (2015) A phase i randomized therapeutic MVA-B vaccination improves the magnitude and quality of the T cell immune responses in HIV-1-infected subjects on HAART. *PLoS One* **10**: e0141456.
121. Mothe B, Climent N, Plana M, Rosas M, Jimenez JL, Munoz-Fernandez MA, Puertas MC, Carrillo J, Gonzalez N, Leon A, et al. (2015) Safety and immunogenicity of a modified vaccinia Ankara-based HIV-1 vaccine (MVA-B) in HIV-1-infected patients alone or in combination with a drug to reactivate latent HIV-1. *J Antimicrob Chemother* **70**: 1833–1842.
122. Putri DH, Sudiro TM, Yunita R, Jaya UA, Dewi BE, Sjatha F, Konishi E, Hotta H, Sudarmono P (2015) Immunogenicity of a Candidate DNA Vaccine Based on the prM/E Genes of a Dengue Type 2 Virus Cosmopolitan Genotype Strain. *Jpn J Infect Dis* **68**: 357–363.
123. Urakami A, Ngwe Tun MM, Moi ML, Sakurai A, Ishikawa M, Kuno S, Ueno R, Morita K, Akahata W (2017) An Envelope-Modified Tetravalent Dengue Virus-Like-Particle Vaccine Has Implications for Flavivirus Vaccine Design. *J Virol* **91**:.
124. Taylor TJ, Diaz F, Colgrove RC, Bernard KA, DeLuca NA, Whelan SPJ, Knipe DM (2016) Production of immunogenic West Nile virus-like particles using a herpes simplex virus 1 recombinant vector. *Virology* **496**: 186–193.
125. Qian P, Zhi X, Wang B, Zhang H, Chen H, Li X (2015) Construction and immune efficacy of recombinant pseudorabies virus expressing PrM-E proteins of Japanese encephalitis virus genotype I. *Virol J* **12**: 214.
126. Higuchi A, Toriniwa H, Komiya T, Nakayama T (2016) Recombinant Measles AIK-C Vaccine Strain Expressing the prM-E Antigen of Japanese Encephalitis Virus. *PLoS One* **11**: e0150213.
127. Barré-Sinoussi F, Chermann JC, Rey F, Nugeyre MT, Chamaret S, Gruest J, Dauguet C, Axler-Blin C, Vézinet-Brun F, Rouzioux C, et al. (1983) Isolation of a T-lymphotropic retrovirus from a patient at risk for acquired immune deficiency syndrome (AIDS). *Science* **220**: 868–871.
128. Broder S, Gallo RC (1984) A Pathogenic Retrovirus (HTLV-III) Linked to AIDS. *N Engl J Med* **311**: 1292–1297.
129. Sarngadharan MG, DeVico AL, Bruch L, Schüpbach J, Gallo RC (1984) HTLV-III:

the etiologic agent of AIDS. *Princess Takamatsu Symp* **15**: 301–308.
130. Votteler J, Schubert U (2008) Human Immunodeficiency Viruses: Molecular Biology. In, *Encyclopedia of Virology* pp 517–525. Academic Press.
131. Frankel AD, Young JAT (1998) HIV-1: Fifteen Proteins and an RNA. *Annu Rev Biochem* **67**: 1–25.
132. Buonaguro L, Tornesello ML, Buonaguro FM (2007) Human Immunodeficiency Virus Type 1 Subtype Distribution in the Worldwide Epidemic: Pathogenetic and Therapeutic Implications. *J Virol* **81**: 10209–10219.
133. Hemelaar J (2012) The origin and diversity of the HIV-1 pandemic. *Trends Mol Med* **18**: 182–192.
134. Sharp PM, Hahn BH (2011) Origins of HIV and the AIDS pandemic. *Cold Spring Harb Perspect Med* **1**: a006841.
135. Cihlar T, Fordyce M (2016) Current status and prospects of HIV treatment. *Curr Opin Virol* **18**: 50–56.
136. Gao Y, McKay PF, Mann JFS (2018) Advances in HIV-1 vaccine development. *Viruses* **10**: 167.
137. Rerks-Ngarm S, Pitisuttithum P, Nitayaphan S, Kaewkungwal J, Chiu J, Paris R, Premsri N, Namwat C, de Souza M, Adams E, et al. (2009) Vaccination with ALVAC and AIDSVAX to Prevent HIV-1 Infection in Thailand. *N Engl J Med* **361**: 2209–2220.
138. Cohen KW, Frahm N (2017) Current views on the potential for development of a HIV vaccine. *Expert Opin Biol Ther* **17**: 295–303.
139. Kuno G, Chang G-JJJ (2007) Full-length sequencing and genomic characterization of Bagaza, Kedougou, and Zika viruses. *Arch Virol* **152**: 687–696.
140. Saiz JC, Vázquez-Calvo Á, Blázquez AB, Merino-Ramos T, Escribano-Romero E, Martín-Acebes MA (2016) Zika virus: The latest newcomer. *Front Microbiol* **7**: 496.
141. Song B-H, Yun S-I, Woolley M, Lee Y-M (2017) Zika virus: History, epidemiology, transmission, and clinical presentation. *J Neuroimmunol* **308**: 50–64.
142. Stettler K, Beltramello M, Espinosa DA, Graham V, Cassotta A, Bianchi S, Vanzetta F, Minola A, Jaconi S, Mele F, et al. (2016) Specificity, cross-reactivity, and function of antibodies elicited by Zika virus infection. *Science (80-)* **353**: 823–826.
143. Singh RK, Dhama K, Malik YS, Ramakrishnan MA, Karthik K, Tiwari R, Saurabh S, Sachan S, Joshi SK (2016) Zika virus – emergence, evolution, pathology, diagnosis, and control: current global scenario and future perspectives – a comprehensive review. *Vet Q* **36**: 150–175.
144. Petersen LR, Jamieson DJ, Powers AM, Honein MA (2016) Zika Virus. *N Engl J Med* **374**: 1552–1563.
145. Leonhard SE, Lant S, Jacobs BC, Wilder-Smith A, Ferreira MLB, Solomon T, Willison HJ (2018) Zika virus infection in the returning traveller: What every neurologist should know. *Pract Neurol* **18**: 271–277.
146. Aragao MFVV, Brainer-Lima AM, Holanda AC, Van Der Linden V, Aragao LV, Silva MLM, Sarteschi C, Petribu NCL, Valença MM (2017) Spectrum of spinal cord, spinal root, and brain mri abnormalities in congenital Zika syndrome with and without Arthrogryposis. *Am J Neuroradiol* **38**: 1045–1053.
147. De Oliveira Melo AS, Aguiar RS, Amorim MMR, Arruda MB, De Oliveira Melo F, Ribeiro STC, Batista AGM, Ferreira T, Dos Santos MP, Sampaio VV, et al. (2016) Congenital Zika virus infection: Beyond neonatal microcephaly. *JAMA Neurol* **73**: 1407–1416.
148. Saiz J-C, Martín-Acebes MA (2017) The Race To Find Antivirals for Zika Virus. *Antimicrob Agents Chemother* **61**:.
149. Ishikawa T, Yamanaka A, Konishi E (2014) A review of successful flavivirus vaccines and the problems with those flaviviruses for which vaccines are not yet available. *Vaccine* **32**: 1326–1337.

150. Barrett ADT (2017) Yellow fever live attenuated vaccine: A very successful live attenuated vaccine but still we have problems controlling the disease. *Vaccine* **35**: 5951–5955.
151. Makhluf H, Shresta S (2018) Development of Zika Virus Vaccines. *Vaccines* **6**: 7.
152. Abbink P, Stephenson KE, Barouch DH (2018) Zika virus vaccines. *Nat Rev Microbiol*.
153. Merino-Ramos T, Jiménez de Oya N, Saiz J-C, Martín-Acebes MA (2017) Antiviral Activity of Nordihydroguaiaretic Acid and Its Derivative Tetra-O-Methyl Nordihydroguaiaretic Acid against West Nile Virus and Zika Virus. *Antimicrob Agents Chemother* **61**: e00376-17.
154. Green, M. & Sambrook J (2012) *Molecular Cloning: a laboratory manual.*
155. Gómez CE, Perdiguero B, Cepeda MV, Mingorance L, García-Arriaza J, Vandermeeren A, Sorzano CÓS, Esteban M (2013) High, broad, polyfunctional, and durable T cell immune responses induced in mice by a novel hepatitis C virus (HCV) vaccine candidate (MVA-HCV) based on modified vaccinia virus Ankara expressing the nearly full-length HCV genome. *J Virol* **87**: 7282–7300.
156. Gibson DG, Young L, Chuang R-Y, Venter JC, Hutchison CA, Smith HO (2009) Enzymatic assembly of DNA molecules up to several hundred kilobases. *Nat Methods* **6**: 343–345.
157. Enfissi A, Codrington J, Roosblad J, Kazanji M, Rousset D (2016) Zika virus genome from the Americas. *Lancet (London, England)* **387**: 227–228.
158. Vázquez-Calvo Á, Blázquez A-B, Escribano-Romero E, Merino-Ramos T, Saiz J-C, Martín-Acebes MA, Jiménez de Oya N (2017) Zika virus infection confers protection against West Nile virus challenge in mice. *Emerg Microbes Infect* **6**: e81.
159. Schmittgen TD, Livak KJ (2008) Analyzing real-time PCR data by the comparative CT method. *Nat Protoc* **3**: 1101–1108.
160. Earl PL, Moss B, Wyatt LS, Carroll MW (2004) Generation of Recombinant Vaccinia Viruses. In, *Current Protocols in Molecular Biology* p Unit16.17. John Wiley & Sons, Inc., Hoboken, NJ, USA.
161. Chakrabarti S, Brechling K, Moss B (1985) Vaccinia virus expression vector: coexpression of beta-galactosidase provides visual screening of recombinant virus plaques. *Mol Cell Biol* **5**: 3403–3409.
162. Carroll MW, Moss B (1995) E. coli beta-glucuronidase (GUS) as a marker for recombinant vaccinia viruses. *Biotechniques* **19**: 352–354, 356.
163. Ramírez JC, Gherardi MM, Esteban M (2000) Biology of attenuated modified vaccinia virus Ankara recombinant vector in mice: virus fate and activation of B- and T-cell immune responses in comparison with the Western Reserve strain and advantages as a vaccine. *J Virol* **74**: 923–933.
164. Esteban M (1984) Defective vaccinia virus particles in interferon-treated infected cells. *Virology* **133**: 220–227.
165. Kremer M, Volz A, Kreijtz JHCM, Fux R, Lehmann MH, Sutter G (2012) Easy and efficient protocols for working with recombinant vaccinia virus MVA. *Methods Mol Biol* **890**: 59–92.
166. Joklik WK (1962) The purification fo four strains of poxvirus. *Virology* **18**: 9–18.
167. Faye O, Faye O, Diallo D, Diallo M, Weidmann M, Sall AA (2013) Quantitative real-time PCR detection of Zika virus and evaluation with field-caught Mosquitoes. *Virol J* **10**: 311.
168. Merino-Ramos T, Blázquez A-B, Escribano-Romero E, Cañas-Arranz R, Sobrino F, Saiz J-C, Martín-Acebes MA (2014) Protection of a Single Dose West Nile Virus Recombinant Subviral Particle Vaccine against Lineage 1 or 2 Strains and Analysis of the Cross-Reactivity with Usutu Virus. *PLoS One* **9**: e108056.
169. Nájera JL, Gómez CE, García-Arriaza J, Sorzano CO, Esteban M (2010) Insertion of vaccinia virus C7L host range gene into NYVAC-B genome potentiates immune

responses against HIV-1 antigens. *PLoS One* **5**: e11406.
170. Mooij P, Balla-Jhagjhoorsingh SS, Koopman G, Beenhakker N, van Haaften P, Baak I, Nieuwenhuis IG, Kondova I, Wagner R, Wolf H, et al. (2008) Differential CD4+ versus CD8+ T-Cell Responses Elicited by Different Poxvirus-Based Human Immunodeficiency Virus Type 1 Vaccine Candidates Provide Comparable Efficacies in Primates. *J Virol* **82**: 2975–2988.
171. Ghiglione Y, Falivene J, Ruiz MJ, Laufer N, Socías ME, Cahn P, Giavedoni L, Sued O, Gherardi MM, Salomón H, et al. (2014) Early skewed distribution of total and HIV-specific CD8+T-cell memory phenotypes during primary HIV infection is related to reduced antiviral activity and faster disease progression. *PLoS One* **9**: e104235.
172. Jansen CA, Piriou E, Bronke C, Vingerhoed J, Kostense S, Van Baarle D, Miedema F (2004) Characterization of virus-specific CD8+effector T cells in the course of HIV-1 infection: Longitudinal analyses in slow and rapid progressors. *Clin Immunol* **113**: 299–309.
173. Addo MM, Draenert R, Rathod A, Verrill CL, Davis BT, Gandhi RT, Robbins GK, Basgoz NO, Stone DR, Cohen DE, et al. (2007) Fully differentiated HIV-1 specific CD8+ T effector cells are more frequently detectable in controlled than in progressive HIV-1 infection. *PLoS One* **2**: e321.
174. Bachmann MF, Wolint P, Schwarz K, Oxenius A (2005) Recall Proliferation Potential of Memory CD8+ T Cells and Antiviral Protection. *J Immunol* **175**: 4677–4685.
175. Moysi E, Petrovas C, Koup RA (2018) The role of follicular helper CD4 T cells in the development of HIV-1 specific broadly neutralizing antibody responses. *Retrovirology* **15**: 54.
176. Havenar-Daughton C, Lee JH, Crotty S (2017) Tfh cells and HIV bnAbs, an immunodominance model of the HIV neutralizing antibody generation problem. *Immunol Rev* **275**: 49–61.
177. Vinuesa CG, Linterman MA, Yu D, MacLennan ICM (2016) Follicular Helper T Cells. *Annu Rev Immunol* **34**: 335–368.
178. McElrath MJ, Haynes BF (2010) Induction of immunity to human immunodeficiency virus type-1 by vaccination. *Immunity* **33**: 542–554.
179. Gómez CE, Nájera JL, Jiménez V, Bieler K, Wild J, Kostic L, Heidari S, Chen M, Frachette M-JJ, Pantaleo G, et al. (2007) Generation and immunogenicity of novel HIV/AIDS vaccine candidates targeting HIV-1 Env/Gag-Pol-Nef antigens of clade C. *Vaccine* **25**: 1969–1992.
180. Platt A, Wetzler L (2013) Innate Immunity and Vaccines. *Curr Top Med Chem* **13**: 2597–2608.
181. Xiao W, Wyatt LS, Moss B, Vogt J, Americo JL, Cotter CA, Earl PL (2009) Elucidating and Minimizing the Loss by Recombinant Vaccinia Virus of Human Immunodeficiency Virus Gene Expression Resulting from Spontaneous Mutations and Positive Selection. *J Virol* **83**: 7176–7184.
182. Seder RA, Darrah PA, Roederer M (2008) T-cell quality in memory and protection: Implications for vaccine design. *Nat Rev Immunol* **8**: 247–258.
183. Sallusto F, Lenig D, Förster R, Lipp M, Lanzavecchia A (1999) Two subsets of memory T lymphocytes with distinct homing potentials and effector functions. *Nature* **401**: 708–712.
184. Sallusto F, Geginat J, Lanzavecchia A (2004) Central Memory and Effector Memory T Cell Subsets: Function, Generation, and Maintenance. *Annu Rev Immunol* **22**: 745–763.
185. Champagne P, Ogg GS, King AS, Knabenhans C, Ellefsen K, Nobile M, Appay V, Rizzardi GP, Fleury S, Lipp M, et al. (2001) Skewed maturation of memory HIV-specific CD8 T lymphocytes. *Nature* **410**: 106–111.
186. Boigard H, Alimova A, Martin GR, Katz A, Gottlieb P, Galarza JM (2017) Zika

virus-like particle (VLP) based vaccine. *PLoS Negl Trop Dis* **11**: e0005608.
187. Mukhopadhyay S, Kuhn RJ, Rossmann MG (2005) A structural perspective of the Flavivirus life cycle. *Nat Rev Microbiol* **3**: 13–22.
188. Salvo MA, Kingstad-Bakke B, Salas-Quinchucua C, Camacho E, Osorio JE (2018) Zika virus like particles elicit protective antibodies in mice. *PLoS Negl Trop Dis* **12**: e0006210.
189. Ferlenghi I, Clarke M, Ruttan T, Allison SL, Schalich J, Heinz FX, Harrison SC, Rey FA, Fuller SD (2001) Molecular organization of a recombinant subviral particle from tick-borne encephalitis virus. *Mol Cell* **7**: 593–602.
190. Dowd KA, DeMaso CR, Pelc RS, Speer SD, Smith ARY, Goo L, Platt DJ, Mascola JR, Graham BS, Mulligan MJ, et al. (2016) Broadly Neutralizing Activity of Zika Virus-Immune Sera Identifies a Single Viral Serotype. *Cell Rep* **16**: 1485–1491.
191. Garg H, Sedano M, Plata G, Punke EB, Joshi A (2017) Development of Virus like Particle Vaccine and Reporter Assay for Zika Virus. *J Virol* **91**: JVI.00834-17.
192. Hunt AR, Cropp CB, Chang GJJ (2001) A recombinant particulate antigen of Japanese encephalitis virus produced in stably-transformed cells is an effective noninfectious antigen and subunit immunogen. *J Virol Methods* **97**: 133–149.
193. Schalich J, Allison SL, Stiasny K, Mandl CW, Kunz C, Heinz FX (1996) Recombinant subviral particles from tick-borne encephalitis virus are fusogenic and provide a model system for studying flavivirus envelope glycoprotein functions. *J Virol* **70**: 4549–4557.
194. Hanna SL, Pierson TC, Sanchez MD, Ahmed AA, Murtadha MM, Doms RW (2005) N-Linked Glycosylation of West Nile Virus Envelope Proteins Influences Particle Assembly and Infectivity. *J Virol* **79**: 13262–13274.
195. Martín-Acebes MA, Blázquez A-B, Cañas-Arranz R, Vázquez-Calvo Á, Merino-Ramos T, Escribano-Romero E, Sobrino F, Saiz J-C (2016) A recombinant DNA vaccine protects mice deficient in the alpha/beta interferon receptor against lethal challenge with Usutu virus. *Vaccine* **34**: 2066–2073.
196. Dowd KA, Ko S-Y, Morabito KM, Yang ES, Pelc RS, DeMaso CR, Castilho LR, Abbink P, Boyd M, Nityanandam R, et al. (2016) Rapid development of a DNA vaccine for Zika virus. *Science* **354**: 237–240.
197. Abbink P, Larocca RA, De La Barrera RA, Bricault CA, Moseley ET, Boyd M, Kirilova M, Li Z, Ng'ang'a D, Nanayakkara O, et al. (2016) Protective efficacy of multiple vaccine platforms against Zika virus challenge in rhesus monkeys. *Science* **353**: 1129–1132.
198. Larocca RA, Abbink P, Peron JPS, de A. Zanotto PM, Iampietro MJ, Badamchi-Zadeh A, Boyd M, Ng'ang'a D, Kirilova M, Nityanandam R, et al. (2016) Vaccine protection against Zika virus from Brazil. *Nature* **536**: 474–478.
199. Zhao H, Fernandez E, Dowd KA, Speer SD, Platt DJ, Gorman MJ, Govero J, Nelson CA, Pierson TC, Diamond MS, et al. (2016) Structural Basis of Zika Virus-Specific Antibody Protection. *Cell* **166**: 1016–1027.
200. Elong Ngono A, Vizcarra EA, Tang WW, Sheets N, Joo Y, Kim K, Gorman MJ, Diamond MS, Shresta S (2017) Mapping and Role of the CD8+ T Cell Response During Primary Zika Virus Infection in Mice. *Cell Host Microbe* **21**: 35–46.
201. Pardy RD, Rajah MM, Condotta SA, Taylor NG, Sagan SM, Richer MJ (2017) Analysis of the T Cell Response to Zika Virus and Identification of a Novel CD8+ T Cell Epitope in Immunocompetent Mice. *PLOS Pathog* **13**: e1006184.
202. Huang H, Li S, Zhang Y, Han X, Jia B, Liu H, Liu D, Tan S, Wang Q, Bi Y, et al. (2017) CD8 + T Cell Immune Response in Immunocompetent Mice during Zika Virus Infection. *J Virol* **91**: JVI.00900-17.
203. Nazerai L, Schøller AS, Rasmussen POS, Buus S, Stryhn A, Christensen JP, Thomsen AR (2018) A new in vivo model to study protective immunity to Zika virus infection in mice with intact type I interferon signaling. *Front Immunol* **8**: 593.
204. Lazear HMMM, Govero J, Smith AMMM, Platt DJJJ, Fernandez E, Miner JJJJ,

Diamond MSSS (2016) A Mouse Model of Zika Virus Pathogenesis. *Cell Host Microbe* **19**: 720–730.
205. Morrison TE, Diamond MS (2017) Animal Models of Zika Virus Infection, Pathogenesis, and Immunity. *J Virol* **91**: e00009-17.
206. Nagata LP, Irwin CR, Hu W gang, Evans DH (2018) Vaccinia-based vaccines to biothreat and emerging viruses. *Biotechnol Genet Eng Rev* **34**: 107–121.
207. Iyer S, Amara R (2014) DNA/MVA Vaccines for HIV/AIDS. *Vaccines* **2**: 160–178.
208. Gómez CE, Perdiguero B, García-Arriaza J, Esteban M (2012) Poxvirus vectors as HIV/AIDS vaccines in humans. *Hum Vaccines Immunother* **8**: 1192–1207.
209. Pantaleo G, Esteban M, Jacobs B, Tartaglia J (2010) Poxvirus vector-based HIV vaccines. *Curr Opin HIV AIDS* **5**: 391–396.
210. Baden LR, Walsh SR, Seaman MS, Cohen YZ, Johnson JA, Licona JH, Filter RD, Kleinjan JA, Gothing JA, Jennings J, et al. (2018) First-in-Human Randomized, Controlled Trial of Mosaic HIV-1 Immunogens Delivered via a Modified Vaccinia Ankara Vector. *J Infect Dis* **218**: 633–644.
211. Barouch DH, Tomaka FL, Wegmann F, Stieh DJ, Alter G, Robb ML, Michael NL, Peter L, Nkolola JP, Borducchi EN, et al. (2018) Evaluation of a mosaic HIV-1 vaccine in a multicentre, randomised, double-blind, placebo-controlled, phase 1/2a clinical trial (APPROACH) and in rhesus monkeys (NHP 13-19). *Lancet (London, England)* **392**: 232–243.
212. Joseph S, Quinn K, Greenwood A, Cope A V, McKay PF, Hayes PJ, Kopycinski JT, Gilmour J, Miller AN, Geldmacher C, et al. (2017) A Comparative Phase I Study of Combination, Homologous Subtype-C DNA, MVA, and Env gp140 Protein/Adjuvant HIV Vaccines in Two Immunization Regimes. *Front Immunol* **8**: 149.
213. Mutua G, Farah B, Langat R, Indangasi J, Ogola S, Onsembe B, Kopycinski JT, Hayes P, Borthwick NJ, Ashraf A, et al. (2016) Broad HIV-1 inhibition in vitro by vaccine-elicited CD8+ T cells in African adults. *Mol Ther - Methods Clin Dev* **3**: 16061.
214. Ake JA, Schuetz A, Pegu P, Wieczorek L, Eller MA, Kibuuka H, Sawe F, Maboko L, Polonis V, Karasavva N, et al. (2017) Safety and Immunogenicity of PENNVAX-G DNA Prime Administered by Biojector 2000 or CELLECTRA Electroporation Device With Modified Vaccinia Ankara-CMDR Boost. *J Infect Dis* **216**: 1080–1090.
215. Hsu DC, O'Connell RJ (2017) Progress in HIV vaccine development. *Hum Vaccines Immunother* **13**: 1018–1030.
216. Wennier ST, Brinkmann K, Steinhäußer C, Mayländer N, Mnich C, Wielert U, Dirmeier U, Hausmann J, Chaplin P, Steigerwald R (2013) A Novel Naturally Occurring Tandem Promoter in Modified Vaccinia Virus Ankara Drives Very Early Gene Expression and Potent Immune Responses. *PLoS One* **8**: e73511.
217. Isshiki M, Zhang X, Sato H, Ohashi T, Inoue M, Shida H (2014) Effects of different promoters on the virulence and immunogenicity of a HIV-1 Env-expressing recombinant vaccinia vaccine. *Vaccine* **32**: 839–845.
218. Wyatt LS, Shors ST, Murphy BR, Moss B (1996) Development of a replication-deficient recombinant vaccinia virus vaccine effective against parainfluenza virus 3 infection in an animal model. *Vaccine* **14**: 1451–1458.
219. Wang Z, Martinez J, Zhou W, La Rosa C, Srivastava T, Dasgupta A, Rawal R, Li Z, Britt WJ, Diamond D (2010) Modified H5 promoter improves stability of insert genes while maintaining immunogenicity during extended passage of genetically engineered MVA vaccines. *Vaccine* **28**: 1547–1557.
220. Earl PL, Cotter C, Moss B, VanCott T, Currier J, Eller LA, McCutchan F, Birx DL, Michael NL, Marovich MA, et al. (2009) Design and evaluation of multi-gene, multi-clade HIV-1 MVA vaccines. *Vaccine* **27**: 5885–5895.
221. Chakrabarti S, Sisler JR, Moss B (1997) Compact, synthetic, vaccinia virus early/late promoter for protein expression. *Biotechniques* **23**: 1094–1097.

222. Cochran MA, Puckett C, Moss B (1985) In vitro mutagenesis of the promoter region for a vaccinia virus gene: evidence for tandem early and late regulatory signals. *J Virol* **54**: 30–37.
223. McMichael AJ, Rowland-Jones SL (2001) Cellular immune responses to HIV. *Nature* **410**: 980–987.
224. Hansen SG, Ford JC, Lewis MS, Ventura AB, Hughes CM, Coyne-Johnson L, Whizin N, Oswald K, Shoemaker R, Swanson T, et al. (2011) Profound early control of highly pathogenic SIV by an effector memory T-cell vaccine. *Nature* **473**: 523–527.
225. Hansen SG, Vieville C, Whizin N, Coyne-Johnson L, Siess DC, Drummond DD, Legasse AW, Axthelm MK, Oswald K, Trubey CM, et al. (2009) Effector memory T cell responses are associated with protection of rhesus monkeys from mucosal simian immunodeficiency virus challenge. *Nat Med* **15**: 293–299.
226. Breitfeld D, Ohl L, Kremmer E, Ellwart J, Sallusto F, Lipp M, Förster R (2000) Follicular B helper T cells express CXC chemokine receptor 5, localize to B cell follicles, and support immunoglobulin production. *J Exp Med* **192**: 1545–1552.
227. Schultz BT, Teigler JE, Pissani F, Oster AF, Kranias G, Alter G, Marovich M, Eller MA, Dittmer U, Robb ML, et al. (2016) Circulating HIV-Specific Interleukin-21+CD4+T Cells Represent Peripheral Tfh Cells with Antigen-Dependent Helper Functions. *Immunity* **44**: 167–178.
228. Locci M, Havenar-Daughton C, Landais E, Wu J, Kroenke MA, Arlehamn CL, Su LF, Cubas R, Davis MM, Sette A, et al. (2013) Human Circulating PD-1+CXCR3−CXCR5+ Memory Tfh Cells Are Highly Functional and Correlate with Broadly Neutralizing HIV Antibody Responses. *Immunity* **39**: 758–769.
229. Claireaux M, Galperin M, Benati D, Nouël A, Mukhopadhyay M, Klingler J, de Truchis P, Zucman D, Hendou S, Boufassa F, et al. (2018) A high frequency of HIV-Specific circulating follicular helper T cells is associated with preserved memory B cell responses in HIV Controllers. *MBio* **9**:.
230. Perdiguero B, Raman SC, Sánchez-Corzo C, Sorzano COS, Valverde JR, Esteban M, Gómez CE (2018) Potent HIV-1-specific CD8 T cell responses induced in mice after priming with a multiepitopic DNA-TMEP and boosting with the HIV vaccine MVA-B. *Viruses* **10**: 424.
231. Davies DH, Wyatt LS, Newman FK, Earl PL, Chun S, Hernandez JE, Molina DM, Hirst S, Moss B, Frey SE, et al. (2008) Antibody profiling by proteome microarray reveals the immunogenicity of the attenuated smallpox vaccine modified vaccinia virus ankara is comparable to that of Dryvax. *J Virol* **82**: 652–663.
232. Haynes BF, Gilbert PB, Mcelrath MJ, Zolla-Pazner S, Tomaras GD, Alam SM, Evans DT, Montefiori DC, Karnasuta C, Sutthent R, et al. (2012) Immune-Correlates Analysis of an HIV-1 Vaccine Efficacy Trial. *n engl j med* **36614366**: 1275–1286.
233. Falivene J, Del Mé Zajac MP, Pascutti MF, Rodríguez AM, Maeto C, Perdiguero B, Gómez CE, Esteban M, Calamante G, Gherardi MM (2012) Improving the MVA vaccine potential by deleting the viral gene coding for the IL-18 binding protein. *PLoS One* **7**: e32220.
234. Altfeld M, Gale Jr M (2015) Innate immunity against HIV-1 infection. *Nat Immunol* **16**: 554–562.
235. Perdiguero B, Gómez CE, Di Pilato M, Sorzano COS, Delaloye J, Roger T, Calandra T, Pantaleo G, Esteban M (2013) Deletion of the Vaccinia Virus Gene A46R, Encoding for an Inhibitor of TLR Signalling, Is an Effective Approach to Enhance the Immunogenicity in Mice of the HIV/AIDS Vaccine Candidate NYVAC-C. *PLoS One* **8**: e74831.
236. Gómez CE, Perdiguero B, Sánchez-Corzo C, Sorzano COS, Esteban M, Gómez CE, Perdiguero B, Sánchez-Corzo C, Sorzano COS, Esteban M (2018) Immune modulation of NYVAC-based HIV vaccines by combined deletion of viral genes

that act on several signalling pathways. *Viruses* **10**: 7.
237. Gómez CE, Perdiguero B, Nájera JL, Sorzano COS, Jiménez V, González-Sanz R, Esteban M (2012) Removal of Vaccinia Virus Genes That Block Interferon Type I and II Pathways Improves Adaptive and Memory Responses of the HIV/AIDS Vaccine Candidate NYVAC-C in Mice. *J Virol* **86**: 5026–5038.
238. Di Pilato M, Mejías-Pérez E, Sorzano COS, Esteban M (2017) Distinct Roles of Vaccinia Virus NF-κB Inhibitor Proteins A52, B15, and K7 in the Immune Response. *J Virol* **91**: e00575-17.
239. Izmailyan R, Chang W (2008) Vaccinia Virus WR53.5/F14.5 Protein Is a New Component of Intracellular Mature Virus and Is Important for Calcium-Independent Cell Adhesion and Vaccinia Virus Virulence in Mice. *J Virol* **82**: 10079–10087.
240. Eudailey JA, Dennis ML, Parker ME, Phillips BL, Huffman TN, Bay CP, Hudgens MG, Wiseman RW, Pollara JJ, Fouda GG, et al. (2018) Maternal HIV-1 Env Vaccination for Systemic and Breast Milk Immunity To Prevent Oral SHIV Acquisition in Infant Macaques. *mSphere* **3**: e00505-17.
241. Watad A, Quaresma M, Brown S, Cohen Tervaert JW, Rodríguez-Pint I, Cervera R, Perricone C, Shoenfeld Y (2017) Autoimmune/inflammatory syndrome induced by adjuvants (Shoenfeld's syndrome) – An update. *Lupus* **26**: 675–681.
242. Pellegrino P, Clementi E, Radice S (2015) On vaccine's adjuvants and autoimmunity: Current evidence and future perspectives. *Autoimmun Rev* **14**: 880–888.
243. Roques P, Ljungberg K, Kümmerer BM, Gosse L, Dereuddre-Bosquet N, Tchitchek N, Hallengärd D, García-Arriaza J, Meinke A, Esteban M, et al. (2017) Attenuated and vectored vaccines protect nonhuman primates against Chikungunya virus. *JCI Insight* **2**: e83527.
244. Lanciotti RS, Lambert AJ, Holodniy M, Saavedra S, Signor LDCC (2016) Phylogeny of Zika Virus in Western Hemisphere, 2015. *Emerg Infect Dis* **22**: 933–935.
245. Kostyuchenko VA, Lim EXY, Zhang S, Fibriansah G, Ng TS, Ooi JSG, Shi J, Lok SM (2016) Structure of the thermally stable Zika virus. *Nature* **533**: 425–428.
246. Sirohi D, Chen Z, Sun L, Klose T, Pierson TC, Rossmann MG, Kuhn RJ (2016) The 3.8 Å resolution cryo-EM structure of Zika virus. *Science* **352**: 467–470.
247. Kim E, Erdos G, Huang S, Kenniston T, Falo LD, Gambotto A, Gambotto A (2016) Preventative Vaccines for Zika Virus Outbreak: Preliminary Evaluation. *EBioMedicine* **13**: 315–320.
248. Abbink P, Larocca RA, Visitsunthorn K, Boyd M, De La Barrera RA, Gromowski GD, Kirilova M, Peterson R, Li Z, Nanayakkara O, et al. (2017) Durability and correlates of vaccine protection against Zika virus in rhesus monkeys. *Sci Transl Med* **9**: 1–8.
249. Guo Q, Chan JF-W, Poon VK-M, Wu S, Chan CC-S, Hou L, Yip CC-Y, Ren C, Cai J-P, Zhao M, et al. (2018) Immunization with a Novel Human type 5 Adenovirus-Vectored Vaccine Expressing the Premembrane and Envelope Proteins of Zika Virus Provides Consistent and Sterilizing Protection in Multiple Immunocompetent and Immunocompromised Animal Models. *J Infect Dis*.
250. Cox F, Van Der Fits L, Abbink P, Larocca RA, Van Huizen E, Saeland E, Verhagen J, Peterson R, Tolboom J, Kaufmann B, et al. (2018) Adenoviral vector type 26 encoding Zika virus (ZIKV) M-Env antigen induces humoral and cellular immune responses and protects mice and nonhuman primates against ZIKV challenge. *PLoS One* **13**: e0202820.
251. Jagger BW, Miner JJ, Cao B, Arora N, Smith AM, Kovacs A, Mysorekar IU, Coyne CB, Diamond MS (2017) Gestational Stage and IFN-λ Signaling Regulate ZIKV Infection In Utero. *Cell Host Microbe* **22**: 366–376.e3.
252. Bowen JR, Quicke KM, Maddur MS, O'Neal JT, McDonald CE, Fedorova NB, Puri

V, Shabman RS, Pulendran B, Suthar MS (2017) Zika Virus Antagonizes Type I Interferon Responses during Infection of Human Dendritic Cells. *PLoS Pathog* **13**: e1006164.
253. Hombach J, Solomon T, Kurane I, Jacobson J, Wood D (2005) Report on a WHO consultation on immunological endpoints for evaluation of new Japanese encephalitis vaccines, WHO, Geneva, 2-3 September, 2004. *Vaccine* **23**: 5205–5211.
254. Richner JM, Himansu S, Dowd KA, Butler SL, Salazar V, Fox JM, Julander JG, Tang WW, Shresta S, Pierson TC, et al. (2017) Modified mRNA Vaccines Protect against Zika Virus Infection. *Cell* **168**: 1114–1125.e10.
255. Sumathy K, Kulkarni B, Gondu RK, Ponnuru SK, Bonguram N, Eligeti R, Gadiyaram S, Praturi U, Chougule B, Karunakaran L, et al. (2017) Protective efficacy of Zika vaccine in AG129 mouse model. *Sci Rep* **7**: 46375.
256. Zhang S, Cubas R, Li M, Chen C, Yao Q (2009) Virus-like particle vaccine activates conventional B2 cells and promotes B cell differentiation to IgG2a producing plasma cells. *Mol Immunol* **46**: 1988–2001.
257. Akahata W, Yang ZY, Andersen H, Sun S, Holdaway HA, Kong WP, Lewis MG, Higgs S, Rossmann MG, Rao S, et al. (2010) A virus-like particle vaccine for epidemic Chikungunya virus protects nonhuman primates against infection. *Nat Med* **16**: 334–338.
258. Russo FB, Jungmann P, Beltrão-Braga PCB (2017) Zika infection and the development of neurological defects. *Cell Microbiol* **19**: e12744.
259. Magnani DM, Rogers TF, Maness NJ, Grubaugh ND, Beutler N, Bailey VK, Gonzalez-Nieto L, Gutman MJ, Pedreño-Lopez N, Kwal JM, et al. (2018) Fetal demise and failed antibody therapy during Zika virus infection of pregnant macaques. *Nat Commun* **9**: 1624.
260. Mor G, Cardenas I (2010) The Immune System in Pregnancy: A Unique Complexity. *Am J Reprod Immunol* **63**: 425–433.
261. Li XF, Dong HL, Wang HJ, Huang XY, Qiu YF, Ji X, Ye Q, Li C, Liu Y, Deng YQ, et al. (2018) Development of a chimeric Zika vaccine using a licensed live-attenuated flavivirus vaccine as backbone. *Nat Commun* **9**:.
262. Aid M, Abbink P, Larocca RA, Boyd M, Nityanandam R, Nanayakkara O, Martinot AJ, Moseley ET, Blass E, Borducchi EN, et al. (2017) Zika Virus Persistence in the Central Nervous System and Lymph Nodes of Rhesus Monkeys. *Cell* **169**: 610–620.e14.
263. Marzi A, Emanuel J, Callison J, McNally KL, Arndt N, Chadinha S, Martellaro C, Rosenke R, Scott DP, Safronetz D, et al. (2018) Lethal Zika Virus Disease Models in Young and Older Interferon α/β Receptor Knock Out Mice. *Front Cell Infect Microbiol* **8**:.
264. Shan C, Muruato AE, Nunes BTDD, Luo H, Xie X, Medeiros DBAA, Wakamiya M, Tesh RB, Barrett AD, Wang T, et al. (2017) A live-attenuated Zika virus vaccine candidate induces sterilizing immunity in mouse models. *Nat Med* **23**: 763–767.
265. Rossi SL, Tesh RB, Azar SR, Muruato AE, Hanley KA, Auguste AJ, Langsjoen RM, Paessler S, Vasilakis N, Weaver SC (2016) Characterization of a novel murine model to study zika virus. *Am J Trop Med Hyg* **94**: 1362–1369.